CRITICAL EVALUATION OF TECHNIQUES FOR THE IDENTIFICATION OF ARCHAEOLOGICAL BAST FIBRES: FLAX, HEMP AND NETTLE

D. B. WAUDBY

PHD

2019

Critical Evaluation of Techniques for the Identification of Archaeological Bast Fibres: Flax, Hemp And Nettle

Denis Brian WAUDBY

Submitted for the degree of

Doctor of Philosophy

Faculty of Life Sciences

School of Archaeological and Forensic Sciences

University of Bradford

2019

Abstract

Denis Brian Waudby

Critical Evaluation of Techniques for the Identification of Archaeological Bast Fibres: Flax, Hemp and Nettle

Keywords: Flax, nettle, hemp, textile-tools, archaeological assemblage blind-testing, degradation

Fibre plants favour different growth conditions and require different levels of husbandry. However, the fibres share some physical and material properties, which make them difficult to distinguish in the archaeological record. This thesis evaluates the effectiveness of methods for characterising bast fibres including; fibre chemical analysis, mechanical testing and fibre morphology, to propose that longitudinal microfibrillar angle (MFA) and cross-sectional circularity (Ct) used in a two-step procedure to analyse selected modern fibres of nettle (*Urtica dioica* L.*),* flax (*Linum usitatissimum* L.) and hemp (*Cannabis sativa* L.) could offer an alternative approach.

The reliability of MFA and Ct, as diagnostic features, was evaluated under a temperature accelerated degradation 48week trial with eight fibre types from three deposition soils Post deposition, surviving fibres were subjected to evaluation of changes in MFA and Ct. An additional check on the diagnostic efficacy was conducted within a blind-test protocol.

Finally, the research programme employs MFA and Ct in the diagnosis of a range of archaeological textile fibres from museum collections and fibres from the Kasr el Yahud mass burial. The thesis includes recommendations to address future post thesis research programmes.

Acknowledgements

I would like to express my appreciation and gratitude to my Supervisors, Dr Gillian Thompson and Dr Adrian Evans for their support, patience and encouragement in the research and preparation for this dissertation. My thanks also go to Dr Peter Twist, Faculty of Engineering and Informatics, University of Bradford for his guidance on plant fibre material properties and his introduction to the Biomomentum Mach-1^{TM} Mechanical testing equipment. In addition, I would like to thank Professor Howell Edwards, Research Department Molecular Spectroscopy, Faculty of Life Sciences, University of Bradford, for his assistance in formulating my introductory research into FT Raman Spectroscopy. The research work benefitted enormously from the support of Edna Barker, Chairperson, Bradford District Guild of Handweavers, Spinners, and Dyers, and her colleagues with their advice and practical expertise in support of the reconstruction process. I am equally indebted to Graham Berry, Technical Support Manager, Camira Fabrics Ltd of Mirfield for the supply of modern reference material and his invitation to review and compare modern production processes and to Nick Voase Managing Director, East Yorkshire Hemp for the supply of commercial flax and hemp fibre samples.

In particular, I would like to record my thanks to the Experimental and Technical Support Staff, Stuart Fox, Belinda Hill, School of Archaeological and Forensic Sciences University of Bradford, for their guidance and support in laboratory sampling and imaging techniques. A considerable level of research time was expended on plant fibre material properties and I am grateful for access to the testing equipment and for the encouragement and training provided by Engineering Technical Support Staff, Glen Thompson and Dimitrios Vgenopoulos

Faculty of Engineering and Informatics, University of Bradford. The research benefitted from access to various museum collections and I am indebted to Gerard McGowan, Museum Archivist, Curator of Natural Sciences, Bradford Museum and Galleries, Cliffe Castle Museum, Keighley, Uthra Rajgopal, Assistant Curator, (Textiles and Wallpaper), University of Manchester, Whitworth Art Gallery and Elinor Camille-Wood, Curator, Calderdale Museums Service Bankfield Museum Halifax.

Dedication

Dedicated to the memory of Maureen Elizabeth Waudby 1942-2011 for her wisdom, encouragement and belief in my pursuit of a lifelong ambition.

TABLE OF CONTENTS

Abstract ..... **i**

Acknowledgements ..... **ii**

Dedication ..... **iii**

LIST OF FIGURES ..... **xii**

LIST OF TABLES ..... **xxvi**

Chapter One **1**

Introduction and initial considerations **1**

1. 0 Introduction 1

1.1 Background progress in fibre identification 1 2

1.1.1 Ceramic material provenance 3

1.1.2 Lithic provenance 3

1.1.3 Metal isotope provenance 4

1.2 Resume plant fibre diagnosis 4

1.3. General project aims 6

1.4 Technological horizons 7

1.5 Bast fibre usage 8

1.6 Research Programme Hypothesis 9

1.6 1 Research Aims and objectives. 9

1.7. Research Project construction 10

1.8 Thesis assemblage -individual chapter outlines 11

Chapter Two **14**

Background – Plant Fibre Structure, Cultivation **14**

and Cultural History **14**

2.0 Introduction 14

2.1 Plant fibre utilisation 15

2.2 Basic fibre plant structure 16

2.3 Area cross section-SEM imaging - nettle (*Urtica dioica)*, flax (*Linum usitatissimum)* and hemp (*Cannabis sativa)* 21

2.4 Area cross section-SEM imaging tree bast fibre 23

2.5 Vascular bundle- definition of a “fibre” 25

2.6 Plant fibre stem sectioning 26

2.6.1 SEM imaging plant fibre area cross-sections 29

2.7 Plant fibre cultivation 30

2.8 Ethnographic reports 32

2.9 Plant taxonomy 33
2.9.1 Flax. (*Linum usitatissimum* L.) Family Linaceae, Genus *Linum,* Species *Usitatissimum* 33
2.9.2 Nettle (*Urtica dioica* L.) Family Urticaceae*,* Genus *Urtica,* Species *Dioica.* 34
2.9.3 Hemp (*Cannabis sativa* L.) Family Cannabaceae, Genus *Cannabis,* Species *Sativa* 35
2.10 Plant fibre sources-Progression of flax and hemp cultivation 36
2.10.1 Nettle (Urticaceae) 36
2.10.2 Flax (Linaceae) 38
2.10.3 Hemp *(*Cannabaceae) 42
2.11 Summary -plant fibre cultivation and history 44

Chapter Three 46

Appraisal of Textile Fibre Assemblage, ... 46

Research Design Parameters: -Aims and Objectives 46
3.0 Interpretive dilemma 46
3.1 Commonality of Chronology 48
3.2 Review of archaeological assemblages in Central Europe 50
3.3 Archaeological assemblages 56
3.3.1 Selection of archaeological assemblages 56
3.3.1.1Lascaux Cave-Dordogne France Palaeolithic 56
3.3 1.2 Ohalo II-Tiberias Israel Palaeolithic 57
3.3 1.3 Dzudzuana Cave-Caucasus-Eurasia Upper-Palaeolithic 57
3.3.1.4 Bouldnor Cliff-Solent England Mesolithic 57
3.3.1.5 Robenhausen-Wetzikon Switzerland EBA 58
3.3.1.6 Sweet Track-Somerset Levels England Neolithic 59
3.3.1.7 Ditfurt-Germany Late Neolithic 59
3.3.1.8 Latdorf-Germany Late Neolithic 59
3.3.1.9 East Switzerland Late Neolithic 59
3.3.1.10 Cueva Sagrada-Spain Early Bronze Age 60
3.3.1.11 Molina de Ledro-Italy Early Bronze Age 60
3.3.1.12 Vulci-Italy Early Bronze Age 60
3.3.1.13 Whitehorse Hill-Dartmoor England Early Bronze Age 61
3.3.1.14 Arslantepe-Malatya Turkey Bronze Age 61
3.3.1.17 Over-Barrow-Cambridgeshire England Bronze Age 62
3.3.1.18 Lusehøj Barrow-Voldtoft Denmark Late Bronze Age 63
3.3.1.19 Must Farm-Cambridge England Late Bronze Age 63
3.3.1.20 Valle delle-Paiole Italy Late Bronze Age 64
3.3.1.21 Casale Marittimo-Italy Early Iron Age 64
3.3.1.22 Civita Castellana-Italy Early Iron Age 64
3.3.1.23 Eberdingen-Hochdorf Germany Early Iron Age 64
3.3.1.25 Belish-Bulgaria Iron Age 65

3.3.1.26 Zagreb-Croatia Iron Age 65
3.3.1.27 Bučovice-Vyškov Moravia Late Iron Age 65
3.3.1.28 Seden Funen-Denmark Late Iron Age 66
3.3.1.29 Söderby-Sweden Late Iron Age 66
3.3.1.31 Moravia Museum (Site unknown)-Moravia Late Iron Age 66
3.3.1.32 Schrattenberg Mistelbach Austria Late Iron Age 67
3.3.1.33 Slavkov Vyškov-Moravia Late Iron Age 67
3.4 Summary: Diagnosis of plant fibre archaeological assemblages 68
3.5 Research design parameters 70

Chapter Four 72

***Chaîne opératoire* – fibre preparation archaeobotanical analysis and inferential diagnosis from textile tools 72**
4.0 Introduction 72
4.1 *Chaîne opératoire* Fibre preparation sequence 72
4.2 Process stages 73
4.3 Archaeobotanical considerations 74
4.4 Plant fibre seeds 75
4.5 Tree bast fibre 76
4.6 Plant fibre modern reference material 77
4.7 Plant fibre retting 81
4.8 Plant fibre inferential diagnosis-Reflections 84
4.9 Spinning: introduction 84
4.9.1 Spindle-whorl assemblages 85
4.9.2 Spindle-whorl performance 86
4.9.3 Analysis of fibre residue on spinning whorls 88
4.10 Loom weights 91
4.11 Textile production 93
4.12 Textile fragments recovered in association with loom weight assemblage from Quartier Mu V Malia Crete. 95
4.13 Summary 96

Chapter Five 97

Plant fibre diagnostic features-their efficacy, reliability and durability 97
5.0 Principal diagnostic features 97
5.1 Fibre chemical constituents 97
5.2 Chemical composition: plant fibre: acid detergent fibre (ADF) and neutral detergent fibre (NDF)) 98
5.3 Comments on NDF/ADF chemical analysis 102
5.4 Fourier Transfer Raman Spectrometry (FTRS) 103
5.5 Alternative spectra from Fourier Transfer Infrared Spectrometry (FTIRS) 105
5.5.1 Processing effects on FTIRS 107
5.6 Fibre Deoxyribonucleic acid (DNA) analysis 110

5.7 Potential of phytoliths to distinguishing between fibres from nettle, hemp and flax 112
5.7.1 Dicotyledon plant fibre phytolith 113
5.7.2 Phytolith shape 115
5.8 Method-phytolith extraction 116
5.8.1 Extraction method 116
5.9 Phytolith ImageJ analysis 118
5.10 Summary 121

Chapter Six 123

Plant fibre material properties-tensile strength and young's modulus 123
6.0 Introduction 123
6.1 Availability of fibre samples 123
6.2 Fibre preparation 125
6.3 Evaluation of breaking load for two-ply nettle fibre 126
6.4 Spun nettle fibre breaking load 127
6.5 Fibres in composite materials 129
6.6 Trial with Biomomentum mechanical testing equipment 134
6.6.1 Initial tensile test trial 134
6.6.2 Biomomentum Mach-1 trial test results 136
6.7 Young's moduli (*E*) for flax, nettle and hemp 136
6.8 Summary 142

Chapter Seven 145

Plant fibre morphology - microfibrillar angle (MFA) 145
7.0 Introduction 145
7.1 Plant fibre morphology - MFA Research 147
7.1.1 Plant fibre morphology; Hypothesis and Objectives 148
7.2 Fibre microfibrillar angle MFA 148
7.3 Fibre orientation S and Z angular twist 149
7.4 Fibre dislocation markings 152
7.4.1 Fibre dislocation observation 153
7.5 Fibre twist test rotation 154
7.6 Microscope observation of microfibrillar angle (MFA) under CPL with a 530nm wave compensator fitted inline (Red Plate Shift) 155
7.6.1 Red Plate test: archaeological investigations of textile fibres 156
7.6.2. Herzog Test Research outcomes 157
7.6.3 Herzog test limitations 159
7.7 Effect of MFA upon tensile test as illustrated by variation in elasticity slope 160
7.7.1 Trendline deviation as indicative of MFA 161
.7.2 Calculation of MFA based on trendline deviation 162

7.8 Optical microscope imagery of fibre longitudinal sections: cross-polarised light (CPL) 166
7.8.1 Method - MFA analysis by optical microscope under CPL 166
7.8.2 Results from MFA analysis – compound microscope with CPL 168
7.9 Summary 170
7.9.1 Fibre dislocation marks 170
7.9.2 Twist test 171
7.9.3 Red Plate- Herzog test colour change 171
7.9.4 MFA analysis by optical microscope under CPL 172

Chapter Eight 173

Fibre geometric morphology - Cross-sectional shape analysis 173
8.0 Introduction 173
8.1 Background 173
8.2 Determination of plant fibre cross-sectional area ratio: photographic images 174
8.3 Determination of plant fibre cross-sectional area ratio - SEM images 180
8.3.1 Method for preparation of fibre plant stems for SEM evaluation of fibre CSA cell morphology 180
8.3.2 SEM imaging of stems 182
8.3.3 ImageJ analysis of fibre diametrical dimensional ratio 183
8.4 Fibre CSA evaluation 185
8.4.1 Fibre cross-sectional sample preparation 185
8.4.3 Fibre CSA: sample preparation, casting and polishing 188
8.5. Determination of cross-sectional area circularity 192
8.5.1 ImageJ analysis of fibre circularity ratio 192
8.6 Summary 197

Chapter Nine 199

Combination diagnosis, microfibrillar angle (MFA) and circularity (Ct) ... 199
9.0 Introduction 199
9.1 Principal component analysis (PCA) 199
9.2 MFA/Ct Ratio analysis 199
9.3 Vector Analysis 200
9.4 Graphical relationship 202
9.5 Summary 203

Chapter Ten 204

Blind test - fibre MFA/CT appraisal 204
10.0 Introduction 204
10.1 Experimental archaeology 205
10.2 Experimental archaeological research programme 205

10.2.1 Radiocarbon C14 Dating 206
10.2.2 Fishbone identification 206
10.2.3 Faunal bone analysis 207
10.2.4 Lithic use-wear (MicrowearAnalysis) 207
10.3 Blind testing - Aims and objectives 210
10.4 Blind test protocol 211
10.4.1 Introduction 211
10.4.2 Method - sample size and source of fibres 213
10.4.3 Method - the selection of fibre samples 213
10.4.4 MFA sample preparation and procedure 214
10.4.5 Cross-sectional circularity (Ct) sample preparation and procedure 216
10.4.6 Statistical evaluation of MFA and Ct 218
10.4.7 Results 219
10.5 Summary 225

Chapter Eleven 227

Fibre degradation - accelerated ageing evaluation 228
11.0 Introduction 228
11.1. Background 228
11.2 The degradation process 229
11.3 General degradation procedure 232
11.4 Method 234
11.4.1 Soil types 236
11.4.2 Soil conditioning 236
11.4.3 Sample mounting 237
11.4.4 Soil containers 238
11.4.5 Burial temperature - accelerated ageing 239
11.4.6 Post-deposition treatment 241
11.4.7 Evaluation of fibre degradation 241
11.4.8 Fibre - degradation of physical properties 242
11.5 Fibre degradation - CSA geometric morphology (Shape analysis) 243
11.5.1 Fibre - mechanical deformation 244
11.5.2 Soil sample - particle size and relative humidity 245
11.5.3 Correction of water content 246
11.5.4 Soil acidity measurement 247
11.6 Results 249
11.6.1 12week degradation results 250
11.6.2 24week degradation results 251
11.6.3 36week degradation of submerged fibres results 252
11.6.4 40week degradation results 253
11.7 Considerations of survival of morphological features MFA and Ct. 254
11.7.1 Determination of degradation effects on the microfibrillar angle (MFA) of fibres 255

11.7.2 Measurement of MFA and Ct of surviving samples 261
11.7.3 Determination of degradation effects on the Circularity (Ct) of fibres 262
11.8 Biomomentum tensile test of degraded samples..... 267
11.9. Supplementary testing - a re-evaluation of 12week peat deposit 275
11 10 Summary- fibre degradation evaluation 277
11.10.1. Tensile properties of degraded fibres 277
11.10.2 Degradation- associated metallic assemblages..... 278
11.10.3 Degradation: MFA/Ct comparison..... 279

Chapter Twelve..... 280

Archaeological assemblages - Case Studies..... 280
12.0 Introduction - archaeological assemblages 280
12.1. Case Study 1 - Confirmation of diagnosis attributed to samples held at Temple Newsam (Leeds Museums and Galleries)..... 281
12.1.1 Introduction..... 281
12.1.2 Review of textile diagnostic features..... 281
12.1.3 The Roger Warner Textile Collection Temple Newsam (Leeds) UK282
12.1.4 The Warren collection catalogue 283
12.1.5 Artefacts selected for fibre identification. 284
12.1.6 Weave construction and description 285
12.1.7 Determination of microfibrillar angle and circularity for samples 286
12.1.8 Comments on Temple Newsam Warren Collection 293
12.2. Case Study 2 - Cliffe Castle Egyptian Coptic Collection 294
12.2.1 Principal sites excavated by Petrie 294
12.2.2 Tunic fibre construction Qumran (Jordan) 296
12.2.3 Tunic Design..... 296
12.2.4 Bankfield Museum - tunic tapestry and embordered features..... 298
12.2.5 Sample preparation and determination of MFA and Ct..... 300
12.2.6. Method for preparation of fibre mounting and analysis 300
12.2.7. Fibre diagnosis Cliffe Castle assemblages 302
12.2.8 Cliff Castle: discussion and resume..... 305
12.3 Case 3- Mass burial rescue excavation - Kasr-el-Yahud (Qasr-al-Yahud) Jordan 306
12.3.1. Geographic location Kasr-el-Yahud (31.84ºN- 35.54ºE) 307
12.3.2. Egyptian Tunic design, construction and decoration..... 309
12.3.3 Nature of fibre sample recovered from Kasr-el-Yahud..... 314
12.3.4 General assessment of the collection 316
12.3.5 Method- preparation of sections and imaging..... 318
12.3.6 Determination of microfibrillar angle (MFA) and circularity (Ct) for KY 12 fibre..... 319
12.3.7 Extension of MFA and Ct evaluation to random samples drawn from the Kasr-el-Yahud collection..... 322

12.3.8. Review of diagnosis of MFA and Ct for Kasr-el-Yahud collection .. 329
12.4 Summary and plot of archaeological assemblage diagnostic determinants 329
12.4.1 Review of Case Study 1: Temple Newsam 329
12.4.2 Review of Case Study 2: Cliff Castle 330
12.4.3 Review of Case Study 3 Kasr-el-Yahud 331
12.4.4. General MFA/Ct determinants from Case Studies compared with experimental results. 332

Chapter Thirteen 334

Discussions and conclusions 334
13.0 Introduction 334
13.1 Review of research programme results 335
13.1.2 Response to results achieved in the initial research phase 337
13.1.3 Plant fibre morphology - MFA/Ct analysis 338
13.1.4 Blind-test protocol 339
13.1.5 Accelerated degradation effects 340
13.1.6 Absence of evidence 340
13.1.7 Subjective Judgement 341
13.2 Potential for MFA and CT diagnosis in future research programmes 342
13.2.1 Plant fibre pseudomorphic presence 343
13.2.2 Textile tool plant fibre residue 344
13.2.3 The flaxseed oil/fibre, primary/secondary product dilemma 345
3.2.4 Tree bast fibre 346
13.3 Enhancement of MFA/Ct determinations and coextensive representations 347
13.3.1 Vector analysis, diagnosis of nodal dislocations spatial location 348
13.3.2 Fibre Ct determine by computer-based artificial 349
intelligence (AI) 349
13.4 Case study reviews 350
13.4 1 Case study 1: Temple Newsam furnishing fabrics 351
13.4 2 Case study 2: Cliffe Castle 351
13.4.3 Case Study 3 Kasr el Yahud 352
13.5 Conclusions 354

REFERENCES 355

INTERNET SITES ACCESSED 394

APPENDIX 396

LIST OF FIGURES

Figure 2.1. Illustration of stem with leaf and auxiliary shoot of *Linum usitatissimum* (Pandey 2012: 153). 17

Figure 2.2. Traverse cross-section through the radial axis of *Linum usitatissimum*; the location of the primary phloem fibres (sclerenchyma) is shown (x320). (Evert et al. 2009: 179, Fig. 8.4.with additions). 18

Figure 2.3. A schematic image of the support system for dicotyledons with positions and descriptions of sections indicated. The bottom right cross-sectional image details the fibres held in the phloem (Cutler et al. 2008: 5 Fig. 1.2). 19

Figure 2.4 A-C. SEM images of traverse sections of plant fibre stems prepared by hand sectioning. The images are presented for comparison with the descriptions provided by the authors and listed in Figure 2.7. 22

Figure 2.5. Lime Bast (*Tilia americana* L.), primary phloem fibres from the shoot axis. A. Cross-section B. Longitudinal section. The longitudinal view (B) shows only a section of the total length of the fibres (A x620; B x375) (Evert 2009: 176, Fig.8.10). C. (*Tilla vulgaris*), bark and xylem traverse section (x60). Note blocks of fibre alternating with conducting tissue (Gale and Cutler 2000: 257, Fig.1) D. Sketch of traverse section of (*Tilia* sp.) stem with fibres in the primary and secondary phloem and the secondary xylem (Pandey 2012: 365, Fig.16.4). 24

Figure 2.6 Illustration of variation in flax fibre dimensions and description (Bos and Donald 1999: 3030 with additions) 25

Figure 2.7.A comparison of fibre cross-sectional area taken from the SEM images included in Figure 2.4 for comparison with images and descriptions taken from other sources (Gale and Cutler 2000, Rast-Eicher. 2016). 28

Figure 2.8. Consideration of social organisation strategies supporting wild and cultivated plant processing. Adapted from (Harris 1989: 11-26). 31

Figure 2.9. Distribution of the *Urtica dioica* group in Europe. The map includes *U. dioica, U. galeopsifolia, U.pubescens* and *U. sondenii.* (Taylor 2009: 1437, Fig.2 with additions*)* Growth intensity indicated by the black dots. 35

Figure 2.10. German WW1 Poster Sammelt Brennessell wenn ihr kleidung und Faden wollt. Auskunft Bayer Nesselstelle Munchen (Trans.) Collect nettle if you want clothing and thread. Information from Bavaria Nettle München Fürstenstr. 37

Figure 2.11. Presence of wild and domestic flax seeds/capsules and textiles impressions in aceramic and early Neolithic sites (Karg 2011: 506-508 and Fig.1 with additions.). (The map is credited to Sue Colledge (UCL, UK) and James Conolly (Trent University, Canada). 41

Figure 2.12. Distribution of archaeological finds of wild flax in Europe: (Linum usitatissimum L.) subspecies (*Linum bienne* L.) in the PPN Neolithic (Weiss and Zohary 2011: Fig. 8). 41

Figure 2.13. Illustration that proposes the introduction of flax to the UK at (4000 BC) and the presence of wild and domestic flax seeds /capsules and textile impressions to early European Neolithic sites. (Karg 2011: 508; Harris 2014: 9 and Fig. 1. with additions). 42

Figure 2.14. Dispersal of *Cannabis* and its uses, in Europe and North Africa. The map is based mostly on historical evidence (Cartography by M. Barbee). (Clark and Merlin 2013: 101(Map 7) with additions). Note the date for the dispersal of hemp into the UK at 100AD. Nomenclature. NLH Narrow leafed hemp (*Cannabis sativa*) ssp s*ativa* Europe. BLH Broad leaf hemp (*Cannabis indica*) ssp *chinensis* China, Korea Japan and South East Asia. NLD Narrow leaf hemp (*Cannabis indica)* ssp *indica* South and South East Asia. 44

Figure 3.1. Plot of locations of sites listed and numbered in Table 3.4 numbered in chronologoical order. 53

Figure 3.2. Lascaux Cave fragment (Glory1959: 135-169 (no scale)).This 30cm length of cord, dated to the Palaeolithic (15,000 BC) was discovered by Abbé Glory in 1953. 56

Figure 3.3. String fragment, Bouldnor Cliff (Peeters and Momber 2014). 57

Figure 3.4. Twinned material from waterlogged site at Robenhausen (Higgitt et al. 2011: 86 Fig.3b, Fig.6). 58

Figure 3.5. Early Bronze Age folded textile (Alfaro 2019: 338). 60

Figure 3.6. Early Bronze Age cremation assemblage Whitehorse Hill (Harris 2016: 49-51; Williams 2016: 25-32, Fig. 3.23). 61

Figure 3.7. Bronze Age Fibre fragments from Over-Barrow (Harris 2015: 73-81, Fig 6.3). 62

Figue 3.8. Lusehøj Barrow Late Bronze Age fibres (Hald 1980: 126, Fig 117; Bergfjord et al. 2012: Fig 1A). 63

Figure 3.9. Textile fragments from the Eberdingen-Hochdorf Princely Burial (Banck-Burgess 2019: 143, 146, Fig. 5.10). 64

Figure 3.10 Late Iron Age bronze arm ring Image, (A) Hollow armband, (B) fabric (Bender-Jørgensen 2005:143(85) (no scale)). (C-D) REM images of the fibres (Grömer et al. 2019: 18). 67

Figure 3.11. The plot represents consideration of the fluctuation in the frequency of utilisation of the three principal fibres as determined in the analysis of 12,061 specimens recovered from a 1980 excavation at Qasr Ibrim in Egyptian Nubia (Adams 2007: 203, Fig.33.2 with additions). 69

Figure 4.1. Test-bed planting University of Bradford. Left bed. Seeded nettle and transplanted nettle rhizomes. Right bed. Flax (v. Marilyn) a textile variety. Below. Left, nettle flowering stage at harvesting, centre flax flowering stage at harvesting, right flax capsule enlargement at maturity..... 78

Figure 4.2.SEM cross sections of hemp, flax, and nettle. The images illustrate the stem anatomy with the following tissues identified, Ep (epidermis), C (cortex), Bf (bast fibre). Images produced on SEM (ETD High Vacuum) at 20kV, Flax 250X, Hemp and Nettle 500X. 81

Figure 5.1. Principle of ADF/NDF detergent partitioning of the fibre fraction “Van Soest Methodology” Image from Ghent University (2016) with additions)..... 99

Figure 5.2. Plant fibre comparison of mean and standard variation in cellulose content. Analysis of variance (ANOVA) in cellulose content based on the analysis of 80 samples. Nettle (n=28), flax (n=34) and Hemp (n=18) found there to be some significant variation between the grouped samples F= 5.21577, df=81, p=0.00751. The graph shows some difference between Nettle and Hemp (T=2.7581, df=44, p=0.00422) and some difference between Flax and Hemp (T=3.0888, df=50, p= 0.00164). However, there was no significant difference between Nettle and Flax. (Note. Outliers have been excluded from this ANOVA comparison) 100

Figure 5.3 Perkins Elmer Spectrum 100 FTIR-ATR. 107

Figure 5.4 Flax FTIR spectra. Intensities (*I)* identified. Intensity ratios $R'(I^{1121/1096})$ 0.019/0.0275 = 0.69 $R=(I^{1096/2900})$ 0.0275/0.005= 5.5..... 108

Figure 5.5 Nettle FTIR spectra. Intensities (*I)* identified. Intensity ratios $R'(I^{1121/1096})$ 0.048/0.083 = 0.58, $R=(I^{1096/2900})$ 0.083/0.048= 1.73 109

Figure 5.6 Hemp FTIR spectra. Intensities (*I)* identified. Intensity ratios $R'(I^{1121/1096})$ 0.062/0.085= 0.73 $R=(I^{1096/2900})$ 0.085/0.022= 3.90..... 109

Figure 5.7 Micrographs of ropes. Ropes made from A) abaca leaves; B) flax stems; C) hemp stems; D) jute stems; E) hemp stems (sample sold as jute);

F) sisal leaves. All types of ropes, whether made from stems or leaves, had both fibres and parenchyma cells present. (Scale bars = 50μm.) (Dunbar and Murphy (2009: 110). 112

Figure 5.8 Image of triangular silica cystolith with fine verrucate sculpting format formed in *Urtica dioica*. The bar is 40μm (Bozarth 1992: 209 Fig. 10.7A)..... 114

Figure 5.9 Phytolith image in association with nettle fibre (Bergfjord and Holst 2010: 1195,Fig.4) (Note. MFA visible at fibre centre circa -7º)..... 114

Figure 5.10 Phytolith presence in nettle leaf ash. CPL image evaluated by "ImageJ" particle analysis. a) SEM, CPL image 400x nettle leaf ash for cystolith identification. b) image transformed under ImageJ (336 particles at 82μm^2 ave.area). c) analysis limited to large particles > 900μm^2 ave. area. d) small particle image analysis 21 at 26 μm^2. 119

Figure 5.11 SEM/EDS Analysis of calcium oxalate (CaC_2O_4) cystolith crystals in nettle fibre. Au is present from the gold coating of the sample (Bergfjord and Holst 2010: 1196, Fig.7) 119

Figure 5.12 A phytolith crystal was identified at the top of non-segmented nettle leaf hair. (Spectrum 3) considered to be calcium oxalate. Scale 30μm. Phytolith chemical constituents are listed on the left. 120

Figure 5.13 The ashed nettle leaf assemblage (Figure 5.12 above) was subjected to EDS analysis to propose that the cystolith could be calcium oxalate (CaC2O4) crystal 120

Figure 6.1. Wooden comb and modern equivalent. a) La Draga, Neolithic boxwood comb (Bosch et al. 2006: 93), b) Vindonissa (A.D.1) wooden comb (Wild 1970: 154), c) Modern equivalent used by the Author in the preparation process (Waudby 2014). 125

Figure 6.2 5564 Mechanical stress/strain testing equipment (Instron High Wycombe UK 2016) 126

Figure 6.3 Results of tensile strength test for seven retted Stinging Nettle fibre. Loading measured on Instron 5564 electro-mechanical load frame. Testing equipment (ASTM C1557 2014; Instron2017). Note. For equal Young's moduli values, lines AA and BB on the graph would be parallel. 127

Figure 6.4. The variation in tensile strength for the seven two-ply samples described above were subjected to analysis of variance in Young's modulus of elasticity E. ANOVA analysis shows limited significance between the groups (F=0.796, df=32, p=0.528)..... 128

Figure 6.5 Biomomentum Mach-1^{TM} Mechanical testing equipment. This multiple-axis tester developed originally for cartilage testing, is now being used in various configurations for the evaluation of the mechanical properties of tissue and soft material (Biomomentum 2016). 134

Figure 6.6 (a) Stiffness/extension trendline for flax. The trendline depicts the elasticity slope for evaluation of Young's modulus (*E)* 135

Figure 6.6 (b) Stiffness/extension trendline for nettle. The trendline depicts the elasticity slope for evaluation of Young's modulus *E* 135

Figure 6.7(a) Stress/Strain curve generated from the tensile test of flax sample E-B4. The curve displays three distinct sections, "A" The initial zero extension as the applied load is absorbed by the mounting frame and clamp realignment, "B" the initial deviation from a straight-line elasticity relationship as influenced by the microfibrillar angle (Charlet et al. 2009) and "C" the straight-line representation of the elasticity range *E.* 137

Figure 6.7 (b). The maximum stiffness of the 6mm sampling length subject to the applied load FzN is displayed along with the stress/strain relationship illustrated by the "y" value in the least-osquare straight-line calculation 139

Figure 6.8 A plot of variations in E for the three species. The representation has been simplified by eliminating all outliers for *E* values above 1000 141

Figure 7.1. The two flax seed types from Late Neolithic wetland sites. a) large-seeded ''Pfyn-type'' flax from Litzelstetten-Krahenhorn I (4000–3800 cal. B.C.). b) small-seeded ''Horgen-type'' flax from Alleshausen–Grundwiesen (ca. 2900 cal. B.C.). Scale 1 mm (Herbig and Maier 2011: 531). c) Hemp seed (v Santhica) (Bouayoun et al. 2018). 146

Figure 7.2. Nettle and flax seeds: flax seeds bottom left, length 4mm, nettle seeds top right length 0.25mm. 146

Figure 7.3. Illustration of nettle flax and hemp. General plant structure leaf, flower, and seed capsules depicted (Thomé 1885: npn). 147

Figure 7.4. Composition and structure of flax fibre (Bos and Donald 1999: 3030 with additions). 149

Figure 7.5 Illustration of plant fibre structure. Primary outer layer P and the Secondary layers S1, S2, and S3. The thickest section, S2, carries the micro-fibre in either S or Z orientation. (Based on Bourmaud et al. 2013: 344). 150

Figure 7.6 S anticlockwise and Z clockwise MFA orientation 151

Figure 7.7. Images viewed under cross-polarised light showing nodal deformation. Left. Flax cross banding. Middle. Nettle showing straight..... 152

Figure 7.8 (A). Flax 25µm flax fibre under CPL and 56nm Red Plate: MFA - 7º: Top left, fibre at extinction. Top right, fibre displaying MFA. Bottom left, fibre at 90º under 56nm Red plate. Bottom right, fibre at 180º under 56nm Red plate..... 158

Figure 7.8 (B). Nettle 10µm nettle fibre under CPL and 56nm Red Plate: MFA -6º. Top left, fibre at extinction. Top right, fibre displaying MFA. Bottom left, fibre at 90º under 56nm Red plate. Bottom right, fibre at 180º under 56nm Red plate. 158

Figure 7.8 (C). Hemp fibre under CPL and 56nm Red Plate: MFA 5º. Top left, fibre at extinction. Top right, fibre displaying MFA 5º. Bottom left, fibre at 90º under 56nm Red plate (vague red). Bottom right, fibre at 180º under 56nm Red plate (vague blue). 159

Figure 7.9. The curve presents the calculated values for MFA based on the assessment of the initial deviation of the tensile test curve from the straight-line elasticity range. Calculated from Formula 1 (Charlet 2009: 235). 163

Figure 7.10. Comparison of recorded Biomomentum tensile test. Top. Graphic representation based on tensile test data. Bottom. Adjustment to recorded data to depict “elasticity region” and deviation (See Chapter 6) the deviations at maximum levels shown in the bottom plots are those proposed as indicative of MFA Table 7.2. 165

Figure 7.11. Illustration of error in measuring MFA by incorrect microscope focusing. In the image on the left, the high transparency allows both sides to be viewed, and the necessity to observe close focusing demonstrated. 167

Figure 7.12. MFA images. MFA determined with microscopic viewing under CPL. Measured by stage rotation angular variation and confirmed with AnalySIS software. Nettle -6º, flax -10º. Hemp 5º. 167

Figure 8.1 Nettle plant fibre CSA images. Selected cells identified for measurement of the ratio of fibre overall diameter to lumina diameter (Ryder and Gaber-Saunders 1987) (with additions)..... 175

Figure 8.2 Çatalhöyük. Flax plant fibre cell images Selected cells identified for measurement of overall fibre diameter to lumina diameter ratio (Ryder and Gabra-Sanders 1987) (with additions)..... 175

Figure 8.3 Transverse sections of hemp fibres. These fibres are thicker than the nettle and flax fibres and have narrower lumina. As the hemp lumen are

narrower and indistinct, this image was not used in the subsequent analysis of lumen/cell diameter ratios. (Ryder and Gabra-Sanders 1987). 176

Figure 8.4 Nettle plant fibre comparative cell diameter dimensional ratios. Lumina diameter/ overall diameter. Data from Table 8.1 below (Waudby 2014: 29-30). 176

Figure 8.5 Flax plant fibre comparative cell diameter dimensions. Lumina diameter/ overall diameter. Table 8.2 below 177

Figure 8.6 SEM images of microtomed cross-sections of plant fibre stems. a) SEM image of nettle fibre 1000X, b) SEM image of flax fibre 500X 179

Figure 8.7. Cross-sections of hemp, flax and nettle. The images illustrate the plant anatomy with the following tissues identified. Ep (epidermis), C (cortex) and Bf (bast fibre). Images produced on SEM (EDT High Vacuum). 182

Figure 8.8. (Right)Selected fibres numbered.Scale in µm 184

Figure 8.9 Section of multi-stage assemblage for 6mm diameter mountants. The plastic mould was a 6mm diameter drinking straw, the different colours for the straws were the principal labelling used with green=nettle, yellow=flax and red=hemp. 189

Figure 8.10 Grinding and polishing 6mm sample.Top left. Metaserv Hand Grinder 1200,600,450 and 320 grade emery paper with water flush. Top right. Mataserv Universal Polisher with diamond suspension polishing fluid. Yellow 6µm, blue 1 µm. Bottom Centre. 13mm drill chuck inclusion shows detail of mounted circular levelling bubble to ensure correct presentation to polisher to achieve a level surface 190

Figure 8.11 Method of sectioning fibre samples into 2 mm thick cross-sections. The image shows how repeated sections can be ground, polished and sectioned to achieve the quality of fibre CSA required. 191

Figure 8.12 Buehler Isomet Low-Speed Rotary Microtome. Used for the cutting of 1-2mm thick sections from the 6mm diameter epoxy resin mould. The cutting wheel used was a 5ins. diameter diamond wafering blade. 191

Figure 8.13 Microfibre cross-sectional Ct imaged with Nikon Optiphot under transmitted cross-polarised lighting (CPL). Typical CSA images analysed with ImageJ software to evaluate circularity, a non-dimensional ratio of CSA. Left. Nettle, (n=15), mean Ct 0.53, St. Dev. 0.109, SE. 0.028. Centre. Flax, (n=14), mean Ct 0.76, St. Dev. 0.05, SE. 0.13. Right. Hemp, (n=21), mean Ct 0.80, St. Dev. 0.06, SE. 0.013. 193

Note There was a variation in the number of microfibres contained within each “theoretical fibre” this variation reduces the number of microfibre samples available for measurement within the total assemblage. 193

Figure 8.14 Flax W6 area cross-sectional Ct. Data assembled from ImageJ analysis of microfibrillar CSA. 194

Figure 9.1. Vector diagram: based on the fibre mean values of MFA and (Ctx10) 201

Figure 9.2. A plot of mean MFA v Mean Ct values: as determined for the three modern natural fibres flax, nettle and hemp. The enclosing circles define the 99% (3 St Errors) confidence range for each fibre type. 202

Figure 10.3. Box and whisker comparison of MFA for the three fibre species. (Previously noted reported Figure 7.15). 215

Figure 10.4. Examples of Nettle and Flax fibres differences in cross-sectional appearance and Ct measurement. Scale bar is 25µm. 216

Figure 10.5. Database established for CSA Circularity (See Figure 8.14) The multi-fibre CSA images were evaluated using ImageJ software (Rasband 2016). 217

Figure 11.1. Laboratory temperature and relative humidity over the duration of the degradation test. 235

Figure 11.2. Carrier mounting and labelling of fibre samples. Numbered fibre samples mounted into slots cut into the acetate sheet carrier (no adhesive used). 237

Figure 11.3. Degradation acceleration. Equivalent deposition rate factor for accelerated temperatures based on calculated temperature rate factors. (Acceleration factor 50kj/mol). 240

Figure 11.4. Biomomentum Mach-1TM Mechanical testing equipment. With camera mounting showing clamping arrangement. Card mounting details are shown right. 243

Figure 11.5. Images under cross-polarised light showing nodal deformation. Left. Flax 30µm dia. (400x) cross banding. Right. Nettle 90µm dia. (200x), showing straight striations (Waudby 2014, 60). 245

Figure 11.6. Jenway 3510 pH meter. Soil pH level measurement. 247

Figure 11.7. Percentage of fibre survivals over time. The peak for peat at 2.2yr results from the underwater submergence of the samples. 254

Figure 11.8. MFA. All surviving fibres were analysed, and MFA measured for the enclosed angle of microfibre using AnalySIS software. The “S” twist of both nettle and flax fibres at -9.35º and -6.30º are visible, the “Z”twist of the hemp fibre at 2.80º is also partially evident. 255

Figure 11.9. MFA of Control fibres. Individual fibre MFA measurements are shown above each fibre type. (For simplicity of display, the +/- angular orientation has been excluded from this representation 257

Figure 11.10. Comparison of MFA for surviving fibres against the Control fibre. The MFA for surviving fibres from each deposition soil and period are illustrated above the equivalent fibre species. The data labels depict the full range of samples deposited from 1) Control (blue) to (6) 40week in dry sand (green). The gaps show no result for degraded fibres. (For simplicity of display the +/- orientation has been excluded from this representation). 257

Figure 11.11a. MFA images for deposited fibres in each environment and different periods. Microfibrillar angled determined by rotational measurement and AnalySIS Software. (Black squares show non-survivors; blank squares show fibres failing MFA). 259

Figure 11.11b. MFA images for deposited fibres in each environment and for different periods. Microfibrillar angles determined by rotational measurement and AnalySIS Software. (The question marks denote uncertain diagnosis. Black squares show non-survivors; blank squares show fibres failing MFA presentation). 260

Figure 11.12. Comparison of the mean and standard deviation of fibre for MFA measurements for all surviving fibres (Control fibres excluded). 261

Figure 11.13. MFA of original non-degraded modern reference material (see Chapter 9). 262

Figure 11.14. Comparison of the mean and standard deviation of fibre circularity for 108 fibres deposited in dry sand. 263

Figure 11.15. Plant fibre comparison of the mean and standard deviation of fibre circularity for 66 fibres deposited in peat. 264

Figure 11.16. Fibres surviving 24week deposition: a selection of six CSA from each image was selected for measurement of Ct with ImageJ software. 266

Figure 11.17a. Illustration of stress/strain database from Biomomentum test for NWC1. 267

Figure 11.17b. Illustration of stress/strain database from Biomomentum test for NU3. Fibre, nettle from the University testbed, was held in Assemblage No 3. The trendline is added to determine the straight-line relationship, “Stiffness (Fz/N)”, used to calculate Young’s Modulus (*E*). (For determination of “*E*” data points preceding and following the straight-line elastic region have been removed). 268

Figure 11.18. Representation of “*E*” values for dry sand deposition. Values calculated for a range of fibres deposited in dry sand for 12, 24 and 40 weeks taken from Table 11.15. (The decrease in modulus reflects the degraded tensile strength)..... 273

Figure 11.19. Representation of “*E*” values for peat deposition. Values calculated for a range of fibres deposited in peat for 24weeks and 36weeks submerged. (The decrease in modulus reflects the degraded tensile strength). 273

Figure 11.20. Plot of recorded oven temperature: variation for 12week period of supplementary degradation trial for set-point at 40º. 276

Figure 12.1.1. RW 337. A 19th. Century seat cover (Ginsberg Catalogue No. 154). Late 19th-century cotton and bast furnishing of Brocatelle weave. 46.3 x 57.1 cm. Cotton warp ends 12/cm Z twist (average dia. 0.64mm). Bast fibre weft picks 28/cm 2ply Z twist (average dia.0.8mm). 284

Figure 12.1.2. RW 338. A late 19th- century furnishing (Ginsberg Catalogue No. 176). Late 19h century of Damask weave 57 x 90 cm acquired from S.W. Wolsey Ltd. London. 285

Figure 12.1.3. MFA and Ct RW 337 Cotton warp fibre imaging. Images of the cotton fibre under CPL multi-colour changes along fibre length are identified as cotton (Bouchard and Tengberg 2011: Fig.3; Petraco and Kubic 2004: 104). 287

Figure 12.1.4. RW 337 Images of chair seat cover cotton and bast construct. A) Front view of chair cover showing white cotton fibre weft 8/cm, 2ply Z twist (20º) average fibre diameter 0.8mm. B) Reversed side of chair seat cover showing purple bast fibre warp 18/cm, 2ply S twist (-30º) average fibre diameter 0.6mm. (The 1cm square aids the thread count). 287

Figure 12.1.5. RW337. Area cross-section for bast fibre sample. Individual fibre CSA’s identified for ImageJ analysis of circularity. 288

Figure 12.1.6. RW 337 Bast weft fibre imaging. A) Fibre rotated under CPL to attain extinction. B) Image under CPL with 56nm Red Plate inserted MFA illustrated at -6º. C) Image viewed under 56nm Red Plate at 90º, image

colour a vague red. D) Image rotated to 180º, some green/blue colour change noted 289

Figure 12.1.7. RW 338 Images of wool and bast furnishing. A) Front view showing bast fibre warp 6/cm Z twist (10º), average fibre diameter 0.5mm. B) Reversed side with wool weft fibre10/cm 2ply S twist(-20º) twist average fibre diameter 0.8mm. (The 1cm square aids the thread count). 290

Figure 12.1.8. RW388 Wool (A) and bast fibre (B) identity: fibre Ct determined with ImageJ Table 12.1.2. 290

Figure 12.1.9. RW 338 Wool and bast weft fibre imaging. A) Fibre rotated under CPL to attain extinction. B) Image under CPL with 56nm Red Plate inserted MFA illustrated at -6º. C) Image with 56nm Red Plate at 90º, poor quality image vague red. D) Image rotated to 180º, a poor-quality image with some green/blue colour change noted. 291

Figure 12.1.10. This a section from RW 338 of fibre imaging under CPL that shows three different fibres in the same location. A) bast fibre B) cotton fibr.e and C) a fibre that responds to Red Plate shift. (See comments in 12.1.8 below)..... 293

Figure 12.2.1. Illustrations of tunic tapestry and embroidery decorations A. Hemline embroidered geometric border and cross (indicated on image); the cross has been interpreted as a Christian symbol. Fragment size 50x30cm. B. Part of a clavus with a small 6.5cm diameter medallion. C. A range of flower shapes woven into a light-coloured tunic. D. Maenads (dancing figures) with flower surround woven into the clavus. Images courtesy of Bankfield Library and Museum Halifax UK 299

Figure 12.2.2. Tunic 40cm diameter central medallion: geometric embroidery design. Courtesy of Bankfield Museum Halifax. 300

Figure 12.2.3. The revised design of mounting for degraded 5mm length archaeological fibre circa 25µm diameter. The design included an opening in the upper surface of the 9mm diameter plastic forma with wooden sealing blocks secured at each end. 301

Figure 12.2.4. Details of MFA and Ct measurements. Sample No CC9 from Cliffe Castle Coptic fibre (DMU 95/071.1-13). Courtesy of Cliffe Castle Museum Keighley UK 302

Figure 12.2.5. Details of Herzog Red Plate Test for MFA. Sample No 9 from Cliffe Castle Coptic fibre (DMU 95/071.1-13). Courtesy of Cliffe Castle Museum Keighley UK. 303

Figure 12.2.6. MFA and Ct determination for sample CC1. Left. Inadequate quality image for MFA analysis. Right. CSA with fibres numbered, Ct visible but outline obscure. 304

Figure 12.2.7. Herzog Test. Sample CC1 imaged but not a clear indication of Red Plate shift. 304

Figure 12.3.1. The vicinity of Qasr el-Yahud. (Dina Shalem 2019, Ostracon, Israel Nature and Parks Authority). 307

Figure 12.3.2. Diagrams of ornamented tunics (M. Houston, Ancient Greek, Roman and Byzantine Costume and Decoration. London 1931: Fig.131-134). Dimensions in inches 310

Figure12.3.3. Diagram of wide-sleeved linen tunic T.1995.145. (Pritchard 2004: 53) Photographs courtesy of Whitworth Museum Manchester 311

Figure 12.3.4. ‘Leukyon´e’; A. Gayet, Fantˆomes d’Antino´e (Paris 1904) (Thomas 2007: 139). 312

Figure 12.3.5. Details of Coptic child’s tunic design. Whitworth Museum ID T 1993.27. Childs linen tunic (585 mm height) with simple neck and sleeve bands the tunic has side gores inserted to fit larger sizes. (Pritchard 2004: 110) Photograph courtesy of Whitworth Museum Manchester. 313

Figure 12.3.6. Detail of sleeve band design Whitworth Museum ID T 8397. Sleeve bands from a linen tunic. The tongues of the hare and lion and the duck’s beaks and feet are highlighted with red wool. (Pritchard 2004: 62). Whitworth Museum ID T 1993.27. 313

Photograph courtesy of Whitworth Museum Manchester. 313

Figure 12.3.7. Detail of wide-sleeved tunic design Whitworth Museum ID T 1995.145. Wide-sleeved linen tunic (1.19m height) showing short clavi with terminals, shoulder medallions (260mm diameter) with smaller medallion repeats at the knee, and hem and sleeve bands. The sleeves are 565mm wide. (Pritchard 2004, 110) Photograph courtesy of Whitworth Museum Manchester. 314

Figure 12.3.8. Kasr-el-Yahud textile assemblage: typical comingled assortment of textile fibre recovered 315

..... 316

Figure 12.3.9. Illustrations of textile colour range that may be related to fibre type. 316

Figure 12.3.10. Sample KY7 Rear of tunic: rolled neck seam evident on the right(a) and rolled side seam top-left (b). Size 38 x 23cm. 317

Figure 12.3.11. KY2 Large textile fragment: evidence of rolled side seam at bottom left at “A”. Size 24x21 cm. 317

Figure 12.3.12. Detail of dark banding woven into tunic fabric: banding shown on both left and right edges..... 318

Figure 12.3.13. KY 12 Circularity of fibre samples. ImageJ analysis of fibres in cross-sectional area of K12. 320

Figure 12.3.14. KY12 fibre 12µm diameter rotated from extinction at 90º. With Red Plate (56nm) introduced, the colour change is evident from red at 90º to blue at 180, a flax fibre..... 320

Figure 12.3.15. KY 12 Determination of MFA Transmitted light under CPL with 56nm Red Plate inserted. The angle of microfibrillar at -7ºcan be seen to the right of the sloping line. 321

Figure 12.3.16. KY 11 Left. Fragment of textile basic tabby weave 9/9 threads per. cm. Right. 13µm thread under 56nm Red Plate, no extinctions are shown and there was no attendant colour change. A degraded cotton fibre, no CSA imagining was possible. Scale 25mm. 322

Figure 12.3.17. KY 26. Fragment of textile basic tabby weave 16/16 threads per cm. Seam present along the centre. Right. 8µm thread under 56nm Red Plate, no extinction shown and no attendant colour change. A degraded cotton fibre, no CSA imagining was possible. Scale 25mm..... 323

Figure 12.3.18. KY 36. Left. Fragment of textile basic tabby weave 9/9 threads per.cm. Right. 22µm thread under 56nm Red Plate, no extinction shown and no attendant colour change. A degraded cotton fibre, no CSA imagining was possible. Scale 25mm..... 323

Figure 12.3.19. KY 3 Left. Fragment of textile basic tabby weave 16/16 threads per cm. Repaired section visible centre bottom and horizontal seam visible near the top. Top Right. 15µm thread under 56nm Red Plate. Top Right Red at 90º. Bottom Right. Blue showed at 180º. A flax fibre. Unfortunately, the CSA image was of poor quality and unsuitable for ImageJ analysis. There was no visible MFA included within the imaging Scale 25mm. 324

Figure 12.3.20. KY 8. Top Left Fragment of textile basic tabby weave 16/16 threads per cm. Bottom Left. 10µm thread under 56nm Red Plate, red at 90º. Bottom centre, blue shown at 180º, a flax fibre. Bottom Right, MFA (-10º)

measurable here with microfibrillar visible top right of the image. Top Right cross-sectional image suitable for measurement of Ct with ImageJ Table 12.3.1. Scale 25mm. 325

Figure 12.3.21. KY 22 Top Left. Fragment of textile basic tabby weave 12/12 threads per.cm. Bottom Left. 13µm thread under 56nm Red Plate, red at 90º. Bottom Centre, blue shown at 180º, a flax fibre. Bottom Right. MFA no microfibrillar visible. Top Right cross-sectional image suitable for measurement of Ct with ImageJ Table 12.3.2. Scale 25mm. 326

Figure 12.3.22. KY 31. Top Left. Fragment of textile basic tabby weave 12/12 threads per cm. Bottom left. 13µm thread under 56nm Red Plate, red at 90º. Bottom Centre, green shown at 180º, possibly a flax fibre. Bottom Right, MFA microfibrillar visible at 10.5º. Top Right cross-sectional image unsuitable for measurement of Ct with ImageJ Scale 25mm. 327

Figure 12.3.23. KY 41. Top Left. Fragment of textile basic tabby weave 14/12 threads per cm, with rolled seam evident on the right. Bottom Left. 18µm (average diameter of three threads), under 56nm Red Plate, red at 90º. Bottom Centre, blue shown at 180º, a flax fibre. Bottom Right, MFA microfibrillar visible at 10.5º. Top Right cross-sectional image for measurement of Ct with ImageJ Table 12.3.3. Scale 25mm. 328

Figure 12.5.1 A plot of MFA/Ct relationships as determined from diagnosis of fibres from archaeological assemblages: the results are labelled as identified in Table 12.5.1 and plotted on the comparative plot assembled in Chapter 9. Flax (yellow), nettle (green) and hemp (red). 333

LIST OF TABLES

Table 2.1 Tabulation ethnographic reports detailing the use of nettle plant fibre in the Northern Hemisphere (Yale University Human Relations Area File (eHRAF 2013) World Culture and Archaeology) 32

Table 3.1 Central European chronology. The availability and intensity of plant fibre utilisation are illustrated by the increasing/decreasing image width within the cells. The arrows depict the North/South limits of the Central European chronological periods ascribed (Gleba and Mannering 2019: 90.121,184,242,265,274,292,305,333,348.366,398,427) (The tabulation includes a reflective view on the utilisation of tree-bast and nettle to illustrate the relationship of the threshold to the introduction of flax and hemp). 49

Table 3.2. Detail extracted from catalogues of fibre assemblages in Western Europe listed and reviewed. A. Listed by Bender-Jørgensen (2005: 140-148), B. Listed by Gleba (2008: 43-63): C. Listed by Grömer (2019: 45). 50

Table 3.3. A reappraisal of plant fibre identification with the exclusion of pseudomorphs and non-descriptive fibre. 51

Table 3.4 Chronological listing of archaeological textile artefacts with fibre material diagnoses, as attributed by the authors. Diagnosis, the listings show uncertain diagnosis, i.e. Flax? or alternative diagnoses, e.g. Wool/Plant. Type is as described by the authors. 54

Table 3.4 (cont.) Chronological listing of archaeological textile artefacts with fibre material diagnoses, as attributed by the authors. Diagnosis, listing shows uncertain diagnosis, i.e. Flax? or alternative diagnoses, e.g. Wool/Plant. Type is as described by the authors. 55

Table 5.1 Tabulation of the percentage of fibre cellulose content. (Authors as listed)..... 101

Table 5.1(cont.) Tabulation of the percentage of fibre cellulose content. (Authors as listed) 102

Table 5.2 Intensity (I) ratios $R' = (I^{1121/1096})$ and $R=(I^{1096/2900})$. Established from FT-Raman spectra of soft bast fibres. (Edwards et al. 1997: 2387) 103

Table 5.3. ID 1-3. Results from FTRS diagnosis of plant fibre. Ratios derived from spectra of fibre samples Edwards et al. (1997) Table 5.2 above. ID 4-5. Results obtained from Perkins Elmer FTIR Spectrum 100 added for comparison..... 108

Table 6.1 Plant fibre tenacity and ultimate strength. (Luniak 1953:Table 5; Bodros and Baley 2008: Table 1) with additions. Note. Luniak provides factors for the conversion of tenacity to GPa). The final column shows the comparison of Bodros and Baley (2008) with GPa for ramie and flax to be in close agreement, the authors report the figure calculated for hemp as "suspect". 123

Table 6.2 Breaking load for two-ply nettle fibre 127

Table 6.3 (a) *E* modulus derived from various publications 130

Table 6.3 (b) *E* modulus derived from various publications (Continued over) 131

Table 6.3 (c) *E* modulus derived from various publication (continued overleaf) 132

Table 6.3(d) *E* modulus derived from various publications 133

Table 6.4. Results from Biomomentum Mach 1 testing. Maximum Load (N), stiffness (N/mm) strain (MPa) and *E* (Young's moduli) (MPa for four samples of retted flax and four samples of nettle are tabulated. The table evaluates the straight-line relationship of Stiffness/Strain to calculate Young's modulus (*E*). 136

Table 6.5 Tabulation of *E* for flax samples Flax E (A1-C7) 138

Table 6.6. Young's modulus (*E*). Analysis of Variance (ANOVA) in *E* for the three species found there to be minimal variation between the grouped samples (F=0.485905, df= 39, p= 0.619012) (n=40), flax (n=11), nettle (n=15) and hemp (n=14) 139

(The shaded areas indicate outlying values for *E).* 139

Hemp (non-fractured) 162

1-3.27 162

Table 7.1 MFA reported, based on trendline deviation 162

Table 7.2. Variation in MFA determination based on strain% Determined at the point of initial deviation from the tensile strain trendline. 164

Table 7.3. Fibre microfibrillar angle MFA: measured as an enclosed angle with AnalySIS software. (Blank squares depicted failed examinations due to the poor quality of the images). 168

Table 8.1. Nettle Fibre Cell Dimensions Comparative Measurement. Lumina/fibre length dimensions. Samples 1-8 taken from Ryder and Gabra-Saunders 1987: 91-108. Samples 8-20 taken from Di Virgilio 2013: 1-56)..... 177

Table 8.2 Flax fibre cell comparative measurement. Lumina/fibre length dimensions. Samples 1-7 taken from (Ryder and Gabra-Saunders 1987: 91-108), Samples 8-29 taken from (Aslan et al. 2011:). 178

Table 8.3 (Left) CSA overall/lumina diameter ratios for SEM images. 184

Table 8.4 Plant fibre sources for nettle, hemp and flax. (from Chapter 4 Table 4) 193

Table 8.5. (a) Ct determination for nettle and hemp fibres. 195

Nettle Ct. n= 60, Average = 0.530, St. Dev.= 0.123, SE= 0.016 195

Hemp Ct. = 44, Average = 0.778, St. Dev.= 0.105, SE= 0.016 195

Table 8.5. (b) Ct determination for flax fibres. Flax Ct. 196

n= 126, Average = 0.778, St. Dev.= 0.079, SE= 0.007 196

Table 9.1. Ratio of maximum/minimum and minimum/maximum of MFA and Ct ratio values to illustrate the overlap. 200

Table 9.2 Tabulation of Mean values MFA and (Ct x 10) 201

Table 9.3 Determination of vector angular direction and magnitude: calculated for MFA and Ct mean values..... 201

Table 9.4 Range of MFA and Ct maximum and minimum values: based on a 99% confidence level at 3 SE..... 202

Table 10.1. Determination of blind test sample size (Drennan 2004: 132-133). 213

Table 10.2. Blind test: fibre material sources. 213

Table 10.3. Summary of blind test results and accuracy of diagnosis. 218

Table 10.4 (a). Comparison..... 221

Table 10.4 (b). Comparison..... 222

Table 10.4 (c). Comparison..... 223

Table 10.4 (d). Comparison..... 224

Table 11.1. List of varieties of fibre selection and cultivation environment. 235

Table 11.2. Selected soils. Moisture content and pH levels are shown. The burial temperature is determined as detailed below (Section 11.4.5). 236

Table 11.3. Ageing protocol. Times necessary for simulating 42-315year thermal ageing of paint canvas at 105 deg. C. (94kj/mol Activation energy) (Seves et al. 2000: 316 Table 1). 239

Table 11.4. Arrhenius equivalent degradation periods in weeks for various acceleration temperatures. (Acceleration factor 50kj/mol)..... 241

Table 11.5. Deposition soil properties and water content at the start of the experiment. 246

Table 11.6. Tabulation for numbered samples, deposition soils, period and pH levels. (Note, for operational reasons the end period was adjusted from 36weeks to 40weeks). 248

Table11.7. Survival of samples after 12 weeks of degradation. (Arrhenius equivalent period of 45 weeks)..... 250

Table 11.8. Survival of samples after 24week degradation. (Arrhenius equivalent period 89weeks)..... 251

Table 11.9. Survival of samples after 36weeks submerged degradation. (Arrhenius equivalent period 134weeks). 252

Table 11.11. Summary of surviving fibres for each period. Deposition soils, period and pH levels. (Note. For operation reasons the end period was adjusted from 36 weeks to 40weeks and the additional submerged 36week period added 253

Table 11.12. Microfibrillar angles MFA. The data is assembled for the Control fibres and fibres from various depositions and periods. (Grey cells show where no measures were possible, black cell depict no survival). 256

Table 11.13. Fibres from 24week deposition: Ct determinations listed. 265

Table 11.14. Young's Modulus for degraded samples from the 12week deposition in dry sand. 270

Table 11.15 (Part 1). Determination Young's Modulus "E" (GPa). Tests were conducted on four samples of each surviving fibre sample mounted (see Section 11.4.8 and Figure 11.4 above). 271

Table 11.15 (Part 2). Determination Young's Modulus "*E*" (GPa). Tests were conducted on four samples of each surviving fibre sample mounted (see Section 11.4.8 and Figure 11.4 above). (The shaded areas indicate fibres that were too fragile to survive the test loading). 272

Table 11.16. Comparative plant fibre Young's Modulus *E*. (Bodros and Baley 2008: Table 1. with additions). 274

Table 11.17. Cumulative figures for mean values of *E* for each fibre species, within each deposition period, are provided for comparison with Table 11.16 above. 274

Table 11.18. Fibres surviving 12 weeks (Arrhenius 45weeks) in peat soil. The fragments surviving this supplementary12week peat were too fragile to evaluate MFA or Ct. All control samples from the dry-sand deposit survived..... 276

Table 12.1.1. RW337. Individual fibre circularity. Circularity (Ct) for identified fibres with a mean of 0.914. 288

Table12.1.2. Tabulation of Ct values: wool and bast fibres identified in Figure 12.1.8. 291

Table 12.3.1. KY 8 ImageJ analysis of circularity (Ct). Fibres identified 1-6 on area cross-sectional image in Figure 11.4..... 325

Table 12.3.2. KY 22. ImageJ analysis of circularity (Ct). Fibres identified 1-6 on area cross-sectional image in Figure 12.3.21..... 326

Table 12.3.3 KY 41. ImageJ analysis of circularity (Ct). Fibres identified 1-6 on area cross-sectional image in Figure 12.3.23..... 328

Table 12.5.1. Tabulation of archaeological MFA and Ct. diagnosis: results for indeterminant figures have been averaged and are shown in shaded cells above 332

Chapter One
Introduction and initial considerations

1. 0 Introduction

In meeting strangers, the concept of “first impressions” applies: that corpus of information gathered on first sight of another individual. While stature may be attributed at a distance on further, closer inspection, it is the consideration of the clothing that provides the interpretive detail of status, ethnographic societal and cultural relationships and, based on this first impression, whether the observed individual presents themselves as friend or foe (Gleba 2008: 1; Gleba and Mannering 201: 1; Bender Jorgensen 2007: 7; Gillis and Nosch 2007: vii). Additionally, the extent to which the clothing displays recognition of the harsh environmental and climate conditions may question the suitability of the individual’s attire and a possible interpretation of their need for aid or assistance (Bender Jorgensen 2008, 7; Dimova 2016, 652; Gleba 2008, 1; Gleba and Mannering 2019, 1).

Cultural status, ethnographic societal and cultural relationships are also represented in furnishing fabrics as evident from interpretations of textile fabric artefacts recovered in burial depositions from the numerous (230 plus) Bronze Age (1400BCE) and Early Iron Age (800-400BCE) miner’s clothing preserved within the salt site at Hallstatt (Grömer 2015: 17-40; Grömer 2019: 27-64). Additionally, furnishing fabrics used to wrap grave goods and colourful cloth coverings on accompanying furnishings were also recovered from elite burial chamber from the Princess’s Grave at Leśno (Cybulska et al.2010: 37) and Eberdingen-Hochdorf (Bank-Burgess 2019: 139-150 (See **Section 3.5.1 23**).

Textile fabrics recovered from artefact wrappings funerary mats and body wrappings are also noted (Lipkin 2012: 77; Bolohan and Lazanu 2015: 143-150: Gleba and Turfa 2007: 35-40).

1.1 Background progress in fibre identification 1

The thesis considers natural plant fibres and their diagnostic differential to understand plant fibre processing and utilisation that form attendant diagnostic potential. However, before considering the diagnostic features presented by textile artefacts, it is necessary to recognise the important contribution to the advances in spinning and weaving knowledge that informs an understanding of textile seriation and typological comparisons. Evidence from early in assessing textile finds works are noted Wild (2007: 2) who commend Hald's (1980) on Danish bog bodies burial textiles. Recent evaluations of textile fabrications have established a wider understanding (Bender-Jørgensen 2007; Andersson-Strand 2010; Harris 2010; Bender Jørgensen and Grömer 2013; Gleba and Mannering 2019)

As noted above, there are textile diagnostic features to aid determinations of spinning and weaving that inform seriation and typological horizons and enhance the understanding of textile production. However, the poor preservation of organic material results in the limited availability of archaeological artefact for appraisal and directs diagnostic trials to the evaluation of modern reference material. This factor, coupled with the high degree of degradation in all but the most favourable depositional environments, is in direct contrast to inorganic analysis

Inorganic material analysis benefits from petrological, and metallic isotope identification, coupled with seriation and typological comparisons that support the materials provenance and chronology. Examples for ceramic material, lithic assemblages and metallic isotope analysis are compared below.

1.1.1 Ceramic material provenance

Petrological provenance was undertaken for Akrotiri textile tools to differentiate local clay production from Naxos Crete imported clay (Vakirtzi 2019: 480).

Thin section petrography of Early Minoan pottery was reviewed by Day and Kiriatzi (1999: 1025-1036) illustrate the complex relationship between the composition of a ceramic body, its origin, and process practices. The differential of inorganic and organic materials 157) was reviewed by Hurcombe (2014: 13, and 152-157) who proposed a holistic approach to resolve the "missing material majority" dilemma for organic remains.

1.1.2 Lithic provenance

In lithic utilisation, the investigation of tool wear traces to compare evidence of their application in the preparation of nettle and bast fibre was conducted by Hurcombe (2010: 129-139). Frahm and Brody (2019: 608-622) employed X-Ray fluorescence to review obsidian origins from the Dura- Europos (Syria) excavation to determine the lithic as locally sourced. The 3D illustrations included by Frahm and Brody (2019: 618-620) are of interest in that they display the potential of 3D vector analysis

Petrography, coupled with shape circularity analysis, was employed to evaluate quartzite lithic assemblage from two Cantabrian Mountain (Spain) sites to determine Neolithic navigation and trade routes (Prieto et al. 2019: 14-30).

Provenance studies, by macroscopic analysis of clay characteristics of spindle whorl manufacture taken from two sites on Thassos Greece, were undertaken by Vakirtzi et al. (2014)

1.1.3 Metal isotope provenance

While recognising the difficulty in applying provenance to remelted metal amalgamations the isotopic analysis of unadulterated copper, lead, silver and gold can establish possible provenance sources

Provenance and processing for copper production in north-eastern Balkan Neolithic culture based on metallography investigations were determined by Ryndina (1999: 1059-1068) and the lead isotopes and chemical composition of metal objects from the “Royal” tomb at Arslantepe Eastern Anatolia are considered by Hauptmann et al. (2002: 1059-1068). Piccardo et al. (2010: 10-14), conducted metallographic investigations to determine the composition and manufacturing process of an Etruscan bronze mirror.

1.2 Resume plant fibre diagnosis

In consideration of fibre identification, it is most important to confirm that the proposed diagnostic analysis may be partially destructive and require validation before its utilisation on archaeological assemblages of historical merit.

Recent advances in textile fabrication have identified diagnostic features including, fibre spin angle and weaving construction enable diagnosis of fibre utilisation with seriation and typological characteristic. However, unlike inorganics, the identification and provenance of organic textile fibres and associated chronologies prove more challenging.

Plant fibre interpretations still present an “interpretive dilemma” regarding the difficulty in ascribing “text” to the interpretation of non-textual archaeological assemblages (Wylie 1989).

The foundation in the identification of textile fibres has been extended considerably in recent times (Peacock 2001: 181-192; Gleba 2008; Andersson Strand et al. 2010; Bender Jorgenson and Grömer 2012: 91-111; Rast-Eicher 2016: 48-112; Bender Jorgensen and Rast Eicher 2018, 25-36: Gleba and Harris 2019: 2329-2346; Gleba and Mannering 2019).

Therefore, it is disappointing to note that, even in current publications, there are still concerns regarding the number of textile assemblages available for analysis. Excavation reports included in Gleba and Mannering (2019) listings note the following.

Möller-Wiering (2019: 122) remarked that excavations were “rather scant” in Germany.

Spantidaki and Moulherat (2019: 185) that Greece “was still in its infancy”.

Maik (2019: 293) confirms that “only a small number of extant archaeological textile finds were available” in Poland.

From an additional source Mazăre (2014: 1) reported: “that textile production was generally ignored by Romanian archaeologists”.

The above comments are in contrast to the report from Italy,

> “textile archaeology is well documented” (Bazzanella 2019: 203).

and Denmark,

> “one of the largest collections of prehistoric textiles.
>
> (Mannering et al. 2019: 91).”

In this research review, it is recognised that, in comparison to inorganic lithic tools, ceramic pottery sherds and precious metals, textiles only survive in exceptional archaeological environments.

Those that survive may be degraded to the extent that fibre diagnosis is difficult. This work is formulated on the evaluation of existing diagnostic techniques and the potential for alternative interpretive procedures.

1.3. General project aims

The project encompasses the chronological period from the Mesolithic to the Late Iron Age, with occasional references to periods beyond this range, to address the concerns detailed in **Sector 1.1** within the following broad areas of interest.

1. A review and appraisal of current diagnostic techniques.
2. The identification and evaluation of alternative diagnostic processes working singularly or collectively.
3. An assessment of the reliability of the proposed alternative within a blind test protocol.

4. The appraisal of the resilience of the diagnostic features that survive degradation depositions.
5. The application of the derived diagnostic techniques to the re-examination of fibre selected from case study assemblages.
6. A consideration of the broader application and potential enhancement of the research programs determinations.

1.4 Technological horizons

Fibre diagnosis and the attributable chronology is mostly related to their stratigraphic relationship with associated depositional material. However, there are notable technological horizons presented by the adaptation of alternative fibre sources.

Horizons that, for Central Europe, are evidenced in the identified of the adaptation of non-native plant fibre, flax (5000 BCE), and hemp (1100 BCE) (Barber 1991; Bosch et al. 2006; Harris 2010 30-31; Karg, 2011: 506-508; Weiss and Zohary 2011; Bergfjord et al. 2012: Harris 2014). These factors are considered and reviewed in **Chapter 3**, **Section 3.1.**

The chronology, for the introduction wool fibre as a secondary product, is attested by evaluation of the age/sex of faunal skeletal assemblage (Sherratt 1983: 90-104: Gleba 2008: 72-74; Wild 2008: 4-10: Bender Jørgensen and Rast-Eicher 2018: 25-36; Rast Eicher 2016: 127-130; Gleba and Mannering 2019: 6-9).

Sabatini et al. (2019) also reviewed the genetic profile of DNA from both local and non-local sheep types to propose the introduction of wool to continental Europe in the Early Bronze Age (2000 BCE). In particular, the extensive assemblages from Hallstatt Austria, present a significant source of evidence for the use of wool fibre (Grömer 2005: 81-90, Grömer 2005: 17-40; Bender Jørgensen and Grömer 2012: 102-103).

1.5 Bast fibre usage

However, within the extensive listing described above, the use of other bast fibres such as nettle and tree-bast have no defined horizons. Ethnographic reports, coupled with the analysis of basketry weaving, cord and netting assemblages, and Palaeolithic fibre artefact, Lascaux Cave-France (Glory 1959), Ohalo-Israel (Nadel et al. 1994), Dzudzuana-Caucasus (Bar-Yosef et al. 2011), Bouldnor Cliff-England (Gaffney et al. 2015), reinforced by the examination of Otzi (The Ice-man) (Acs et al. 2005), confirms the extensive chronology for their initial use of bast fibres as primary fibre sources. A usage, which may have declined through time but remains today, although at a much-reduced level.

While this research programme considers only flax, hemp and nettle bast fibre results from this work may aid future research on the diagnosis of other bast fibres, with particular reference to early tree bast fibre usage (Médard 2005: 99-105; Rast-Eicher 2005: 118; Harris 2010; 1070; Rast-Eicher 2016: 81-86)

1.6 Research Programme Hypothesis

In addressing the above parameters, the following hypothesis is proposed.

Hypothesis

Can diagnostic techniques be developed for the three principal fibre species, flax, nettle and hemp, that are robust, reliable, minimally invasive and suitable for replication and efficacy trials?

1.6 1 Research Aims and objectives.

In formulating the Research Programme, the following Aims and Objectives were proposed.

Aims To develop and evaluate techniques that determine diagnostic differentials for flax, nettle and hemp fibres, techniques that are robust, reliable and minimally invasive.

Objectives

1. To review the human/plant fibre relationship and the chronology of non-native fibre introduction.
2. To consider the *chaîne opératoire* for plant fibres processing from crop planting through to end-use.
3. To assess a selection from multiple archaeological assemblages and review their diagnostic outcomes.
4. To evaluate how past diagnostic technique would meet the research parameters.

5. To propose improved or alternative techniques that may resolve the interpretive dilemma.
6. To develop and appraise experimental methods for the determination of the proposed diagnostic trials.
7. To subject the findings to a statistical confirmation of the diagnostic analysis.
8. To investigate how the degradation effects of burial environments may modify the features.
9. To confirm the reliability of the fibre diagnosis under a blind test protocol.
10. To utilise the diagnostic programme in the appraisal of archaeological assemblages.
11. To produce a report for peer review and dissemination of the findings.

1.7. Research Project construction

The following chapters are described as a representation of a programme of reflections on the exploitation of bast fibres in textile manufacturing and to address the problem in ascribing diagnostic interpretations as indicative of the chronological utilisation of native and non-native plant fibre species.

In this review, the research “Aims and Objectives” are presented as they address the interpretive dilemma in ascribing meaning to those scarce fragmented textile remains available for archaeological evaluation.

Prehistoric archaeological assemblages are reviewed that attest to plant fibre textile adoptions from the Palaeolithic to the Late Iron Age. Current techniques are reviewed, and alternatives are proposed that may enhance diagnostic interpretations.

1.8 Thesis assemblage -individual chapter outlines

The thesis is presented in twelve chapters that follow this **Chapter 1** introduction. The chapters have been arranged to follow the sequence of fibre identification, cultivation and processing to archaeological deposition, past and present diagnosis techniques and the formulation of alternative diagnostic features.

Chapter 2 presents the background information regarding plant fibre structure, cultivation, and cultural history availability, and the utilisation of the three principal plant fibres flax, nettle and hemp are discussed.

Chapter 3 reviews and appraises archaeological assemblages and the accompanying fibre diagnosis attributed to them.

Chapter 4 considers the *chaîne opératoire* (production sequence) to evaluate those processes and textile tools that modify the plant fibre from harvesting through to the refined end product.

Chapter 5 lists the principal diagnostic techniques currently employed and reflects their efficacy, reliability, and age-related endurance within the depositional environment.

Chapter 6 contrasts and evaluates the material properties of plant fibre using two alternative electromechanical load frames for the determination of fibre tensile strength and elasticity (*E)*.

Chapter 7 outlines the sampling processes and analytical techniques employed to identify and quantify the microfibrillar angle (MFA) as a reliable and minimally invasive diagnostic feature.

Chapter 8 extends the research programme to evaluate the measurement of fibre cross-sectional area as a potential secondary diagnostic feature to complement and support MFA in the confirmation of plant fibre diagnosis.

Chapter 9 presents the combined MFA/Ct diagnostic relationship and displays these as illustrative of the statistical confirmation of variance and accredited high level of confidence attributed to the combined relationship's reliability.

Chapter 10 details the criteria established for a randomised Blind Test protocol and the resultant outcome percentage of successful fibre identification reported.

Chapter 11 reports the findings obtained from a temperature-accelerated 48week degradation trial of fibres to confirm the resilience of the associated MFA/Ct features within a depositional environment.

Chapter 12 reports the reliability of MFA and Ct diagnostic features as applied to three case study samples, Coptic Collection held at Cliffe Castle Museum Keighley U.K., Textile Collection from Temple Newsam Museum Leeds U.K. and samples from the Kasr al Yahud mass burial provided by the University of Bradford U.K.

Chapter 13 summarise the thesis deliberations and results to propose areas worthy of further investigation in pursuit of an improvement in the identification of plant fibres recovered from archaeological sites. Recommendations for the extension and enhancement of the research protocol are included here.

Chapter Two
Background – Plant Fibre Structure, Cultivation and Cultural History

2.0 Introduction

A broad range of natural fibres is likely to have been used for textiles, string, and cordage in prehistoric material cultures. Three significant plant resources are thought to have been nettle (*Urtica dioica* L.), flax (*Linum usitatissimum* L.) and hemp (*Cannabis sativa* L.). These plants favour different growth conditions and require different levels of husbandry, but their products undergo broadly similar processing methods. Plant fibres share some physical and material properties which make them difficult to distinguish in the archaeological record and this project sets out to investigate identification methods for the diagnosis of plant fibre. The research programme evaluates approaches to defining diagnostic features in modern reference material for identifying archaeological plant fibres from archaeological textiles, with the long-term aim to aid understanding of past fibre processing and use. Identification of bast fibres from archaeological textile assemblages makes an essential contribution to the understanding of prehistoric material culture and social structures. It has long been recognised that only a small proportion of plant products used in the past are represented in the archaeological record.

In contrast to the inorganic lithic and ceramic material cultures, a large proportion (95%) of organic material culture, goes unrecognised or misidentified (Soffer et al. 2000: 511-537; Hurcombe 2014: 1-4).

While recognising this past dichotomy, in the interpretation of food plant and non-food plant utilisation, there is now a growing interest in the holistic understanding of plant exploitation by past human populations. Previous authors have estimated that the poor preservation of plant remains lead to a significant misrepresentation of the plant material culture and the attendant human-environmental interaction (Adovasio et al. 2014; Hurcombe 2014: 4-10). Improvements in diagnostic techniques may serve to re-evaluate non-food plant exploitation. As noted by Barber (1991),

> “(L)ack of domestication does not in itself imply non-use; and so we must look at our few pitiful scraps of evidence for textile within a much wider, palaeobiological world: the range of habitats of the wild as well as domestic species of fibre-bearing plants” (Barber 1991: 11).

2.1 Plant fibre utilisation

Botanical sciences promote the understanding of plant fibre constructs and the advantage derived from the utilisation of the fibre's mechanical strength and durability. An understanding that, in a pre-agrarian hunter-gatherer society, directs attention to the selection, care and protection of native resources, a "para-cultivation" partnership (Dounias 2001). Knowledge and expertise gained in the preparation of fibres for textile and cordage manufacture direct attention to the similar, potentially superior, fibre properties of non-native plant species.

The adaptation of non-native species and the attendant changes in agricultural practices formed the foundation of Late Neolithic flax exploitation and subsequent advances in fibre processing and textile production.

Additionally, the selection of non-native species provides evidence of the movement of people and materials and the attendant social, and cultural interchange (Gleba 2008: 1-9; Bender-Jørgensen and Grömer 2012: 91-111; Hardy and Kubiak-Martens 2016: 71-90; Rast-Eicher 2016: 87-88; Hardy et al. 2020).

2.2 Basic fibre plant structure

Fibre stem ground tissue (parenchyma) includes all tissues that are neither dermal (skin) nor vascular vessels (tube) and is composed of three types based on the nature of the cell walls that embed the vascular tissue.

1. Parenchyma cells form the "filler" tissue in the soft parts of plants and are usually present in the cortex, pericycle, pith, and medullary rays in primary stem and root. These primary thin fibre walls that remain alive after they become mature.

2.Collenchyma cells provide extra mechanical and structural support, particularly in root and apex regions of new growth. These cells have thin primary walls with some areas of secondary thickening.

3. Sclerenchyma provides the primary structural support to a plant and have thickened, typically lignified, walls. For mature cells, the protoplast

declines, and the permanent sclerenchyma become unnucleated (Cutler et al. 2008: 7-9; Beck 2010: 18- 22; Pandey 2012: 94-98).

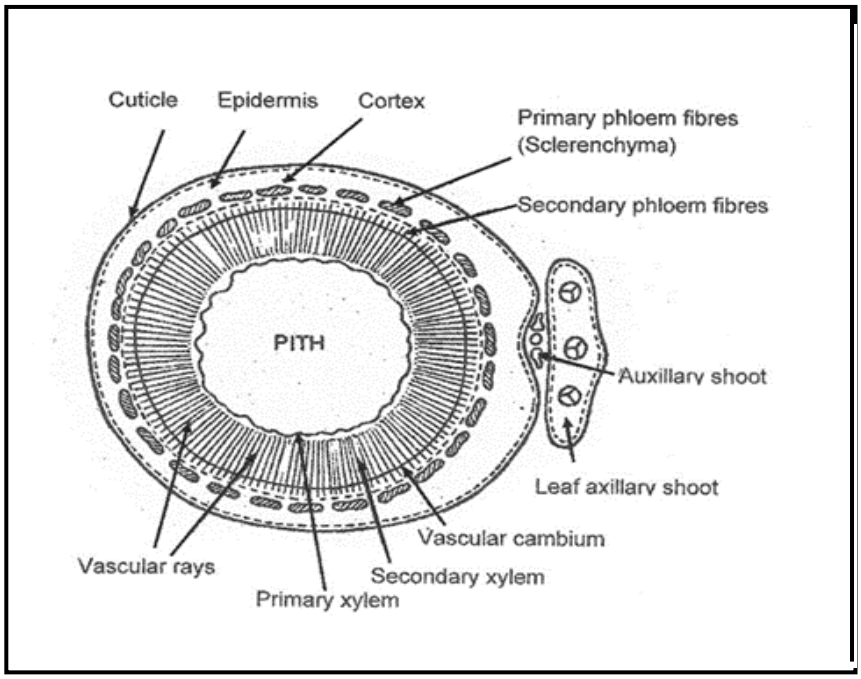

Figure 2.1. Illustration of stem with leaf and auxiliary shoot of *Linum usitatissimum* (Pandey 2012: 153).

Figure 2.1 provides additional information describing a further sub-division of the multi-layered flax stem fibre zone. The layers are identified from the outside as cuticle, epidermis, primary phloem fibres, secondary phloem fibres, vascular cambium (main vascular sheath), secondary xylem and primary xylem with the pith and vascular rays occupying the centre core. The vascular bundles are shown as located circumferential within the cortex adjacent to the epidermis (Pandey 2012: 153).

An expanded view of the stem cross-sectional structure is illustrated by Evert et al. (2009: 179) as shown in Figure 2.2, note the variations in cell notation.

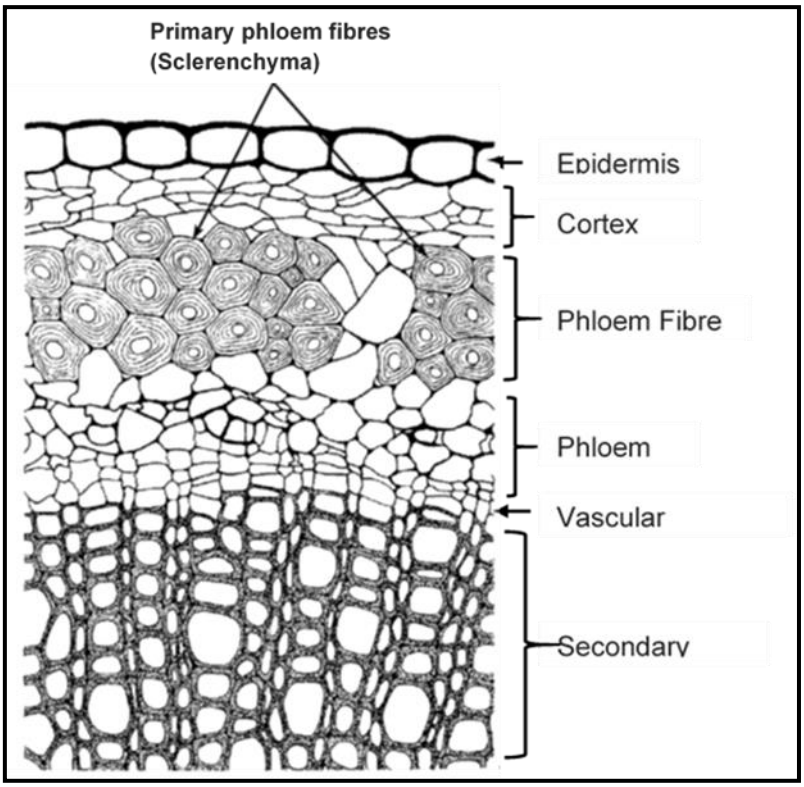

Figure 2.2. Traverse cross-section through the radial axis of *Linum usitatissimum*; the location of the primary phloem fibres (sclerenchyma) is shown (x320). (Evert et al. 2009: 179, Fig. 8.4.with additions).

For a dicotyledon stem, Beck (2010: 16 Fig. 2.10a) lists, in order from the outside, epidermis, cortex, and pith, with primary xylem and primary phloem, and radially orientated vascular vessel arranged centrally. The plant species is not identified.

In the initially planned examination, traverse sections of the angiosperm dicotyledon plants were prepared for the examination of the comparative cross-sectional area under both Scanning Electron Microscope (SEM) and Optical Microscope with cross-polarised lighting (CPL).

To ensure that the selected sections are representative of the textile fibre under consideration, the traverse sections were taken from the mid-inter-nodal point to avoid the immature material present at root and stem apex Figure 2.3.

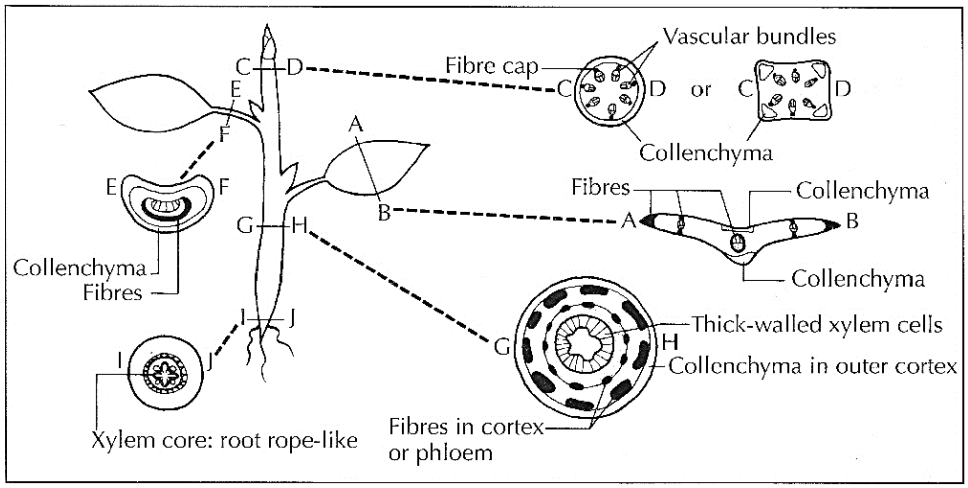

Figure 2.3. A schematic image of the support system for dicotyledons with positions and descriptions of sections indicated. The bottom right cross-sectional image details the fibres held in the phloem (Cutler et al. 2008: 5 Fig. 1.2).

It is recommended that transverse sections be taken from the inter-nodal area G-H, as detailed in Figure 2.3. The illustration of the transverse section details the vascular sclerenchyma bundles that provide the principal mechanical support for the plant fibre stem. The orientation, shape and distribution of these mature fibre vascular bundles are a principal focus for plant fibre diagnostic evaluation.

The extended aerial plant stems of flax, nettle and hemp all share similar attributes including mechanical strength, water retention capability and systems for water and mineral transpiration. The stems contain a central pith surrounded by xylem and phloem vascular tissue.

Mechanical stem strength is provided by thick-walled sclerenchyma fibres described by reference to the initial xylem vascular tissue. These cells conduct water and nutrients from the root core and the extraxylary (bast) cells related to the phloem. Secondary cells fibre walls are usually lignified with pronounced lamella tissue surrounding them. Upon maturity, the walls may thicken to the extent that the central lumen is obliterated as the protoplast hardens, and the cell dies. With no surviving cells, these fibres become unnucleated and unsuitable for DNA analysis. (Bergfjord and Holst 2010: 1192; Pandey 2012: 98; Beck 2020: 426).

The exposed waxy outer layer of stem epidermis and surrounding cuticle layer combine to control and maintain water retention. Control of transportation is enabled by regulation of evaporation through the manipulation of stomata stem pores that maintain the effective transport of water and soluble minerals to the growth areas (Pandey 1978: 136-143; Cutler et al. 2008: 83-87; Beck 2010: 149-156).

The transportation of mineral salts and water is provided by xylem and phloem vascular bundles that have different characteristics. Primary cells, that elongate and form the basis of plant fibre sclerenchyma, and secondary cells that have ceased to elongate. Evert (2009) describes two types of vascular tissue, xylem the water-conducting tissue, and phloem, the food-conducting tissue. There are references to Evert (2009) nomenclature of “xylem” and “extraxylary fibres” located in the cortical and phloem regions referred to as “bast fibres” (Pandey 2012: 98).

In a reflection of the classification of plant fibres, it is reported that there are added difficulties in describing archaeological textile fibre as the attendant floral and seed remnants may not be available for analysis (Rast-Eicher 2016: 72).

2.3 Area cross section-SEM imaging - nettle (*Urtica dioica)*, flax (*Linum usitatissimum)* and hemp (*Cannabis sativa)*

The sections shown in Figure 2.4 A-C, include the identification of the epidermis (E) cortex (C), and bast-fibre (BF). Specimens were prepared as detailed above Figure 2.3, and image sections are compared and described in Figure 2.7 referencing the diagnostic criteria offered by Gale and Cutler (2000) and Rast-Eicher (2016).

The similarity of the prepared stem sectional images and the comparable descriptions from Gale and Cutler (2000) and Rast-Eicher (2016) emphasise the difficulty in ascribing diagnostic differentials to the attendant fibres. Additionally, and relevant to the research programme, the images display the fibre cross-sections as they are constrained by the stem's epidermis and surrounding parenchyma structure.

When released from constraint, by chemical or mechanical processes, the diagnostic features are further modified, a modification influenced by ageing, burial environmental degradation, fibre hydrophilic absorption, post-excavation storage, and conservation treatments.

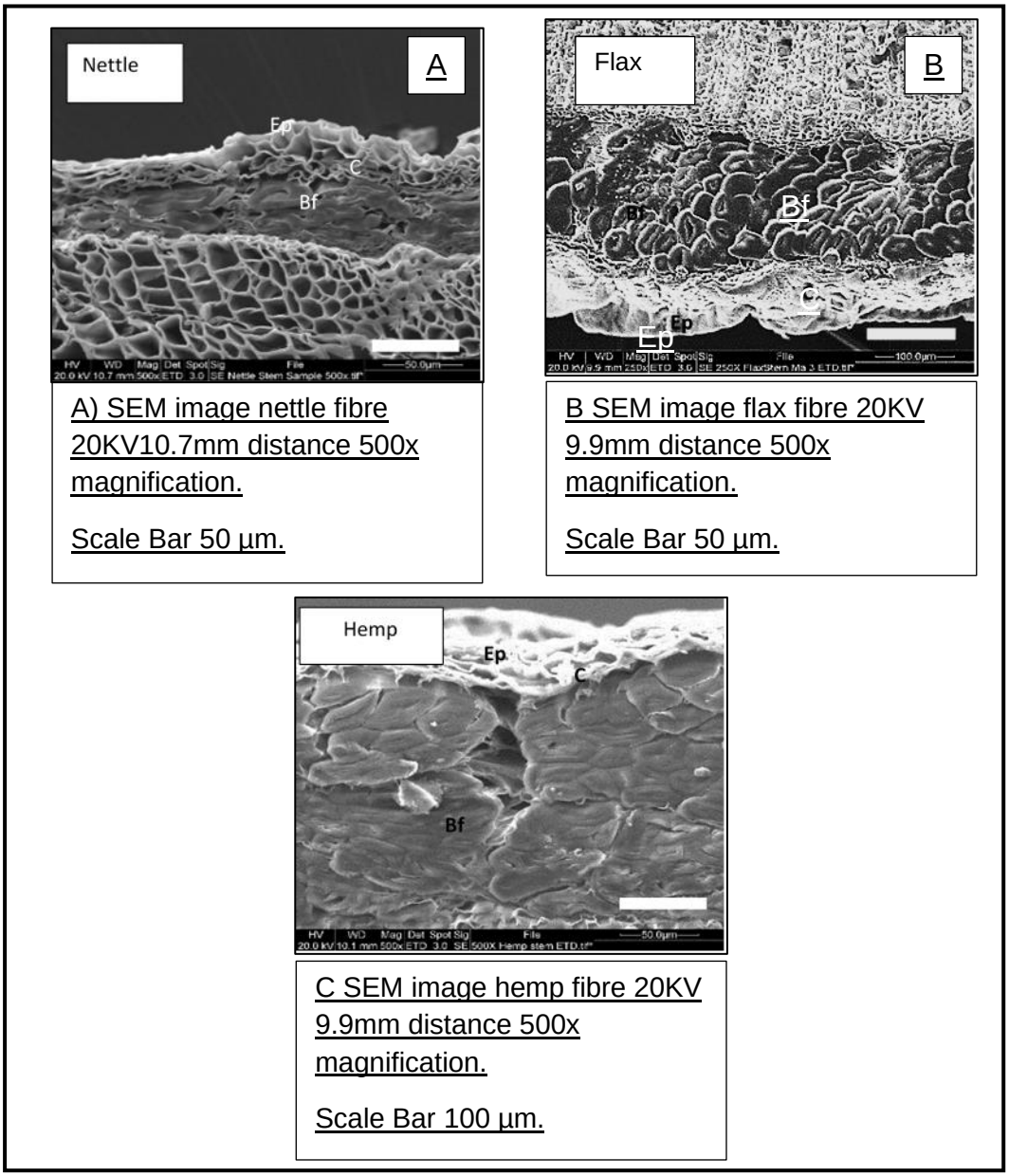

Figure 2.4 A-C. SEM images of traverse sections of plant fibre stems prepared by hand sectioning. The images are presented for comparison with the descriptions provided by the authors and listed in Figure 2.7.

2.4 Area cross section-SEM imaging tree bast fibre

As demonstrated above, the three plant fibres under consideration within this work are flax, nettle and hemp. However, it should be noted that in the Mesolithic and Early Neolithic there is evidence to support the utilisation of tree-bast particularly lime tree bast fibres (*Tilia* sp) (Médard 2005: 99-105; Rast-Eicher 2005: 118; Harris 2010: 1070; Rast-Eicher 2016: 81-86). Médard (2005) in reporting on the lack of tree bast fibre representation undertook a review of tree bast from elm, lime, and oak to determine their potential as textile fibres. Medard (2005) concluded that there was evidence from these three species to support further work in the identification of prehistoric textiles of other useful plant species available in the environment at the time (Medard 2005: 99-105).

There is a significant corpus of information on fibre production from the palynological examination of botanical remains recovered from the study of the lake-dwellings of the Circum-Alpine region (Jacomet 2006; Menotti 2015; Bank -Burgess 2019) and for Hallstatt (Austria) (Bichler et al. 2005). In particular, for the Mesolithic and Early Neolithic, the findings included the use of bast from lime trees (*Tilia cordata* L. and *Tilia europaea* L.) (Myking et al. 2005; Harris 2010; Higgitt et al. 2011; Leuzinger and Rast-Eicher 2011; Bender- Jørgensen and Grömer 2013; Harris 2010; Harris 2014; Harris et al. 2017; Bender Jørgensen and Rast-Eicher 2018; Médard 2019: 367-377).

Médard (2019) notes the variety of bast fibres from similar species but limits consideration to those fibres documented in archaeological evidence as utilised in Switzerland during the Neolithic period, lime (*Tilia* sp) and flax, with lime predominant.

It is advantageous at this stage to add the botanical anatomy of lime to the record for comparison with the flax, nettle and hemp fibre morphologies listed.

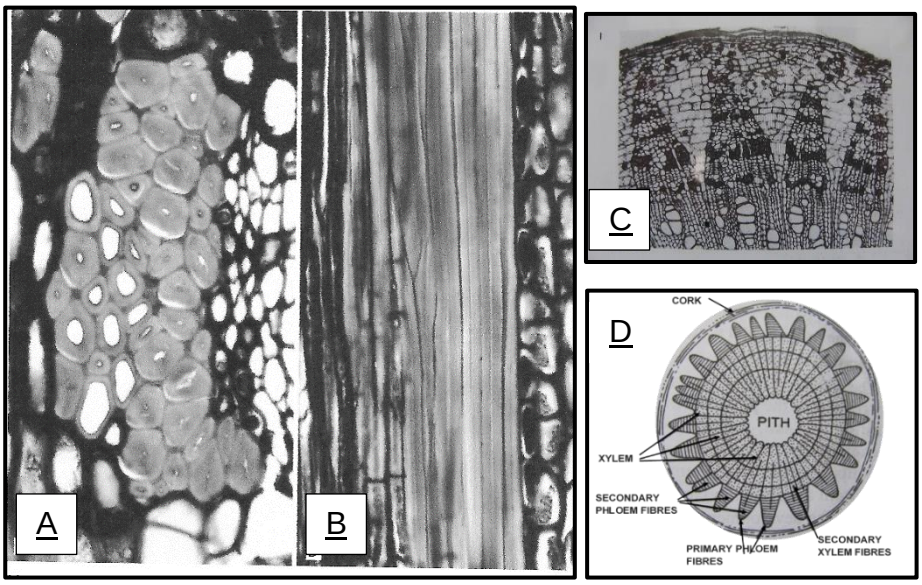

Figure 2.5. Lime Bast (*Tilia americana* L.), primary phloem fibres from the shoot axis. A. Cross-section B. Longitudinal section. The longitudinal view (B) shows only a section of the total length of the fibres (A x620; B x375) (Evert 2009: 176, Fig.8.10). C. (*Tilla vulgaris*), bark and xylem traverse section (x60). Note blocks of fibre alternating with conducting tissue (Gale and Cutler 2000: 257, Fig.1) D. Sketch of traverse section of (*Tilia* sp.) stem with fibres in the primary and secondary phloem and the secondary xylem (Pandey 2012: 365, Fig.16.4).

The rate of decline in lime bast utilisation on the Swiss Plateau increases from 5000BC as evidenced by the increase in non-arboreal pollen (NAP) indicative of large-scale forest clearances circa 1350BC (Jacomet 2006; Kühn and Weniger 2015; Bank- Burgess 2019).

2.5 Vascular bundle- definition of a “fibre”

The comparative microfibre images presented in Figure 2.4 A-C demonstrate some of the difficulties experienced in formulating an archaeological description for fibre assemblages that are mostly composed of fibre bundles.

There is a loose description of “fibre”, a term used as a collective generic, covering a range of fibre diameters. The fibre has been defined as an “archaeological fibre” a “theoretical fibre” or a “fibre bundle”. In material science, “fibres” are considered to be less than 100µm in diameter. For textile fibres, the term is used as descriptive of fibre material that can be worked into thread and fabric (Gleba and Mannering 2012: 5). Harris (2017: 580) proposes that these fibre bundles are best described as “strips”. Bos and Donald (1999: 3030) refer to a “technical fibre” with a diametric range of 50-100µm Figure 2.6. In this work fibres of 20-50 µm diameter described as “theoretical fibre” will be employed.

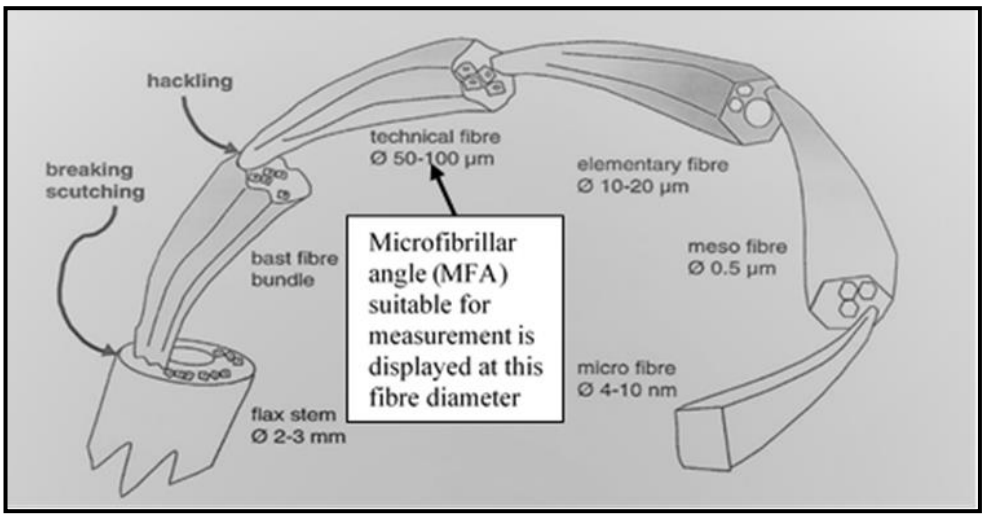

Figure 2.6 Illustration of variation in flax fibre dimensions and description (Bos and Donald 1999: 3030 with additions)

The theoretical fibre morphological, microfibrillar angle (MFA) and area cross-sectional, diagnostic shapes and features are evaluated in more detail in **Chapter 7 and 8**.

2.6 Plant fibre stem sectioning

In the appraisal of fibre botanical structures and the listing of fibre diagnostic features, suggestions on the preparation and sectioning of the stem- material is referenced in publications to include recommended practices (Gale and Cutler 2000: 1-20; Cutler et al. 2008: 175-179; Beck 2010: 230-234; Rast-Eicher 2016: 62-73).

Concerns are expressed regarding the use of razor blade sectioning and it is recommended that multiple sectioning, by rotary or rocking microtome, be used particularly for sections below 10µ (Cutler et al. 2008: 175). The possibility of misleading effects, resulting from the decay or breakdown of cellular tissue, is noted with additional guidance on the preparation of dry material and the advantages and disadvantages of angular sectioning (Gale and Cutler 2000: 18-20: Rast-Eicher 2016: 65).

Fibre cross-sections, for the initial research programme, were cleaned, prepared, and embedded in paraffin wax. The method for the preparation of plant stems for SEM evaluation of fibre CSA cell morphology is detailed in **Chapter 8**.

The traverse sections were subsequently chemically dewaxed and sectioned with a rotary microtome. However, the dewaxing removal process proved inadequate, with some embedding still present. Cell material was also removed by the rotary action and the SEM images were compromised

While resin embedding is available as an alternative, the assemblage proved too hard for rotary microtome sectioning. The SEM images included below were prepared by razor cutting hand sectioning from wet stem material.

The sample preparation of longitudinal and traverse sections of plant fibre material is a principal focus for the successful identification of the fibre diagnostic features and are discussed in more detail in later chapters.

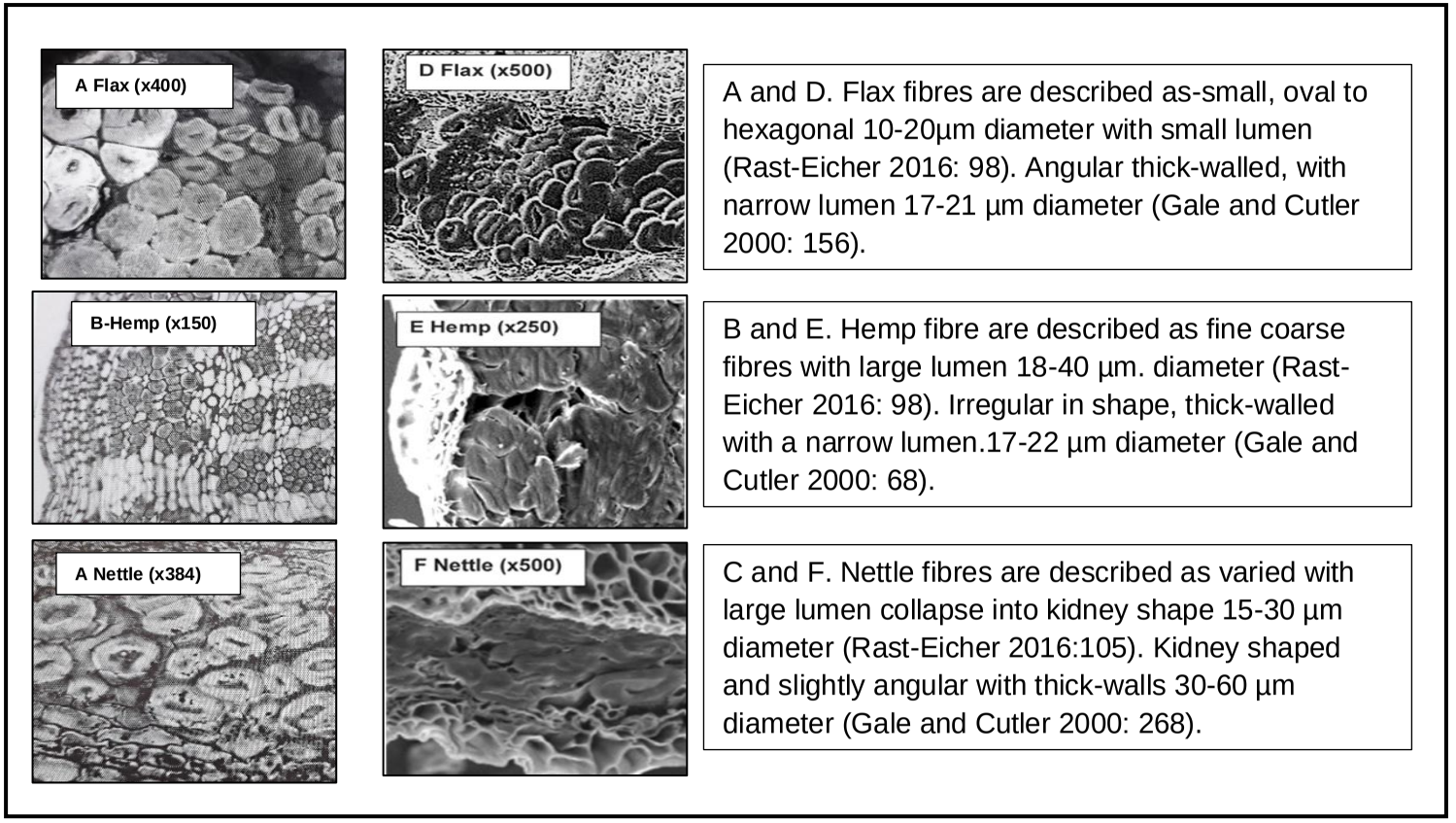

Figure 2.7.A comparison of fibre cross-sectional area taken from the SEM images included in Figure 2.4 for comparison with images and descriptions taken from other sources (Gale and Cutler 2000, Rast-Eicher. 2016).

2.6.1 SEM imaging plant fibre area cross-sections

As illustrated above, SEM imaging was proposed for the production of calibrated fibre images and was the initial choice for the research programme. Sample preparation, to an acceptable standard for comparative measuring, is reliant on the accurate placement and orientation of the samples and precision in cutting the thin sections. Also, splatter coating and adjustment of the SEM parameters, coupled with the slow traverse across the sampling area, placed considerable demands on the SEM access periods allocated. A further consideration was the image quality achieved in the reflective mode presented in SEM and the effect of autofluorescence (Peetla et al. 2006: 689). A topic addressed in later chapters.

Trails were conducted on a Nikon Optiphot Polarising Microscope with reflective cross-polarised light (CPL) coupled with Nikon BD Plan 40/0.65 objective lens. The longitudinal sections mounted under a glass slip (nD 1.52), and 1mm thick section of fibre (nD 1.4) cross-sectional areas were viewed under cross-polarised light. The transmitted light provided translucent microfibrillar images from both anterior and posterior fibre from the longitudinal surfaces and quality cross-sectional images for analysis of circularity. While magnification on the optical microscope is limited to x400, it was decided that, for microfibrillar angle (MFA) and fibre cross circular area circularity (Ct), this was the most effective procedure. SEM imaging was available for more detailed fibre analysis if required.

2.7 Plant fibre cultivation

Textile research and ethnographic studies allow a review of material cultural heritage and the husbandry practises employed by past societies to protect and enhance their fauna and flora resources. Previous plant studies recognised their use as a food source, for medicinal use, in fibre production, and textile/body colouring (Pinelli et al. 2008; Bodros and Bailey 2008). Ancient skills of weaving, knitting and fabrication practised in hunter-gatherer societies continued to supplement the material cultures developed through the Mesolithic and Neolithic period and continue into modern times. This study considers plant fibre textiles and methods for classifying plant fibres to aid understanding of their use in the past.

The project recognises the poor preservation and low visibility of plant fibre material within the archaeological record that challenges the archaeological principle.

“Absence of evidence is not evidence of absence."

Additionally, it is noted that the presence of flaxseeds within archaeological excavations, as detailed in archaeobotanical records, receives consideration as a farmed crop while nettle is only acknowledged as a common weed. This classification is at odds with ethnographic hunter-gatherer studies where nettle fibre in the Northern Hemisphere is seen as a beneficial crop with numerous uses (Hald 1980: 121-147; Dunsmore 1985: 1-57; Hurcombe 2000: 155-173; Edom 2010: 1-10). Reports from Nepal on the utilisation of Himalayan nettle (*Girardinia diversifolia* L. *(“*allo” in Nepal) serves to broaden our consideration

of plant fibre utilisation where harvesting and processing have parallels with plant fibre usage in Europe (Dunsmore 1985: 1-57).

The relationship involved in the utilisation of plant material and the change in emphasis between a culture of working with nature in the enhancement and protection of natural resources is described by Dounias (2001: 135-156) as “para cultivation”, through the cultivation, hybridisation and guardianship of crops. It is recognised that tending wild and cultivated plants involves different social organisation strategies **Figure 2.8**.

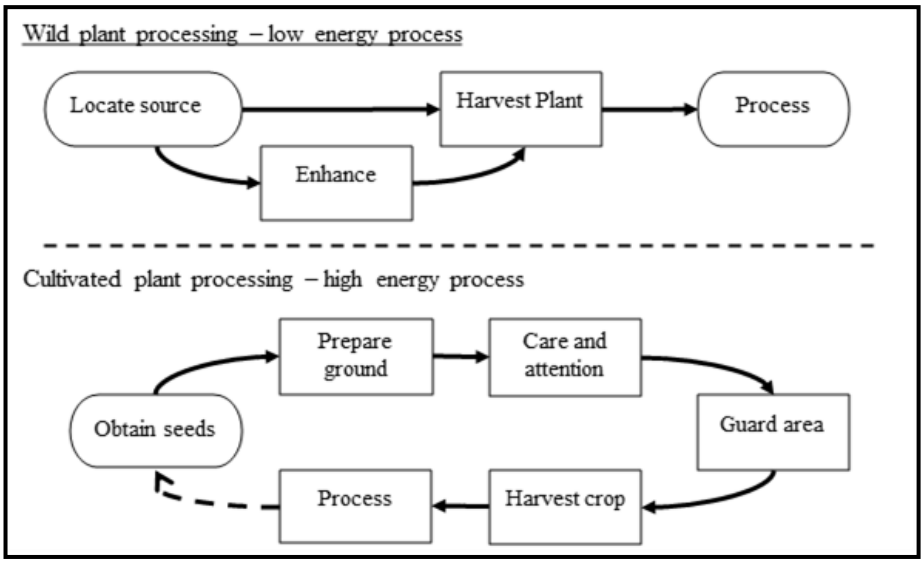

Figure 2.8. Consideration of social organisation strategies supporting wild and cultivated plant processing. Adapted from (Harris 1989: 11-26).

It is essential to define the type of plant being processed if the relationship of past societies and cultivation of specific plants for food and other uses are to be recognised (Ryder and Gabra-Sanders 1999; Larsson and Lagerás 2015; Soltvedt and Henningsmoen 2016).

Improvements in techniques for diagnosing plant fibres will aid the re-evaluation of some archaeological specimens to support the identification of the broad range of plant products used in past societies.

2.8 Ethnographic reports

	Location	Fibres	Period	Usage
North America				
Drucker (1911)	Nootkan-Vancouver	Nettle	1860-1885	Harpoon Fishing lines
Renker and Gunther (1990)	Makah-Vancouver	Nettle	1883-1888	Lanyard String
Densmore (1979)	Chippewa-Minnesota	Nettle	1905-1925	Bowstring, Fishing nets, Cordage
Hilger (1951)	Chippewa-Minnesota	Nettle	1932-1940	Bowstrings, Fishing lines
Asia				
Black (1973)	Nivkh-Amur	Nettle	1850-1899	Cordage, Thread
Schrenck (1854)	Gylyak-Amur	Nettle	1826-1894	Cordage, Thread
Jochelson (1908)	Koryaks-Kamchatka	Nettle	1897-1902	Fishing nets, Thread
Northern Europe				
Edom (2010)	Europe	Nettle	NA	Nettle cloth, String
Hald (1980)	Scandinavia	Nettle	NA	Nettle cloth, Fishing nets
Sirelius (1904)	Wogel, Finland	Nettle	1932-1940	Thread

Table 2.1 Tabulation ethnographic reports detailing the use of nettle plant fibre in the Northern Hemisphere (Yale University Human Relations Area File (eHRAF 2013) World Culture and Archaeology)

In compiling this resume of ethnographical reports on bast fibre utilisation, the ethnography data available from Yale University's information system "Human Relations Area Files" was reviewed (Yale University Human Relations Area File (eHRAF 2013)) World Culture and Archaeology. Table 2.1.

In general, the principal source of information drawn from this database is predominantly North American and Asian with minimal reporting from European sources. However, additional sources of European plant fibre usage are available from Scandinavia in studies by other authors (Hald 1980: 121-147; Hurcombe 2000: 155-173).

Additional, as previously noted, the history of nettle fibre usage in northern Europe and reports on the utilisation of nettle plant serves to broaden our consideration of plant fibre utilisation (Dunsmore 1985: 1-57; Edom 2010: 1-10).

2.9 Plant taxonomy

The principal fibres under investigation flax, nettle and hemp are all dicotyledons from the Angiosperm group, and their Linnaean binomial classification is shown below.

2.9.1 Flax. (*Linum usitatissimum* L.) Family Linaceae, Genus *Linum,* Species *Usitatissimum*

The genus *Linum,* totalling approximately 200 species, is mainly grown in temperate or sub-tropical climates and is further sub-divided by consideration of their end-use as oleaginous (oil seeds) or as textiles fibres. There are 36 *Linum* species detailed (Rast-Eicher 2016: 87-95; Gale and Cutler 2000: 152-155).

In an evaluation by the University of Wales, a total of 28 varieties of fibre flax were analysed to determine their productivity with a range 40-80kg/acre reported (Dimmock et al. 2005). Flax is grown in well-drained rich damp soil and the oil varieties are now favoured over flax textiles that have been overtaken by modern manufactured fibres. The genus is widely spread across Europe with 36 species listed in Flora Europa Vol.2 that includes several species recorded as “difficult to identify” (Tutin et al.1990: 206-211)

2.9.2 Nettle (*Urtica dioica* L.) Family Urticaceae, Genus *Urtica,* Species *Dioica.*

Urticaceae are common in the north temperate zone with approximately 30 species recognised. There are four species reported for the U.K. including fen nettle (*Urtica. galeopsifolia* L.), small nettle (*Urtica. urens* L.), “Pellitory of the Wall” (*Parietaria judaica* L.) and “mind your own business” (*Soleirolia soleirolii* L.) (Mabey 1996: 66-69; Gale and Cutler 2000: 268-270; Rast-Eicher 2016: 104-106). Flora Europa Vol. 1 lists eight *Urtica* species including the small nettle (*Urtica urens* L.) and the Roman nettle (*Urtica pilulifera* L.) (Tutin et al. (1993: 67-68). Nettle is recognised in its close association with human settlements where ground disturbances and the high phosphate soil levels produce fertile soils (Anderson 1952: 136-149). **Figure 2.9** illustrates the distribution of *Urtica dioica* in Europe.

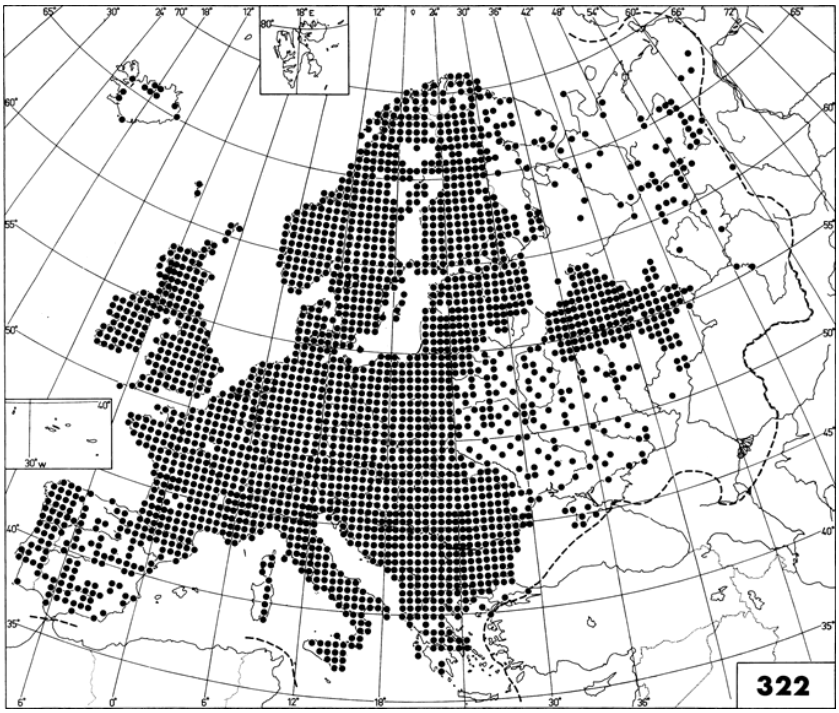

Figure 2.9. Distribution of the *Urtica dioica* group in Europe. The map includes *U. dioica, U. galeopsifolia, U.pubescens* and *U. sondenii.* (Taylor 2009: 1437, Fig.2 with additions*)* Growth intensity indicated by the black dots.

2.9.3 Hemp (*Cannabis sativa* L.) Family Cannabaceae, Genus *Cannabis,* Species *Sativa*

This annual, dioecious plant is native to the alluvial sands of South-East Russia and Asia, where the earliest usage in China 9000 B.C. as a narcotic is recorded (Gale and Cutler 2000: 64; Rast-Eicher 2016: 96-103). Hemp spread widely throughout Europe and was naturalised as both a medicinal plant and a textile before the Roman period (Mabey 1996: 62-63). There are records of seeds found in the excavation of an Augustinian Monastery in East Lothian Scotland (Moffat et al. 1989). In view of the narcotic content, the cultivation of hemp is now restricted in Europe and North America to varieties of low tetrahydrocannabinol (THC) content (THC) (Misuse of Drugs Act 1971,38(2) Class II).

2.10 Plant fibre sources-Progression of flax and hemp cultivation

In establishing a foundation structure for consideration of plant fibre utilisation, and to review the availability of nettle, flax and hemp as the primary sources of vegetable plant fibre it is necessary to place these plant sources within their geographic and chronological availability. This consideration is, of course, reliant upon the adequacy of the information provided, especially concerning the bias attributed to the crop/weed dilemma. While the information on flax and hemp cultivation is extensive, there are few similar reports for the nettle family *Urticaceae* of which the Stinging Nettle (*Urtica dioica*) is one of 500 species worldwide. Gleba (2008), in her discussions on pre-Roman textile production, tabulates both Bronze Age and Iron Age textile finds from a range of excavation sites. In the Bronze Age listing of 18 textile fibres, all but four are linen with one of the remainders noted as "bast". In the Iron Age listing of 37, the author reports all but ten as wool (probably reflecting the increase in animal husbandry), with two of the remainder noted as plant fibre, possibly "linen" (Gleba 2008: 82-84 and Tables 2a 2b).

2.10.1 Nettle (Urticaceae)

Hald (1980) and Edom (2010) are early reporters for nettle as a raw material in the Northern hemisphere. In addition to its use as a textile fibre material, nettle supplied additional benefits of food, fodder and medicine (Bodros and Bailey 2008; Pinelli et al. 2008).

The symbiotic relationship of humans to nettle plant is attested to in that humans produce the high phosphates and nitrates required to stimulate plant growth (Hald 1980: 124-147; Edom 2010: 5-7).

Figure 2.10. German WW1 Poster Sammelt Brennessell wenn ihr kleidung und Faden wollt. Auskunft Bayer Nesselstelle Munchen (Trans.) Collect nettle if you want clothing and thread. Information from Bavaria Nettle München Fürstenstr.

The self-cultivation of nettle, in contrast to the later exploitation of hybrid commercial plant, is seen as requiring no horticultural cultivation or care. However, this interpretation, perhaps based on current diagnostic bias, leads to an assumption that the plant only exists as an exploited weed. The concept of care, nurture, ownership, and protection of a valuable resource of the past are disregarded. Dunsmore (1985) reinforces this concept in a report on the use of (*Girardina diversifolia*) "*allo*" by the natives of Sankhuwasabha in Nepal where cultivation is controlled both by the villagers' ownership of harvesting areas and government supervision (Dunsmore 1985: 2-10). In response to the growing interest in nettle as a commercial crop, investigations were undertaken in Germany in the late 19th century.

With the trade embargo on the importation of cotton fibre in World War 1, German manufacturers used nettle fibre as a substitute in the manufacture of tents, rucksacks, undershirts and socks Figure 2.10.

Horne et al. (2008) reported on the work undertaken by Bredemann in the 1920s immediately following the war, and Dreyer et al. (1996) note the scheme initiated by the Institute of Applied Botany Hamburg, to select 30 of Bredemann's Stinging Nettle clones for re-evaluation. The study aimed to review the commercial potential of the clones to define the growth behaviour and fibre content achieved (Bredemann 1950: npn, [Cited in Horne et al. 2008: 63-70]; Dreyer et al. 1996: 28-39; Horne et al. 2008: 63-70). In contrast to the increased activity in Germany in the early 1940s, as outlined above, we note Bredemann's (1950) work and the significant wartime contribution of the commercial utilisation of Stinging Nettle as a textile fibre.

2.10.2 Flax (Linaceae)

The considerable corpus of information on the cultivation and chronological availability of flax provides an illustrative contrast to the above comments on nettle utilisation from early considerations (Pounds 1974: 219, Hald 1980: 127) Zohary and Hopf 2000: 126-132; Gleba 2008: 66-67; Cruikshank 2011: 239-260; Karg 2011: 506–508; Viklund 2011: 509-515)

Zohary and Hopf (2000), note that flax cultivation serves two products, linseed oil and linen textile fibre. The original oil producing *Linum bienne* is recorded as widely distributed in the Mediterranean basin, North Africa, the Near East, Iran and parts of eastern Europe (Zohary and Hopf 2000: 126-127). The flax fibre plant, *Linum usitatissimum*, is a derivative from this wild version *Linum bienne* and Wild (1970) details the chronological expansion from its origins to Syria 6000 BC, Mesopotamia 5000 BC, Central Europe 4000 BC to be present in Spain and Portugal circa 2000 BC. In terms of distribution the review of Roman textile manufacturing, suggests that linen did not have a wide circulation in the "northern provinces" and that any recorded finds may have resulted from Italy and Gaul imports (Wild 1970: 15 and 44).

Hald (1980) confirms this understanding with a comment that,

> "(F)lax has not been established with certainty among Danish finds before the pre-Roman Iron Age" (Hald 1980: 127).

Gleba (2008), refers to considerations of plant fibre textile in pre-Roman Italy to confirm the above dates and adds that, until recently, it was considered that,

> "(I)n view of the few archaeological textile finds in Northern Italy the fibre was imported from Asia Minor" (Gleba 2008: 65-67).

Karg (2011) provides the map Figure 2.11 to illustrate the distribution of both wild and domesticated flax and the differential oilseed/textile end-use diagnosed in the early Pre-Pottery Neolithic (PPN) and Neolithic.

Harris (2014: 9 and Fig.1) adds to Karg (2011) to include textile finds associated with the flax seed Figure 2.13. Pounds (1974) and Walton (1989) discuss an extract from the 9th century inventory of Saint-Pierre at Ghent monastic landholdings to provide the earliest reference to flax as a commercial crop. In the listing, approximately a quarter of the holdings are detailed as bipartite in that the produce is shared with the abbey. From the "*demesne mansus"* Villa of Businiacas the products listed include:

> "(A) pound of flax a chicken and five eggs" (Pounds 1974: 51-52; Walton 1989: 313).

The earliest reference to flax growing in England is given by Swanton (1975) in his "*Anglo Saxon Prose"* where he records an Anglo-Saxon reference to the duties of the manorial reeve associated with flax cultivation and the supply of flax lines, reel yard-winders, and combs (Swanton 1975: 26-27). In a similar illustration, Zohary and Hopf (2000) depict the expansion of Near East Neolithic crop assemblages in Europe, West Asia and the Nile Valley (Zohary and Hopf 2000: 243-246 and Map 20).

Barber (1991) considers the relationship between loom type and textile fibre to provide a series of isochrone maps to represent the fibre distribution pattern in the European second millennium BC (Barber 1991: 249-2512 and Fig. 11.1).

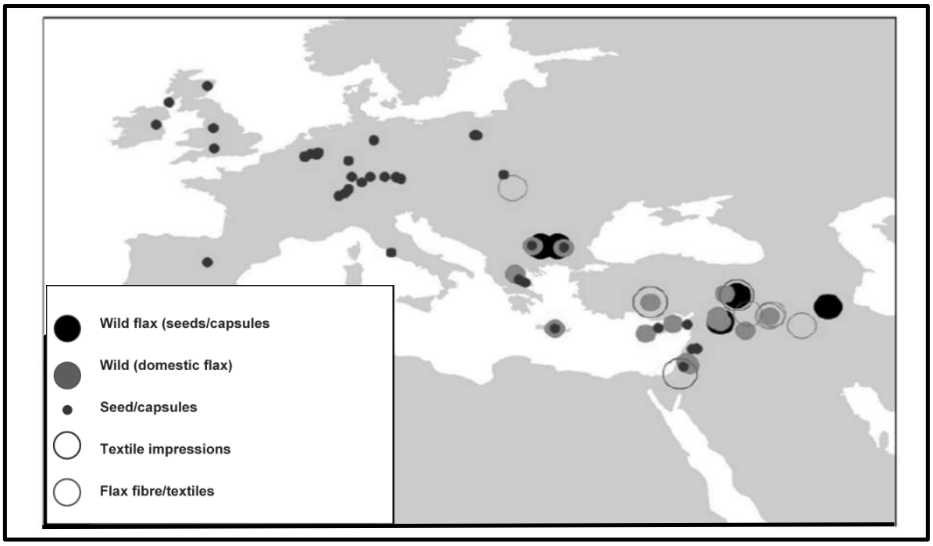

Figure 2.11. Presence of wild and domestic flax seeds/capsules and textiles impressions in aceramic and early Neolithic sites (Karg 2011: 506-508 and Fig.1 with additions.). (The map is credited to Sue Colledge (UCL, UK) and James Conolly (Trent University, Canada).

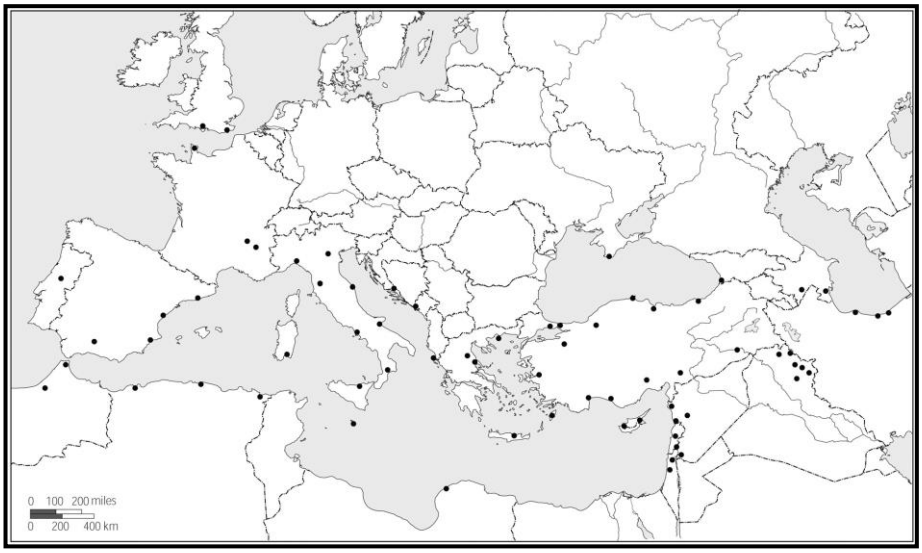

Figure 2.12. Distribution of archaeological finds of wild flax in Europe: (Linum usitatissimum L.) subspecies (*Linum bienne* L.) in the PPN Neolithic (Weiss and Zohary 2011: Fig. 8).

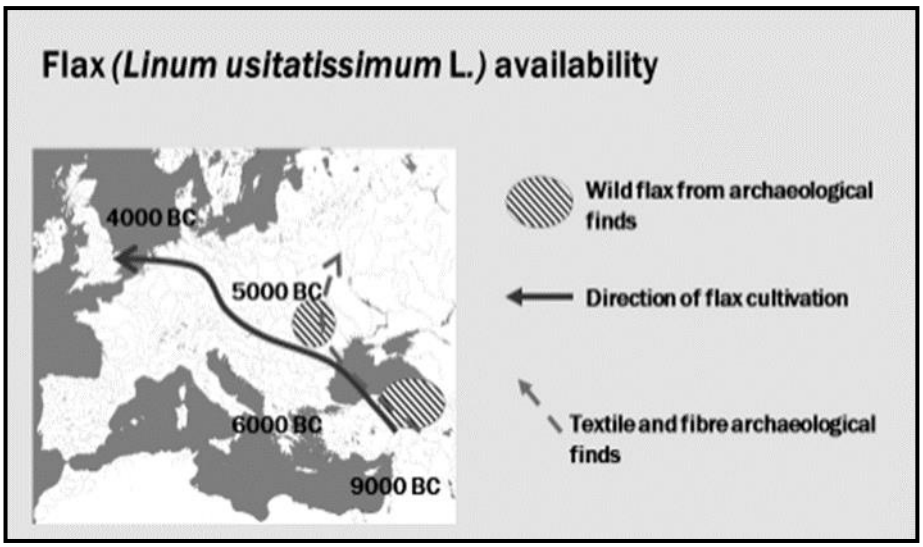

Figure 2.13. Illustration that proposes the introduction of flax to the UK at (4000 BC) and the presence of wild and domestic flax seeds /capsules and textile impressions to early European Neolithic sites. (Karg 2011: 508; Harris 2014: 9 and Fig. 1. with additions).

Weiss and Zohary (2011: Fig.8), in their consideration of the domestication of Southwest Asian founder crops during the Pre-Pottery Neolithic period (PPN), included two flax subspecies, oil varieties, which are relatively short (30–70 cm) and branched and usually bear large seeds, while fibre varieties are taller and sparsely branched and usually produce small seeds.

2.10.3 Hemp *(*Cannabaceae)

Hemp fibres are strong but less fine than nettle or linen; and are therefore generally restricted in use to the production of rope or cordage or as a coarse weave for sack or sailcloth manufacture (Zohary and Hopf 2000: 16-17

The slow westward progress of hemp before the Roman period advanced along two different routes, north of the Danube to Germany and, in the mid-third century BC, via a Mediterranean route to the Rhone Valley (Zohary and Hopf 2000). Hemp serves three purposes, as a supply of bast fibre, for oil extraction from seeds, and as a psychotomimetic drug (Zohary and Hopf 2000: 132-133 Clark and Merlin 2013).;). The authors note that, at the date of their report, there were no archaeological records to inform the early establishment of the plant and propose that the plant would have originated early in temperate Asia (Zohary and Hopf 2000: 132-133). A view that was subsequently confirmed by Clark and Merlin (2013)and Rast-Eicher 2016: 96).

Clarke and Merlin (2013: 59-133), in an extensive review of the cultivation of *Cannabis* sp. (L.), prepared an isochrone dispersal map based on plant biotypes and as evidenced by fibre and textile finds to construct the map shown below **Figure 2.14**. However, there are difficulties in obtaining modern reference hemp fibres due to the restriction in hemp farming. This embargo was lifted in 1997, whereby hemp cultivation is regulated by licence for commercial farming of 0% tetrahydrocannabinol (THC) (Misuse of Drugs Act 1971,38 (2) Class II). *Cannabis sativa* L. v. Santhica is now grown for oil-seed production and samples of commercial hemp plant fibres were harvested for evaluation (East Yorkshire Hemp 2017). Traditional textile hemp with high THC may be available from overseas; however, the present samples will suffice as base diagnostic material.

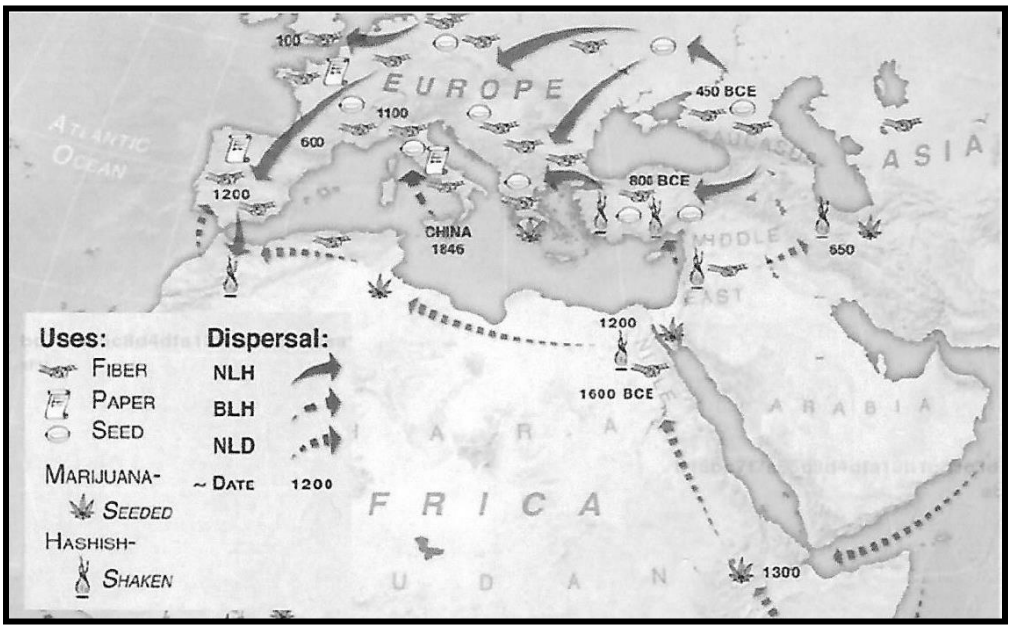

Figure 2.14. Dispersal of *Cannabis* and its uses, in Europe and North Africa. The map is based mostly on historical evidence (Cartography by M. Barbee). (Clark and Merlin 2013: 101(Map 7) with additions). Note the date for the dispersal of hemp into the UK at 100AD. Nomenclature. NLH Narrow leafed hemp (*Cannabis sativa*) ssp s*ativa* Europe. BLH Broad leaf hemp (*Cannabis indica*) ssp *chinensis* China, Korea Japan and South East Asia. NLD Narrow leaf hemp (*Cannabis indica)* ssp *indica* South and South East Asia.

2.11 Summary -plant fibre cultivation and history

In the above, evidence for the introduction and utilisation of native and non-native plant fibre have been reviewed. The comparison of organic and inorganic archaeological assemblages, with 95% of organic material undetected, results in an understatement of their archaeological presence. For native plant fibres, there are extensive ethnographic reports for a variety of cord and rope manufacture and primary textile assembling that confirm their usage even in modern times.

As is evident from the botanical images presented above, there is a commonality of plant fibre morphological features that enhances the interpretive dilemma. A diagnostic dilemma that is additionally challenged by fibre processing, fungal and micro bacterial degradation, and post-excavation treatments. In conclusion, in order to rationalise the chronological threshold for the introduction and utilisation of alternative plant fibre resources, there is a requirement to improve both the recovery of fibre traces from site depositions and the enhancement of plant fibre diagnostic techniques.

Chapter Three
Appraisal of Textile Fibre Assemblage, Research Design Parameters: -Aims and Objectives

3.0 Interpretive dilemma

In the preceding chapter, the chronological horizons for the introduction of non-native plant fibres, flax and hemp, and the botanical attributes that support their application within textile utilisation, have been reviewed. The limited availability of archaeological remains reinforces the "interpretive dilemma" in that the artefacts are diagnosed within a subjective judgement based on the analyst's experience (Wiley 1989: 1-6). The diagnosis of archaeological fibre can thus be based on a deductive or inductive process (Peacock 2001: 181-189; Bender-Jørgensen 2007: 7-12; Wild 2007: 1-6; Hurcombe 2008: 83-105; Outram 2008: 1-67).

Additionally, the deductive diagnosis based on inferential evidence from fibre/textile remains held in close association with textile tools and production processes spindle whorls, loom weights, and retting pits, adds to the interpretive dilemma. (Hedges 1983: 73-85; Martin and Murphy; 1988: 353-358; Barber 1991: 249-251 and Fig. 11; Moore and Jennings 1992; Walton Rogers 1997: 1737; Peyronel 2007: 26-35; Fuller 2008: 1-19; Andersson-Strand 2010: 149-173; Stolcova and Grömer 2010: 9-10; Andresen and Karg 2011: 517:526; Cruikshank 2011: 239-260; Dimova 2016: 652-680; Grömer 2016: 22-82). The relationship between textile tools and structures that serve to support evidence of textile production is explored further in **Chapter Four**.

Inductive diagnosis, the compliance with derived hypothesis tested within an experimental format is directed to reconstructing the textile production processes to establish evidence of the changes that could be indicative of a

diagnostic relationship. Of particular interest is the investigation of tool wear as evidence of the association with the cultivation and harvesting of plant fibre and the subsequent extraction and processing of the fibre material (Gonzalez et al. 2003: 481-489; Evans and Donahue 2005: 1733-1740; Andersson-Strand et al. 2010: 2; Hurcombe 2010: 129-139; Evans 2014b: 5; Van-Gijn and Little 2016: 135-153; Hayes et al. 2017: 245-260). Also, Forte and Lemorini (2017) conducted an appraisal of spindle whorl and spool tool wear to ascertain that funereal depositions held within tool wear striations were indicative of practical usage and were not unused symbolic depositions (Forte and Lemorini 2017). The presence of non-native species such as flax or hemp with textile tools enhances the interpretive determinacy as their presence is indicative of purpose-driven human intervention. In contrast, for nettle, a ruderal weed, the dilemma arises from the nettle plants tendency to colonise dump heaps on human occupation sites, which adds difficulty to their diagnosis.

3.1 Commonality of Chronology

In a review of diagnostic features, fibre types are considered within their chronological horizons as outlined below. Placement, within the particular typological age, reflects the variation in the determination of the periods of introduction of non-native plant across Europe. In order to provide a standard chronological reference, the data reviewed below will adhere to a chronological structure based on a Central Europe chronology as illustrated in Table 3.1 below.

The chronological periods depicted in Table 3.1 reflect both the commonality of period description (shaded) with arrows tom indicate the variation in duration.

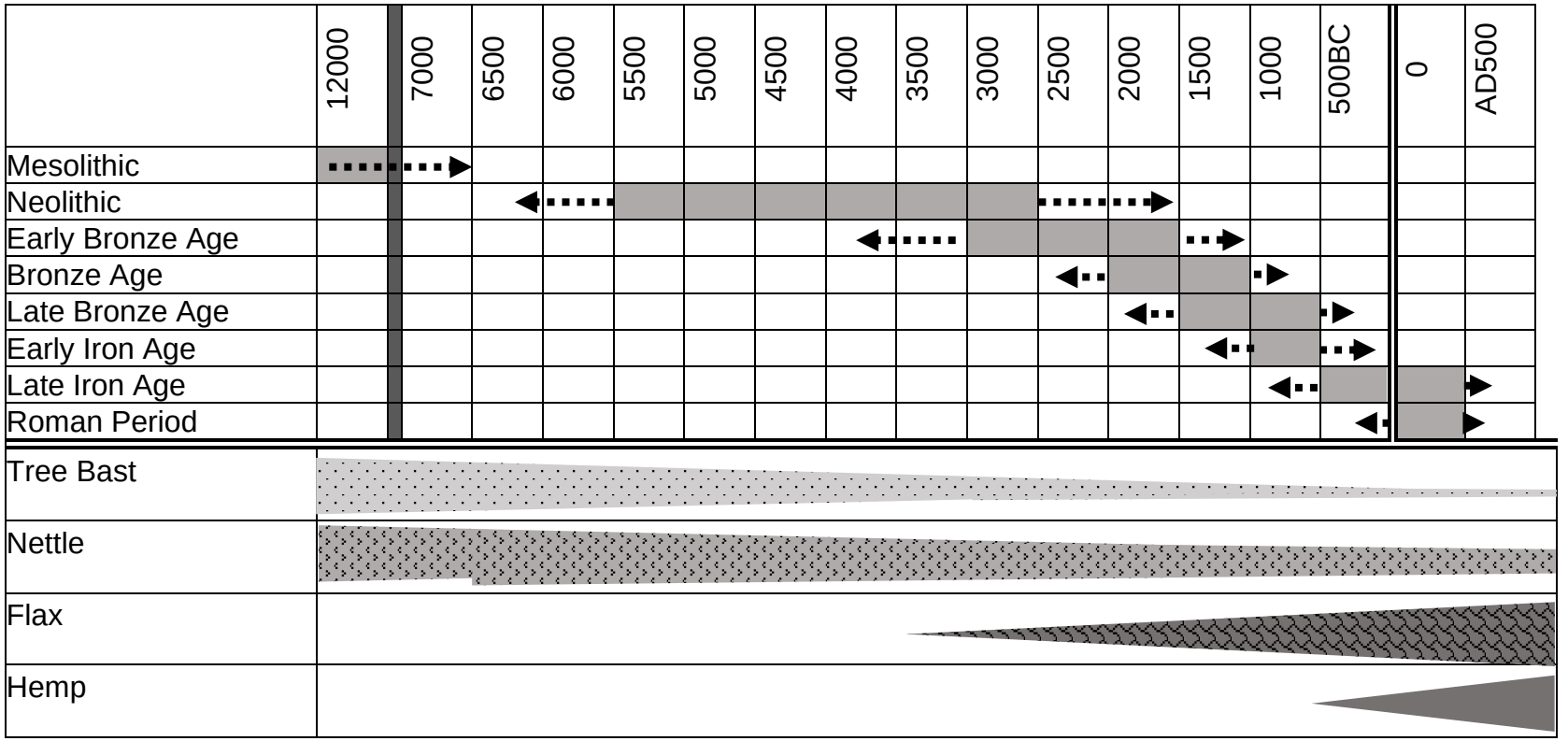

Table 3.1 Central European chronology. The availability and intensity of plant fibre utilisation are illustrated by the increasing/decreasing image width within the cells. The arrows depict the North/South limits of the Central European chronological periods ascribed (Gleba and Mannering 2019: 90.121,184,242,265,274,292,305,333,348.366,398,427) (The tabulation includes a reflective view on the utilisation of tree-bast and nettle to illustrate the relationship of the threshold to the introduction of flax and hemp).

3.2 Review of archaeological assemblages in Central Europe

The recording of plant fibre identifications included within archaeological assemblages for Central Europe has been catalogued and these listings were reviewed to determine those reports that register flax/fibre identifications as unreliable or listed as unknown plant fibre (Bender-Jørgensen 2005: 133-150; Gleba 2008: 43-63; Grömer 2019: 45).

Listing	Wool	Pseudomorphs undefined	2	Flax?? uncertain diagnosis	Hemp positive diagnosis	Plant fibre unspecified	Unnamed fibre	String/Cord unspecified	Unknown	Total
A	21	172	5	5	0	0	3	5	1	212
B	5	39	8	0	3	4	29	2	2	92
C	4	0	0	5	0	0	9	0	1	19
Total	30	211	13	10	3	4	41	7	4	323
%age.	10%	65%	4%	3%	1%	1%	13%	2%	1%	100%

Table 3.2. Detail extracted from catalogues of fibre assemblages in Western Europe listed and reviewed. A. Listed by Bender-Jørgensen (2005: 140-148), B. Listed by Gleba (2008: 43-63): C. Listed by Grömer (2019: 45).

Table 3.2 illustrates the difficulty in determining plant fibre types from pseudomorph impressions in calcified deposits or held in close association with a metallic material. While the pseudomorph images, 65% of the total, served to identify thread count and fabric spinning and weaving structure, the fibre types are undefined. A further 13% were described generally as fibre, with only 5% diagnosed as flax or hemp. The wool fibre was classified in 10% of the samples. The limited number of plant fibre samples and the uncertain diagnoses directs attention to the requirement for a review of methods employed in plant fibre identification Table 3.3.

Listing	Wool	Flax	Flax??	Hemp	String/Cord	Unknown	Total
A	21	5	5	0	5	1	37
B	5	8	0	3	2	2	20
C	4	0	5	0	0	1	10
Total	30	13	10	3	7	4	67
Total%	46%	19%	15%	4%	10%	6%	100%

Table 3.3. A reappraisal of plant fibre identification with the exclusion of pseudomorphs and non-descriptive fibre.

Table 3.3 confirms the difficulty of attributing a positive plant fibre diagnosis. Even where pseudomorphs and non-identified fibres are excluded only 19% of the records were positive identifications and 15% were tenuous fibre determinations. These positive and tenuous diagnoses are plotted in **Figure 3.1**. and listed in **Table 3.4.**

Figure 3.1and **Table 3.4** include indeterminate fibre diagnosis from archaeological assemblages plus reports from assemblages outside the selected region, included for illustrative purposes, to provide a total of 33 archaeological samples that demonstrate the interpretive dilemma.

Section 3.3.1 provides details for each assemblage and illustrations where appropriate. The site locations are shown in **Figure 3.1**. **Table 3.2** and **Table 3.3** The accompanying map, **Figure 3.1,** illustrate the variation in the number of plant fibre identifications listed, assemblages from France, Germany and Spain are particularly concerning. For Germany it is noted that,

> "(I)n comparison to the size of the country and the long time span the actual amount of extant fabrics is rather scant and German scholars were forced to rely on Danish finds" (Möller-Wiering 2019: 122).

In the entries for France Bender-Jørgensen (2005: 147) listed seven assemblages where six were associated with metal objects and only one fibre identified as wool. Spanish assemblages were not included in Bender-Jørgensen's (2005) Central European tabulation. However, while Alfaro (2019: 334-346) reports several assemblages from Spain, including Cueva Sagrada, (in **Figure 3.1)** it is noted,

> "(T)hat scholarship in Spain generally consists of publications of textile tools" (Alfaro 2019: 337).

Figure 3.1. Plot of locations of sites listed and numbered in Table 3.4 numbered in chronologoical order.

No	Location	Diagnosis	Type	Period	Author
1	Lascaux Cave France	Bast?	Cord	Paleo	Glory (1959)
2	Ohalo Israel	Bast?	Rope	Paleo	Nael et al. (1994)
3	Dzudzuana Caucasus	Flax?	Fibre	U Paleo	Bar-Yosef et al. (2011)
4	Bouldnor Cliff England	Bast?	String	Neo	Gaffney et al. (2015)
5	Robenhausen Switzerland	Flax/Lime	Fibre	Neo	Higgett et al. (2011)
6	Sweet Track England	Nettle?	Fibre	Neo	Coles et al. (1973)
7	Ditfurt Germany	Wool/Flax	Fragment	L Neo	Möller-Wiering (2019: 126)
8	Latdorf Germany	Wool/Flax	Fragment	L Neo	Möller-Wiering (2019: 126)
9	East Switzerland	Flax/Lime	Fibre	L Neo	Leuzinger and Rast-Eicher (2011)
10	Cueva Sagrada Spain	Flax?	Textile	EBA	Alfaro (2019: 338)
11	Molina de Ledro Italy	Flax?	Fragment	EBA	Bazzenella (2003)
12	Vulci Italy	Plant/Flax	Fibres	EBA	Gleba and Turfa (2007)
13	Whitehorse Hill England	Nettle?	Fibre	EBA	Harris (2016)
14	Arslantepe Malatya Turkey	Bast?	Fragment	BA	Frangipane et al. (2009)
15	Harlyn Bay England	Flax?	Fibre	BA	Jones et al. (2011: 92, Fig. 4)
16	Pyotdykes Scotland	Flax?	Fibre	BA	Coles et al. (1964)
17	Over-Barrow England	Flax/Nettle	Fibre	BA	Harris (2015: 73-81, Fig. 6.3)
18	Lusehøj Voltoft Denmark	Flax/Nettle	Textile	LBA	Bergfjord et al. (2012)
19	Must Farm England	Nettle?	Fibre	LBA	Cambridge Arch. Unit (2016)

Table 3.4 Chronological listing of archaeological textile artefacts with fibre material diagnoses, as attributed by the authors. Diagnosis, the listings show uncertain diagnosis, i.e. Flax? or alternative diagnoses, e.g. Wool/Plant. Type is as described by the authors.

No	Location	Diagnosis	Type	Period	Author
20	Valle delle Paiole Italy	Plant?	Textile	LBA	Gleba (2008: 44(4))
21	Casale Marittimo Italy	Bast?	Fabric	EIA	Gleba (2008: 50(22))
22	Civita Castellana Italy	Plant?	Fragment	EIA	De Lucia Brolli (1998)
23	Eberdingen-Hochdorf Germany	Hemp?	Textile	EIA	Bank-Burgess (2019: 147)
24	Huldremose Denmark	Nettle?	Textile	EIA	Mannering et al (2019: 103)
25	Belish Bulgaria	Plant/Hemp	Fabric	IA	Dimova (2016)
26	Zagreb Croatia	Flax?	Fabric	IA	Uranić (2006)
27	Bucovice Brno Moravia	Flax?	Fibre	LIA	Bender Jørgensen (2005: 140(10))
28	Funen Denmark	Flax/Nettle	Residue	LIA	Henriksen and Runge (2009)
29	Söderby Sweden	Flax?	Fragments	LIA	Franzén et al (2019)
30	Komárno Slovakia	Flax?	Fibre	LIA	Bender Jørgensen (2005: 141(29))
31	(Museum Moravia) Brno	Flax?	Textile	LIA	Bender Jørgensen (2005: 141(26))
32	Schrattenberg Austria	Flax?	Fibre	LIA	Bender Jørgensen (2005: 143(85)
33	Slavkov Moravia	Flax?	Textile	LIA	Bender Jørgensen (2005: 141(22)

Table 3.4 (cont.) Chronological listing of archaeological textile artefacts with fibre material diagnoses, as attributed by the authors. Diagnosis, listing shows uncertain diagnosis, i.e. Flax? or alternative diagnoses, e.g. Wool/Plant. Type is as described by the authors.

3.3 Archaeological assemblages

The fibre textile assemblage tabulations appraised are detailed above to offer a base for further consideration of the plant fibre diagnostic features identified. As listed in **Table 3.**4, additional information for references that record the absence of fibre identity, or doubts expressed on the validity of the diagnosis are included in the following section.

3.3.1 Selection of archaeological assemblages

A selection of prehistoric archaeological assemblages that include fibres, mainly from Northern European sites, along with their fibre identifications is shown below. The reported fibres include string, cord and prepared mixed fibres, nettle/flax, hemp and nettle.

3.3.1.1Lascaux Cave-Dordogne France Palaeolithic

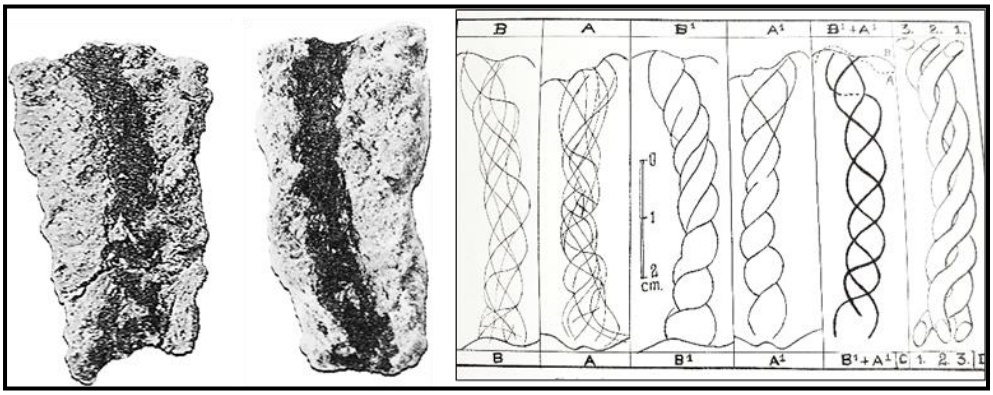

Figure 3.2. Lascaux Cave fragment (Glory1959: 135-169 (no scale)).This 30cm length of cord, dated to the Palaeolithic (15,000 BC) was discovered by Abbé Glory in 1953.

The cord was twisted in the “S” direction and incorporated three “Z” plied strands. Although the cord had deteriorated, considerably it was identified as bast fibre. The image on the right is Gory’s reconstruction of the encrusted three-ply fibre construction (Glory 1959: 135-169(no scale); Barber 1991: 40).

3.3 1.2 Ohalo II-Tiberias Israel Palaeolithic

At Ohalo ll, a Palaeolithic site was exposed due to a significant drop in the water level of the Sea of Galilee in 1989. In the excavation of the floor of a burnt hut, three charred fibre fragments (circa 20-30 mm) were found. The fibres dated at 17,000 BC. with a fibrillar orientation of 20^0, were identified as monocotyledons hence neither nettle nor flax. These fibres, from stems or leaves, are recognised as the oldest rope (Nadel et al. 1994: 454, Fig.4).

3.3 1.3 Dzudzuana Cave-Caucasus-Eurasia Upper-Palaeolithic

There are claims that this find, radiocarbon dated to circa. 20000 BCE is the oldest fibre in Europe. The cave finds included lithics, bone tools, and coloured fibres identified as wild flax (Bar-Yosef et al. 2011). However, there are queries as to the validity of the claim, suggesting that the fibre could have been blown into the cave and became twisted due to disturbance by natural air currents (Breniquet 2013: 6). Additionally, there are concerns regarding the identification of the fibre as flax (Bergfjord et al. 2010: 1634; Bar Yosef et al. 2011).

3.3.1.4 Bouldnor Cliff-Solent England Mesolithic

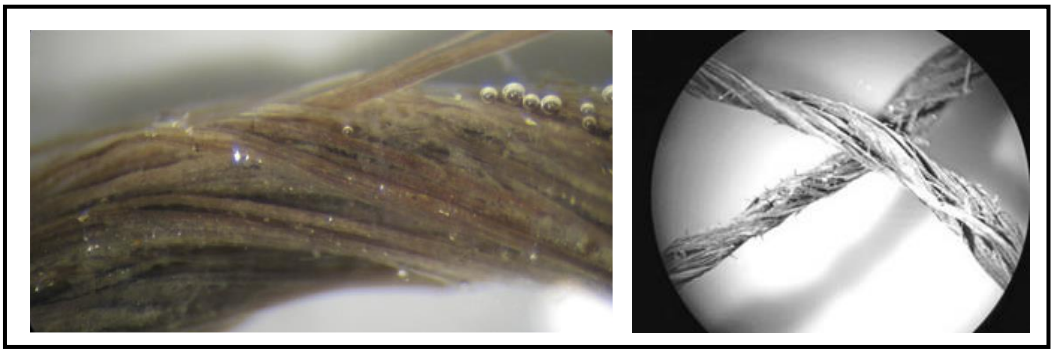

Figure 3.3. String fragment, Bouldnor Cliff (Peeters and Momber 2014).

At Bouldnor Cliff the archaeological assemblage was reported to include twisted fibre excavated from a submerged hunter-gatherer camp off the Isle of Wight. Shown right, the 11cm length of string was excavated from an organic layer, carbon 14 dated to 6240-6000 BCE, and as such is recognised as the oldest prepared fibre string found in the U.K. Shown left, fibre Z twist detail (Peeters and Momber 2014; Gaffney et al. 2015).

3.3.1.5 Robenhausen-Wetzikon Switzerland EBA

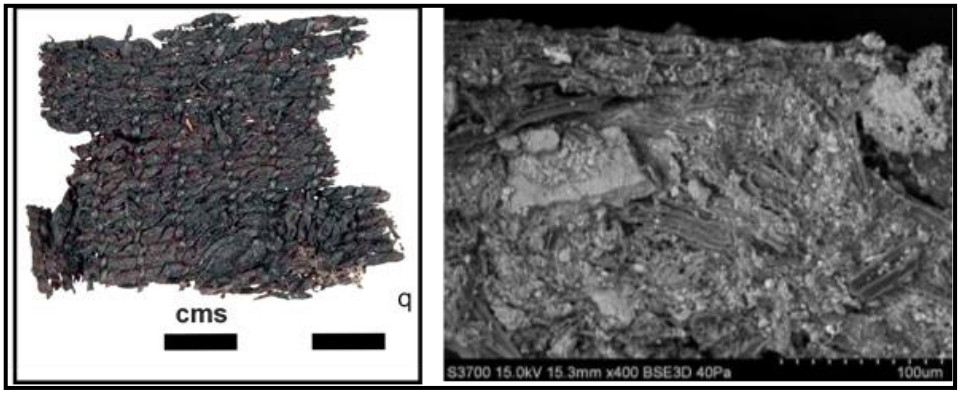

Figure 3.4. Twinned material from waterlogged site at Robenhausen (Higgitt et al. 2011: 86 Fig.3b, Fig.6).

This open twined material comes from waterlogged settlements excavated from the shores of alpine lakes. The main features of the fibres, diagnosed originally as flax, but may be tree-bast, were visible although the diameters and dimensions of the fibres have changed due to being waterlogged and dried out. The SEM image on the right illustrates the poor condition and tangled assortment of the fragmented flax and lime fibres (Higgitt et al. 2011: 86 Fig.3b, Fig.6).

3.3.1.6 Sweet Track-Somerset Levels England Neolithic

In the excavation of the Sweet Track in Somerset, within the debris of Site B, fragments of grass-rope were found along with fibres attached to an arrowhead. These were tentatively identified as nettle used to attach the arrowheads although the diagnosis is still under review. The waterlogged environment served to preserve the fibre. The authors suggested that, while the rope may have had many potential uses, there was insufficient information to confirm this (Coles et al.1973: Fig 29; Hurcombe 2008: 86).

3.3.1.7 Ditfurt-Germany Late Neolithic

A Late Neolithic tabby fragment of woven textile was identified as constructed from long wool fibres. A later examination described the fibres as plant fibre probably flax (Hertel and Grömer 2019: 130, Fig. 4; Möller-Wiering 2019: 126).

3.3.1.8 Latdorf-Germany Late Neolithic

In a similar report to the above, wool fragments from Spitzes Hoch were re-examined to confirm that these could be flax (Hertel and Grömer 2019: 13, Fig.5; Möller-Wiering 2019: 126).

3.3.1.9 East Switzerland Late Neolithic

In consideration of Neolithic fibre processing in East Switzerland, a comparative evaluation was undertaken between flax and lime bast fibre. Flax fibre, S plied 0.3mm diameter, were from Zurich-Breitingerstrasse, and a lime-bast fibre, S plied 0.7mm diameter, from Zurich-Mythenschloss were compared. The study proposed that, where the retting process was incomplete, there would be difficulty in distinguishing between the two fibres (Leuzinger and Rast-Eicher 2011)

3.3.1.10 Cueva Sagrada-Spain Early Bronze Age

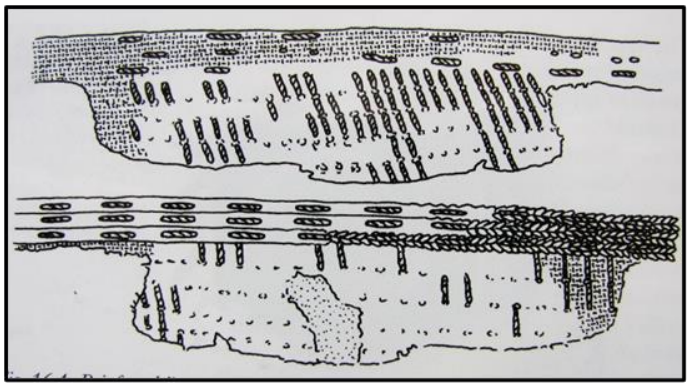

Figure 3.5. Early Bronze Age folded textile (Alfaro 2019: 338).

A folded two-piece Early Bronze Age textile was discovered in Lorca Mercia beneath a dual burial. The construction, shown above, suggests a fabric intended for clothing. This textile, described as very fine balanced tabby, was woven from 0.1-0.2 mm threads with a thread count 21/28 threads/cm. While only part of the textile was preserved in this rich set of grave goods, the fine fibre was judged to be linen (Alfaro 2019: 338).

3.3.1.11 Molina de Ledro-Italy Early Bronze Age

There is an extensive collection of textiles from this EBA site in Northern Italy, including a fragment composed of flax, tree bast and wool. The authors note that, while the primary fibre was flax, the carbonised remains make diagnosis difficult (Bazzanella 2009: 206).

3.3.1.12 Vulci-Italy Early Bronze Age

These fibres were discovered in association with 44 bronze buttons among the cremated remains of a young woman. Microscopic examination of the burial urn contents revealed fibre threads securing the buttons. The threads were described as fibres of plant origin, probably linen (Gleba and Turfa 2007).

3.3.1.13 Whitehorse Hill-Dartmoor England Early Bronze Age

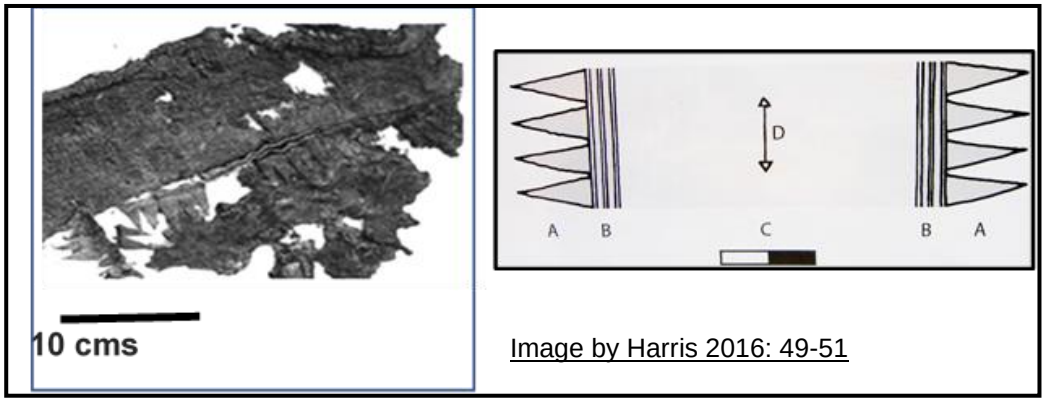

Figure 3.6. Early Bronze Age cremation assemblage Whitehorse Hill (Harris 2016: 49-51; Williams 2016: 25-32, Fig. 3.23).

This fibre, attributed to nettle, was found in an Early Bronze Age cremation assemblage of organic and other items. The item was identified as well-preserved calfskin held together with a series of two-ply woven nettle.

The image on the right illustrates the construction of the fabrics piece. As with previous identifications, this nettle interpretation is described as “cautious” (Cameron et al. 2016: 64-68; Cartwright 2016: 72-74; Harris 2016: 49-51; Williams 2016: 25-32, Fig. 3.23).

3.3.1.14 Arslantepe-Malatya Turkey Bronze Age

There were circa 300 textile tools recovered from this long and continuous habitation site at Arslantepe, mainly loom weights and spindle whorls. Unfortunately, while their presence is evidence of textile working, the textile fibres are not identified other than in generic terms as fibres (Frangipane et al. 2009).

3.3.1.15 Harlyn Bay-Cornwall England Bronze Age

At Harlyn Bay, Cornwall, a vessel was found in a stone covered pit. The assemblage included a small bronze pendant with mineralised fibres attached. A rectangular longitudinal section of plant fibres was identified as similar to flax (Jones et al. 2011: 92).

3.3.1.16 Pyotdykes-Angus Scotland Bronze Age

A plug of vegetable textile fibre was found in the socket of a spearhead recovered from the excavation of a Bronze Age site at Pyotdykes in Angus, Scotland. This small fragment (38mm x 19mm) of rare Bronze Age textile was woven with unpigmented straight fibres of vegetable origin.

The diagnosis, as fine flax fibres, was confirmed by the reaction with Shirlastain, a chemical reagent of unknown specification, to confirm the fibre as probably flax (Coles et al. 1964: Fig.20).

3.3.1.17 Over-Barrow-Cambridgeshire England Bronze Age

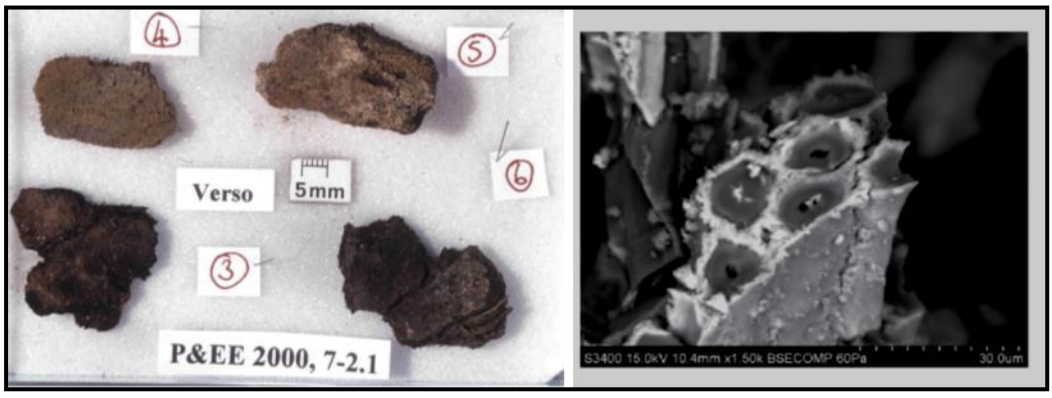

Figure 3.7. Bronze Age Fibre fragments from Over-Barrow (Harris 2015: 73-81, Fig 6.3).

Four amalgamations of charred plant fibre are shown on the left. The charred fibre was found within a pit cremation, preserved in heavy dirt encrustation.

The SEM analysis of plant fibre morphology and fibre cell characteristic cross-sections are shown on the right to confirm these as bast fibres, possibly flax or nettle. However, no firm identification was made (Harris 2015: 73-81, Fig 6.3).

3.3.1.18 Lusehøj Barrow-Voldtoft Denmark Late Bronze Age

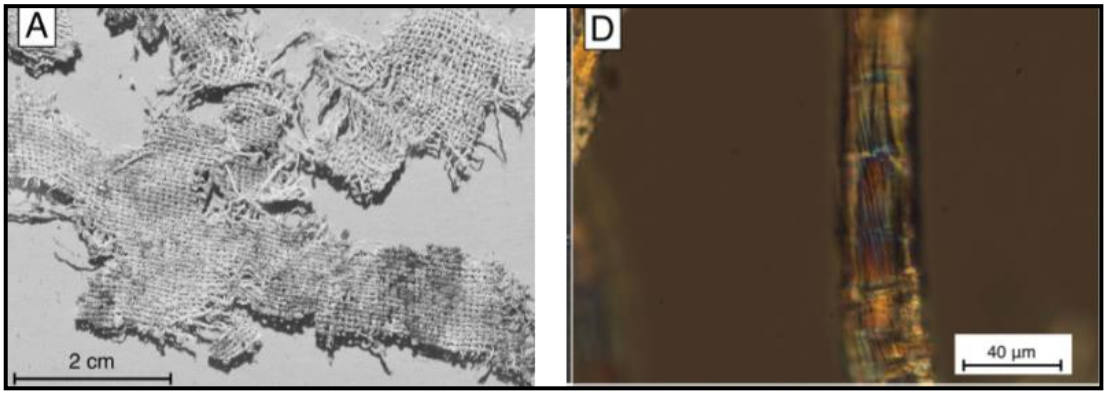

Figue 3.8. Lusehøj Barrow Late Bronze Age fibres (Hald 1980: 126, Fig 117; Bergfjord et al. 2012: Fig 1A).

These pieces of LBA woven textiles were found inside a bronze urn wrapped around cremated human remains. The fibres were initially identified as flax (Hald 1980:126: Fig 117). A subsequent review, using polarised light microscopy and analysis of calcium oxalate cystolith crystals, was used to redefine the fibre as nettle (Bergfjord et al. 2012: Fig 1A).

3.3.1.19 Must Farm-Cambridge England Late Bronze Age

The Late Bronze Age excavation at Must Farm was carried out by Cambridge Archaeological Unit while investigating a well-preserved settlement. Among the assemblage was a weft-wound collection of textile-fibres preserved in the river sediment. The fibre has been tentatively identified as nettle. Diagnosis is currently under review (Cambridge Archaeological Unit 2016).

3.3.1.20 Valle delle-Paiole Italy Late Bronze Age

Fragments of a folded EBA tabby textiles were recovered from this North Italy site. The weave was determined as two-ply Z wool and plant fibre construction (Gleba 2008: 44 (4)).

3.3.1.21 Casale Marittimo-Italy Early Iron Age

The EIA tombs at Castle Marittimo contained animal and bast fibre pieces along with a selection of indefinable utilitarian fabrics. In Tomb A and Tomb G, fibres were located in pseudomorph form (Gleba 2008: 50(22), Fig. 32).

3.3.1.22 Civita Castellana-Italy Early Iron Age

Several mineralised textile fragments were found in multiple Early Iron Age deposition. There were traces of plant fibre attached to an iron dagger, and an iron razor blade (De Luca Brolli 1998: 188, Fig. 4,5,6,7; Gleba 2008: 54(42)).

3.3.1.23 Eberdingen-Hochdorf Germany Early Iron Age

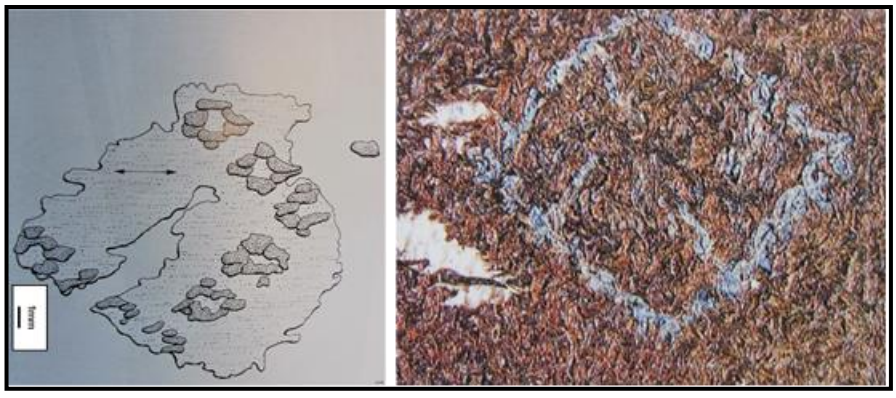

Figure 3.9. Textile fragments from the Eberdingen-Hochdorf Princely Burial (Banck-Burgess 2019: 143, 146, Fig. 5.10).

A rose-patterned tablet weave from the chariot, shown left and textile from the cauldron with a diamond symbol in blue, shown right. Both fibres were identified as plant fibre, possibly hemp (Banck-Burgess 2019: 143, 146, Fig. 5.10).

3.3.1.24 Huldremose-Denmark Early Iron Age

There are reports that the Huldremose Woman, in addition to her outer wool clothing, was also wearing a nettle fibre garment. This determination suggests the possibility that similar burials from the same period may also have textiles manufactured from plant fibre (Mannering et al. 2019: 103-104).

3.3.1.25 Belish-Bulgaria Iron Age

Dimova (2016) comments on the lack of knowledge of plant fibre in Bulgaria. The presence of flax has been established in Early Iron Age contexts at Svilengrad and from a grave at Belish in northern Bulgaria where a small fragment of tabby-woven hemp fabric and loose threads were found (Dimova 2016: 670).

3.3.1.26 Zagreb-Croatia Iron Age

The famous Zagreb Mummy at the Archaeological Museum Zagreb is of interest in that the body is encased within a linen wrapping the *Liber linteus* Zagrebiensis (The Linen Book of Zagreb). While the first diagnosis proposed that the fabric was papyrus, it was later confirmed as linen. X-Ray and pathology analysis of the body and paint colouring was undertaken, but there has been no detailed investigation of the fibre type (Uranic 2006).

3.3.1.27 Bučovice-Vyškov Moravia Late Iron Age

Moravske Muzeum held samples from grave 14. The mineralised fibres, attached to bronze rings, were diagnosed initially as wool but subsequently later determined as possible flax. The fragments were tabby weave, spin warp: z, spin weft: z 15/14 count (Bender-Jørgensen 2005: 140(10)).

3.3.1.28 Seden Funen-Denmark Late Iron Age

In wells, excavated on this Late Iron Age site, preserved organic material residue were discovered. The proposal was that, based on evidence of flax stalks without seed heads, these wells served as retting stations. One of the wells contained nettle stalks to suggest that this fibre was also processed (Henricksen and Runge 2009: 20-21).

3.3.1.29 Söderby-Sweden Late Iron Age

Mineralised tabby weave fragments were recovered from a cairn, the fibre held in association with weapon burial and jewellery. Three textiles fragment were found together with several silver artefacts. The fragments were sufficiently detailed to determine the weave structure but the fibre could only be diagnose as plant material, possibly flax (Franzen et al. 2019: 360, Fig. 17.16)

3.3.1.30 Dolný Peter Komárno-Slovakia Late Iron Age

Fibre recovered from the Akademie Vlad grave 55 was encased within hollow bronze rings. The tabby weave was recorded as warp: spin z, weft: spin z, 14/14 weft count. The fibre identification was undecided, perhaps flax fibre (Bender-Jørgensen 2005: 141(29)).

3.3.1.31 Moravia Museum (Site unknown)-Moravia Late Iron Age

The excavation site for these two museum deposits of iron fragments with textile remains was unknown. They were described as tabby weave, spin warp: z, spin weft: z. Sample 1 thread count 10/7 possibly wool, sample 2, thread count 15/16, could be flax. (Bender-Jørgensen 2005: 141(26)).

3.3.1.32 Schrattenberg Mistelbach Austria Late Iron Age

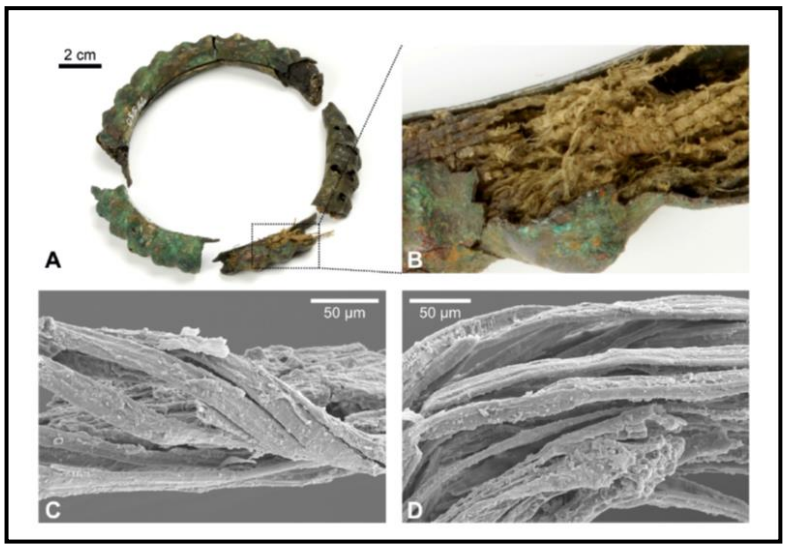

Figure 3.10 Late Iron Age bronze arm ring Image, (A) Hollow armband, (B) fabric (Bender-Jørgensen 2005:143(85) (no scale)). (C-D) REM images of the fibres (Grömer et al. 2019: 18).

The assemblage is held at the Naturhistorisches Museum Wien. An example of a hollow bronze arm ring with textile filling. The images show the general construction of these artefacts with some indication of their manufacture. While there is evidence of the fibre, tabby weave, warp: z, spin, weft: z spin, 19/18 thread count. The fibre could only be described tentatively as flax (Bender-Jorgensen 2005: 143 (85).There are many catalogue references to pseudomorph assemblages of plant fibre used to fabricate leg bands. The above images illustrate the technology (Bender-Jørgensen 2005: 140-150; Grömer et al. 2019: 18).

3.3.1.33 Slavkov Vyškov-Moravia Late Iron Age

This iron fragment, with textile remains, deposited at the Moravske Muzeum is described as tabby weave, spin warp: z, spin weft: z, thread count 14/15. However, the fibre diagnosis was uncertain but could be flax (Bender-Jorgensen 2005: 141(22)).

3.4 Summary: Diagnosis of plant fibre archaeological assemblages

It is recognised that the above listing is not a representative sample. However, it does illustrate the difficulty, not just in the separation between nettle, flax, and hemp but also in determining the fibre within the overall bast fibre grouping including tree-bast and assemblage where the fibres may be an interwoven collection of two or more fibres. An additional concern is the large percentage of fibre assemblages held in close attendance with metal artefacts where the interaction results in a skeuomorphic modified fibre representation (Janaway 2001). While the retained impressions enable Z and S angles of fibre twist and weave patterns to be qualified in most cases, fibre diagnosis is difficult if not impossible. However, the problem, in identifying single fibres types from these skeuomorphic images, highlights the potential for future research.

Recent publications reporting on progress in addressing fibre analysis from spindle whorl residue and fibre attachment to stone tools could serve as a foundation for further studies (Forte and Lemorini 2017: 165-182; Forte et al. 2019; Hardy et al. 2020).

The limited assemblages drawn from the catalogue tabulations above directs attention to those advantages arising from the determination of fibre types within the Western European geographic and. chronological zones appraised.There is a comparison with the analysis undertaken on a significant collection of preserved fibre assemblages recovered from excavations undertaken at Qasr Ibrim in Egyptian Nubia through 2000years of occupational deposits from 200 BC-1800 AD (Adams 2003: 201-207).

The following plot, **Figure 3.11**, is based on Adams (2007) fibre analysis of the utilisation of flax, wool and cotton fibres identified from 12,061 specimens deposited through 2100 years of occupation

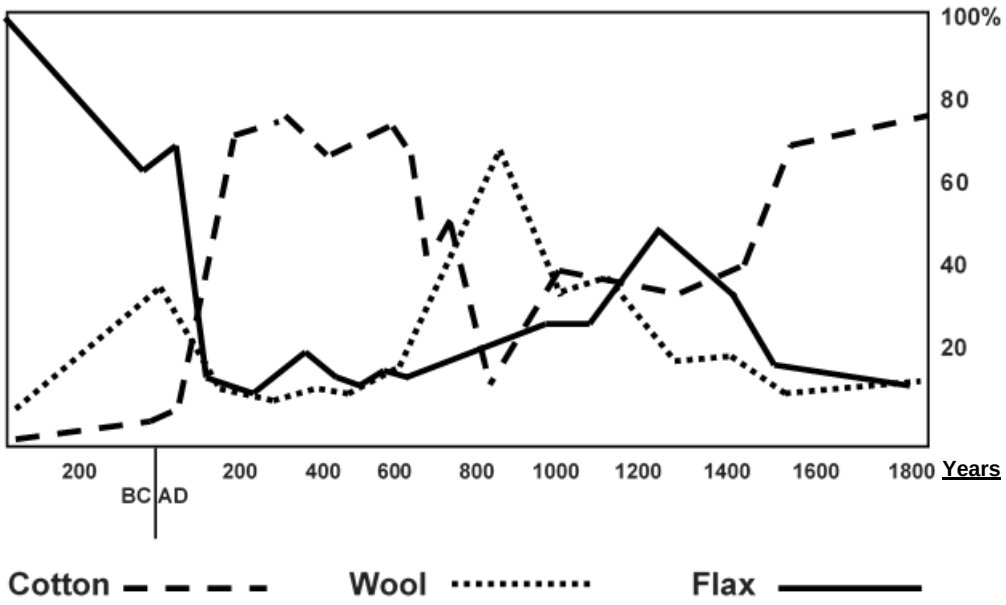

Figure 3.11. The plot represents consideration of the fluctuation in the frequency of utilisation of the three principal fibres as determined in the analysis of 12,061 specimens recovered from a 1980 excavation at Qasr Ibrim in Egyptian Nubia (Adams 2007: 203, Fig.33.2 with additions)

Adams (2007) notes the correlation of fibre usage through the period extending from the Ptolemaic, with flax as the dominant source to the Roman conquest in 30 BC, to note a significant increase in the use of wool. Flax and wool were still evident but declined considerably following the departure of the Romans and the introduction of Mero cotton from Sudan. The plot confirms that the use of cotton slumped with the introduction of Christianity in 550 AD.Cotton was replaced with wool until the early middle ages when cotton was reintroduced around 800 AD.

The survival of a significant collection of fibre artefacts in dry climate soil environment offers an exceptional opportunity for numerical analysis. An opportunity that is, unfortunately, unavailable for most Western European depositions. However, there is an additional area of interest in the diagnosis of flax. In a radiation analysis at the Grenoble Synchrotron Radiation Facilities (SRF), the microfibrillar angle of flax recovered from the Dead Sea Caves at Khirbet Qumran was evaluated (Muller et al. 2004). The authors recorded concerns in the analysis to note the difficulty in eliminating ramie fibres from the specimens submitted. As ramie was grown extensively in Egypt 5000-3000BC is there a possibility that, in a similar comparison to the differentiation of nettle and flax in European assemblages, there could be a similar dichotomy for the Egyptian flax/ramie textile diagnosis?

3.5 Research design parameters

In response to the interpretive dilemma demonstrated by the difficulty in diagnosing the archaeological assemblages detailed in **Section 3.5** above and in recognition of the poor survival for plant fibre remains, and the need to conserve this limited assemblage, the following research design parameters are proposed.

- Procedures should be sufficiently robust such that the identified diagnostic features will survive within the deposition or conservation environment.
- The diagnosis should be reliable in the determination of the differential identity between species and suitable for reproduction by others.

- Analytical techniques employed should be minimally invasive and, for samples removed from the assemblage, the diagnostic features require preservation and conservation for future re-evaluation.
- The research diagnostic and analytical procedures employed must be suitable for replication using standard University research facilities.
- A blind-test protocol will be structured to confirm the validity of the research findings.
- The extent to which the diagnostic features survive a range of burial or storage degradation will be recorded and evaluated.
- A selection of archaeological assemblages will be subjected to evaluation within the diagnostic parameters established above.
- The research outcomes will be subjected to peer review.

Chapter Four
Chaîne opératoire – fibre preparation archaeobotanical analysis and inferential diagnosis from textile tools

4.0 Introduction

In reviewing the processes for prehistoric textile production, it is noted that ideally the evaluation of plant fibre utilisation would be focussed on archaeological fibres and textiles recovered from site excavations. The diagnostic features to be considered are susceptible to both the growth environment and the subsequent processing techniques employed. Process modifications to plant fibre chemical composition, material properties and morphological features require consideration within the research programme to determine their influence on any proposed diagnostic parameters.

However, most depositional conditions do not support the survival of organic materials and in consequence textile production research is also directed to the investigation of those textile tools, structures and process activities within the chaíne opératoire that complete textile production.

4.1 *Chaîne opératoire* Fibre preparation sequence

In consideration of the fibre preparation sequences, there is a requirement to evaluate those activities that modify the raw material as it is refined into its end-product. Bleed (2001) defines this sequencing model as,

> *"(T)he operation of activities that progress through time"* (Bleed 2001: 102).

The activity is described as "archaeologically based" in that it deals with past events as they change through time (Bleed 2001: 101-127).

4.2 Process stages

Several authors report the preparation of the raw materials, nettle, flax and hemp with the process stages identified and these are in general agreement with those listed below (Barber 1991: 9-16; Hurcombe 2000; 155-173; Vogl and Hartl 2003: 119-128; Karg 2011; 506-508). This process sequence is generally referred to as the *chaîne opératoire* and can be represented in graphical network format although some authors, reflecting iconographic images, use pictorial representation (Barber 1991: 90-91, Fig. 3.8 and 3.9; Hurcombe 2008: 83-115; Lumb 2013: 54-77 and Fig. 4.1).

Plant fibre preparation-*chaîne opératoire*

- Harvesting - the collecting of plant fibre stems.
- Retting – decortication by partial biological or chemical decomposition of pectin.
- Scutching - mechanical beating and scraping of plant straw.
- Hackling - cleaning and aligning long-line fibres.
- Combing - to produce staple length and width.
- "Tow" - waste stem-wood fibre removal.

Hurcombe (2000) reviewed a wide range of ethnographic reports to provide a summary of both the skill factor and the time required to complete each of the above stages (Hurcombe 2000: 155-173 and Table14.1).

4.3 Archaeobotanical considerations

The low visibility and small size of seeds and pollen from fibre producing plants may result in poor recovery except in the most rigorous chemical or sediment flotation processes (Pearsall 1989: 33-97). Furthermore, particularly for wild species, it is challenging at the microscopic level to differentiate the natural dissipation of nettle pollen and seeds from the debris associated with fibre production. In contrast, the larger seeds of cultivated flax (*Linum usitatissimum* L.) or hemp (*Cannabis sativa* L.) from Neolithic sites are interpreted as evidence of cultivation of oil-bearing plants (Kenward and Hall 1995).

Consideration of European reports and references from site surveys provides evidence for the interpretation of plant material usage through the Mesolithic and Neolithic period (Van Zeist et al. 1984; Wasylikova 1984; Zohary and Hopf 2000). Küster (1984) considered the Neolithic plant remains from Eberdingen-Hochdorf to identify *Linum* as a cultivated plant for linseed oil but regards nettle as a ruderal weed (Küster 1984: 308-312). In contrast, the remains of nettle (*Urtica dioica* L.) from a lakeside Neolithic site at Clairvaux in France, are interpreted as having numerous uses such as alimentation, medicinal, dye and weaving (Lundstrüm-Baudais 1984: 295-306; Harwood and Edom 2012: 107-119; Andualem et al 2015: 1-9). In the tabulation of plant remains from the Neolithic coastal site at Aartswoud, Pals (1984), identified nettle as a crop plant in Table 1. However, the potential of *Urtica dioica* as a useful textile “crop” is ignored in Table 3 (Pals 1984: 313-321,Table 1 and 3). In an extensive review of domesticated fibre crop plants from the old world, (Zohary and Hopf 2000: 125-133) list both flax and hemp but disregard nettle.

Unfortunately, as nettle is a native ruderal weed throughout most of Europe, its presence, as a textile plant fibre within an archaeological site, can be challenging to differentiate. Hence, the diagnostic techniques employed to identify nettle as a textile fibre requires experience and a degree of subjective judgement (Küster 1984; Lunddström-Baudais 1984).

4.4 Plant fibre seeds

Tabulation of archaeobotanical data of soil samples revealed a spectrum of cultivated plants that reflect the chronological and cultural influences that determine the production and utilisation of plant fibre material through the prehistoric period (Jacomet 2006: 65-84; Bank-Burgess 2019: 141). From the Late Neolithic onward numerous flax seed finds are listed with particular reference to the seed diameter as illustrative of the primary product oil or fibre (Van Zeist and Bakker-Heeres 1975; Herbig and Maier 2011: 531; Bouayon et al. 2018).

Mature flax oil seed content of capsules has been determined at circa 35% and is evidence by larger seed size. This interpretation is questionable, for fibre production the flax plants are pulled before maturity to facilitate the ease of fibre extraction from less mature stems with harder epidermis (Bond and Hunter 1987; Oplinger et al. 1997; Cruickshank 2011).

Consequently, the seed capsules would also be under-mature and smaller. However, some flax fibre growth would have to be left to full-maturity to provide seeds for future flax crops. Seed debris associated with fibre production would therefore be smaller and underdeveloped, while larger mature flax crop seeds may have been retained for sowing (Maier and Schlichtherle 2011: 576).

The oil/fibre dichotomy has been addressed in detail in a Special Report published in Vegetation History and Archaeobotany (2011). The following authors contributed, Israel, (Kislev et al. 2011); Italy, (Bosi et al. 2011); SW Germany, (Herbig 2011); Denmark, (Anderssen 2011); Sweden, (Viklund 2011); Sweden, (Karg 2011); Switzerland, (Leuzinger and Rast-Eicher 2011); Greece, (Valamoti 2011) and Upper Swabia Germany, (Maier and Schlichtherle 2011). The authors' general conclusions were that there was insufficient evidence to support oil as the primary flax product.

4.5 Tree bast fibre

While this work is formulated to consider flax, nettle and hemp fibre morphologies as listed in **Chapter Two**, it is appropriate at this stage to recognise the utilisation of tree bast fibre in the Mesolithic and Early Neolithic period. Rast-Eicher (2016: 21-25), Harris (2010) (Medard (2005) and Myking et al. (2005) address the manufacture of lime bast cordage in the North European Mesolithic (9000 – 3000 BC) to confirm the material properties of the fibre and details of both collection and processing of the tree bast fibre.

THEBO, a joint project of five co-partners, (The acronym subsumes the project title "Textile craftsmanship in the prehistoric wetland settlements on Lake Constance and Upper Swabia". The project addressed the understanding of the critical elements of textile production and the cultural development in southern German arable farming (Bank- Burgess 2019). The comingling of flax fibres and lime bast bark fragments are listed for seven of the eight assemblages from Swiss Lake dwelling textile fragments held in the British Museum (Higgitt et al. 2011: 85, Table 1).

Samples, including textiles, threads, netting and cord, were subjected to Scanning Electron-Microscopy (SEM) and Fourier Transfer Raman Spectroscopy (FTRS) and were determined as detrital material of flax/lime bast mixtures (Higgitt et al. 2011: 84-87).

The rate of decline in lime bast utilisation on the Swiss Plateau increases from 5000BC as evidenced by the increase in non-arboreal pollen (NAP) as indicative of large-scale forest clearances circa 1350BC (Jacomet 2006; Kühn and Weniger 2015; Bank- Burgess 2019).

4.6 Plant fibre modern reference material

In recognising the limited availability of archaeological samples, the initial research phase was based on trials conducted with modern reference material as tabulated below **Table 4.1a and 4 1b.** Nettle fibres were gathered from local woodlands for retting, decortication and basic combing.

Additional supplies of nettle were provided by Camira Fabrics Mirfield (2014) who were conducting a trial of commercially farmed nettle as part of a study sponsored by the Department of the Environment, Food and Rural Affairs (DEFRA). This study was undertaken by De Montfort University's Textile Engineering and Material Research Group to evaluate the fineness and yield of the fibre (Horne et al. 2008: 63-70).

Samples of two varieties of commercial flax fibres from oil-seed plantings, (*Linum usitatissimum* (v. Winterlyn and v Eden) were obtained from farmed crops in North and East Yorkshire. Hemp fibres samples were also provided by Camira Fabrics (*Cannabis sativa v. Santhica*) and an unknown variety.

Concerns regarding the provenance for commercial fibres was noted by Dunbar and Murphy (2009, 110) who reported the misidentification of jute fibre provided for their fibre DNA study.

Hence, the fibre sources for the research programme were supplemented with a flax crop (v. Marilyn) and nettle plants from the University testbed planting Figure 4.1.

Figure 4.1. Test-bed planting University of Bradford. **Left bed.** Seeded nettle and transplanted nettle rhizomes. **Right bed.** Flax (v. Marilyn) a textile variety. **Below**. Left, nettle flowering stage at harvesting, centre flax flowering stage at harvesting, right flax capsule enlargement at maturity.

Plant	Species	Source	Location	Process	Harvesting	References
Nettle	*Urtica dioica*	Wild (open woodland)	Bradford West Yorkshire UK	Retted and hand-decortication		NGR SE 14112 27408
Nettle	*Urtica dioica*	Wild (closed woodland)	Bradford West Yorkshire UK	Retted and hand-decortication	Hand gathering	NGR SE 14112 27408
Nettle	*Urtica dioica*	Commercial crop	Driffield East Yorkshire UK	Chemical and mechanical decortication and bleached	Springdale Crop Synergy Ltd	http://www.springdale-group.com (1) (accessed 21/06/2018). NGR TA 04486 60665
Nettle	*Urtica dioica*	Commercial crop	n/a	Chemical and mechanical decortication unbleached	Camira Fabrics Mirfield	http://www.camirafabrics.com/ fabrics (accessed 15/06/2018).
Nettle	*Urtica dioica*	Crop from seed and rhizomes	University of Bradford UK	Retted and hand-decortication	Testbed cultivation	NGR SE 15307 32811

Table 4.1a. Lists of fibre material source, location, process and harvesting/supply criteria. (1) Refers to the STING Pilot, a project for the cultivation and decortication of nettle fibre at Springdale (Horne et al. 2008).

Plant	Species	Source	Location	Process	Harvesting	References
Hemp	*Cannabis sativa v. n/a*	Commercial crop	n/a	Mechanical decortication unbleached	Camira Fabrics Mirfield	http://www.camirafabrics.com/fabrics (accessed 15/06/2018).
Hemp	*Cannabis sativa* v. Santhica	Commercial crop	n/a	Mechanical decortication and bleached	Camira Fabrics Mirfield	http://www.camirafabrics.com/fabrics (accessed 15/06/2018).
Flax	*Linum usitatissimum v. Winterlyn*	Commercial crop	Dunkeswick North Yorkshire UK	Mechanical decortication	Snowden Farm Dunkeswick North Yorkshire	NGR SE 30663 46939
Flax	*Linum usitatissimum* v. Eden	Commercial crop	East Yorkshire Hemp Baswick East Yorkshire UK	Mechanical decortication	Inn Carr Farm, Baswick, Brandesburton	http://www.eastyorkshirehemp (accessed 15/06/2018). NGR TA 01051 48118
Flax	*Linum usitatissimum* v. Marilyn	Crop from seed and rhizomes	University of Bradford UK	Retted and hand-decortication	Testbed cultivation	http://www.wildfibres.co.uk (accessed 21/06/2018). NGR SE 15307 32811

Table 4.1b. Lists of fibre material source, location, process and harvesting/supply criteria.

4.7 Plant fibre retting

The next stage in the textile production operation is concerned with the retting process, the release of the bast fibre from the plant stem epidermis. Retting can be achieved in a simple process by scattering the stems on the ground and leaving them subjective to fungal and micro botanical erosion of the lignum adhesive. Alternatively, the stem bundles could be immersed in moving water for 7-10 days to achieve the same result.

The extraction process is determined by the need to release the bast fibre from within the parenchyma by decortication of the epidermal surface and removal of the pectin adherence through the retting process. The fibres are then separated from the subsurface in the “scutching” process that may require beating and scraping with wood, bone, lithic or metal tools.

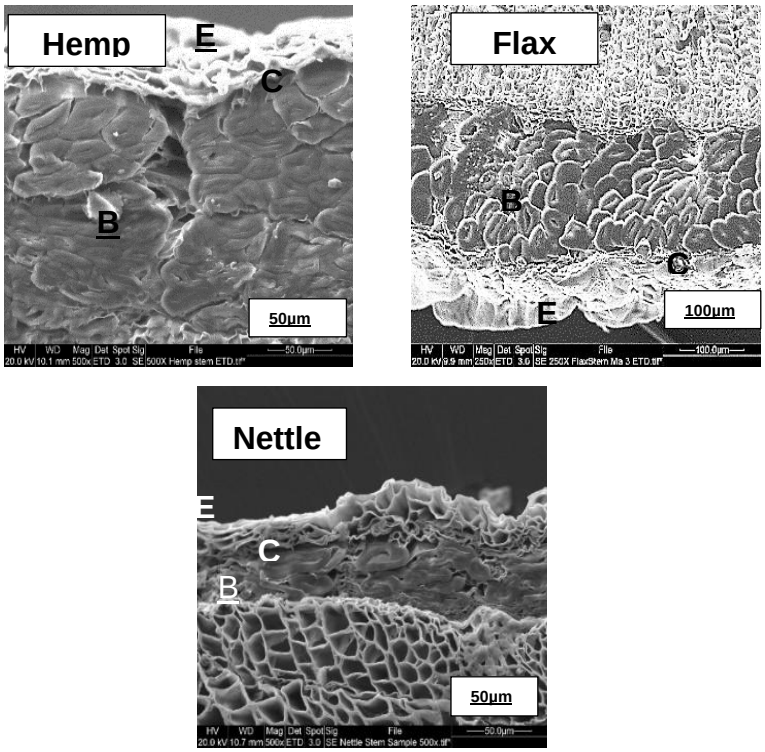

Figure 4.2.SEM cross sections of hemp, flax, and nettle. The images illustrate the stem anatomy with the following tissues identified, Ep (epidermis), C (cortex), Bf (bast fibre). Images produced on SEM (ETD High Vacuum) at 20kV, Flax 250X, Hemp and Nettle 500X.

The close association and location of fibres within the plant stem are shown in the Scanning Electron Microscope (SEM) images Figure 4 2. with the fibres held tightly within the stem, and it is this feature, and the relative difficulty of separation that is a major factor in the choice of plant fibre.

The hemp, nettle and flax images illustrate the relationship of the fibres to the stem. However, the fibres present different levels of resistance to the process mainly for nettle where, compared with flax and hemp, the difficulty in removing effectively the epidermis requires biological or chemical decomposition of the pectin (Horne et al. 2008).

In order to further appreciate the effects of harvesting and processing upon the fibre shape and material properties, nettle fibres from a woodland site in Bradford West Yorkshire UK Table 4.1 were harvested and retted for 10days in a purpose-built rain flushed retting station Figure 4 3. The retted stems were manually decortication, with basic combing, and spun to produce fibres suitable for primary diagnostic evaluation.

The stem sections illustrated in Figure 4.2 show the close relationship of the bast fibre formed below the cortex. This close association of the fibres with pectin, a polysaccharide that binds the fibre cells, is a major consideration in terms of the selection of the decortication process to be employed. In a practical demonstration undertaken in partnership with the Bradford Guild of Handweavers, Spinners and Dyers (2014), nettle stems collected from local areas were retted in a purpose-built retting station before mechanical decortication and trial spinning **Figure 4.3**.

Figure 4.3. Retting station**.** Constructed for natural rainwater flush supplemented by manual flushing as required.

Retting pits, along with reused wells, lakes, and pools were also noted for textile fibre plant preparation. However, most of these sites were from the late Bronze Age onwards (Andresen and Karg 2011: 517-526). There are noted concerns that excessive retting releases the fibre into the water to coagulate at the surface and are lost from the production process, a problem also reported for nettle and flax processed by others. (Di-Virgillio 2013: npn) in a field trial of nettle fibre in Tuscany noted the problem of cellulose degradation due to an extended retting period. Levy and Gilead (2013: 26-44), reporting on the Ghassulian textile industry of the Southern Levant, conducted an extensive research programme on the propagation of flax to note the degradation of fibre strength due to over-retting.

At the West Row Fen, Suffolk UK, a Bronze Age site, flax seeds found in close association with stem remains within the retting pits are interpreted as evidence of flax processing, no comments on potential alternative fibre plant remains were reported (Martin and Murphy 1988).

In contrast, seeds of both flax and nettle (*Urtica dioica* L.) were found at Reading Business Park, again in association with retting pits, and the possibility of both plant fibres being used was reported (Moore and Jennings 1992).

4.8 Plant fibre inferential diagnosis-Reflections

It is noted that while fibre chemical and morphological differentials, as diagnostic features, may be the principal research focus, other supportive textile processing assemblages offer inferential diagnostic attributes. It is recognised, as noted above, that within the overall textile production *chaîne opératoire* there are inorganic textile tool remains such as retting pits spindle whorls, spools and loom weights, that provide an interpretive potential that attests to textile fabrication.

4.9 Spinning: introduction

Fibre retting changes the morphology of the fibres through water absorption and fibre separation. The presence of discarded seed and stem fragments, suitable for diagnosis, that remain within retting stations provide an ideal opportunity to diagnose plant fibres present within the residue analysis. While the diagnosis of the fibre undergoing processing is problematic, the fibre preparation *chaîne opératoire* designations can be extended into considerations of the textile tools employed. In particular the presence of spindle whorls and loom weights offer inferential fibre diagnostic potential.

4.9.1 Spindle-whorl assemblages

A review of 5200 plus European spindle whorl assemblage reflects the attendant evaluation of weight, diameter and shape along with their Moment of Inertia (MI) as indicative of the quality and fineness of the spun fibres (Médard 2003: 375-391; Grömer 2005: 107-116: Peyronel 2007: 27-35; Gleba 2008: 103-109; Gostenčnik 2010: 73-89; Štolcova and Grömer 2010: 9-20 Sauvage 2013: 189-204 Mazăre 2014: 1-42; Sauvage 2014: 184-226 Vakirtzi et al. 2014: 43-56 Dimova 2016: 652-680; Grömer 2016: 74-88; Vakirtzi 2019: 479-500).

Verhecken (2010: 257-270), adds to the above in an extensive consideration of spindle-whorl performance world-wide with a similar evaluation of 1700 assemblages.

In a review of the Central European whorls the variation in shape and choice of material, with clay being replaced by ceramic sherds in the Middle and Late La Téne period reported. It was proposed that this change was indicative of the establishment of mass production (Štolcova and Grömer 2010: 9-20, Fig.3.4). Also, the authors reported on a comparison of fibre type in that the number of flax textiles recovered from the Dürrnberg salt mine is high, at 24% in contrasts with the Hallstatt assemblage where 95% of textiles were made of wool and minimum use of flax recorded (Štolcova and Grömer 2010: 10; Grömer 2013: 45).

Gostenčnik (2010: 73) adds to the comments regarding the deterioration in spindle-whorl design and describes 866 from 902 whorls recovered from Late Roman Iron Age assemblage from Magdalensberg as low-quality coarse pottery or discarded marble.

4.9.2 Spindle-whorl performance

Spindle-whorl Moment of Inertia (MI) has been proposed as a parameter for determining the functional classification of whorls. The mathematical derivation of MI is based on the form, size and mass of the whorl. A qualitative analysis experiment was undertaken to confirm the hypothesis that the fineness of the yarn is dependent on the weight of the spindle-whorl used and that heavy weights were only suited to coarse fibre production (Verhecken 2010: 257:270; Verhecken 2013: 97-101). The experiment concluded with a test run on a small sample of flax and cotton to conclude that, while the results showed a relatively good relationship between MI and fineness, they were untrustworthy. Further tests, on wool spun by six operators, found a minimum correlation between MI and fineness to conclude that the principal determinant for spun fibre fineness was the skill and experience of the spinner.

Kania (2015) in a similar series of test, conducted in response to the above, a detailed description of the drafting process was provided to direct appraisal of the spinner/spindle-whorl relationship. The conclusion, based on the output of 140 samples produced from a group of 14 spinners, was that,

> "(T)he dominant factor influencing the yarn was the individual spinner, neither whorl mass, nor whorl moment of inertia nor fibre did influence the spun yarn significantly (Kania 2015: 113).

Furthermore, in a review of two millennia of textile tools recovered from the Bronze Age site at Arslantepe Mound in Turkey, the authors considered the weight, diameter and shape of 88 spindle whorls to remark on the lack of correlation between spindle-whorl shape and their weight and diameter ratios.

It was concluded that, as weight and diameter were the functional parameters that defined the spun fibre quality, whorl shape was non-functional and was based on tradition, taste, or manufacturing convenience. Also, reported was that, when spinning a thin thread on a heavy whorl, the thread broke due to the heavy load. Conversely, the alternative of spinning a thick multi-fibre thread on a light spindle whorl with the attendant reduction in rotational speed resulted in producing a fibre that is not strong enough to weave (Frangipane et al. 2009: 7 and Fig.3).

Neolithic and Copper Age textile production in Transylvania (Romania) was reviewed by Mazăre (2014) to include an evaluation of spindle whorls and loom weights from 51 archaeological sites. The spinning whorls, 58 in total, were sub-divided into fired clay and pierced pottery shards and classified by raw material, weight, group, morphology and profile, based on a classification attributed to Medard (2012) (Mazăre 2014: 12-14).

Mazăre (2014) notes Chmielewski and Gardyński's (2010) inclusion of MI and rotational speed within the appraisal of spinning-whorls to proposes that this modified classification affords a comparison of performance to include suspended short, thick spindles suitable for finer threads, and longer thinner spindles, with the whorl carried on the upper side, suitable for bast fibres or yarn plying.

Vakirtzi et al. (2014) reviewed spindle whorls from two prehistoric sites on Thassos North Aegean, Aghios Ioannis (39 whorls) and Skala Sotiris (169 whorls) to compare and contrast spindle whorl weight, diameter and shape.

The determined site variations were noted as descriptive of the change in fibre processing, from plant fibre to finer wool fibre for the two sites based on radiocarbon dating to determine Aghios Ioannis, as a Final Neolithic transitional site, and Skala Sotiris, an Early Bronze Age site (Vakirtzi 2014: 43-56).

4.9.3 Analysis of fibre residue on spinning whorls

In an extension to the consideration of the relationship of spinning whorls to the spun fibre, an appraisal of spindle-whorl residue was initiated (Forte et al. 2019: 1-8). The analytical research protocol employed replicated spindle-whorls manufactured with a diverse composition of clays kiln-fired to 800-900ºC for use in experimental fibre spinning. Flax, cotton and wool fibres were spun by experienced spinners under two spinning techniques, low whorl drop spindle and spinning in a bowl. Spinning sessions in excess of 15 hours resulted in the deposition of tool wear spun fibre and wood residue on all nine samples (Forte et al. 2019: 1-8).

The residue was examined through Nikon SMZ stereomicroscopy with a 1x objective, 10x ocular with a magnification range 0.75x-75x low magnification and SEM2 Hitachi TM3000 magnification 50x-2000x the shape and description are shown in **Figure 4 4** and **Table 4.2** to confirm that while several fibres fragments were visible, there was insufficient original surface morphology to support a fibre diagnosis (Forte et al. 2019: 5).

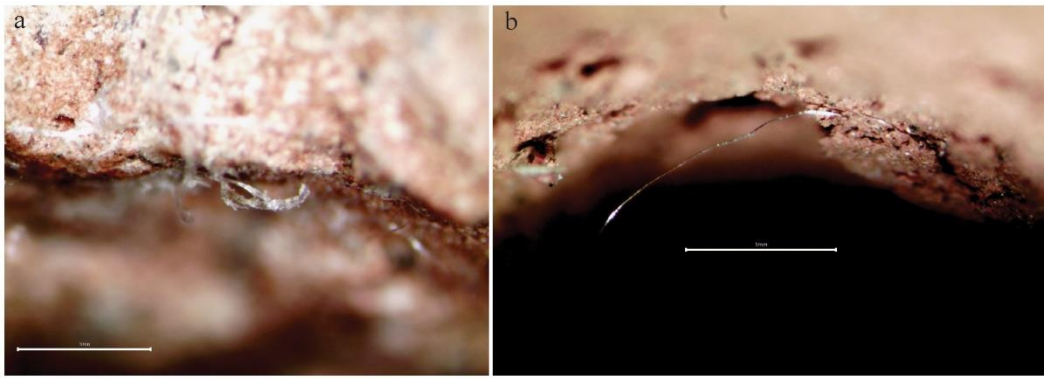

Figure 4.4. Fibre residue recovered from spindle-whorls. a) Fibre residue on experimental spindle-whorl ID1. b) Fibre residue on spindle-whorl ID4. **Scale Bar 1mm**. (Forte et al 2019: Fig. 4).

However, the authors confirm that,

> "(A)lthough many fibre fragments were in a poor state of preservation, two samples, ID1 and 4 **Table 4.2,** were still recognisable according to the characteristic elements of the bast fibre morphology, such as nodes or kinkbands perpendicular to the fibre axis and the oval or polygonal shape."
>
> (Forte et al. 2019: Fig.5 and 6)

Features of Fibre Residues				
ID	**Type**	**Size**	**Shape**	**Guide Elements preserved**
1	Bast fibres	Flattened areas: 18-19 μm Well preserved areas: 10-14 μm	Ovoidal/polygonal	Nodes polygonal shape
3	Unrecognizable Fibre split	-	-	-
5	Wool	31-36 μm	Round/ovoidal	Scales and medulla (badly preserved)
6	Unrecognizable Fibre split	-	-	-
7	Bast fibres	10 μm	Polygonal	Nodes, polygonal shape
8	Cotton	9-12 μm	Spiral ribbon-shaped	Helix structure
9	Unrecognizable Fibre split	-	-	-

Table 4.2. Spindle whorl residue analysis determined with Optical Microscopy and SEM imaging through Nikon SMZ stereomicroscopy (1x objective, 10x ocular, range 0.75x-75x and SEM2 Hitachi TM3000 magnification 50x-2000x (Forte et al. 2019).

4.10 Loom weights

In textile production, it is the inorganic archaeological assemblages, mostly lithic and ceramic textile tools, that are the more common evidence for textile production. In contrast to organic material, such as wood and plant fibre, inorganic materials survive in archaeological stratigraphic context. Hence, in the absence of plant fibre in the assemblage, the presence of inorganic textile tools provides artefacts that inform the interpretation of textile fabrication. The weight and diameter of spindle-whorls discussed above are assessed as factors that prescribe the quality of spun yarn suitably prepared for weaving and are indicators of the yarn length that can be processed in a given time. Loom weights, categorised by weight, thickness and shape are appraised as determinants of warp tension and thread count density (Schiere 2005: 101-105; Militello 2007: 36-45; Peyronel 2007: 26-36; Gleb 2008: 127-138; Andersson Strand et al. 2013: 191-196; Guzowski et al. 2015: 309-328; Belanova 2019: 306-331; Vakirtzi 2019: 485-50).

As described above, in reference to spindle-whorls, a similar approach is adopted to classify 563 loom weights from a total of twenty-two Neolithic and Copper Age sites in Transylvania. The classification, in terms of shape, weight and thickness are proposed as illustrative of functionality in textile weaving quality. These determinants of the loom weights are listed under the following classes.

- Presence and location of the mounting hole
- Weight
- Thickness
- Morphology

A tabulation of the loom weight/warp thread tension calculation is included to illustrate the productivity in terms of yarn consumption per square meter of finished cloth (Mazăre 2014: 14-24, Table 1.7). In a closing summary, Mazăre (2014), remarks on the lack of textile remains to aid fibre identification. However, Mazăre's (2014) analysis did include the interpretation of textile imprints from the Neolithic 4th century, as mostly twinned tree bast and woven fabrics of flax.

Dimova (2016) reviewed textile production based on the evaluation of a 400 plus spindle whorls and 3000 plus loom weights assemblages from three Late Iron Age locations in Thrace. The author notes the limitation of the spatial data in identifying production workshops to propose that textiles were produced in separate households (Dimova 2016: 652-680).

At Arslantepe (Turkey) from the excavation of a Middle Bronze Age site, an assemblage of fifty-five loom weights was found held in the debris of Room A58. Examination of the loom weight shapes demonstrated the changes that occurred over the three occupation periods from hemispherical to conical and finally elliptical-discoid. From forty-two thin, fired clay discoid weights, range 277g-584g, an estimate of the size of finished products that could be woven was proposed. With sixteen fine threads and a warp tension of 10g/thread per loom weight a denser weave, could be produce. The same loom weight, carrying five threads, could also produce a heavier fabric (Frangipane et al. 2009: 24-25).

The above discussion has reviewed the assemblages of loom-weights and their appraisal in terms of physical and morphological attributes and how the selection of appropriate loom weights influences the textile construction and informs the choice of fibre.

4.11 Textile production

As previously noted, there are adaptations of production quantity and quality that are indicative of the scale of production from the primary household single premise production for personal usage through to the household specialist crafters working for the community and finally, full-scale purpose-built workshops providing textiles trading with a more extensive customer base over an extended area. An accumulation of numerous spindle whorls and loom weights in close association are interpreted as indicative of this expansion in production quantity (Arnold 1985: 225-231; Gleba 2008: 192-193; Mazăre 2014: 31; Dimova 2016: 653).

For example, the site at Troia in northwest Anatolia is located in the silted-up estuary of two rivers on a site occupied for over 3000years. Archaeological assemblages from the Early Bronze Age to the late Roman have been recovered from this mound-site. The recovered textile tools include both spindle-whorls (1493) and loom weights (189) and other tools from seven different occupation periods. In Room B “The Citadel” (E9) thirty-three weights, mostly conical, were recovered from the final period floor deposit.

Consideration of the analysis of 1493 loom weights, rejected the assumption that the assemblages were evidence of specialisation (Guzowski et al. 20)

From the archaeological sites on Crete, Malia, with an occupational history of presence from the Neolithic (6000-3000BC) to the final destruction of the Minoan Palace in the Bronze Age (1450BC), a range of quality artefacts were recovered. Excavation, by the French School of Archaeology (Athens), continues with the results published in the series Études Crétoises. Volume 34 includes reports on textile production at Le Quartier Mu (V) a Middle Minoan Town located north west of the palace (Cutler et al. 2013). In a review of the recovery of loom weights from various building/workshop areas, Cutler et al. (2013) evaluated an assemblage of 641 loom weights to attribute to each area evidence of textile production quality and volume. The findings are listed in **Table 4.3** with a summary of the interpretation of product type and quantity.

Location	Loom weights	Activity/Production outcome
Seal shop	1	No production, administration area
Potter' w/shop	33	Thin threads denser weave product
Workshop	8	Heavier weights higher tension product
South workshop	10	(included in above)
Building A	167	Very thin threads Tabby weave product
Building B	40	Storage area Documentation
Building C	42	Denser Twill weave product
Building D	160	Used for a range fabric weaves
Building E	12	Storage
Building F	4	(no report)
TOTAL	477	
Building F	4	(no report)
TOTAL	477	

Table 4.3. Summary of loom weights numbers recovered from Quartier Mu (V) with comments on activity and possible product (Based on Cutler et al.2013).

4.12 Textile fragments recovered in association with loom weight assemblage from Quartier Mu V Malia Crete.

In addition to the loom weight finds from Quartier Mu V there were fragments of mineralised textiles recovered in an earlier 2005 excavation of the drain in the eastern part of Building A. The fabric, described as tabby weave, 20 thread/cm of 0.3mm S spun thread in one direction and Z spun in the other, was diagnosed as wool. This description is in general agreement with the product description for Building A based on the evaluation of the loom weight assemblage (Cutler et al. 2013; Sarpaki 2007: 884).

Two thread fragments were also recovered in May 2009 from the mounting holes of two pebble loom weights, one in Building B (Sample 72 M 669), the other from Building D (Sample 72M 870). Stereo and optical microscopy and scanning electron microscope (SEM) analysis of the 2009 samples are recorded as follow.

Sample 72 M669 was too small to allow weave or fibre determination, although SEM imaging indicated morphological features attributed to cellulosic bast fibres similar to flax or hemp.

Sample 72M 870 Fibre diameters of 10-17 μm were recorded and SEM imaging indicated morphological features attributed to cellulosic bast fibres similar to flax (Cutler et al. 2013; Sarpaki 2007: 884).

4.13 Summary

As noted for the analysis of spindle whorl residue, there may also be opportunities to analyse thread remnants from both loom weights and whorls. However, it would be preferential to identify their presence immediately upon excavation as subsequent post-excavation cleaning and conservation may not be conducive to fibre diagnosis. The initial 2007 find from Quartier Mu, a 4cm x 4cm textile fragment, presented a sample more suited to analysis, the sample was discovered within an archaeobotanical analysis of the drainage channel deposit. The recovery of this textile fragment confirms the advantage of soil flotation recovery of organic material from sites containing textile tools and associated artefacts.

A retrospective review of the Aims and Objectives determined above directs attention to an evaluation of existing diagnostic methods and techniques to ascertain the extent that they meet the research programme criteria. Hence the following principal diagnostic techniques will be appraised.

- Fibre chemical constitution
- Fibre DNA analysis
- Phytolith presence in fibre assemblages
- Fibre material properties
- Fibre morphology

Areas of interest as identified above, are broadly separated into chemical or morphological features and these are featured in the subsequent chapters.

Chapter Five
Plant fibre diagnostic features-their efficacy, reliability and durability

5.0 Principal diagnostic features

In **Chapter Four** the principal diagnostic techniques to be assessed were listed as below.

- Fibre chemical constituents
- DNA analysis
- Presence and morphology of phytoliths
- Fibre material properties
- Fibre morphology

Here the evaluations for the chemical constituents, DNA analysis and phytolith presence are addressed. Material properties and morphology are address in **Chapters Six and Seven.**

5.1 Fibre chemical constituents

Plant fibre diagnosis is determined from observations of changes in dimension or colour resulting from chemical staining.

Vegetable fibres swell when stained with cuprammonium hydroxide [$Cu(NH_3)_4](OH)_2$, phloroglucinol ($C_6H_6O_3$) and hydrochloride (HCl) and staining of the lignin is determined from comparison of the observed colour change in the sample (Wild 1970: Schaffer 1981). Interpretation of the resulting colour changes is subjective and requires specialised knowledge in their identification.

Fibre chemical analysis has also been used to ascertain the variations in constituent content as they are reflected in response to changes attributable to fibre processing (Sharma et al. 1999; Bacci et al. 2011; Yan et al. 2014),

their variation along the stem growth (Liu et al. 2014), and the variation within hybridised varieties (Sharma and Faughey 1999). Improvement in hemp quality were also reported as influenced by the fibre's chemical make-up (Jinqui and Jianchun 2010).

Current environmental concerns encourage an awareness of the potential for replacing glass fibre in polymer-matrix composites with natural plant fibre where the fibre chemical constituents are indicative of the improvement in mechanical strength (Baley 2002; Hanninen 2012; Yan et al. 2014).

5.2 Chemical composition: plant fibre: acid detergent fibre (ADF) and neutral detergent fibre (NDF))

Plant fibre diagnostics, based on neutral detergent fibre (NDF) and acid detergent fibre, were included in several projects (Sharma et al. 1999; Sharma and Faughey 1999; Bacci et al. 2011). The procedure for evaluating the digestible quality of forages in the diets of herbivores was established by Van Soest (1967). This procedure was refined further (Raffrenato and Van Amburgh 2011; Raffrenato et al. 2011). Van Soest (1967) formulated the concept as an aid to differentiating the starch and sugar digestible cell contents from the less digestible hemicellulose, lignin, and cellulose. Neutral detergent fibre (NDF) is dissolved to remove the easily digestible proteins, lipids, sugars, starches and pectin in the feedstuff. The insoluble fibre residue consists of the plant materials cellulose, hemicellulose and lignin and indigestible nitrogenous matter in animal products (Ankom Technology 2016; Foss Analytics 2016)

The determination of acid detergent fibre (ADF) and neutral detergent fibre (NDF) is achieved by the chemical analysis of animal feedstuff.

The following British Standards (BS) apply, for acid detergent fibre (ADF) and acid detergent lignin (ADL) contents BS EN (ISO13906:2008), and for neutral detergent fibre content (NDF) BS EN ISO 16472:2006 **Figure 5.1.**

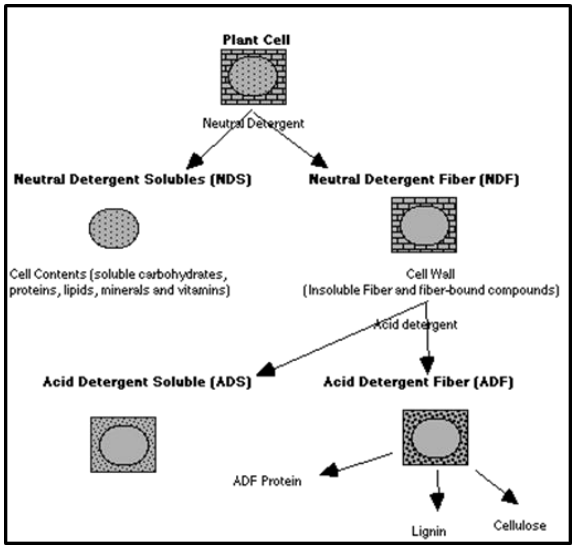

Figure 5.1. Principle of ADF/NDF detergent partitioning of the fibre fraction "Van Soest Methodology" Image from Ghent University (2016) with additions).

ADF is verified in the first stage of the method where the detergent solution is used to remove acidic modified carbohydrates, protein and fats. The remaining fibrous residue is primarily cellulose, lignin or insoluble animal products and damaged feedstuff. The residue is weighed for the determination of ADF. In the second stage, the remaining residue is solubilised in sulphuric acid, leaving the lignin (ADL) which is measured gravimetrically. In the final stage, these two distillations are combined to derive NDF (Hemicellulose + Cellulose + Lignin) ADF (Cellulose + Lignin)

In addition to the analysis detailed above, the technique has also been employed in the chemical analysis of a range of plant fibres including *Urtica simensis* L. (Ethiopian Stinging Nettle) (Andualem et al. 2015), *Urtica dioic* (Stinging nettle) (Sharma and Faughey 1999; Bacci et al. 2011) and *Boehmeria nivea* L. (Ramie) (Conto et al. 2011) (Stinging nettle)

(Sharma and Faughey 1999; Bacci et al. 2011) and *Boehmeria nivea* L. (Ramie) (Conto et al. 2011)

A database of fibre chemical analysis for the three fibre species, flax, nettle and hemp, and comments on the variation influenced by plant growth conditions and location within the plant stem has been reported (Sharma et al. 1999; Sharma and Faughey 1999; Baley 2002; Bacci et al. 2010; Jinqui and Jianchun 2010; Hanninen 2012; Yan et al. 2014). The data has been sub-divided by species for statistical comparison **Figure 5.2** and tabulation, **Table 5.1.**

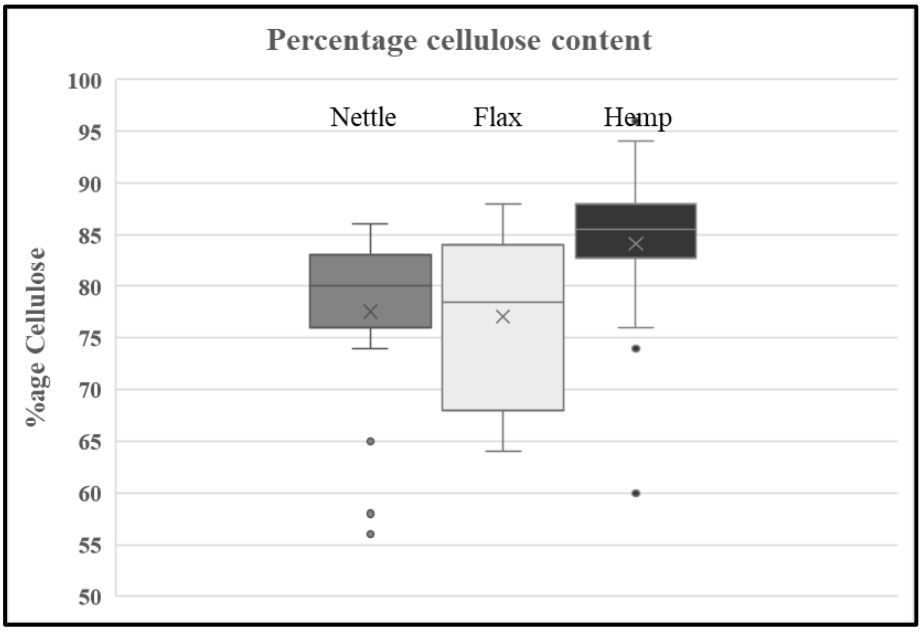

Figure 5.2. Plant fibre comparison of mean and standard variation in cellulose content. Analysis of variance (ANOVA) in cellulose content based on the analysis of 80 samples. Nettle (n=28), flax (n=34) and Hemp (n=18) found there to be some significant variation between the grouped samples F= 5.21577, df=81, p=0.00751. The graph shows some difference between Nettle and Hemp (T=2.7581, df=44, p=0.00422) and some difference between Flax and Hemp (T=3.0888, df=50, p= 0.00164). However, there was no significant difference between Nettle and Flax. (Note. Outliers have been excluded from this ANOVA comparison)**.**

Author	Nettle	Reference	Flax		Hemp
Bacci et al. (2010) Table 2	81	Yarn et al. (2014)	64	Jinqiu and Jianchun (2010)	60
“	78	“	67	“	74
“	80	“	74	“	87
“	78	“	65	“	94
“	84	“	67	“	96
“	82	“	73	“	83
“	83	Hanninen (2012)	75	Kostic et al. (2008)	76
“	80	“	79	“	82
“	81	“	87	“	84
Bacci et al. (2010) Table 4	86	“	83	“	84
“	65	“	84	“	87
“	83	“	84	“	88
“	75	“	86	“	88
“	85	“	86	“	89
Bacci et al. (2010) Table 6	65	Bourmaud et al. (2008)	84	“	84
“	82	“	86	“	84
“	83	“	84	“	85
“	80	“	80	“	87
“	79	“	82	“	86
“	74	“	76		
“	76	“	83		
“	84	“	81		
“	79	“	85		
“	81	“	88		

Table 5.1 Tabulation of the percentage of fibre cellulose content. (Authors as listed)

Author	Nettle	Reference	Flax		Hemp
Virgillio (2013) 2nd year Btm.	84	Bailey (2002)	64		
Virgillio (2013) 2nd year Mid,	79	“	67		
Virgillio (2013) 2nd year Top	81	“	74		
Virgillio (2013) 1st year	84	Sharman et .al (1999)	78		
Waudby (2014)	56	“	76		
“	58	“	82		
“	58	“	74		
		Waudby (2014)	68		
		“	68		
		“	66		
Mean	**79.7**		**78.1**		**84.0**
St. Dev	**8.3**		**7.8**		**8.0**

Table 5.1(cont.) Tabulation of the percentage of fibre cellulose content. (Authors as listed)

5.3 Comments on NDF/ADF chemical analysis

In reviewing the outcome for the applications listed above, all the samples were obtained from the analysis of modern material either from testbed plantings or in research programmes contemplating fibres as a suitable replacement within composite materials.

The statistical analysis confirms that chemical analysis could indicate a minor statistical significance between nettle and hemp and flax and hemp. However, there is no differential between nettle and flax.

In summary, the analytical process is destructive, and the results are variable. Hence, the process would be unsuitable for the diagnosis of archaeological textile remains.

5.4 Fourier Transfer Raman Spectrometry (FTRS)

FTRS is a non-destructive analytical technique employing mass spectrometry of the fibre sample. For plant fibre, the FTRS principle affords a diagnosis based on the variable cellulose, moisture, lignum, and pectin constituents as being indicative of individual plant fibre identities. Edwards et al. (1996) successfully applied this technique to the diagnosis of Egyptian fabric from two different periods, 1900 BCE and AD 614.

Three Grecian 6th to 13th-century fibres, provisionally identified as silk, wool and linen, were subjected to FTIR analysis by (Margaritti et al. 2010) who concluded that, with only one fibre unambiguously identified, the preservation and age of the samples affected the efficacy of the determination. In an extension to the research, Edwards et al. (1997) compared a range of plant fibres and tabulated the results to confirm relative band intensities (*I*) as diagnostically significant between flax and ramie (*Boehmeria nivea* **L.)** with R´ = ($I^{1121/1096}$) and R=($I^{1096/2900}$). These tabulated ratios were obtained from the

FT-Raman spectra on a Bruker IFS 66 (1064nm) as shown in **Table 5.2**

Sample	**R´ ($I^{1121/1096}$)**	**R ($I^{1096/2900}$)**
Flax (FTRS)	0.72	0.85
Ramie (FTRS)	0.70	1.63
Jute (FTRS)	0.77	0.92

Table 5.2 Intensity (*I*) ratios R´ = ($I^{1121/1096}$) and R=($I^{1096/2900}$). Established from FT-Raman spectra of soft bast fibres. (Edwards et al. 1997: 2387)

As Edwards et al. 1997:2383-2392) note in their conclusions,

> "(T)he results of our study of natural untreated plant fibres using FT-Raman spectroscopy are seen to provide a method for the non-destructive characterisation of these materials and indicate future possibilities for the application of this technique to archaeological fabrics" (Edwards 1997: 2388).

In a previous study, fibre samples were submitted to the Molecular Studies Group (MSG), University of Bradford, to evaluate the potential for future studies (Waudby 2014). In their comments, MSG confirmed that the samples were run on both the visible Renishaw (In Via Raman microscope), and Bruker FT Raman (1064nm) and the following results reported as follows.

> "Results were varied, with Raman producing a reasonable 63nm visible wavelength Raman spectrum on the Renishaw. The Renishaw results from other fibres were inconclusive. The Stinging Nettle fibres indicated promising results on the Bruker FT Raman instrument that could be improved if a more modern instrument were available. The other fibres gave only poor-quality results" (Farwell 2014 pers. comm.).

The above results indicate the possibility to extend the study to investigate the potential of FTRS in differentiating between flax, nettle, and hemp plant fibres. In collaboration with the Federal University, Juiz de Flora, Brazil (2016), a sample of plant fibres from various commercial sources was forwarded for FTRS analysis. A summary of their results is listed below.

Samples of nettle, jute and ramie provided by University of Bradford, Archaeological Sciences (Edwards, pers. comm., 18/11/2014)

Analysis:

Common bands were presented by all samples: 382, 438, 524, 1096, 1124, 1152, 1343, 1377. In addition, the following specific bands applicable to each fibre species were noted.

- Nettle :1058, 1460, 1606, 2940.
- Flax: 1460, 902, 1606, 2940.
- Ramie: none of these.

Comments

> "It is possible to differentiate between the three fibres: ramie against, flax/nettle because of the presence of any of the above bands. The differential intensity between flax and nettle through the presence of a weak band at 1058 in nettle and presence of 902 in flax is another possibility. Other bands are common to both. However, to obtain quality spectra for differentiation between the fibres, the effect of archaeological deposition on spectral background emission should be considered" (Edwards pers. comm 2014). (See additional comments in Section **5.5.1**).

5.5 Alternative spectra from Fourier Transfer Infrared Spectrometry (FTIRS)

FTIRS evaluations were used to define the effect of deformation of hemp fibres around kink bands, dislocations and nodes to include consideration of MFA as an aid to understanding the material properties of hemp (Dai and Fan 2010).

It was noted,

> "(T)hat some form of deformation occurred during plant growth, a significant amount of deformation resulted from decortication and other down-line processing" (Dai and Fan (2010: 339).

Dai and Fan (2010: 339. Fig. 2a) used FTIRS to illustrate hemp MFA as 3.27º. However, the sketch displays this as a negative angle relative to the fibre axis ("S") spin. Other writers recorded MFA for hemp as a positive angle ("Z") spin (Garside and Wythe 2006: 205, 209: Fig. 7; Thygesen et al. 2006: 27, 30-Fig.5B). The problem of differentiation of two bast fibre, flax and hemp, that share similar chemistry and microstructure was addressed by FTIRS to consider the secondary S2 fibrillar wind. Microfibrillar angles of circa 7º were evident for both fibres. However, for the flax fibre, this was "Z" wind anticlockwise and, for hemp, "S" wind clockwise which is contrary to accepted determinations (Garside and Wythe 2006: 205, 209: Fig. 7).

The combination of FTIRS along with microscopic analysis to determine the fibre MFA has been considered in various studies (Garside and Wythe 2006: 205, 209 Fig.7; Thygesen et al. 2006: 27, 30 and Fig.5B; Dia and Fan 2010: 339). Other methods of measurement are also available, (Herzog (Red-Plate) colour change, or direct angular measurement of ultimate fibre orientation under cross-polarised light (Herzog 1985).

The methods proposed using FTIR spectra for MFA analysis seems unnecessarily complex in comparison. This topic is addressed in more detail in **Chapter Seven.**

5.5.1 Processing effects on FTIRS

In an alternative spectrographic analysis Fourier Transform Infrared (FTIRS) investigation of the effects of retting and processing on hemp fibre, a significant difference (ANOVA p = 0.05) in mechanical strength between the alkali-treated fibres was recorded and the difficulty in obtaining convincing FT Raman spectra arising from natural fluorescence blanking the Raman signal reported (Peetla et al. 2006: 689). While concerns about the effect of fluorescence on the Raman spectrometry and the preference for near infrared excitation are recognised, (Edwards et al. 1996: 6630; Peetla et al. 2006: 689), it was decided to submit the samples for a comparative infrared evaluation (FTIR) test to compare the results. Nettle, flax and hemp fibre samples were analysed using the FTIR spectrum obtained on a Perkin-Elmer Spectrum 100 ATR-Spectrometer **Figure 5.3.**

Figure 5.3 Perkins Elmer Spectrum 100 FTIR-ATR.

Figures 5.4, 5.5 and 5.6 show the FTIR Intensity ratios derived for flax, nettle and hemp. Comparison with the FTRS results shows the variation attributed to soft bast fibre autofluorescence. The result from both series of tests is shown in **Table 5.3forv comparison**

I.D	Sample	R´ ($I^{1121/1096}$)	R ($I^{1096/2900}$)
1	Flax (FTRS)	0.72	0.85
2	Ramie (FTRS)	0.70	1.63
3	Jute (FTRS)	0.77	0.92
4	Flax (FTIR)	0.69	5.50
5	Nettle (FTIR	0.58	1.73
6	Hemp (FTIR)	0.73	3.90

Table 5.3. ID 1-3. Results from FTRS diagnosis of plant fibre. Ratios derived from spectra of fibre samples Edwards et al. (1997) Table 5.2 above. ID 4-5. Results obtained from Perkins Elmer FTIR Spectrum 100 added for comparison.

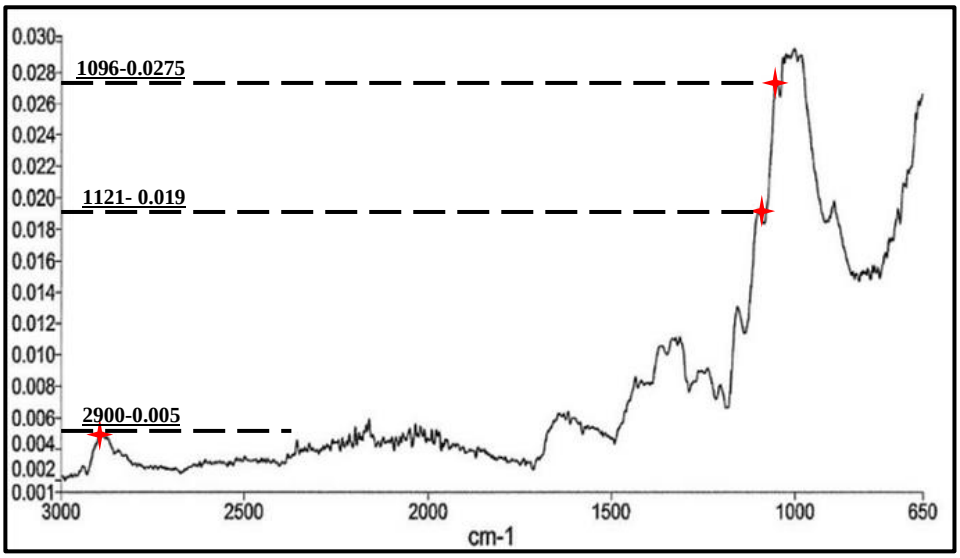

Figure 5.4 Flax FTIR spectra. Intensities (*I*) identified. Intensity ratios R´($I^{1121/1096}$) 0.019/0.0275 = 0.69 R=($I^{1096/2900}$) 0.0275/0.005= 5.5

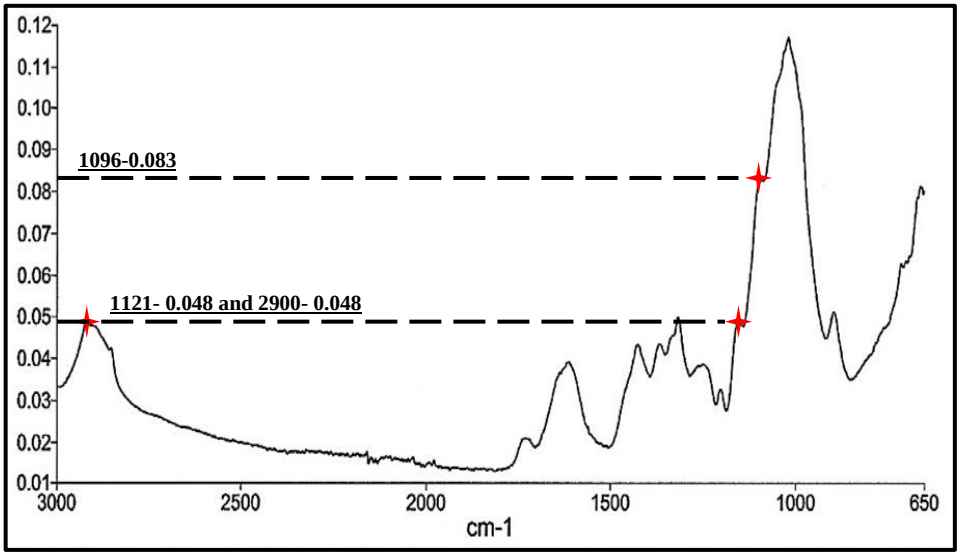

Figure 5.5 Nettle FTIR spectra. Intensities (*I)* identified. Intensity ratios R´($I^{1121/1096}$) 0.048/0.083 = 0.58, R=($I^{1096/2900}$) 0.083/0.048= 1.73

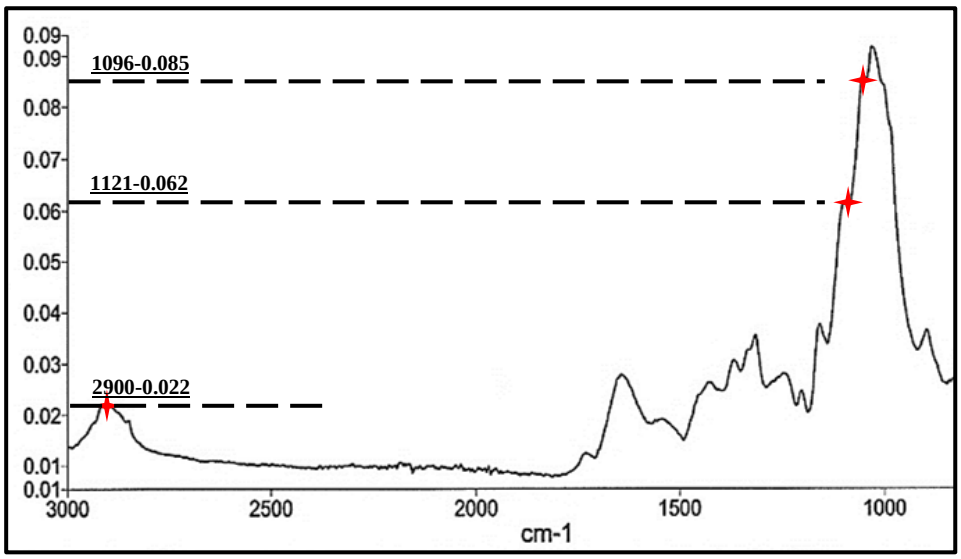

Figure 5.6 Hemp FTIR spectra. Intensities (*I)* identified. Intensity ratios R´($I^{1121/1096}$) 0.062/0.085= 0.73 R=($I^{1096/2900}$) 0.085/0.022= 3.90

The FTRS and FTIR plots for flax, nettle and hemp as listed in **Table 5.3** to display the variation in the calculated R´and R ratios. While the results for nettle are comparable, both flax and hemp display increased ratios for R. A differential that could be attributed to autofluorescence effect.

In a response to concerns regarding the detrimental effect of autofluorescence Peetla et al. (2006: 689) and Holder et al. (2000) confirm the potential for the utilisation of Fourier Transfer Near Infrared at 1064nm to eliminate the interference.

5.6 Fibre Deoxyribonucleic acid (DNA) analysis

The extraction of DNA from archaeological plant fibres could provide a useful identification tool. However, DNA analysis of bast fibres is not considered possible since they are made of dead cells without a nucleus, (**Section 2.2**), and analysis can only be performed on plant fibre samples if undamaged tissue such as parenchyma cells are present (Bergfjord and Holst 2010: 1192). In a study of Scandinavian Viking and Early Middle Age textiles, Skogland et al. (2013: npn) comment that DNA extraction and analysis of bast fibres are usually not possible particularly where exposure to water in the retting process results in hydrolytic damage to the DNA.

In contrast to the lack of DNA in the non-nucleus fibre, Allaby et al. (2005) in their work on flax domestication extracted DNA from flax leave to conclude that the genetic evidence indicated that flax oil was the initially primary product (Allaby et al. 2005).

Dunbar and Murphy (2009) express concerns regarding the accuracy of identifications based on microscopic characteristics and proposed DNA analysis of parenchyma cells for identifying rope samples from crime scenes, including flax but not nettle. In Dunbar and Murphy's micrographs of their work, the presence of parenchyma fragments is illustrated **Figure 5.7** and identified in **(A)**.

Whilst initial comparison of hemp, flax, sisal and jute DNA parenchyma cells associated with the plant fibre were encouraging, in that they were species-specific, Dunbar and Murphy (2009: 111) in their comments on the results for grass-stained sisal rope report,

> "(T)hat, if this were an unknown piece of rope, it would be difficult to determine its identity" Dunbar and Murphy 2009: 111).

Dunbar and Murphy's work confirms Bergfjord and Holst (2010: 1192) findings that DNA analysis was only reliable for uncontaminated archaeological fibre samples retaining associated tissue. Also, hydrolytic damage, oxidation and age degradation of DNA have to be considered in the preparation and diagnosis of samples.

However, in reviewing the above, it is recognised that the rapidly increasing technical capability for DNA analysis may provide opportunities to re-evaluate plant fibre diagnosis in the future.

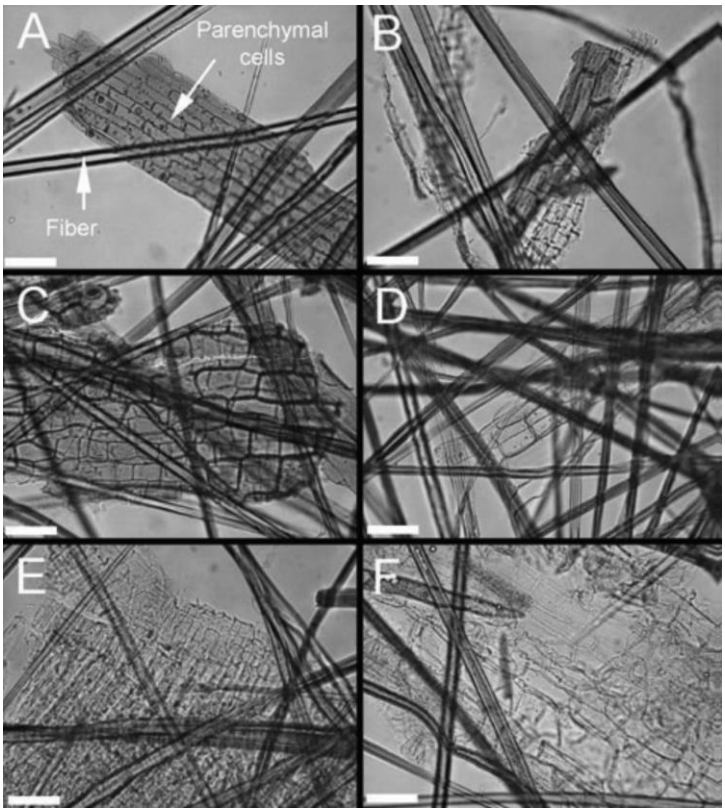

Figure 5.7 Micrographs of ropes. Ropes made from A) abaca leaves; B) flax stems; C) hemp stems; D) jute stems; E) hemp stems (sample sold as jute); F) sisal leaves. All types of ropes, whether made from stems or leaves, had both fibres and parenchyma cells present. (Scale bars = 50μm.) (Dunbar and Murphy (2009: 110).

5.7 Potential of phytoliths to distinguishing between fibres from nettle, hemp and flax

Opal phytolitharia derived from epidermal cells of grass leaves has been identified in atmospheric dust, soils, palaeosol and deep-sea sediments. These were reported by Powers (1992: 15-35) who comments on the early works and includes reference to Darwin's description and analysis of fine dust settling on Beagle. Archaeological applications are attributed to Schellenberg (1983) for his work on archaeological contexts in Turkestan (Rosen 1992: 129-147; Piperno 2006: 2-3). However, not until the 1970s was phytolith analysis included as part of archaeological research.

While seeds and pollen are produced in a recognisable repetitive format, phytoliths, even those from a single plant, vary in form, size, and chemical constituency (Piperno 1988: 50-107; Pearsall and Dinan 1992: 37-64; Piperno 2006: 23-44; Ball et al. 2016). These variations have been catalogued to establish a database in support of the development of a phytolith classification system (Pearsall and Dinan 1992: 37-64; Piperno 2006: 23-44). The major corpus of phytolith morphological references has been assembled from their presence within the monocotyledon grasses, cereal and assorted food plants. Data for dicotyledon phytoliths (cystoliths) shapes are still limited (Bozarth 1992: 193-214, Figs.10.1-10.8, Table 10.1; Canti 2003; Bremond et al. 2005).

5.7.1 Dicotyledon plant fibre phytolith

The diagnosis of opal phytolith associated with dicotyledons (dicots) is listed for phytoliths from herbaceous species native to the Great Plains (USA) (Bozarth 1992). The listing includes a classification of phytoliths shapes present in the leaves of dicotyledons. Of the three species considered in this research programme, unfortunately Bozarth (1992: 193-214) only included nettle as flax and hemp are not native to the Great Plains.

Comparison of Bozarth (1992) image, of the cystoliths collected from nettle leaf structures. **Figure 5.8,** includes a 40µm scale bar that shows the crystal is circa 50µm diameter. The “theoretical fibres” employed in this research programme are circa 25µm diameter a different order of magnitude.

A comparison is available with Bergfjord and Holst (2010: 1195, Fig.4) where the cystolith crystals can be measured from the 30µm scale bar to estimate their diameter at circa 7µm **Figure 5.9**.

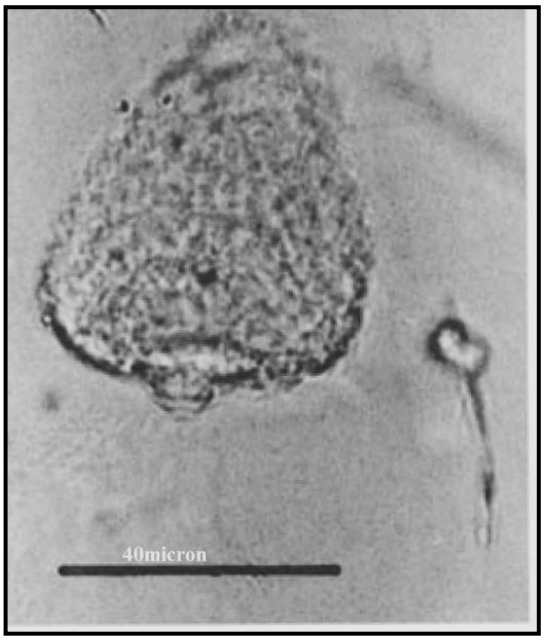

Figure 5.8 Image of triangular silica cystolith with fine verrucate sculpting format formed in *Urtica dioica*. The bar is 40µm (Bozarth 1992: 209 Fig. 10.7A).

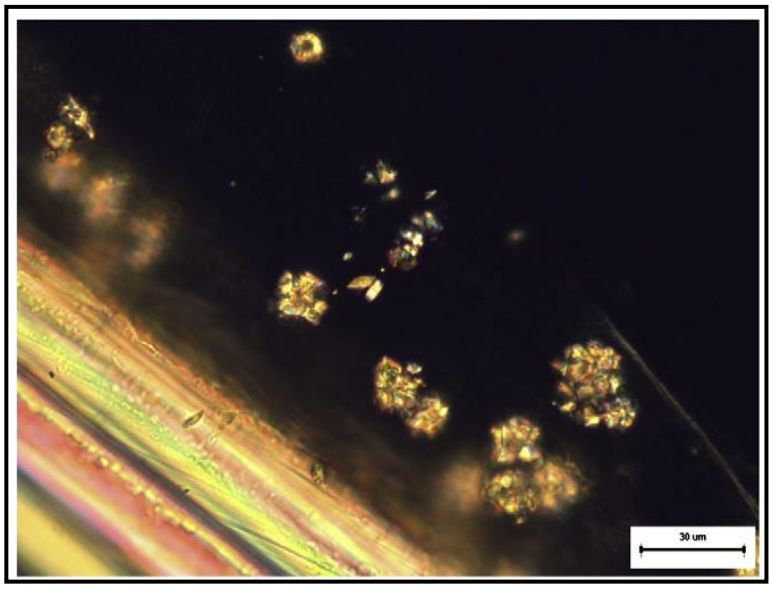

Figure 5.9 Phytolith image in association with nettle fibre (Bergfjord and Holst 2010: 1195,Fig.4) (Note. MFA visible at fibre centre circa -7º)

The presence of phytoliths on textile tools is also reported, although again these are not species-specific (Hurcombe 2000: 155-173; Bowdery 2001: 225-238; Hurcombe 2007: 89-90). However, as with other aspects of tool-wear analysis. There is difficulty in determining whether the tools under consideration were solely dedicated to use on a single species of plant fibre or were employed in multiple processes such as sickles for harvesting (Hurcombe 2000; Domíngues-Rodrigo 2008; Evans 2014a).

5.7.2 Phytolith shape

In addition to silica dioxide (SiO_2), phytoliths derived from calcium absorption are also reported. These needle-like calcium oxalates (CaC_2O_4) and calcium carbonate ($CaCO_3$) druse and raphide structures are usually referred to as cystoliths. The shape of these cystoliths is reported by various authors as spherical, with low contiguous verrucate sculpting, or triangular with fine verrucate sculpting or mace-like druses (Bergfjord et al. 2012: 1193).

Piperno (1988) reports silicified and calcified cystoliths as non-diagnostic. However, images of some cystoliths present in Urticaceae, and their diagnostic shapes and abundant presence are included in the tabulation (Piperno 1988: Table 2.4, Fig. 46, and 65-68).

Barber (1991) remark on the absence of cystoliths in association with flax fibres to propose this as a diagnostic differential. There are suggestions that the absorption of silica and calcium from the soil is limited due to the presence of a "fatty" coating around the plant roots (Parry and Kelso 1975; Parry and Winslow 1977; Sangster and Hodson 1992).

5.8 Method-phytolith extraction

Methods, for the extraction of phytoliths from plant material, are described for two principal processes, dry-ashing and wet-ashing (Pearsall and Dinan 1992: 37-64; Piperno 1988: 119-129; Bozarth 1992: 193-214; Piperno 2006: 89-103). While concerns are expressed regarding dry-ashing, with plant samples incinerated at temperatures from 500-1000C, and higher temperatures affecting phytolithic morphology and Piperno (2006: 97) recommended this method with a proviso that the furnace temperature be limited to 500ºC.

5.8.1 Extraction method

In this research, it was decided to adopt the dry-ash method utilising diluted hydrochloric acid (HCl) and diluted hydrogen peroxide (H_2O_2). The process was conducted within a fume-cupboard.

- Sample of ten grams were selected, and excess retained pith and core material removed before packing the sample into individual clean crucibles and labelled.

- The muffle furnace was cleaned before insertion of the crucibles, and the location within the furnace for each sample logged.

- The furnace temperature was set to 500ºC. and start-time and data-log initiated.

- Regular inspections were undertaken to confirm temperature stability.

- In a fume cupboard, the ash content was removed from the crucibles and transferred to test tubes for further processing.

- Remaining organic material was removed with the addition of 10% HCl and the sealed test-tubes heated in a water-bath at 70ºC.for 20 minutes until the reaction ceased.

- The sealed test-tubes were transferred to a centrifuge (3500 rpm. for 5 mins.) and the clear HCl residue removed by pipette for discarding under a water-stream.

- 10ml distilled water was added and each tube and returned to the centrifuge (3500 for 5 mins.) and the clear fluid decanted under a water stream.

- In the fume cupboard 10ml. of hydrogen peroxide (H_2O_2) was added by pipette and the centrifuge process continued (3500 rpm. for 5 mins.). The waste residue was decanted in a water stream.

- The above process was repeated, and the rinsing process finished with a distilled water flush.

- The remaining ash was transferred to absorbent paper and returned to the fume cupboard to dry overnight.

- Finally, the ash residue was stub mounted and prepared for carbon coating and SEM microscopic imaging.

- Identified phytolith presence was noted, and the images were measured under ImageJ Particle Analysis to quantify size, shape and number.

5.9 Phytolith ImageJ analysis

Each of these source samples was divided into their plant growth section, flowers, leaves, stem, fibre, root, and the phytolith/cystolith presence determined by the dry ash process. **Figure 5.9** illustrates the shape, variety and colour of nettle fibre cystoliths as observed under a Nikon Optiphot compound microscope with cross-polarised light (CPL) at 40x magnification and a Nikon BD Plan 40/0.65 objective lens. The images were subsequently analysed with “ImageJ" software to determine particle dimensions (Rasband 2016; Broeke et al. 2015).

In an evaluation of the presence of calcium oxalates cystoliths in nettle fibre, a sample of ashed nettle stalk was submitted to Scanning Electronic Microscopy (SEM) and Energy Dispersive Spectrometry (EDS) analysis by Bergfjord and Holst (2010) who commented that,

> If mainly calcium oxalate crystals are found, it indicates that the fibre is either nettle ramie or hemp" (Bergfjord and Holst 2010: 1195)

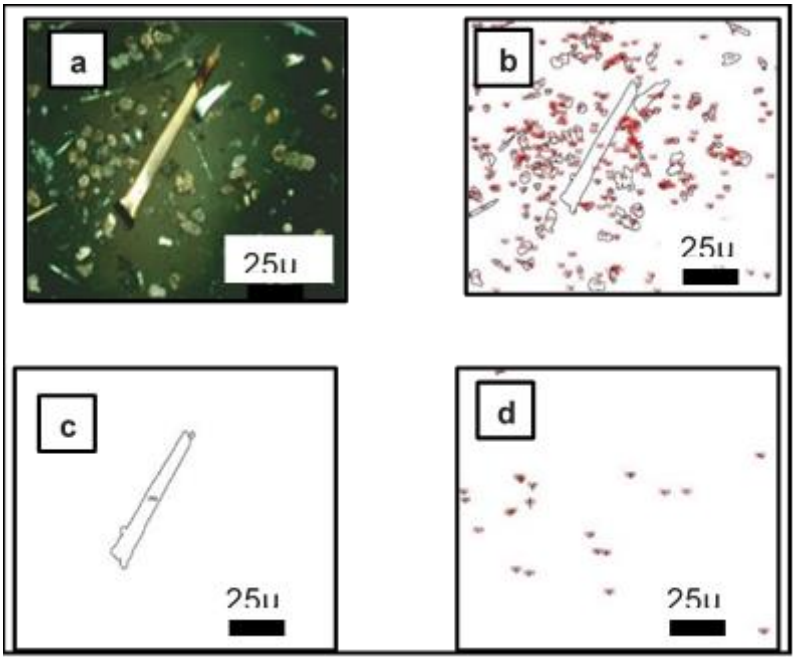

Figure 5.10 Phytolith presence in nettle leaf ash. CPL image evaluated by "ImageJ" particle analysis. a) SEM, CPL image 400x nettle leaf ash for cystolith identification. b) image transformed under ImageJ (336 particles at 82µm^2 ave.area). c) analysis limited to large particles > 900µm^2 ave. area. d) small particle image analysis 21 at 26 µm^2.

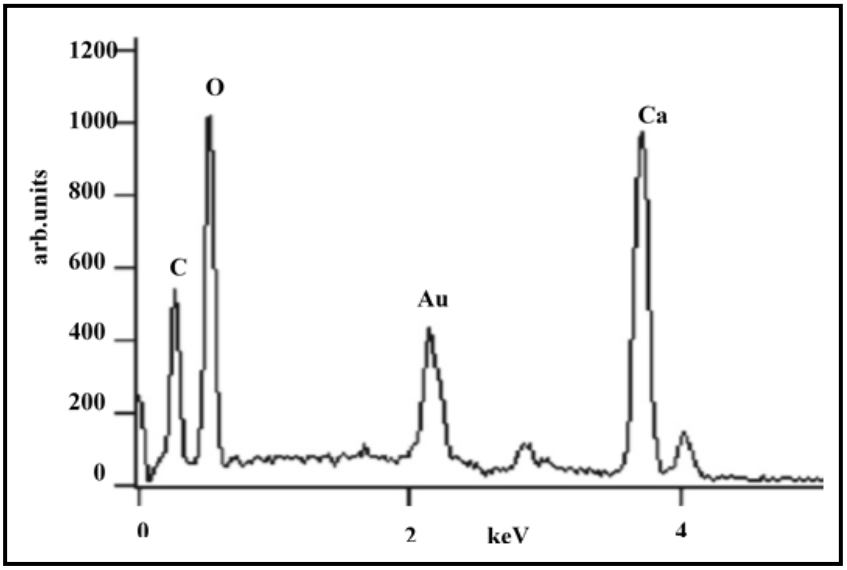

Figure 5.11 SEM/EDS Analysis of calcium oxalate (CaC_2O_4) cystolith crystals in nettle fibre. Au is present from the gold coating of the sample (Bergfjord and Holst 2010: 1196, Fig.7)

A similar trial to the above with *(SEM*) with (EDS) was conducted on the nettle leaf sample illustrated in **Figure 5.10 (a)** to evaluate the process with a phytolith crystal identified at the top of the non-segmented nettle leaf hair

Element	Weight %	Atomic %
OK	46.75	66.51
MgK	0.71	0.66
SiK	0.77	0.63
SK	15.50	11.01
ClK	6.60	4.24
KK	7.21	4.20
CaK	22.47	12.76
Totals	100.00	

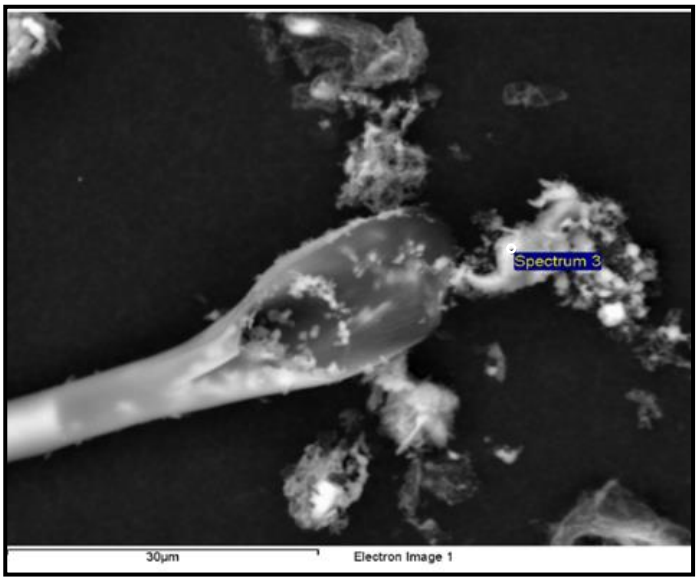

Figure 5.12 A phytolith crystal was identified at the top of non-segmented nettle leaf hair. (Spectrum 3) considered to be calcium oxalate. Scale 30µm. Phytolith chemical constituents are listed on the left.

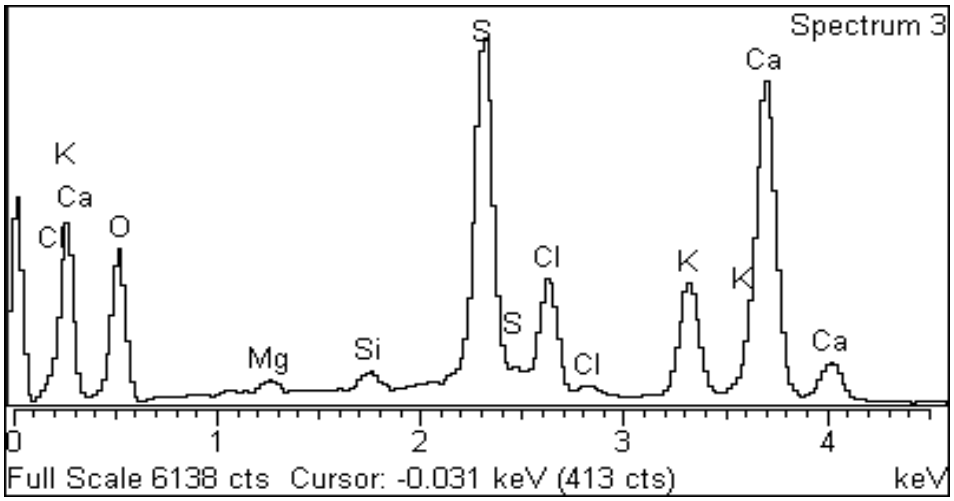

Figure 5.13 The ashed nettle leaf assemblage (Figure 5.12 above) was subjected to EDS analysis to propose that the cystolith could be calcium oxalate (CaC2O4) crystal

5.10 Summary

In this chapter, fibre chemical analysis by ADF/NDF, DNA and phytolith presence have been evaluated as fibre diagnostic features that may meet the Aims and Objectives as detailed in **Chapter 1**A review based on the analysis of variance (ANOVA) in the evaluation of the chemical constituents of 80 plant fibre samples reveals a minimal differential in the principal constituent, cellulose. There are minor variations between both nettle and hemp and flax and hemp. However, there was no significant difference between the nettle and flax constituents. In addition, and a significant deviation from the research design criteria, the ADF/NDF processes are destructive and as such unsuitable for the analysis of archaeological fibre assemblages

DNA offers limited potential as the fibres themselves have no nuclei. Hence, DNA will only be available from associated nuclei-rich plant material accompanying the fibre sample. While the process, with minimal sample size, meets the objective, the presence of associated plant material limits the application to the analysis of fibres obtained from less rigorous processing. Improvements in DNA, coupled with research on flax plant hybridisation, may offer advantages in the diagnosis for the differentiation of the hybrids developed with a preference for either oil or fibre production. The identification of hybrid variations may assist in resolving the oil/fibre dichotomy in allocating end-use diagnosis ascribed to the presence of flax seeds in archaeological assemblages.

The comments on future developments in FTRS and the proposal that Fourier Transfer Near Infrared Spectrometry FTNIRS, may overcome the difficulty associated with autofluorescence interference with image quality is noted. Consequently, the improvements in diagnosis, with reduced sample sizes

would be less invasive and may provide improvements. However, it is necessary to accept that any FTRS analysis could only confirm the chemical constituents that are, as noted above, variable and dependent upon growth conditions and fibre processing.

Chapter Six
Plant fibre material properties-tensile strength and young's modulus

6.0 Introduction

In **Chapter 5** the diagnostic potential available from plant fibre chemical analysis, DNA analysis and phytolith presence were compared. Here the material properties of nettle, flax and hemp are evaluated. The possibility of establishing a database of textile fibre mechanical properties was included in an early study of the mechanical properties of single fibres as an extension to other physical methods of qualitative analysis. The results where tabulated with the proviso that the fibre conditions are dependent upon growing environment, production processes and the testing environment (Luniak 1953: 87-88 and Table 5).

Fibre Type	Tenacity g/den.	Density g/cc	Calculated GPa	Bodros and Baley 2008 Table 1. GPa
Ramie	4.5-8.8	1.51-1.55	0.60-1.203	0.56-0.90
Flax	2.6-8.0	1.48-1.50	0.34-1.058	0.85- 1.80
Hemp	3.0-7.0	1.48-1.49	0.40-0.920	0.23-0.31 (?)
Jute	2.0-6.3	1.44-1.49	-------	Not shown

Table 6.1 Plant fibre tenacity and ultimate strength. (Luniak 1953:Table 5; Bodros and Baley 2008: Table 1) with additions. Note. Luniak provides factors for the conversion of tenacity to GPa). The final column shows the comparison of Bodros and Baley (2008) with GPa for ramie and flax to be in close agreement, the authors report the figure calculated for hemp as "suspect".

6.1 Availability of fibre samples

Investigations to assess the potential for cultivation of nettle were undertaken in Germany in the late 19th century in response to the growing interest in nettle as a commercial crop. However, there were doubts expressed as to the suitability of *Urtica dioica.* Nettle cultivation proved extremely valuable during World War 1 as, with a trade embargo on the importation of cotton fibre.

The German manufacturers used nettle fibre as a substitute in manufacturing tents, rucksacks, undershirts and socks. It is estimated that 85% of these products were made of nettle fibre (Bodros and Baley 2008: 2143-2145).

More recently in the UK the "Sustainable Technology. in Nettle Growing" (STING) project was sponsored by the Department of the Environment, Food and Rural Affairs (DEFRA) to evaluate the potential for the introduction of commercial production of nettle fibre crop to the UK farming community. The project was undertaken by De Montfort University's Textile Engineering and Material Research Group to evaluate the fineness and yield of the fibre (Horne et al. 2008: 63-70; Harwood and Edom 2012). The work entailed the development of a chemical extraction process to optimise fibre extraction rates.

In a retrospective view, Horne et al. (2008) noted that the total production levels achieved in Germany during World War Two (1939-1945), approximately 10,000 tonnes, were obtained from a combination of commercial growing coupled with the encouragement of small-scale public endeavours. Subsequently, it is reported that the organised collection and cultivation of nettles ceased after the war as the commercial interest declined due to cost-effectiveness and technical issues (Horne et al. 2008: 63-70).

Based on the above a test crop was planted and harvested in Driffield East Yorkshire, by Springdale Crop Synergies.

The problematic stem decortication had been was addressed using a pilot chemical process designed by De Montfort University with spinning and weaving completed by Camira Fabrics plc, Meltham, West Yorkshire (2018).

Samples of the commercial nettle fibre and other plant fibre products were provided to the University of Bradford for comparative evaluation. Decortication of the commercial nettle fibre at the pilot plant was completed by soaking the stems in a sodium hydroxide solution followed by a water rinse and drying (Horne et al. 2008: 63-70; Harwood and Edom 2012).

6.2 Fibre preparation

It is noted that there are practical skills and knowledge required in replicating the plant fibre production quality as achieved by the hunter-gatherer groups of the past and of those reported in the ethnographic studies. In recognising the need for practical craft support, it was decided to request the services of the Bradford District Guild of Handweavers, Spinners, and Dyers (2014) to prepare a range of nettle products for testing. Two-ply spun products were provided from the combed nettle fibres obtained from lithic blade combing and shorter fibres from the following heckle combing.

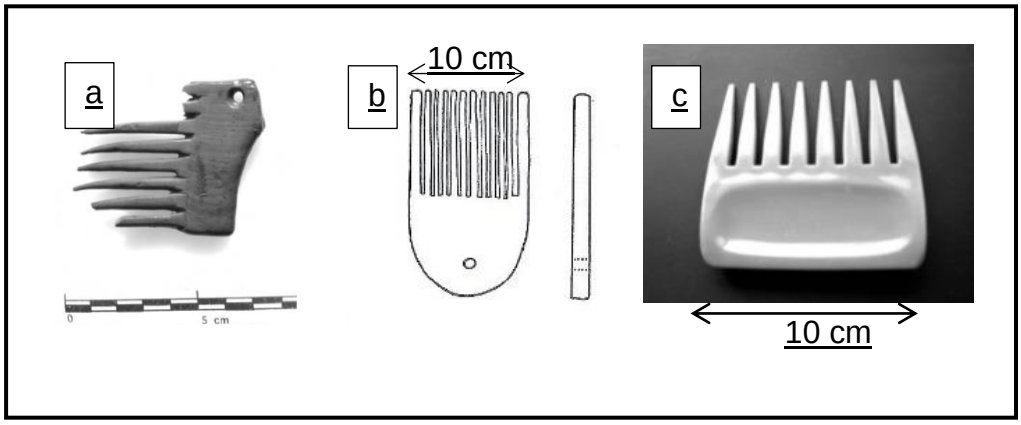

Figure 6.1. Wooden comb and modern equivalent. a) La Draga, Neolithic boxwood comb (Bosch et al. 2006: 93), b) Vindonissa (A.D.1) wooden comb (Wild 1970: 154), c) Modern equivalent used by the Author in the preparation process (Waudby 2014).

6.3 Evaluation of breaking load for two-ply nettle fibre

Facilities for conducting the load tests were available at the University of Bradford, Faculty of Engineering and Informatics, School of Engineering using the Instron 5564 electromechanical load frame testing systems (Instron High Wycombe UK 2016). The Instron 5564 is used to test a wide range of materials in tension or compression, utilising electromechanical load frames designed to apply load to the test specimen via the moving crosshead.

The drive system moves the crosshead up, to apply a tensile load on the specimen, or down, to apply a compressive load on the specimen. A load transducer (load cell), mounted in series with the specimen, measures the applied load. The load cell converts the control system measures to display and tabulate the results. Load cells are interchangeable within a range of capacities, to provide a load measuring capabilities limited only by the maximum capacity of the load frame. Strain transducers (extensometers) can also be used on these systems to measure strain.

Figure 6.2 5564 Mechanical stress/strain testing equipment (Instron High Wycombe UK 2016)

6.4 Spun nettle fibre breaking load

The two-ply nettle fibres from the long fibre and short fibre samples “A” and “B” were tested for breaking load, conducted as specified in ASTM D 3379-75 (1989) The following results were obtained **Table 6.2.**

Type of Fibre (2ply)	Ref. No.	Dia. mm	Breaking Load N
Long fibre (B)	LF2 A1	1.2	84.9
Long fibre (B*)	LF2 A2	1.3	72.7
Short fibre (B)	SF2 B1	2.0	34.9
Short fibre (B)	SF2 B2	1.9	27.15
Retted fibre (A)	RF2 A1	1.2	19.66
Retted fibre (A)	RF2 A2	1.3	17.98

Table 6.2 Breaking load for two-ply nettle fibre

Figure 6.3 shows a plot of typical raw results as obtained through tensile testing. This figure presents the results for seven samples of retted Stinging Nettles and illustrates the wide range of variance.

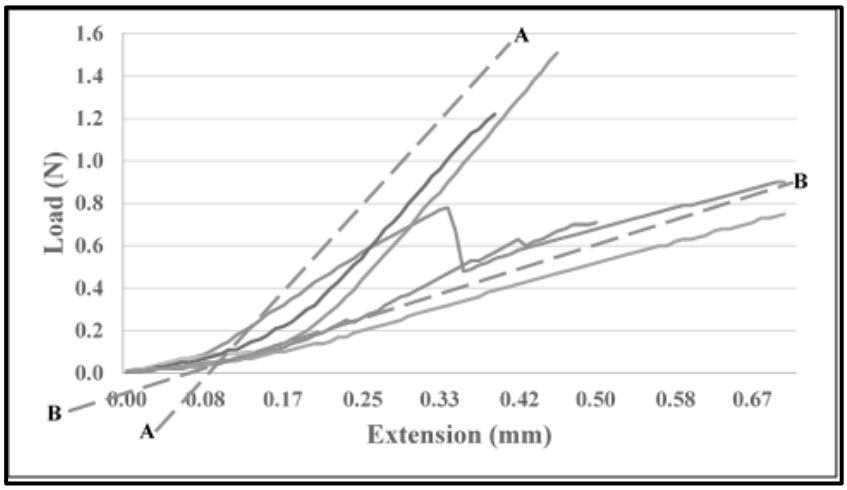

Figure 6.3 Results of tensile strength test for seven retted Stinging Nettle fibre. Loading measured on Instron 5564 electro-mechanical load frame. Testing equipment (ASTM C1557 2014; Instron2017). Note. For equal Young’s moduli values, lines AA and BB on the graph would be parallel.

The tensile test programme was extended to cover a range of fibre samples (n= sample size). **Figure 6.4** shows a boxplot of data for Young's moduli from the seven different types of fibre studied using the tensile testing bench and the results plotted for the 32 samples. The following nomenclature is applied **1.** Wild retted nettle (n=5), **2**. Wild unretted nettle (n=4), **3**. Commercial nettle bleached (n=6), **4.** Commercial nettle unbleached (n=3), **5.** Commercial hemp combed (n=6), **6**. Commercial hemp unbleached (n=5) and **7**. Commercial flax (n=4). There was limited significance between the groups (F=0.796, df=32, p=0.582).

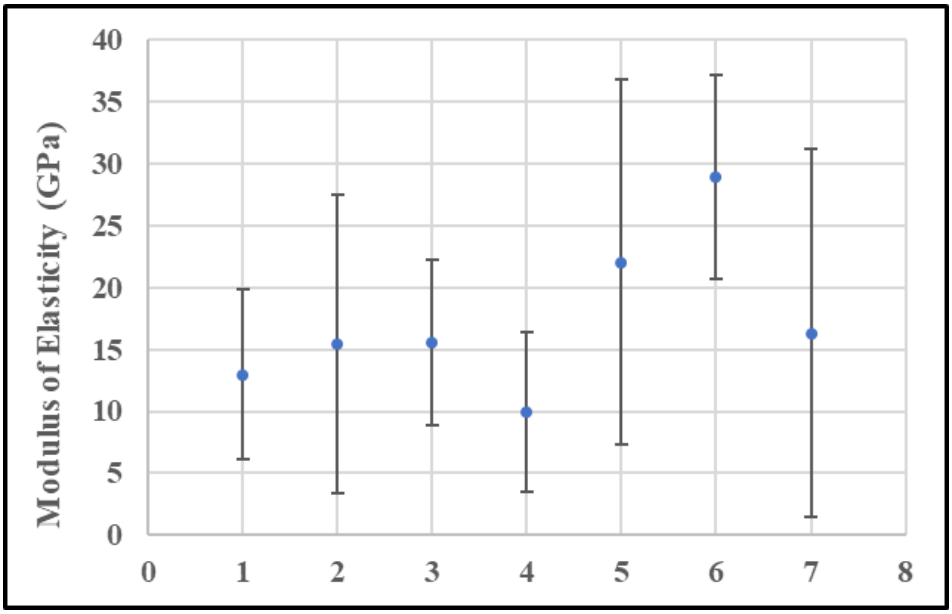

Figure 6.4. The variation in tensile strength for the seven two-ply samples described above were subjected to analysis of variance in Young's modulus of elasticity E. ANOVA analysis shows limited significance between the groups (F=0.796, df=32, p=0.528)

6.5 Fibres in composite materials

Difficulties in the evaluation of material properties have been reported (Haugan and Holst 2014). In recent studies, of plant fibre incorporated into composite materials, there was a need to attain improved predictability in performance and reliability in the quality of production for “load-bearing” components. Assessments of these material composites have been conducted incorporating standard test procedures as specified within ASTM D 3379-75 (1989) utilising the Instron 5564 electro-mechanical load frame testing equipment (Bodros and Baley 2008; Summerscale et al. 2010; Baley and Bourmaud 2014).

Table 6.3 (a,b,c.d) includes these composite identified “C”, within the *E* value listing. The **Table 6.3** listing is subdivided into categories to separate flax for composite use (C) from oil-seed flax varieties to aid statistical comparison. There are 44 composite values listed with an average of 48GPa, for oilseed flax varieties there are 13 listed with an average of 53GPa a close comparison.

No.	Author	Year	Flax GPa	Flax St. Dev.	Hemp GPa	Hemp St. Dev.	Comment
1	Thomason et al.	2011	61.9				(C) 9.57 CSA as indicative of "*E*" for flax is unreliable
2	"		58.8				(C) 7.48 CSA " " "
3	"		51.9				(C) 9.30 CSA " " "
4	"		53.2				(C) 9.03 CSA " " "
5	"		59.2				(C) 8.71 CSA " " "
6	"		57.0				(C) 7.64 CSA " " "
7	"		53.6				(C) 9.98 CSA " " "
8	"		49.8				(C) 10.26 CSA " " "
9	"		50.9				(C) 7.96 CSA " " "
10	"		47.8				(C) 8.76 CSA " " "
11	"		46.9				(C) 11.56 CSA " " "
12	"		43.0				(C) 10.71 CSA " " "
13	"		37.6				(C) 8.77 CSA " " "
14	"		40.9				(C) 10.30 CSA " " "
15	"		36.8				(C) 11.44 CSA " " "
16	Haag and Mussigi	2016	72.0	40.0	64.0	30.0	(C) Flax and Hemp CSA v "*E*" est. from chart. F 72 GPa, H 64 GPa
17	Bodros and Baley	2008	58.0	15.0	19.1	4.3	(C) Nettle for comp. v flax and hemp. (Authors recommend nettle)
18	"		71.0	25.0			" " flax (" " ")

Table 6.3 (a) *E* modulus derived from various publications

No.	Author	Year	Flax GPa	Flax St. Dev.	Hemp GPa	Hemp St. Dev.	Comment
19	Bourmaud et al.	2013	68.2	35.8	19.1	11.3	Relationship "*E*" and MFA for flax varieties Hermes
20	"		54.1	15.1			" " " Ariane
21	"		57.0	29.0			" " " Agatha
22	"		41.0	12.5			" " " Everest 1
23	"		75.0	21.6			" " " Everest 2
24	"		46.3	12.1			" " " Alaska
25	"		67.5	23.7			" " " Hivernal
26	"		47.2	21.3			" " " Oliver
27	Harris et al.	2017	17.0	6.5			Examined Neolithic potential for flax v lime bast (dry)
28	Barbuléé and Gomina	2017	55.0	25.0			Compared fibre strand v bunch and gauge length est. from a graph
29	Fuentes et al.	2017	72		27.0		(C) Uses strain map to confirm "*E*" differentiation (strong fibre)
30	"				24.0		" " " (weak fibre)
31	Placet et al.	2017			19.7	10.2	(C) Considered retting effects on "*E*" hemp 19.7 (retted)
32	"				16.7	6.7	" " 16.7 (non-retted)
33	Gourier et al.	2014	55.0	15.0			(C) Evaluated temperature effect on "*E*". normal temperature
34	"		54.0	16.0			" " 140deg.
35	"		54.0	18.0			" " 190 deg. max. temp

Table 6.3 (b) *E* modulus derived from various publications (continued overleaf)

N0.	Author	Year	Flax GPa	Flax St. Dev.	Hemp GPa	Hemp St. Dev.	Comment
36	Lefeuvre et al.	2014	56.2	11.9			(C) Assessed the variation in "*E*" for Flax varieties. Marylin 1
37	"		50.3	12.2			" " " Marylin 2
38	"		60.5	19.2			" " " Marylin 3
39	"		48.9	11.5			" " " Marylin 4
40	"		66.5	36.3			" " " Hermes
41	"		50.1	27.2			" " " Oliver
42	Pillin et al.	2011	71.7	23.2			(C) Compared "*E*" for Flax (Oil) to replace fibre Hivernal
43	"		49.5	13.2			" " " Alaska
44	"		45.6	16.7			" " " Niagra
45	"		48.0	20.3			" " " Everest
46	"		57.0	20.9			" " " Oliver
47	Goudenhooft et al.	2017	41.2	10.3			(C) Determination of "*E"* for improved fibre yield Liral Prince
48	"		44.3	9.7			" " " Ariane
49	"		55.5	15.1			" " " Eden

Table 6.3 (c) *E* modulus derived from various publication (continued overleaf)

No.	Author	Year	Flax GPa	Flax St. Dev.	Hemp GPa	Hemp St. Dev.	Comment
50	Goudenhooft et al. "		46.1	15.9			" " " Aramis
51							
52	Thygesen et al.	2006			23.0	5.0	(C) Effect of fungus upon "*E*" of hemp (Raw)
53	"				20.0	3.0	" " (Treated)
54	Summerscale et al.	2010	58.0	15.0	70.0		(C) Flax fibre as reinforcement for composite
55	Peetla et al.	2016			11.1	0.1	"*E"* as related to retting time for hemp (H1 2.5 wk.)
56	"				12.8	0.1	" " (H2 5.5 wk.)
57	"				7.8	0.1	" " (H3 7.8 wk.)

Table 6.3(d) *E* modulus derived from various publications

6.6 Trial with Biomomentum mechanical testing equipment

Following discussions with colleagues in the Faculty of Engineering and Informatics (University of Bradford), it was suggested that the Biomomentum test facilities, coupled with statistical analysis, might offer a more rigorous diagnostic parameter (Biomomentum 2016).

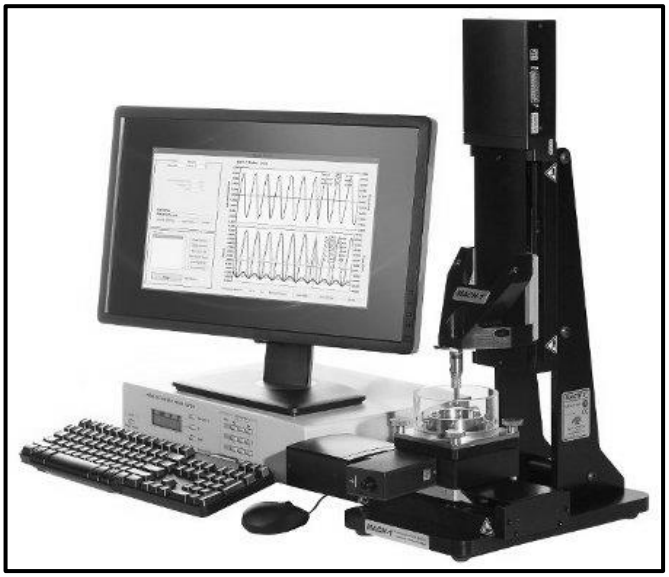

Figure 6.5 Biomomentum Mach-1^{TM} Mechanical testing equipment. This multiple-axis tester developed originally for cartilage testing, is now being used in various configurations for the evaluation of the mechanical properties of tissue and soft material (Biomomentum 2016).

6.6.1 Initial tensile test trial

To determine the potential for tensile testing of plant fibre, it was proposed to evaluate *E* using the Biomomentum Mach-1 testing equipment. The Biomomentum is designed to perform tests on small diameter specimens such as biological tissue and can apply the tensile load through precision displacement control in small increments with variable load cells ± 150 g to ± 10 kg. A trial run, suitable for small diameter plant fibre samples of flax and

nettle was undertaken. Single flax and nettle fibres of varying diameter, 10-35µm, were presented for tensile tests conducted as specified in ASTM D 3379-75 (1989). For the eight samples, four flax and four nettle, included in the trial the following examples of “Stiffness v Extension curves are shown below **Figure 6.6 (a and b).**

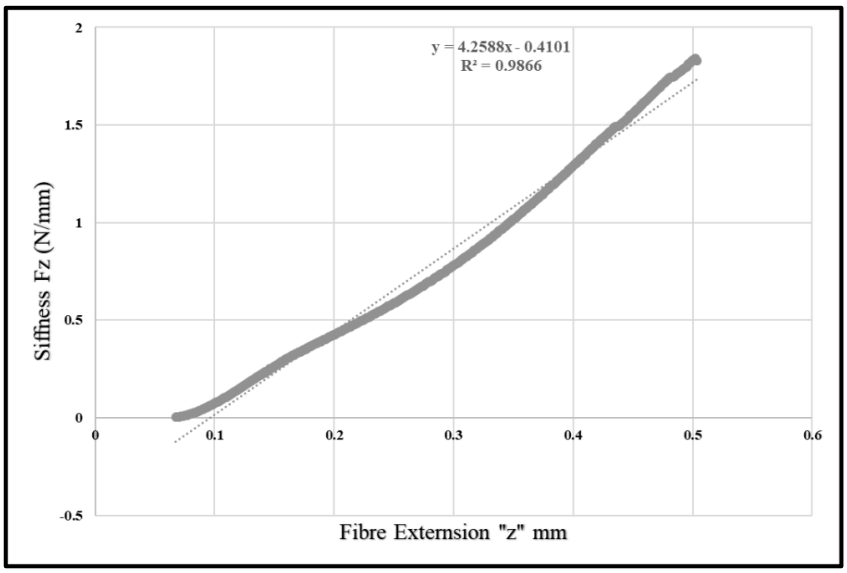

Figure 6.6 (a) Stiffness/extension trendline for flax. The trendline depicts the elasticity slope for evaluation of Young’s modulus (*E)*

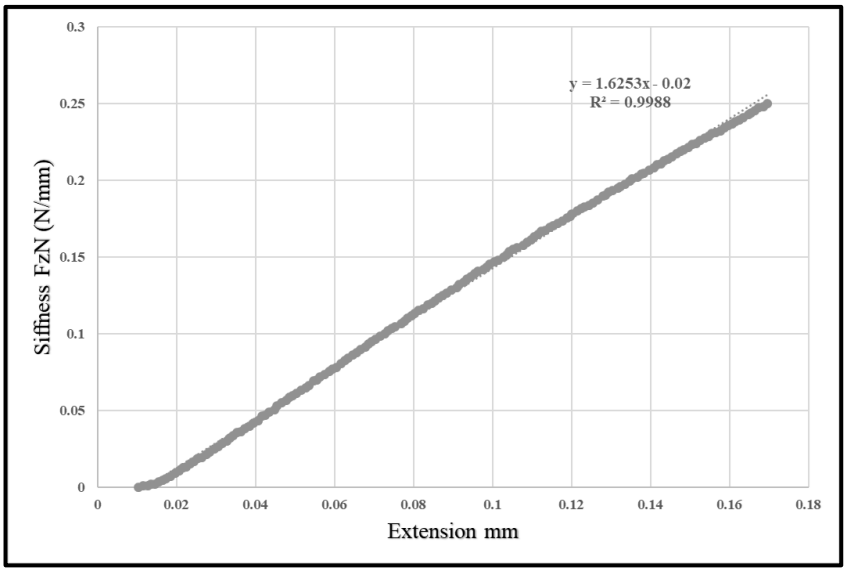

Figure 6.6 (b) Stiffness/extension trendline for nettle. The trendline depicts the elasticity slope for evaluation of Young’s modulus *E*

6.6.2 Biomomentum Mach-1 trial test results

The load-displacement relationship during fibre testing, together with the linear elastic approximations, were used to calculate Young's moduli (*E*). While the least-squares fit to the initial loading curves is good, there are subtle periodic variations in stiffness that appear to be characteristic of the deformation process. The variations in the slopes of individual lines for each fibre reflect the actual value of stiffness as influenced by the individual fibre cellulose content **Table 6.4.**

	Sample	**Dia. (mm)**	**Max. Load (N)**	**Stiff (N/mm)**	**Str. (MPa)**	**Young's Moduli *E* (MPa)**
Flax	1	0.170	1.84	4.26	81	4691
Flax	2	0.197	2.43	8.48	80	6959
Flax	3	0.122	2.34	5.38	200	11506
Flax	4	0.063	0.42	1.05	136	8398
	Mean	**0.138**	**1.76**	**4.79**	**124**	**7889**
	St. Dev	**0.059**	**0.927**	**3.071**	**57**	**2854**
Nettle	1	0.068	0.50	2.52	137	17360
Nettle	2	0.041	0.25	1.63	189	30776
Nettle	3	0.045	0.28	0.63	173	9939
Nettle	4	0.050	0.56	1.27	286	16126
	Mean	**0.051**	**0.40**	**1.51**	**196**	**18550**
	St. Dev	**0.012**	**0.157**	**0.789**	**64**	**8774**

Table 6.4. Results from Biomomentum Mach 1 testing. Maximum Load (N), stiffness (N/mm) strain (MPa) and *E* (Young's moduli) (MPa for four samples of retted flax and four samples of nettle are tabulated. The table evaluates the straight-line relationship of Stiffness/Strain to calculate Young's modulus (*E*).

6.7 Young's moduli (*E*) for flax, nettle and hemp

The above pilot study was extended to review the evaluation of *E* as a diagnostic feature for the three plant fibre species under consideration.

The following fibres were selected for further study.

Flax (*Linum usitatissimum.* L**.**) (v. Eden) A minimally processed cultivated crop provided by East Yorkshire Hemp (2017).

Hemp (*Cannabis sativa* L.) (v. Santhica) Plants grown for oilseed production and provided by East Yorkshire Hemp (2017). Traditional textile hemp with high THC may be available from overseas. However, the present samples will suffice as a base diagnostic material.

Nettle (*Urtica dioica* L.) A wild plant collected from a woodland site in Bradford West Yorkshire.

For each of the above, 24 samples were mounted across a 6mm diameter gap and held within a card support frame. The samples were fitted into the Biomomentum clamping device and tension applied with an on/off variable velocity of 1mm/sec Examples of the resulting stress/strain curves are shown in **Figures 6.7 (a and b).**

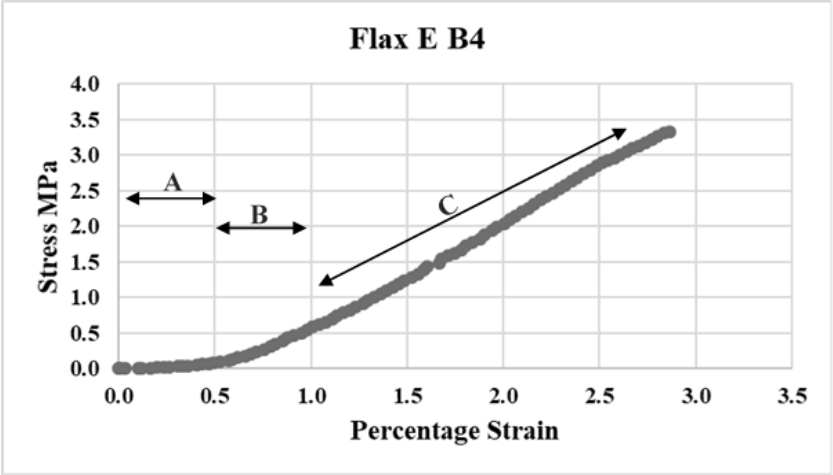

Figure 6.7(a) Stress/Strain curve generated from the tensile test of flax sample E-B4. The curve displays three distinct sections, “A” The initial zero extension as the applied load is absorbed by the mounting frame and clamp realignment, “B” the initial deviation from a straight-line elasticity relationship as influenced by the microfibrillar angle (Charlet et al. 2009) and “C” the straight-line representation of the elasticity range *E.*

The data represented by the curves shown in **Figure 6.7 (a)** requires modification to remove those sections outside the elasticity range to achieve an accurate representation of Young's modulus **(*E*)**. The modified graph is shown in **Figure 6.7(b).**

Sample	Diameter (µm)	Maximum load (N)	Stiffness (FzN/mm)	Area (sq.mm)	Stress (MPa)	*E* (MPa)
A1	114	11.210	31.400	0.01021	1098.1	18455
A6	102	0.600	0.019	0.00817	73.4	14
A8	110	1.730	0.601	0.00950	182.0	379
B1	91	0.448	0.341	0.00650	68.9	315
B2	63	0.174	0.006	0.00312	55.8	11
B3	40	0.450	0.116	0.00126	358.1	554
B4	145	3.240	1.310	0.01652	196.2	476
B7	210	0.460	0.182	0.03464	13.3	32
B8	69	2.560	2.000	0.00374	684.5	3209
C2	86	0.384	0.167	0.00581	66.1	172
C6	81	0.225	0.121	0.00515	43.7	141
				√n=3.46	**Ave. *E***	**2106**
					St. Dev.	**5481**
					SE	**1584**

Table 6.5 Tabulation of *E* for flax samples Flax E (A1-C7).

In **Table 6.5,** eight samples of Flax v Eden (FE) were submitted for each range (A1-C8); some samples did not survive the test. Hence, of the 24 samples submitted, only 11 survived the test. The results achieved for flax FE are, in terms of diagnostic potential, a wide range of *E* values (A1=18455, A6 =14) possibly reflecting the differences in processing. A full comparison of the three species is shown in **Table 6.6.**

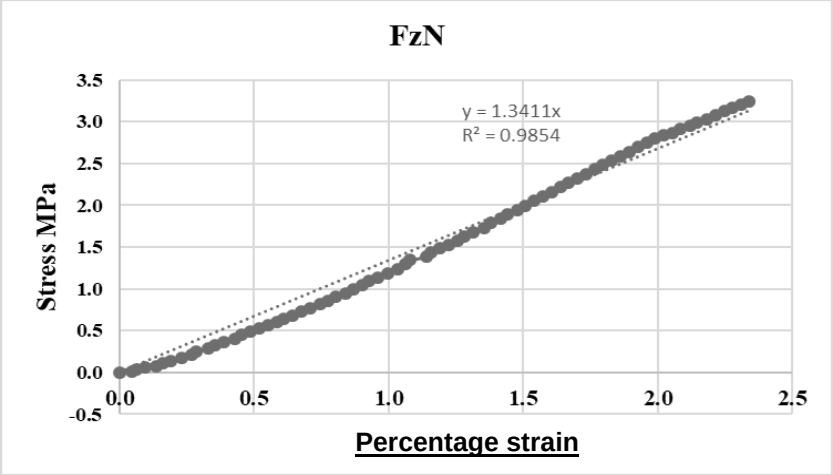

Figure 6.7 (b). The maximum stiffness of the 6mm sampling length subject to the applied load FzN is displayed along with the stress/strain relationship illustrated by the "y" value in the least-square straight-line calculation

No.	Flax	Nettle	Hemp
1	18455	2045	207
2	14	8071	1075
3	379	176	536
4	315	360	6352
5	11	263	16
6	554	784	2064
7	476	11080	256
8	32	39	293
9	3209	115	118
10	172	667	235
11	141	11	256
12		25	1003
13		5775	429
14		69	461
15		2019	
Ave. E	**2160**	**2142**	**950**
St Dev	**5481**	**3407**	**1644**
√n	**3.32**	**3.87**	**3.74**
SE	**1584**	**890**	**440**

Table 6.6. Young's modulus (*E*). Analysis of Variance (ANOVA) in *E* for the three species found there to be minimal variation between the grouped samples (F=0.485905, df= 39, p= 0.619012) (n=40), flax (n=11), nettle (n=15) and hemp (n=14) (The shaded areas indicate outlying values for *E).*

The tabulation in **Table 6.6** is based on the test conducted on those surviving fibres, for some samples the stress induced in the load test or the inadequate mount fixing failed.

Note The database in support of the above is included in Appendix A.

The above database **Table 6.7** is plotted in **Figure 6.8** to illustrates the minimal variation in the measured value of *E* for the three species sampled. This exercise, coupled with the results achieved in previous research (Waudby 2014), indicate that Young's moduli as a diagnostic feature, are unreliable. The range of moduli depicted, 100-800 MPa is in close agreement with the figures reported by Haag and Mussigi (2016) who, in addition to flax and hemp, also included jute, ramie and kenaf in their evaluation. Unfortunately, nettle fibre was not included in their research. As previously noted, there is a range of processes within the *chaîne opératoire* that would modify the material properties of the fibre including plant growth environment, plant maturity at harvesting, the retting and decortication processes and the gauge length and mounting in the tensile test facility (Barbulee et al. 2017).

Additionally, in evaluation of test-bed fibres, it has been confirmed that fibre strength and elasticity values vary along the stem length or from an underestimation of effective fibre cross-sectional area (Charlet et al. 2009; Thomason et al. 2011; Di-Virgilio 2013).

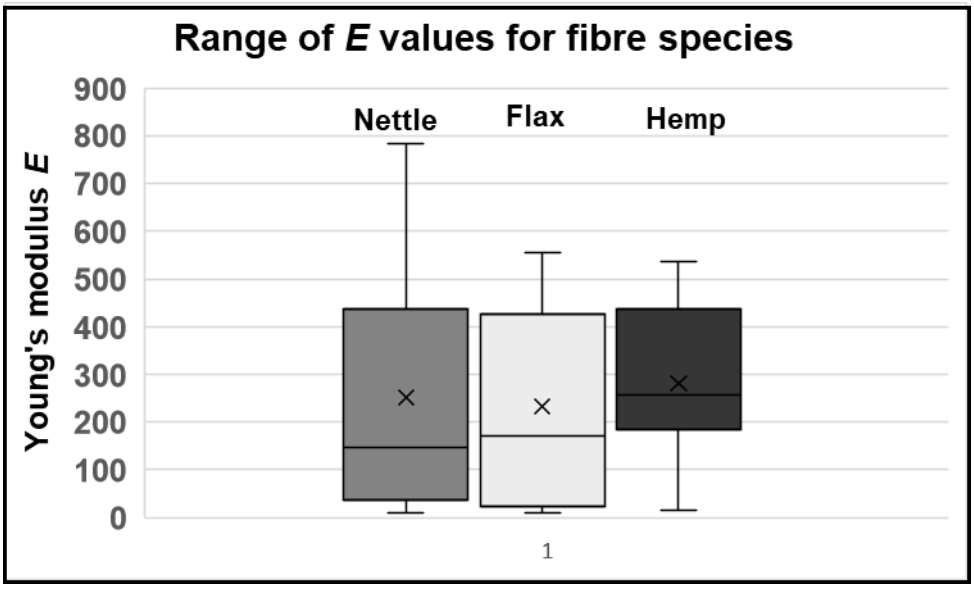

Figure 6.8 A plot of variations in E for the three species**.** The representation has been simplified by eliminating all outliers for *E* values above 1000

The Box and Whisker plot of the database of **Table 6.6** is shown in **Figure 6.8** to demonstrate the commonality of the determination of E as shared by the three plant fibre types and to reinforce the need to explore alternative diagnostic potentials

6.8 Summary

In **Chapter 5** the potential of a range of diagnostic features has been reviewed including,

- Fibre chemical constituents
- The DNA analysis of fibres
- Phytolith presence

It is noted that, for each of the above diagnostic parameters, there are concerns regarding the efficacy and reliability of the methods employed.

The criteria established within the research programme is that the proposed techniques to be employed should be,

- Sufficiently robust, such that the identified diagnostic features will survive within the deposition or conservation environment.
- The diagnosis should be reliable in the determination of the differential diagnostic identity between species and suitable for replication by others.
- Analytical techniques should be minimally invasive and, where samples are removed from the assemblage, the diagnostic features are protected and conserved for future re-evaluation.
- The diagnostic features employed should be capable of replication using standard University research facilities.

The fibre chemical properties' potential to serve as a diagnostic feature, that would comply with the experimental hypothesis and attendant aims and objectives have been discussed previously. Consideration of the variances arising from plant fibre cultivation and the attendant processing *chaíne opérator* plus aspects of post-depositional degradations highlights the

difficulties in formulating reliable diagnostic procedures that meet the research objectives.

Additionally, the data assembled above demonstrate that *E* values vary significantly within individual species both in terms of growing conditions and process treatment and the plant stem location. The final plot in this chapter, **Figure 6.8** and **Table 6.6,** and the attendant analysis of variance (ANOVA) emphasises the requirements to review the plant fibre diagnostic techniques.

Here the fibre material properties, their tensile strength and elasticity were appraised and a corpus of reports on the evaluations Young's Modulus of Elasticity (*E)* was assembled to note and tabulate a database on their use as a replacement for glass-fibre in composite materials. The associated *chaîne opératoire*, harvesting, processing, and assembly techniques would differ from those associated with textile manufacture. Fibres selected for the manufacture of load-bearing construction material would, of necessity, be required to meet stringent quality manufacturing standards.

In measuring *E,* the calculation is based on the straight-line stress/strain relationship (Young's modulus) as depicted by the trend line. E's determination is based on the straight line "elastic range" that includes the need to refine the graphical representation to ensure an appropriate representation of the "elasticity slope" is noted. The adjustments required are detailed as follows,

a) Recognition of the delay in applying the initial stress loading due to initial uptake of load by the mounting mechanism and the consequential delay in the transfer of the load bearing to the fibre

and

b) Determination of the deviation of the loading direction as the microfibres adjust their MFA to take the load-bearing onto a vertical plane.

However, in the evaluation of MFA based on the initial area of trend line deviation, there is a subjective judgement about the location of the stress point displaying the level of maximum deviation. This subjective approximation is a principal concern in the application of this diagnostic technique. It should also be noted as with Herzog's Test the diagnosis can only determine the MFA angle and provides no indication of the negative "S" or negative "Z" twist, a major diagnostic feature in the differentiation of flax/nettle and hemp.

Note The database in support of the above is included in Appendix A.

In **Chapter 7** the potential for additional diagnostic features embedded within the fibre morphology is examined in detail.

Chapter Seven
Plant fibre morphology - microfibrillar angle (MFA)

7.0 Introduction

In previous chapters, fibre diagnostic potentials were appraised, including chemical analysis, fibre DNA, phytolith presence, tensile strength and elasticity. For each of the above, there are concerns regarding the variation in diagnostic determinants as they reflect processes within the *chaîne opératoire*. Fibre diagnostic features are influenced by the environment, climate, soil, cultivation methods, harvesting period and processing. While recognising, particularly for ruderal species, that it is extremely difficult at the microscopic level to differentiate the natural dissipation of pollen and seeds from debris associated with fibre production. The seeds of cultivated flax or hemp from Neolithic sites have been interpreted as evidence of cultivation of oil-bearing plants (Kenward and Hall 1995). In an attempt to identify the seasonality of occupation of the Mesolithic site at Star Carr it was reported that previous research programmes had concentrated on evidence from faunal assemblages, while the potential of plant remains has been largely neglected (Dark 2004). Fibre plant seeds of both flax and nettle were found at Reading Business Park, a Bronze Age landscape, in association with retting pits, and multiple sources of plant fibre, including nettle, were recorded (Moore and Jennings 1992: Ch.9, 122). At the West Row Bronze Age site, flax seeds found in close association with the remains of retting pits are interpreted as evidence of flax processing, no alternative fibre plant remains were identified (Martin and Murphy 1988).

Herbig and Maier (2011), in their morphometric analysis of flaxseed from late Neolithic wetland settlements in southwest Germany, proposed that the variation in seed dimensions between the larger seed (4000-3800 cal. BC), and smaller seed (ca. 2900 cal. BC) reflected the change in the end-use for flax as oil or fibre **Figure 7.1.**

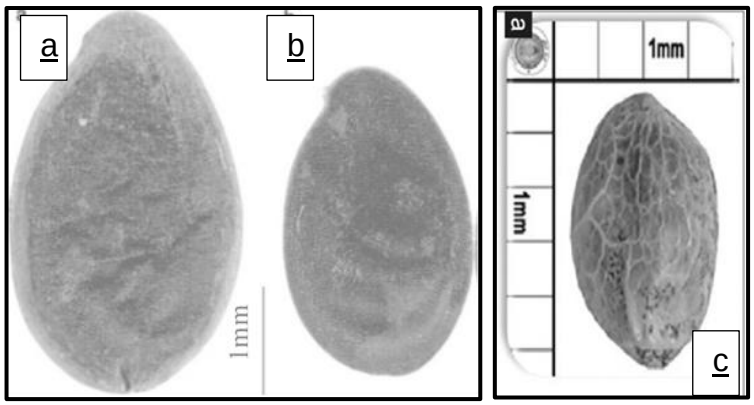

Figure 7.1. The two flax seed types from Late Neolithic wetland sites. a) large-seeded ‘‘Pfyn-type’’ flax from Litzelstetten-Krahenhorn I (4000–3800 cal. B.C.). b) small-seeded ‘‘Horgen-type’’ flax from Alleshausen–Grundwiesen (ca. 2900 cal. B.C.). Scale 1 mm (Herbig and Maier 2011: 531). c) Hemp seed (v Santhica) (Bouayoun et al. 2018).

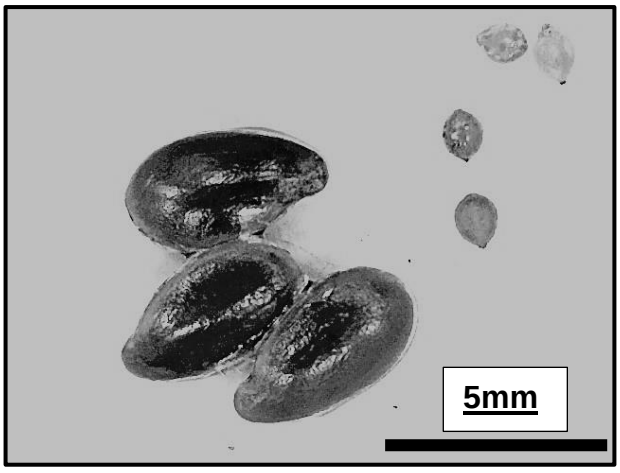

Figure 7.2. Nettle and flax seeds: flax seeds bottom left, length 4mm, nettle seeds top right length 0.25mm.

The size differential shown in **Figures 7.1** and **7.2** illustrates one of the difficulties in separating nettle seed (0.25mm) within the flotation process.

7.1 Plant fibre morphology - MFA Research

It is apparent from the above that plant fibre seeds, preserved within the archaeological assemblage, maintain their morphological shape and, while exhibiting changes in size through time and between regions, shape diagnostic features are maintained over long periods. Also, as illustrated below, **Figure 7.3,** the plant morphology, overall size and shape, leaf, flower, and seed capsule structure offer robust diagnostic features.

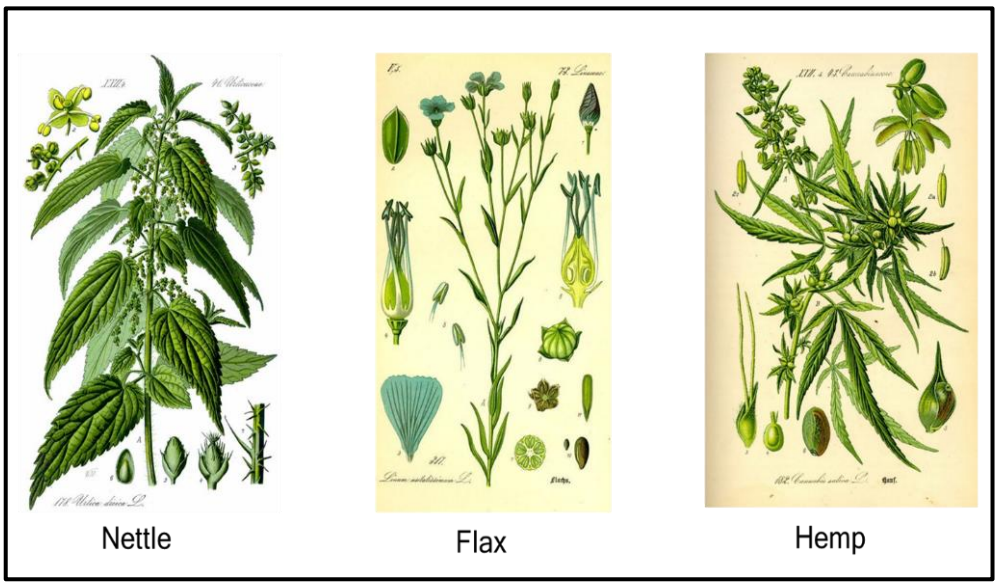

Figure 7.3. Illustration of nettle flax and hemp. General plant structure leaf, flower, and seed capsules depicted (Thomé 1885: npn).

7.1.1 Plant fibre morphology; Hypothesis and Objectives

In recognising the long-term survival of seed morphology, the following hypothesis is proposed.

Hypothesis

Are there other morphological plant fibre features that could serve the diagnosis of ancient textiles?

In support of the hypothesis, the following aims and objectives are presented

Aim To evaluate additional diagnostic potential of plant fibre morphological features

Objectives

- An analytical sampling of plant fibre processes that reveal morphological features.
- To develop analytical techniques that qualify and quantify the features so identified.
- To ensure that the methods adopted to meet the overall objective are reliable, robust, and minimally invasive.
- To determine statistical evaluations that quantify the mathematical relationship between the diagnostic features of the three fibre types.

7.2 Fibre microfibrillar angle MFA

Variations in the description of a “fibre”, were considered previously **Chapter 3, Section 3.3 and Figure 3.4.** The term “fibre” is used as a collective generic to describe a range of fibre diameters with the fibre defined alternatively as an “archaeological fibre” a “theoretical fibre” or a “fibre bundle”.

Bos and Donald (1999: 3030) refer to a “technical fibre” with a diametric range of 50-100µm, as shown in **Figure 7.4** and it is this range of fibre diameters that were investigated within this work.

It is important to recognise that the diagnosis of the bundle of microfibres held at this level will present images suitable for analysis. under microscopic optical techniques.

The angular relationship of the 5-10µm diameter microfibres held within this theoretical fibre structure is the principal focus for MFA determination. If the examination was directed to individual microfibres of 10-20µm diameter, the single microfibre might not present the multifibre images suitable for measurement of the microfibrillar angle MFA.

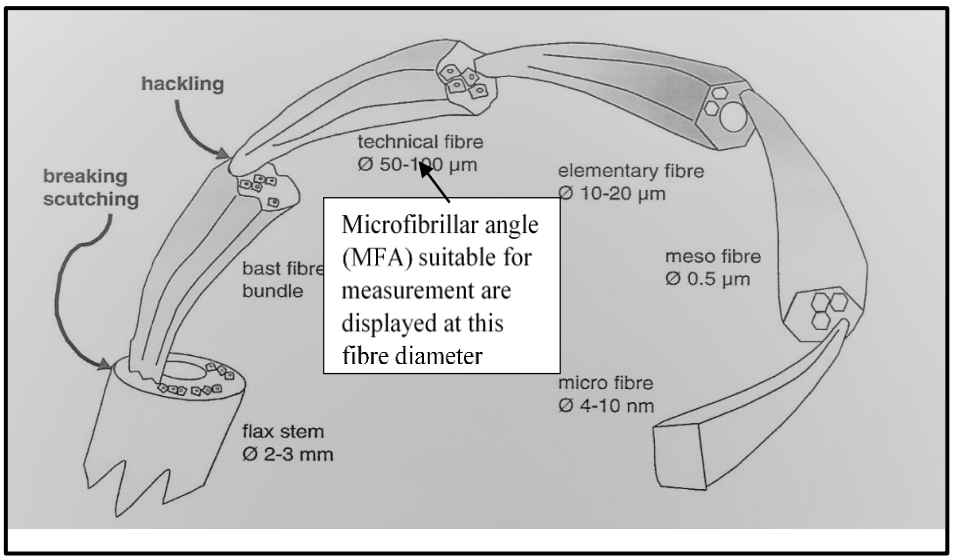

Figure 7.4. Composition and structure of flax fibre (Bos and Donald 1999: 3030 with additions).

7.3 Fibre orientation S and Z angular twist

Plant fibre orientation, described as the direction of the rotation of bast microfibrillar around the fibre, is referred to as Z or S twist (or right- and left-handed fibres) **Figure 7.5.**

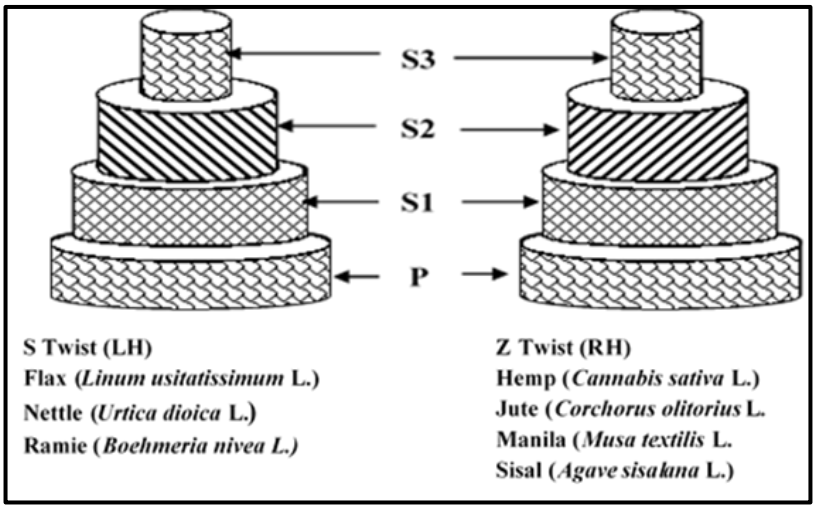

Figure 7.5 Illustration of plant fibre structure**.** Primary outer layer **P** and the Secondary layers **S1**, **S2**, and **S3**. The thickest section, **S2,** carries the micro-fibre in either S or Z orientation. (Based on Bourmaud et al. 2013: 344).

The fibres selected for this study are composed of an outer primary layer, and three distinctive inner layers commonly referred to as S1, S2, and S3 **Figure 7.5.** The microfibrillar are shown in the dominant S2 layer and their twist direction, left or right-handed, are shown. This spiral angle of twist is known as the microfibrillar angle, an indicative feature of the fibre type.

Fibres, having S or Z spin, have been included in **Figure 6** under their appropriate image representation. It is the angle of microfiber contained within the principal section S2 that provides the descriptive “spin angle” for the technical fibre **Figure 7.6.**

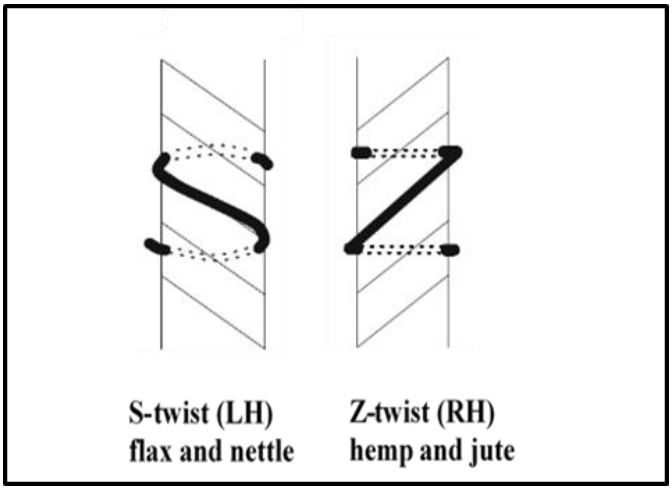

Figure 7.6 S anticlockwise and Z clockwise MFA orientation

The MFA can be observed and evaluated by a range of techniques that are considered and detailed in the following Section paragraphs as shown.

- **7.4.** Microscope imagery of dislocation marks along the fibre length.
- **7.5** Twist test observed as the rotation of a drying fibre when held at one end.
- **7.6** Microscope observation under CPL with a 530nm wave compensator fitted inline (Red Plate Shift).
- **7.7** Effect of MFA upon tensile test, as illustrated by variation in elasticity slope.
- **7.8** Optical microscope imagery of fibre longitudinal sections under cross-polarised light (CPL).

The research programme considered each of the above techniques to review their effectiveness as diagnostic features. Other authors evaluated X-Ray diffraction (Bourmaude et al. 2013), and Field Emission Scanning (Dia and Fan 2010), although these approaches are outside the scope of this current research project.

7.4 Fibre dislocation markings

Plant fibres have irregularities within their fibre wall structure located in the dominant S2 layer. In considering the failure of fibres under tensile strength testing it has been recorded that breakage is most likely to occur at dislocation points and that these points are representative of the change in cellulose content (Hernandez-Estrada et al. 2016). These irreversible weak points are referred to as dislocations and result from both the growth conditions and the subsequent retting, decortication and fibre processing (Baley 2002; Dai and Fan 2010; Haugan and Holst 2014).

> "Dislocation nodes refer to the ring-shaped, slightly thicker areas, which can be seen on many plant fibres" (Haugan and Holst 2014: 952).

These distinguishing dislocation marks presented by the fibre result from growth and fibre processing and are viewed through microscopic observation, as shown below **Figure 7.7.**

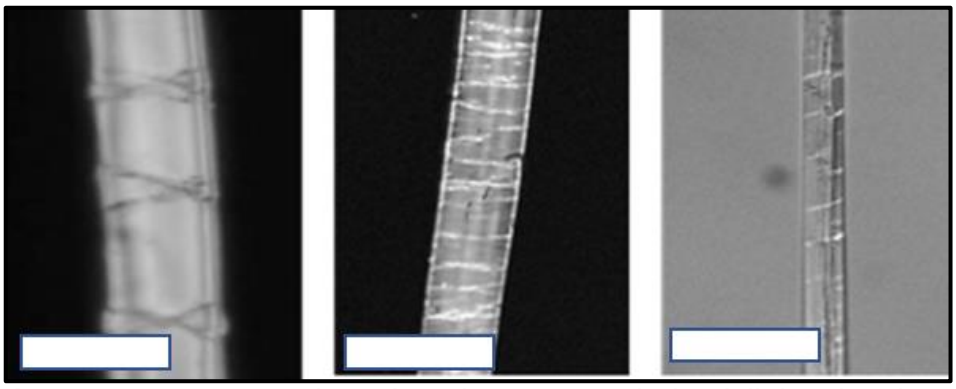

Figure 7.7. Images viewed under cross-polarised light showing nodal deformation. Left. Flax cross banding. Middle. Nettle showing straight striations. **Right.** Hemp showing fewer and straight-line striations **Scale Bar 50µm.**

Bergfjord and Holst (2010: 1192, Fig.1) report on their findings from Scanning Electron Microscopy (SEM) images of plant fibre that the surface characteristics of flax, nettle, ramie, jute and hemp are so similar that they cannot be used to distinguish between the fibres.

7.4.1 Fibre dislocation observation

Several short longitudinal sections of fibre material were cut from a selection of fibre ends to obtain samples 2-5 mm lengths of ultimate fibre. These were mounted in distilled water and placed under a coverslip. Other mountants Canada Balsam, and Eutectic mountants were trialled. However, the mounting layer thickness above the fibre interfered with the ability of close microscopic imaging to focus on the microfibrillar orientation. Also, there was discolouration and deformation of the mountant that interfered with the imaging quality.

Fibre dislocations were investigated under CPL using a Nikon Optiphot-2 microscope and viewed with a Nikon E-Plan objectives at 40x magnification. Observation of the dislocation marks **Figure 7.7** illustrate the differential with flax fibres displaying a cross “X” striation at the nodal point, while nettle has linear striations regularly situated along the fibre length. Hemp is similar to the nettle, but the striations are less regular.

However, Haugan and Holst (2014), in their comments on “flax look-alikes”, advise caution in the interpretation.

> “Interpretations of dislocations can be misleading as, under certain circumstances, the fibre can present characteristic features of another species” (Haugan and Holst 2014: 957).

The possibility of misinterpretation of similar nodal band images viewed at extinction under cross-polarised light (CPL) is also reported (Dai and Fan 2010; Thygesen and Gerling 2013; Hernandez-Estrada et al. 2016; Hanninen et al. 2017).

7.5 Fibre twist test rotation

The S and Z helical fibrillar orientation of fibre cell structures impose a twisting motion to the fibre upon drying, either clockwise ("S") for flax and nettle, or anti-clockwise ("Z") for hemp (*Cannabis sativa* L.), jute (*Corchorus olitorius* L.), manila (*Musa textilis* L.) and sisal (*Agave sisalana* L.) (Barber 1991: 16; Wiener et al. 2003; Haugan and Holst 2013; Skoglund et al. 2013: *npn.*) The twist test is an established practical test that can be conducted without optical imagery or scientific measurement.

While attempts have been made to describe and quantify the rotational outcomes, judgement for this diagnostic technique is subjective and dependent upon operator knowledge and experience. In practice, the fibre is gripped in the fingers or clamped and damped slightly prior to the suspension over a mild heating source. Rotations, where present, are clockwise for flax and nettle and anti-clockwise for hemp. The motions are erratic with delays and variations in the rotational action.

Garside and Wyeth (2006) utilised this inherent cell fibrillar structure to differentiate flax and hemp fibres by reference to the natural "S" or "Z" twist as presented by rotated fibres under Attenuated Total Reflectance Fourier Transform Infra-Red (ATR-FTIR) spectroscopy.

It was concluded that fibrillar angles of approximately -7^0 for the “S” (flax) and +7^0 for the “Z” (hemp) wind direction could serve as a diagnostic criterion. However, in response to the above findings, Skoglund et al. (2013) comments that,

> “S)trictly speaking we can only identify the hemp samples since the samples with S-twist could in principle also be nettle” (Skoglund et al. 2013: npn).

As a practical test, this has its uses for spot-checks of fibres, but the observations are subjective, with a range of rotation description such as “clockwise rapid” (nettle), “clockwise reluctant” (flax), “anti-clockwise” slow (hemp), and “inconclusive” (Wild 1970: 38; Schaffer 1981; Barber 1991: 16; Wiener et al. 2003; Haugan and Holst 2013; Skoglund *et al.* 2013: *npn.*). Other reasons for rejecting this method are based on experiments undertaken in this research.

The practical application of the test revealed that some fibres do not rotate, and the response varied dependent upon the degree or duration of the wetting or drying. The diagnosis was highly subjective.

7.6 Microscope observation of microfibrillar angle (MFA) under CPL with a 530nm wave compensator fitted inline (Red Plate Shift)

The differential was reported as it is presented under crossed polarised light (CPL) when viewed with the addition of a selenite retardation plate “Red 1” as an alternative to the twist test (Lukšová et al. 2017). Examination of the variation in the refractive index along the fibre length is compared to the variations observed at right angle across the fibre.

Changes in the viewed angle of the fibre at 90º from parallel to the right angle displays colour change dependent upon the MFA. For flax, the changes from dark red to blue/yellow are observed while for hemp, the opposite applies.

Red Plate Shift refers to a colour filter of 56nm inserted at 45º to the microscope viewing plane. The test is recognised as Herzog's Red Plate Test (Herzog 1985). A more detailed investigation of the birefringence colour changes and qualification by comparison with data on a Michel-Lévy interference chart were proposed and illustrated as a guide to interpretation (Haugan and Holst 2013).

7.6.1 Red Plate test: archaeological investigations of textile fibres

Archaeological textile artefacts have been investigated within the above protocol to establish the fibre species used in their manufacture (Lukšová et al. 2017). An investigation of ten Scandinavian Viking and Early Middle Age Wall hangings, believed to be flax, successfully identified four as flax.

Lukšová et al. (2017) conducted an extension to this research on ten further fibre samples from grave deposits subjected to the Herzog test with nine confirmed as flax. The remaining fibre was simply identified as bast.

A similar programme was initiated at the Finno-Ugric and Historical Collections of The National Museum of Finland where 12 textile artefacts provided 25 fibres for analysis. Observation under the Herzog test identified 16 nettle fibres, five cotton fibres and one each of flax and hemp (Suomela et al. 2018).

7.6.2. Herzog Test Research outcomes

Test samples from the three species, nettle, flax and hemp, were selected for examination of fibre orientation as evidenced by observations under a Nikon Optiphot-2 CPL stereo-microscope with a full-wave compensator of 56nm inserted at 45 deg. Viewed with a Nikon E-Plan 40/0.65 objective the comparison of colour changes exhibited upon rotation can be observed. The indicative colour change, and associated fibre S or Z rotational angle were recorded and compared in the three sets of images obtained from modern reference material and shown below **Figure 7.8(A), (B) and (C).**

In each set the fibres are shown in extinction under CPL at **(a)** with the image observed under 56nm Red Plate to illustrate the MFA angle at **(b).** In **(c)** and **(d)** the colour change in response to the Herzog Test is shown. With the red at 90º and blue at 180º for flax and nettle confirming the negative MFA angle for both. For hemp, with a positive MFA angle, the colour change is reversed with blue at 90º and red at 180º although for hemp the changes are less distinct**.**

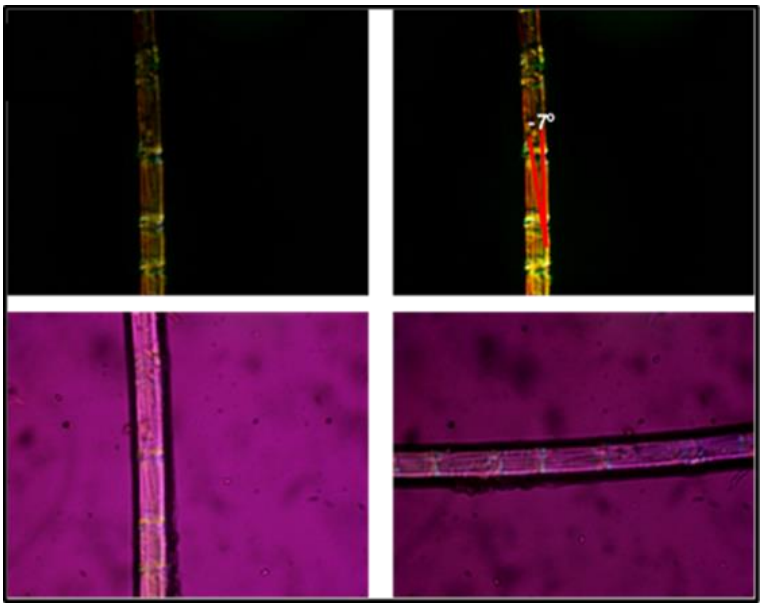

Figure 7.8 (A). Flax 25µm flax fibre under CPL and 56nm Red Plate: MFA -7º: Top left, fibre at extinction. Top right, fibre displaying MFA. Bottom left, fibre at 90º under 56nm Red plate. Bottom right, fibre at 180º under 56nm Red plate

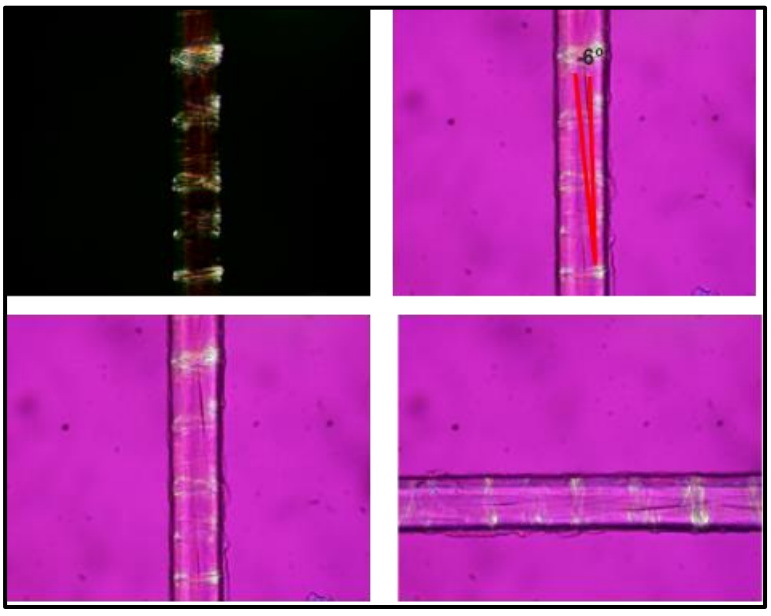

Figure 7.8 (B). Nettle 10µm nettle fibre under CPL and 56nm Red Plate: MFA -6º. Top left, fibre at extinction. Top right, fibre displaying MFA. Bottom left, fibre at 90º under 56nm Red plate. Bottom right, fibre at 180º under 56nm Red plate.

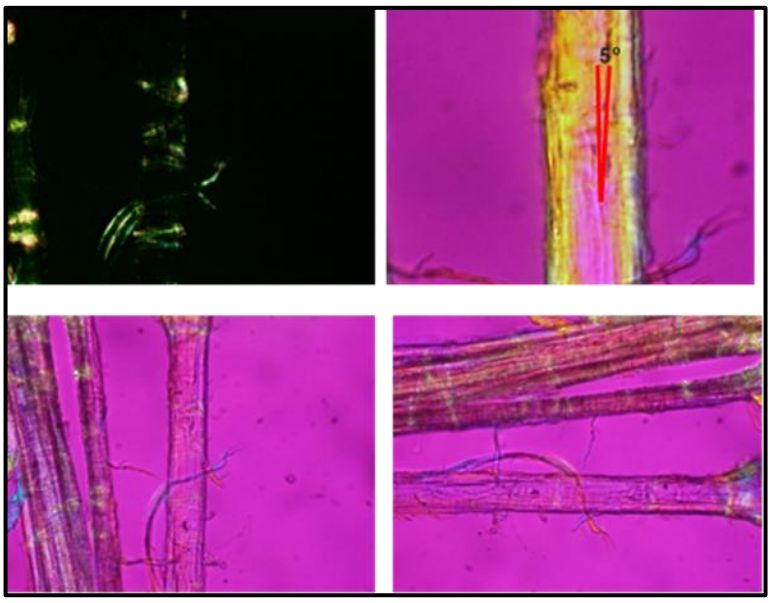

Figure 7.8 (C). Hemp fibre under CPL and 56nm Red Plate: MFA 5º. Top left, fibre at extinction. Top right, fibre displaying MFA 5º. Bottom left, fibre at 90º under 56nm Red plate (vague red). Bottom right, fibre at 180º under 56nm Red plate (vague blue).

7.6.3 Herzog test limitations

Haugan and Holst (2013) published results from the evaluation of the cause and effect of the utilisation of Herzog's test as a diagnostic feature. In a review of their method, it is recorded that a single fibre was analysed. However, fibre definition is problematic. Were the authors describing a single fibre, a "theoretical fibre" (c. 25µm) or a microfibre (c. 10µm).

An explanation for the failure of the Herzog test as dependent upon fibre thickness is proposed as a limitation on the effectiveness. Haugan and Holst (2013) comment on the need to focus on the single section of fibre that is displaying extinction and disregarding other sections.

The test also has limitations in identifying fibre species as the fibre anterior and posterior views present opposing microfibrillar angle. Hence, “S” negative MFA and “Z” positive MFA are not differentiated **(See Section 7.61).**

In this research programme, it was noted that, where two or more fibres, were in the same frame and where subjected to the Herzog Red Plate Test the colour changes. Under identical orientation the fibres each presented a different range of observed colour change a differentiation that eliminated any diagnostic information.

Petraco and Kubic (2004) in a review of the MFA Herzog Test images noted the affected by minor changes in the focus on the anterior fibre surface. The images presented in Petraco and Kubic (2004: 92-93) illustrate the birefringence colours presented by Jute, Ramie and Sisal that display a variation of colours along their length. The colour changes are. labelled as “Tinges”, a limited display, that makes it difficult to identify the diagnostic features attributed to the primary colour changes. Consequentially there was a need to restrict the observation to a short, clean section of fibre.

7.7 Effect of MFA upon tensile test as illustrated by variation in elasticity slope

In a trial of hemp, as a composite material component, Fuentes et al. (2017) considered the variations in the mechanical behaviour of technical fibres to ascertain two typical tensile stress/strain curves that demonstrated non-linear behaviour.

The authors attributed this variation to cell wall composition. A similar variation is also reported from the tensile test of flax varieties Marylin, Oliver and Hermes that produced a range of linear stress/strain curves varying from straight-line relationship to a display of a non-linear section at the beginning of tensile loading. This variation was attributed to both the plant variety and cell-wall composition of the cellulose microfibrillar (Lefeuvre et al. 2014).

The tensile properties of single fibre samples of oleaginous flax fibres were considered in a research programme to provide an explanation and determination of the variation in stress/strain relationship under tensile testing. The non-linear region deformation was exhibited within the range of strain between 0-0.5% for fibres with an MFA of 10º. (**Note** the positive and negative orientation of the fibres is not determined under the Hertzog Test). This variation was attributed to factors considered to affect mechanical properties, such as soil composition, geographic area, condition of culture, agronomic factors, weathering, stocking conditions and mechanical treatments during extraction (Pillin et al. 2011).

7.7.1 Trendline deviation as indicative of MFA

Placet (2009) proposed that the mechanical strength of natural fibres was influenced principally by the cellulose microfibrillar present in the “S2” layer. The tilt of the MFA at 10º serving to offset the tensile load application in the early stages of the tensile test until the microfiber is vertically aligned with the direction of the applied load.

Table 7.1 summarises published findings to provide a tabulation of the MFA measurements as determined by consideration of trendline deviation.

Author	**Fibre**	**MFA Range(deg.)**
Charlet et al. (2009)	Flax	6-18
“ “	Hemp	6.9
“ “	Ramie	6.4
Bourmaud et al. (2013)	Flax	8.1-9.6
“ “	Hemp	11.2
Dasong and Mizi (2010)	Hemp (fractured)	6.16
	Hemp (non-fractured)	1-3.27

Table 7.1 MFA reported, based on trendline deviation

.7.2 Calculation of MFA based on trendline deviation

Charlet (2009) considered that the onset of early non-linear behaviour in a more detailed investigation to propose that this could not be attributed to cross-sectional variations along the fibre profile. Nevertheless, it was related to the cellulose microfibrillar progressive realignment (Charlet et al. 2009). The authors described the variations as presenting in three stages, an initial linear stage up to 0.3% with a second non-linear part 0.3-1.5% and a final linear stage to failure.

This resulting deformation has been calculated and a descriptive formula provided (Charlet et al. 2009). The tension applied to the fibre results in a change in the microfibrils' orientation and a corresponding fibre lengthening. denoted as ΔL

Charlet et al. (2009: 235) offer formula (1) to determine the MFA angle initiating this deformation.

$$\varepsilon = \ln(1+\Delta L/L_o) = -\ln(\cos\alpha) \quad \text{(Formula 1)}$$

Where ε = Strain %, $\Delta L/L_o$ = extension /original length and α = MFA

For the test piece, the authors identified and illustrated a tensile deformation of 1.45%, which corresponds to an MFA of 9.6º (Charlet et al. 2009: 235).

Figure 7.9 shows the relationship between tensile deformation and MFA as determined by the above formula applied to the tensile tests undertaken in this research programme.

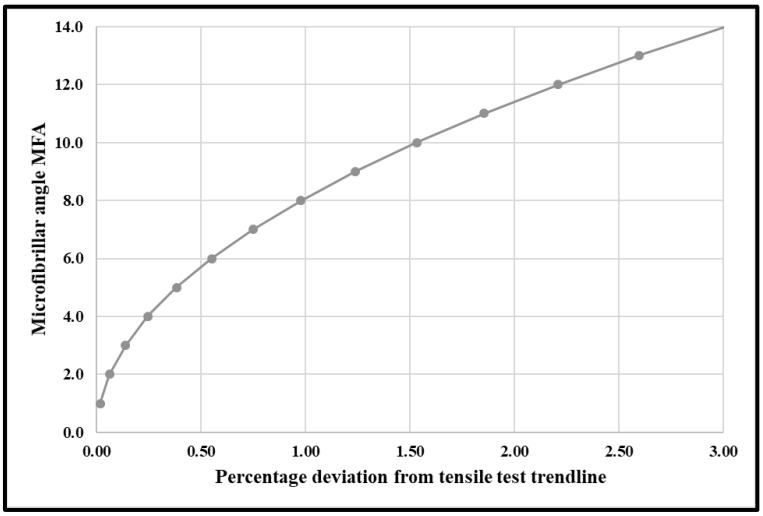

Figure 7.9. The curve presents the calculated values for MFA based on the assessment of the initial deviation of the tensile test curve from the straight-line elasticity range. Calculated from Formula 1 (Charlet 2009: 235).

The tensile tests reported in **Chapter 6** were reconsidered, to evaluate their deviation as a potential diagnostic feature, by inspection of the tensile test curve as recorded. To appraise the maximum deviation from the straight-line, the elasticity relationship was readjusted to incorporate the initial stress/strain relationship and the second stage deviation.

The following graphs **Figure 7.10** illustrate the changes and the deviation derived. There is a variation in MFA as calculated from Formula 1 compared with MFA determined under CPL microscopy. The adjusted MFA values are dependent upon the subjective assessment of the initial deviation, as shown in **Figure 7.11. Table 7.2** lists the variation.

Fibre	Recorded MFA	Adjusted MFA (Formula 1)
Nettle	6.3 deg.	4.6 deg.
Flax	6.4 deg.	3.9 deg.
Hemp	8.4 deg.	6.3 deg.

Table 7.2. Variation in MFA determination based on strain% Determined at the point of initial deviation from the tensile strain trendline.

The diagnosis of variation in deviation, as indicative of MFA, has limitations. Firstly, in the subjective assessment of the point of maximum deviation and secondly, recognising that the MFA angular deviation does not attribute negative “S” or positive “Z” direction, an essential diagnostic feature.

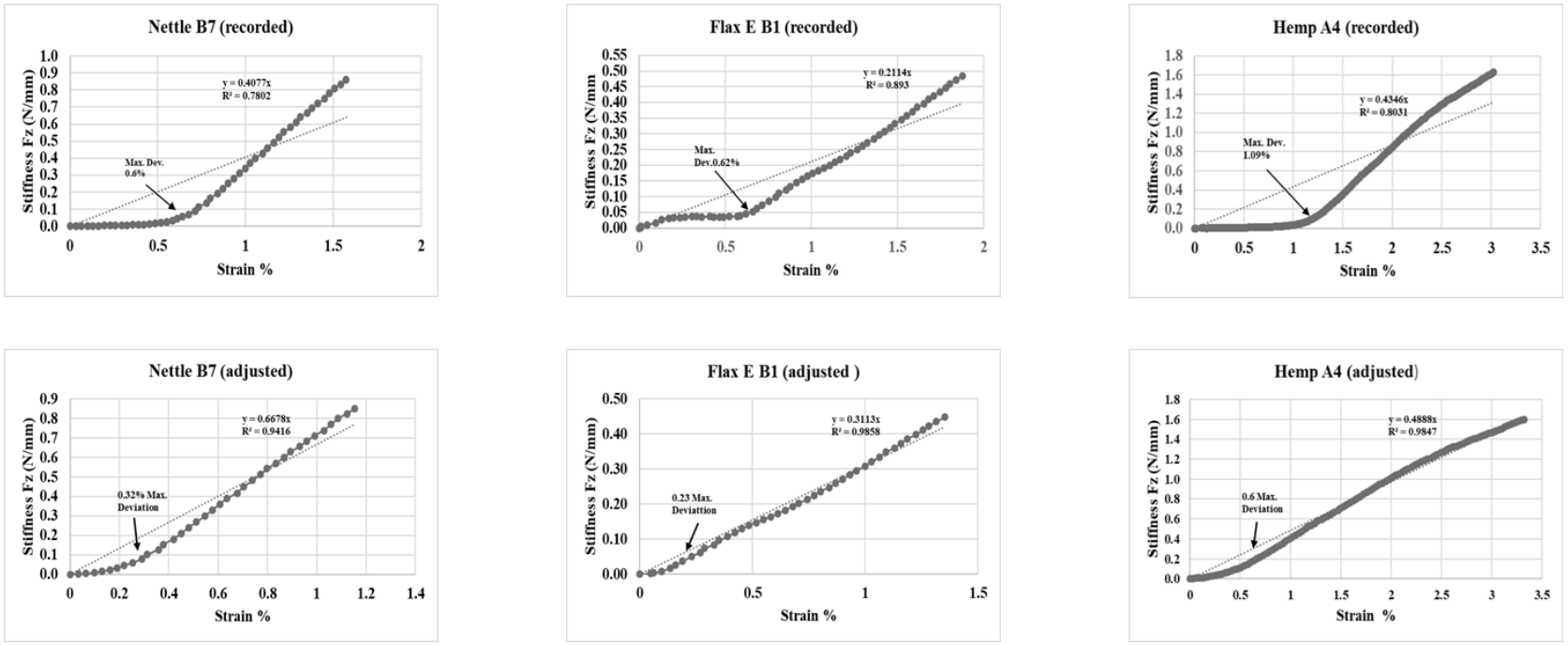

Figure 7.10. Comparison of recorded Biomomentum tensile test. **Top**. Graphic representation based on tensile test data. **Bottom.** Adjustment to recorded data to depict “elasticity region” and deviation **(See Chapter 6)** the deviations at maximum levels shown in the bottom plots are those proposed as indicative of MFA **Table 7.2.**
Note. See Appendix B for database Young’s Moduli

7.8 Optical microscope imagery of fibre longitudinal sections: cross-polarised light (CPL)

The following fibres were selected for submission to the MFA evaluation of flax (v. Eden), hemp (v. Santhica) both collected from field cultivation by East Yorkshire Hemp, and nettle, collected from a wild open woodland, site location in Bradford UK.

7.8.1 Method - MFA analysis by optical microscope under CPL

Samples were prepared as detailed in **Section 7.4.1** Flax, hemp and nettle samples were separated and cut into 2mm sections prior to mounting in distilled water under a glass coverslip and sealed prior to examination under crossed polarised lighting (CPL). For each fibre type, 25, 2mm sections were viewed with a Nikon Optiphot-2 microscope and Nikon E-Plan objectives at 10x and 40x magnification to determine the microfibrillar angle as observed under CPL. It is essential to focus on the fibre's anterior surface to ensure the correct orientation. To focus in error on the posterior surface of the fibre will display the opposite orientation as can be seen in **Figure 7.11.** A total of 25 images of micro-fibrillar angle for each fibre species were recorded, and the MFA measured as an enclosed angle using AnalySIS, Soft Imaging System (Analysis 2018). Typical results are shown in **Figure 7.12.**

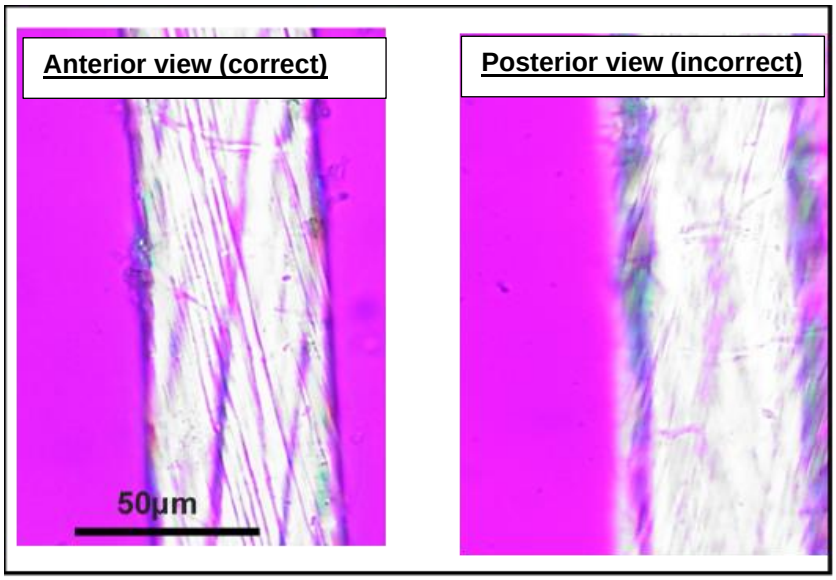

Figure 7.11. Illustration of error in measuring MFA by incorrect microscope focusing. In the image on the left, the high transparency allows both sides to be viewed, and the necessity to observe close focusing demonstrated.

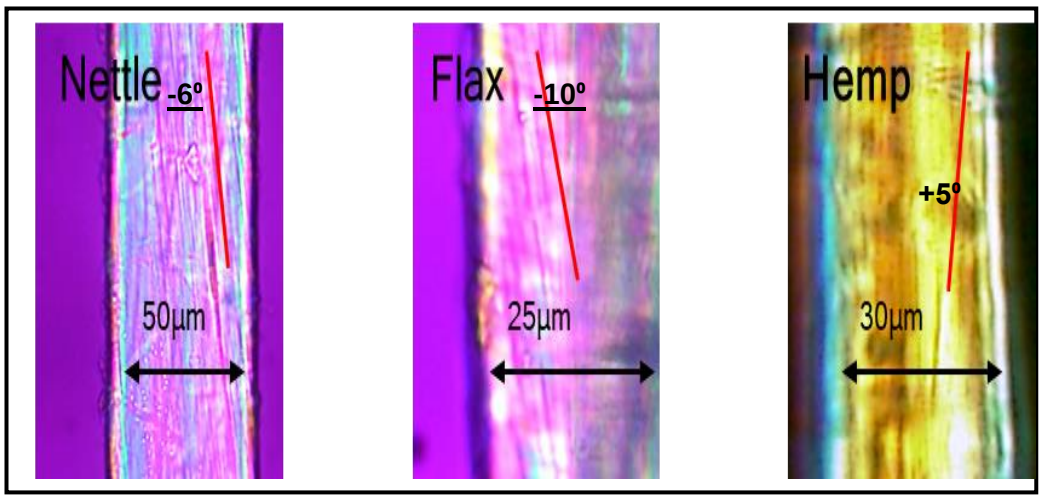

Figure 7.12. MFA images. MFA determined with microscopic viewing under CPL. Measured by stage rotation angular variation and confirmed with AnalySIS software. Nettle -6º, flax -10º. Hemp 5º.

7.8.2 Results from MFA analysis – compound microscope with CPL

The analysis of images obtained from 25 samples of each fibre species is recorded within a database **Table 7.3** and plotted **Figure 7.13.**

Sample	Flax	Nettle	Hemp	No.	Flax	Nettle	Hemp
1	-5.6	-10.5	5.0	**15**	-8.0	-3.2	3.4
2	-4.2	-10.2	4.0	**16**	-5.3	-7.6	3.0
3	-7.4	-4.9	3.5	**17**	-4.8	-8.9	4.6
4	-3.3	-6.9	4.5	**18**	-7.3	-3.3	6.3
5	-3.6	-4.7	4.8	**19**	-8.8	-3.4	3.9
6	-4.0	-3.5	6.9	**20**	-4.8	-7.0	3.6
7	-3.5	-5.3	5.0	**21**	-4.1	-6.2	4.4
8	-4.2	-4.2	4.3	**22**	-5.3	-5.3	4.5
9	-5.9	-7.7	6.5	**23**	-6.9	-8.5	
10	-6.6	-5.8	3.9	**24**		-8.1	
11	-8.4	-5.9	4.6	**25**		-7.9	
12	-7.0	-7.1	4.3	**Ave**	**-5.78**	**-6.52**	**4.591**
13	-6.7	-7.6	3.2	**St Dev**	**1.67**	**2.157**	**1.128**
14	-7.3	-9.4	6.8	**SE**	**0.348**	**0.431**	**0.240**

Table 7.3. Fibre microfibrillar angle MFA: measured as an enclosed angle with AnalySIS software. (Blank squares depicted failed examinations due to the poor quality of the images).

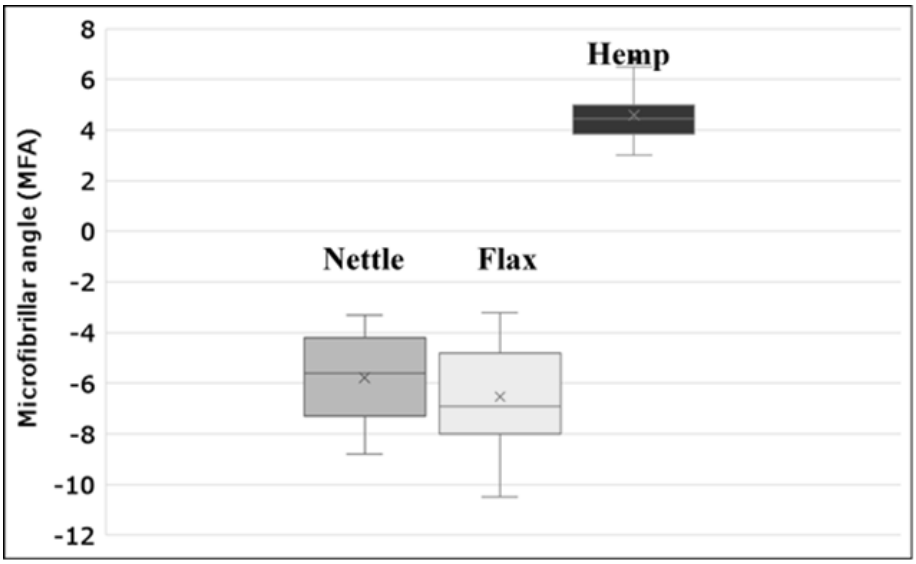

Figure 7.13. Box and whisker comparison of MFA for the three fibre species

Analysis of variance (ANOVA) of MFA values shown in **Figure 7.14** found that, for the MFA samples of the microfibrillar angle measured, (n=70), nettle (n=25), flax (n =23) and hemp (n=22), there is a significant variation between the grouped samples ($F= 293.17$, $df= 67$, $p<0.0001$). The "*t*" test for paired two sample means showed a significant difference between nettle and hemp ($t = 20.60$, $df=21$, $p<0.0001$) and a significant difference between flax and hemp ($t=25.02$, $df=21$, $p<0.0001$. There is no significant difference between flax and nettle.

Measurement of MFA by direct observation and resolution of microfibrillar angle under cross-polarised light provides a statistically viable result with less reliance on the observer's subjective judgement. The mean MFA is determined by averaging the direct observation, with the angle measured by reference to the rotation of the microscope stage, as depicted by microfibrillar image realignment, and the enclosed angle measured with AnalySIS computer image analysis software.

7.9 Summary

For the techniques reported in this chapter, the following comments regarding their efficacy in attaining the research aims and objectives are reviewed. The identification of fibre species within the archaeological record provides a basis for the re-evaluation of archaeological specimens to support reappraisals regarding the broad range of plant products in past societies. Along with considerations of the size and shape of plant seeds and inflorescences, the research hypothesis posed the question as to the potential for other sections of plant anatomy to retain and present a diagnostic potential.

7.9.1 Fibre dislocation marks

The observation of dislocation marks is unreliable and dependent upon the fibre orientation under cross-polarised light (CPL). As shown in **Figure 7.6** and **7.7** images of fibre can be misinterpreted and, in some circumstances, are affected by humidity, cleanliness and processing techniques. A feature of interest in the dislocation image presentation is that all the “cross” dislocation marks hold their base location at both edges of the fibre irrespective of the fibre rotation (**Figure 7.8).** This anomaly, usually attributed to a trauma event affecting the microfibres, is reflected in the change of the CPL light pathway and is worthy of further study but is outside the scope of this current investigation.

7.9.2 Twist test

As a practical test, this has its uses for spot-checks of fibres, but the observations are subjective, with a range of rotation description such as “clockwise rapid” (nettle), “clockwise reluctant” (flax), “anti-clockwise” slow (hemp), and “inconclusive” (Barber 1991: 16; Wiener et al. 2003; Haugan and Holst 2013; Skoglund *et al.* 2013: *npn.*). Other reasons for rejecting this method are based on experiments undertaken in this research. The practical application of the test revealed that some fibres do not rotate, and that the response varied dependent upon the degree or duration of the wetting or drying, and the diagnosis was heavily subjective.

7.9.3 Red Plate- Herzog test colour change

As reported above, there is a range of investigations of fibre species utilising this technique. These are divided between the evaluation of the relative refractivity and practical diagnosis of textile material. When working on poor quality minimally processed fibre, it is difficult to achieve the necessary quality of imaging. Hence, for clarity in diagnosis, it is suggested that the Herzog test would provide improved results from the imaging of a single, quality, processed fibre that had been professionally conserved. Finally, it is recognised that the process is subjective and requires a degree of expertise and, in terms of this research, the test fails to differentiate between flax and nettle.

7.9.4 MFA analysis by optical microscope under CPL

Examining of microfibre angles under CPL provides the researcher with an image suitable for practical measurement either by rotation of the microscope stage or by analysis with computer software. This removes the subjective decision associated with the alternative methods for the diagnosis of MFA. While locating and fine focusing on microfibre longitudinal sections embedded in distilled water under a 0.17mm cover-glass takes time and concentration, the results, as illustrated in **Figure 7.13**, provide suitable images for analysis and measurement. With due regard to the caution regarding anterior or posterior focusing, analysis of MFA by optical microscopy under CPL was the research method selected for the diagnosis of morphological features that could serve in the diagnosis of ancient textiles and one that most clearly met the proposed hypothesis.

Note The database in support of the above is included in Appendix C

Chapter Eight
Fibre geometric morphology - Cross-sectional shape analysis

8.0 Introduction

As noted in previous chapters the recovery of seeds from soil samples of archaeological environments is difficult. The low visibility and small size of seeds and pollen from fibre producing plants may result in poor recovery except in the most rigorous chemical or sediment flotation processes (Pearsall 1989: 33-97). Additionally, there was the conundrum regarding the interpretation of seed presence as the sole indicative factor for the use of plants fibres in textile production, an interpretation which requires support from other related textile artefacts, spindles, loom weights, pin beaters, fibre combs (Walton-Rogers 1997: 1735-1745 and 1749-175, Hurcombe 2010: 129-139, Stolcova and Croma 2005: 9-20).

8.1 Background

Plant fibre shape, material properties, and microscopic imagery have been used extensively to determine the genus of unknown plant fibre material. Previous authors considered fibre dimension, fibre terminal shape, and fibre density as diagnostic features (Catling and Grayson 2012: 6-7; Bodros and Baley 2008; Horne et al. 2008).

However, these features are dependent upon growth environment, geographic location, horticultural practices and fibre processing and hence exhibit a range of diagnostic differentials. Subsequent deposition or conservation environments also serve to amend fibre properties. Nettle, flax, and hemp plants in their natural growing environment have leaf and stem shapes, flower colour and shape that are distinguishable and morphologically recognisable

features. In this chapter, the research proposal is to review geometric morphology and past techniques including; fibre cross-sectional shape and fibrillar to identify potential areas worthy of further investigation.

8.2 Determination of plant fibre cross-sectional area ratio: photographic images

In a previous research programme, Waudby (2014) reported that fibre diameter, length, cross-sectional area and terminal shape had been employed to qualify and quantify differences in fibre dimensions (Catling and Grayson 1982; Bodros and Baley 2008; Horne et al. 2008).

However, dimensional ranges as individual measurements are difficult to compare due to variations in fibre size as influenced by the conditions described above. Non-dimensional ratios resolve this difficulty. The published images, **Figures 8.1, 8.2 and 8.3,** were measured to record fibre lumen/overall cross-sectional area (CSA) cell diameter ratios (Waudby 2014).

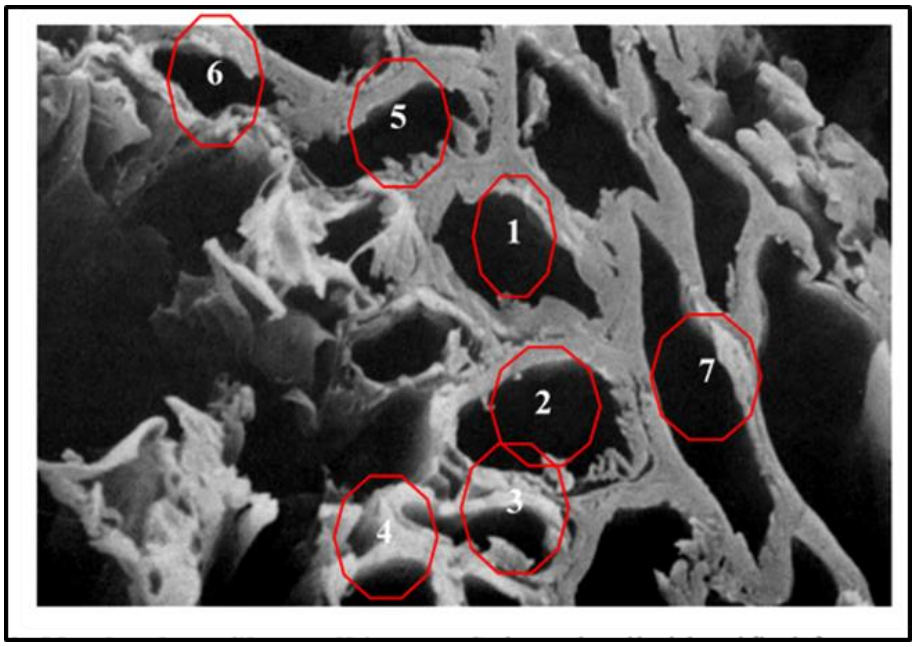

Figure 8.1 Nettle plant fibre CSA images. Selected cells identified for measurement of the ratio of fibre overall diameter to lumina diameter (Ryder and Gaber-Saunders 1987) (with additions)

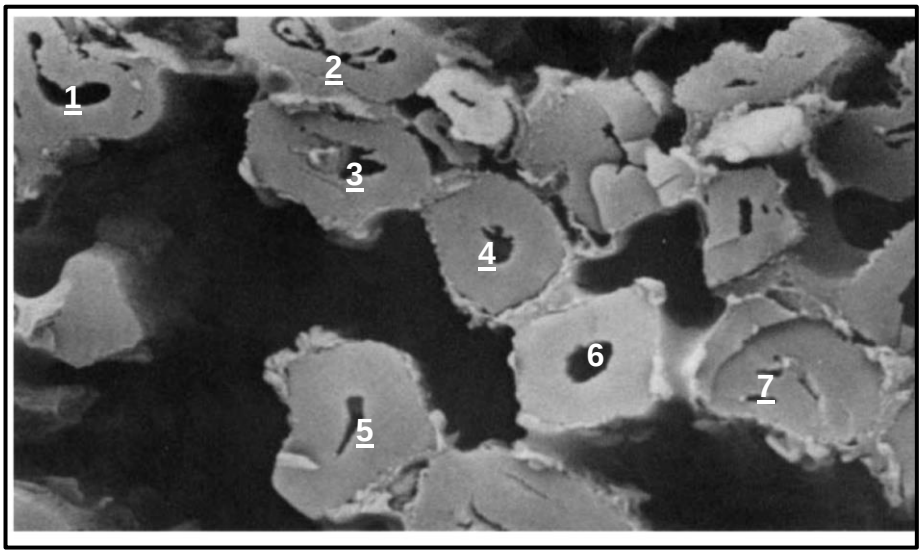

Figure 8.2 Çatalhöyük. Flax plant fibre cell images Selected cells identified for measurement of overall fibre diameter to lumina diameter ratio (Ryder and Gabra-Sanders 1987) (with additions)

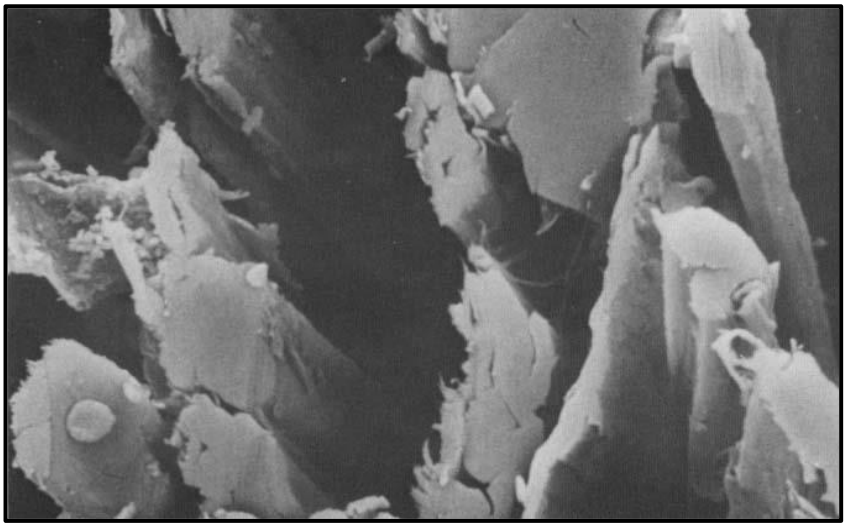

Figure 8.3 Transverse sections of hemp fibres. These fibres are thicker than the nettle and flax fibres and have narrower lumina. As the hemp lumen are narrower and indistinct, this image was not used in the subsequent analysis of lumen/cell diameter ratios. (Ryder and Gabra-Sanders 1987).

Image dimensional data from other sources were included in the analysis to give a total of 20 nettle images, **Table 8.1,** and 29 flax images, **Table 8.2**

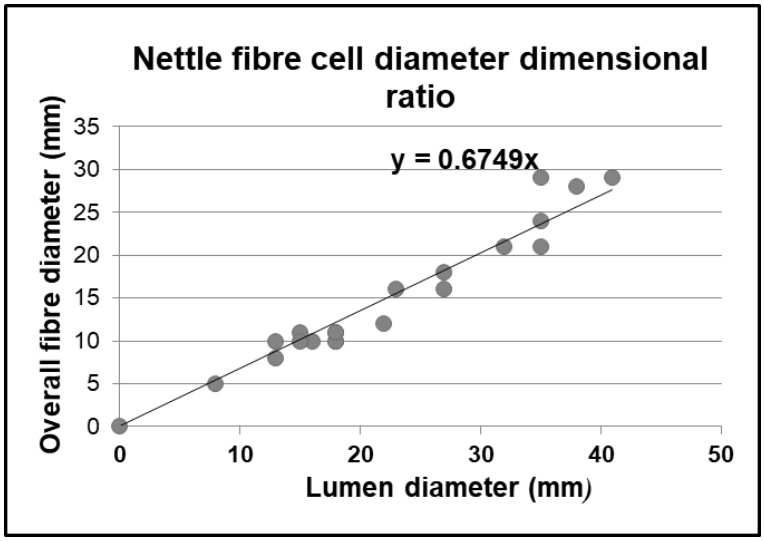

Figure 8.4 Nettle plant fibre comparative cell diameter dimensional ratios**.** Lumina diameter/ overall diameter. Data from **Table 8.1** below (Waudby 2014: 29-30).

Sample	Fibre overall diameter (mm)	Lumina diameter (mm)		Sample	Fibre overall diameter (mm)	Lumina diameter (mm)
1	41	29		**11**	18	10
2	38	28		**12**	18	10
3	35	24		**13**	22	12
4	27	16		**14**	27	18
5	35	29		**15**	18	11
6	35	21		**16**	16	10
7	32	21		**17**	8	5
8	23	16		**18**	18	11
9	13	8		**19**	15	10
10	15	11		**20**	13	10

Table 8.1. Nettle Fibre Cell Dimensions Comparative Measurement. Lumina/fibre length dimensions. Samples 1-8 taken from Ryder and Gabra-Saunders 1987: 91-108. Samples 8-20 taken from Di Virgilio 2013: 1-56).

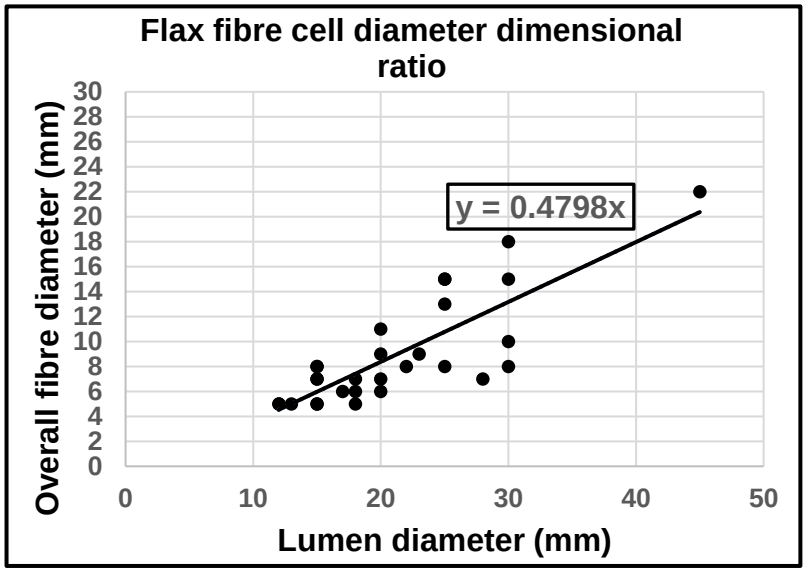

Figure 8.5 Flax plant fibre comparative cell diameter dimensions. Lumina diameter/ overall diameter. Table 8.2 below

Sample	Fibre diameter overall (mm)	Lumen diameter (mm)	Sample	Fibre diameter overall (mm)	Lumen A diameter (mm)	Sample	Fibre diameter overall (mm)	Lumen diameter (mm)
1	25	15	**11**	20	9	**21**	20	7
2	30	18	**12**	15	5	**22**	20	6
3	30	15	**13**	15	7	**23**	15	8
4	25	8	**14**	12	5	**24**	18	6
5	30	10	**15**	18	5	**25**	28	7
6	30	8	**16**	45	22	**26**	20	11
7	22	8	**17**	15	5	**27**	25	13
8	17	6	**18**	15	7	**28**	18	7
9	25	15	**19**	12	5	**29**	13	5
10	15	8	**20**	23	9			

Table 8.2 Flax fibre cell comparative measurement. Lumina/fibre length dimensions. Samples 1-7 taken from (Ryder and Gabra-Saunders 1987: 91-108), Samples 8-29 taken from (Aslan et al. 2011:).

The above tables and plots illustrate the variation in cell wall thickness as determined from photographic images. The nettle “thin wall” fibre with lumen/cell maximum diameter ratio of 67% can be compared with the flax “thick wall” ratio of 48%; the hemp fibres were not included.

Scanning Electron Microscope (SEM) digitised imaging was used to produce comparative fibre images to evaluate the potential for non-dimensional ratios in the diagnosis of locally harvested nettle and flax stem sections.

Images for both SEM samples **Figure 8.6** illustrate concerns regarding the image quality of “plant fibre wall thickness” as a diagnostic feature. The majority of the nettle stem images show distinctive lumen while only one flax fibre within the stem cross-section revealed a small lumen shape.

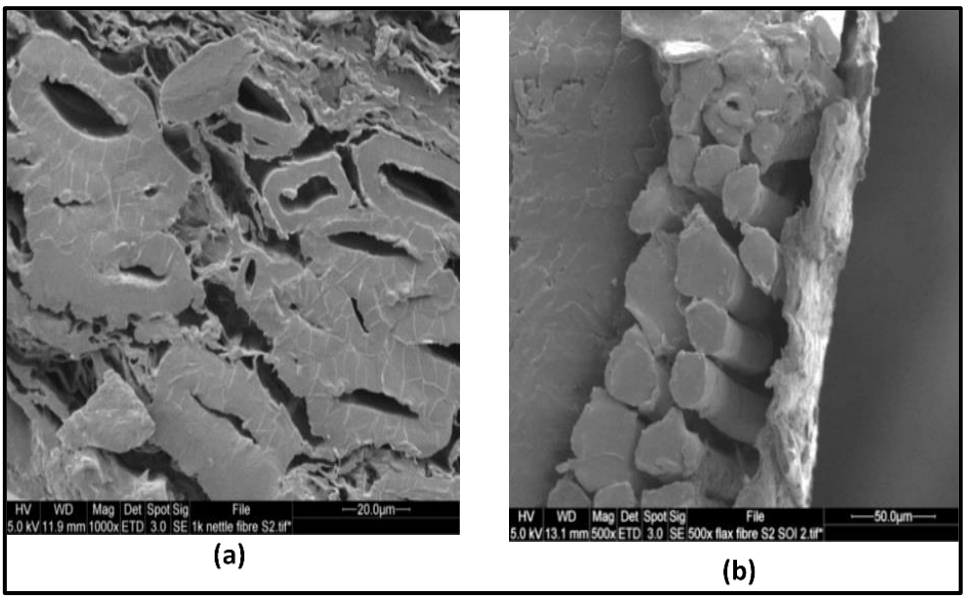

Figure 8.6 SEM images of microtomed cross-sections of plant fibre stems. a) SEM image of nettle fibre 1000X, b) SEM image of flax fibre 500X

The range of cross-sectional morphology, as displayed, raises concern regarding thick wall and thin wall as descriptive generalities that may be subjected to unintentional cognitive bias in their interpretation. A particularly relevant factor where such comparisons are affected by the growing environments, the harvesting and retting processes, the range of subsequent manufacturing processes, and ultimately the taphonomic and conservation conditions.

8.3 Determination of plant fibre cross-sectional area ratio - SEM images

The non-dimensional CSA ratio of fibre is proposed as a potential morphological diagnostic feature to be subjected to more detailed analysis to explore the range of non-dimensional ratios presented by the fibre. Initially, the proposal is to evaluate the possibility of employing a similar analysis to images obtained through Scanning Electron Microscopy (SEM) as shown in **Figure 4.1**.

8.3.1 Method for preparation of fibre plant stems for SEM evaluation of fibre CSA cell morphology

Sample preparation

Fibre plant stems were prepared as follows. 15 mm sections were cut from the sample length and soaked overnight with ethanol a tissue fixative mixture under vacuum. This procedure facilitates the fixative penetration.

The samples were soaked in the isopropyl alcohol solutions for the specified periods and placed in a fume cupboard for the periods shown below.

- 70% isopropyl alcohol --- 2 hours
- 90% isopropyl alcohol --- 2 hours
- 100% isopropyl alcohol --- 2 hours
- 100% isopropyl alcohol --- 2 hours
- 100% isopropyl alcohol --- overnight

Separate jars were used for each preparation stage with the samples blotted between transfers.

Cleaning

Following the above procedure, the samples were immersed in toluene and placed in the fume cupboard for cleaning to remove any traces of isopropyl alcohol. Cleaning was continued for the periods detailed below

- 100% Toluene --- 2 hours
- 100% Toluene --- 2 hours

Separate jars were used for each preparation

Cold Mounting

The dried samples were fitted into a 20mm plastic mould former for embedding within an EpoFix epoxy resin.

Epoxy resin mixed, resin 25 parts, hardener three parts by weight and stirred for two minutes.

Moulding was complete by syringe filling of the 20mm moulds, with the resin remaining viscous for 30 mins.

Place moulds into a vacuum chamber (400m.bar) for 24hrs at room temperature 20deg. C

Preparation of samples for SEM diagnosis

After the curing, the resin moulding was removed from the mould for CSA surface preparation using a series of wet emery paper of increasing fineness

Following the above, the surface of the sample was diamond polished to provide an acceptable surface for SEM analysis and imaging

A 2mm section was removed for stub mounting, stained with methylene blue prior to carbon coating.

The base of the cross-section was subjected to a similar process as in 1) above to facilitate a secure and level mounting onto the SEM stub.

8.3.2 SEM imaging of stems

The SEM images obtained are shown in **Figure 8.7.** with details for the SEM settings included under each image

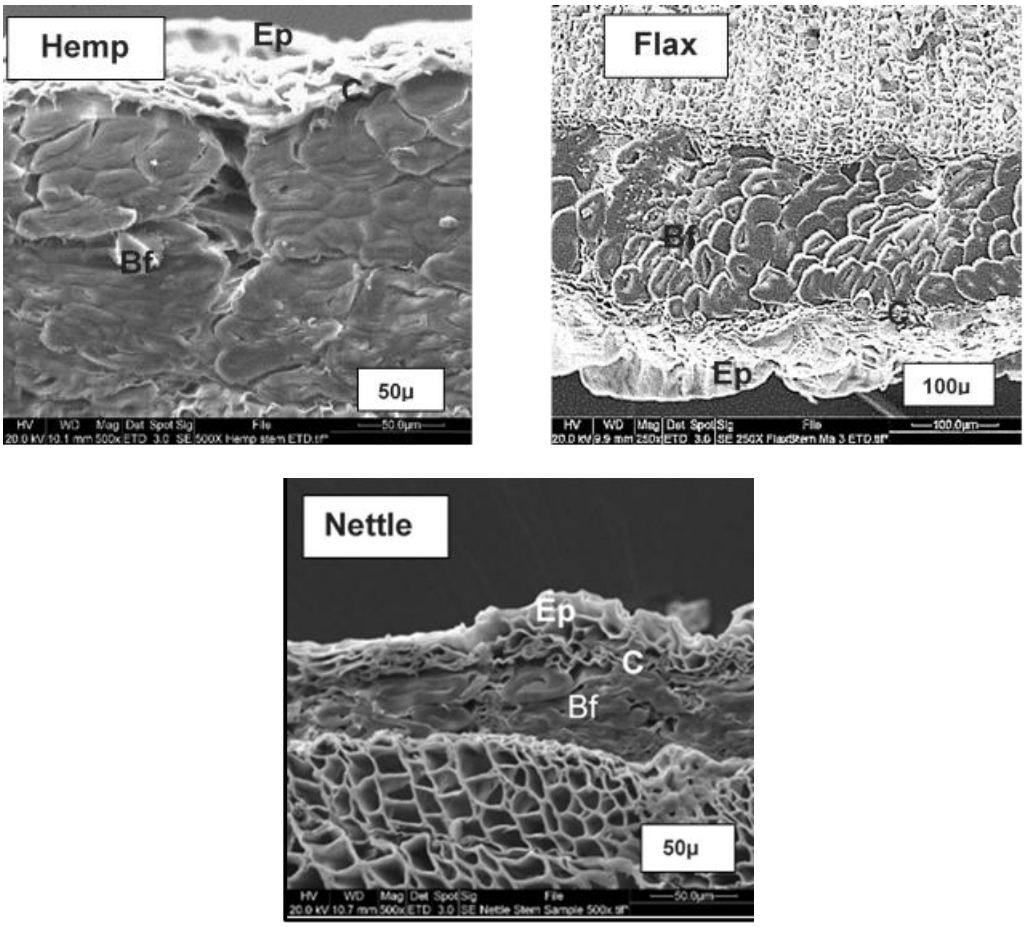

Figure 8.7. Cross-sections of hemp, flax and nettle. The images illustrate the plant anatomy with the following tissues identified. Ep (epidermis), C (cortex) and Bf (bast fibre). Images produced on SEM (EDT High Vacuum).

8.3.3 ImageJ analysis of fibre diametrical dimensional ratio

Sections from each fibre image where selected and six individual fibre CSA's identified and labelled for measurement with ImageJ software (Rasband 2016). The measurements are tabulated in **Table 8.3** to detail the range of diameter ratios derived from the SEM images of hemp, nettle and flax.

The diametrical ratios derived from SEM images demonstrate the ability to overcome variations presented in fibre CSA. The range of cell diameter and the ratio diameters are shown in **Table 8.3** with hemp ranging from 70.3µm to 32.0µm (SE 0.04), nettle 61.8µm to 22.0µm (SE 0.05) and flax 27.8µm to 19.0µm (SE 0.08). The corresponding ratios are hemp 0.63, nettle 0.64 and flax 0.40. Hence while this analysis could differentiate flax from nettle and hemp, there is minimally difference between nettle and hemp at 0.63 and 0.64 respectively.

ImageJ measurement of diametrical ratios (µm)			
Hemp (SEM) ImageJ			
No.	**Length Outer**	**Length Lumina**	**Ratio**
1	48.6	35.2	0.72
2	47.5	32.7	0.69
3	46.2	24.7	0.53
4	38.1	19.3	0.51
5	32.0	18.0	0.56
6	70.3	53.3	0.76
		Ave	**0.63**
		St. Dev.	**0.11**
		SE	**0.04**
Nettle (SEM) ImageJ			
No.	**Length Outer**	**Length Lumina**	**Ratio**
1	61.8	45.2	0.73
2	41.4	23.8	0.57
3	43.6	20.1	0.46
4	22.0	15.0	0.68
5	46.0	27.0	0.59
6	23.0	17.9	0.78
		Ave	**0.64**
		St. Dev.	**0.12**
		SE	**0.05**
Flax (SEM) ImageJ			
No.	**Length Outer**	**Length Lumina**	**Ratio**
1	25.6	10.1	0.39
2	26.5	12.6	0.48
3	22.1	10.0	0.45
4	27.8	8.7	0.31
5	19.0	5.7	0.30
6	25.3	11.6	0.46
		Ave	**0.40**
		St. Dev.	**0.08**
		SE	**0.03**

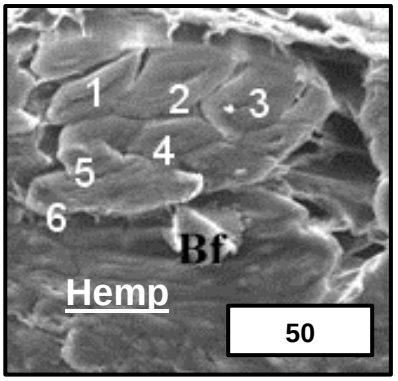

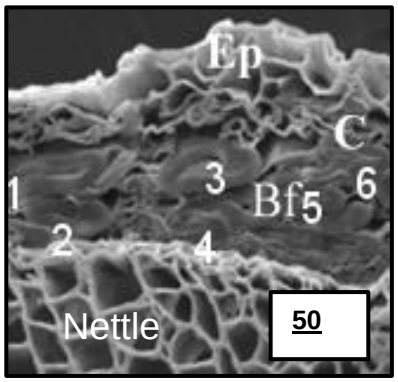

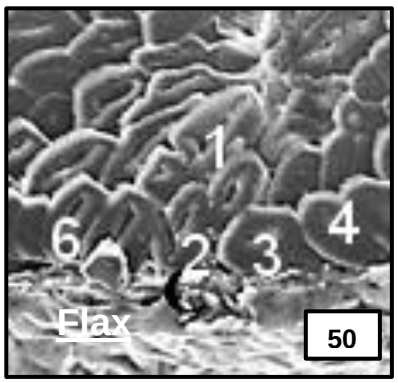

Figure 8.8. (Right)Selected fibres numbered.(See **Fig. 4.1**).Scale in µm

Table 8.3 (Left) CSA overall/lumina diameter ratios for SEM images.

8.4 Fibre CSA evaluation

A consideration of cross-sectional non-dimensional ratios outlined above suggests a potential for the identification of a fibre diagnostic feature and supports further investigations.

There are three parameters to consider in the investigation of this feature.

- What sectional CSA preparation would provide the best quality of images suitable for computer analysis?
- Which fibre CSA, non-dimensional computer-based diagnostic parameter, would provide the most effective differential feature?
- Can the computer-based measurement be formulated to eliminate subjective judgement?

8.4.1 Fibre cross-sectional sample preparation

The proposal was to consider several sample preparation techniques and appraise the quality of presentation of cross-sectional imagery as suitable for evaluation with computer software. For the circa. 25µm technical fibres under investigation the following techniques were considered.

The plate method,

Fibre bundles are pulled through a small diameter hole, with protruding ends sliced off flush to the plate (Greaves 1995, 5-7).

Manually fibre microtome.

Schaffer (1981: 121-122) prepared thin CSA sections with a Mico-Schwarz microtome. The fibres are held in a vertical position within a steel plate and protruding fibres are cut with a razor blade flush to the plate surface

Cross-sections embedding

Samples can also be prepared by embedding them between two pieces of cork and sectioning with a razor blade (Goodway 1987: 27-84). This process is suggested as quicker and less tedious than cutting with a microtome.

Rotary microtomes

The use of rocking or rotary microtomes is recommended by several authors (Haseloff 2003, 1174-1182; Charlet 2009, 1399-1403; Gierlinger.et al. 2012, 1694-1708).

In a previous work, Waudby (2014) prepared plant fibre cross-sections utilising methods broadly in agreement with those proposed above, including both sections cut from wax encapsulated plant stems, to 20µm sections obtained from a rotary microtome American Optical Model AO 820. However, the paraffin wax sections failed to hold the plant fibre specimens within the sample cross-sectional profile. Similarly, poor-quality results were obtained from the Brunel Rocking Microtome (Brunel Microscopes 2016) with fibre CSA material dislodged during microtome slicing

8.4.2 Appraisal of sectioning techniques and recommendations

There were two principal factors to be reviewed in the comparison of the CSA sectioning techniques. Firstly, the effect of the sectioning upon the fibre morphological shape and secondly the need to ensure that any mountant embossing did not interfere with CSA imaging quality and could be removed

successfully prior to a microscope analysis. Additionally, if a true CSA section is to be achieved, it was necessary to limit the distortions produced by excessive tensions placed on the fibre bundle during clamping and slicing. All the above techniques were included within the trial to evaluate the quality of CSA sectioning on microscopic imaging.

In practice, it was noted that samples submitted to microtome slicing were embedded in relatively soft mountants and proved difficult to clean and gave poor quality images. Also, it was apparent, from the MFA preparation detailed in chapter seven, that there is a difference in fibre CSA presentation between the fibres held under restraint within the stem structure and fibre bundles released by retting and combing whereby the CSA became swollen.

Thomason et al. (2011) in their considerations of plant fibre as a composite material, and Di Virgilio (2013), reporting on the properties of commercial Stinging Nettle crop, obtained improved sectioning utilising polished epoxy resin moulding. This process provided rigid epoxy mountings suitable for grinding and polishing and improved sample preparation to determine plant fibre CSA morphology. In researching the availability of epoxy resins to meet the requirements it was accepted that a cold mounting resin, EpoFix from Sigma-Aldrich, best serve the research design.

8.4.3 Fibre CSA: sample preparation, casting and polishing

It was apparent that there were practical considerations to be addressed in the construction CSA casting,

- The epoxy resin moulding conditions, time periods and techniques to be employed.
- The ratio of moulding/CSA diameter ratio that would be most effective
- The location of the CSA image be within the microscope field of view.
- The angle of sample presentation as representative of the fibre CSA, to be at right angles to the fibre longitudinal axis.
- Sectioning of circa 1-2mm thickness, require tom obtain a mirror-polished finish to enable images to be viewed by transmitted light.

A method of presenting fibre samples within a rigid mountant suitable for thin cross-section preparation was developed. The theoretical fibre, circa 25-40μm diameter, had to be centralised vertically within the chosen mountant and weighted to ensure a near-vertical presentation. The epoxy resin specified was of low viscosity; hence, there was a possibility of leakage around or through the mount sealing. With a cold-drying period of 12 hours, the assemblage had to be held in a firm and stable position during the preparation period. A copper trace wire of 230μm was incorporated in close attendance to the specimen to provide guidance on the fibre location within the mountant. The final requirement was to ensure that the finished moulding could be held securely during the subsequent grinding and polishing processes. Many sample moulding and support techniques were trialled, the final tested and approved mounting assemblage is illustrated in **Figure 8.8.**

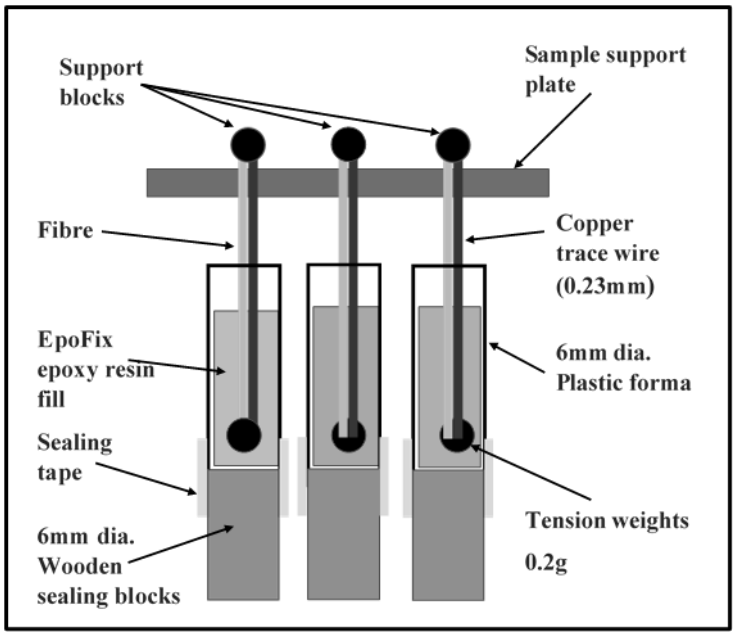

Figure 8.9 Section of multi-stage assemblage for 6mm diameter mountants. The plastic mould was a 6mm diameter drinking straw, the different colours for the straws were the principal labelling used with green=nettle, yellow=flax and red=hemp.

Practical considerations

The bottom sealing block was coated with wood varnish and an adhesive strip added to seal the joint between the plastic mould and the sealing block to prevent egress through the wooden sealing block's cell structure or around the joint.

Sample preparation

Following overnight curing in a fume cupboard, the sealing block was trimmed to reduce the overall size of the sample, and redundant mountant removed from the top of the mould to gain access to fibre samples held below the mountant fluids concaved meniscus.

Sample cutting and polishing

The end of the prepared sample was ground flat using a range of emery papers and diamond polished to give a mirror finish suitable for microscope imaging and computer analysis. To attain a level surface, for optimum orientation in microscope viewing, the samples were held in a 13mm tool “chuck” complete with a circular levelling bubble mounted on top to ensure a vertical orientation of the sample during the grinding and polishing process.

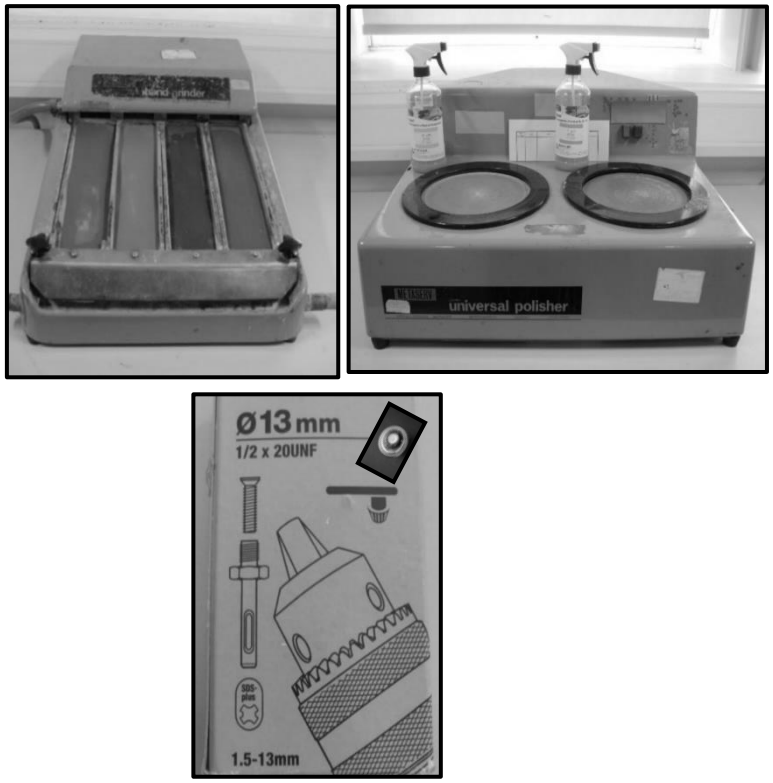

Figure 8.10 Grinding and polishing 6mm sample.**Top left**. Metaserv Hand Grinder 1200,600,450 and 320 grade emery paper with water flush. **Top right.** Mataserv Universal Polisher with diamond suspension polishing fluid. Yellow 6µm, blue 1 µm. **Bottom Centre.** 13mm drill chuck inclusion shows detail of mounted circular levelling bubble to ensure correct presentation to polisher to achieve a level surface

Grinding was undertaken on the Metaserve Hand Grinder using an increasing fineness of emery papers 320, 450, 600 and 1200. Mirror-faced diamond polishing was completed on Buehler Metaserve Universal Polisher on a Lamplan 432 200mm diameter pad with a 6µm diamond suspension spayed lubrication **Figure 8.9.**

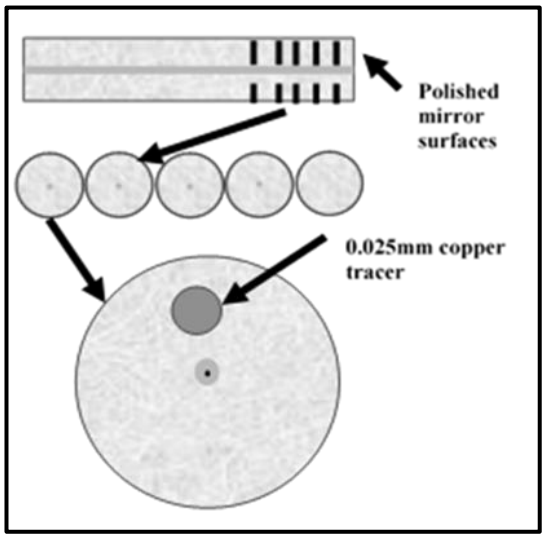

Figure 8.11 Method of sectioning fibre samples into 2 mm thick cross-sections. The image shows how repeated sections can be ground, polished and sectioned to achieve the quality of fibre CSA required.

Figure 8.12 Buehler Isomet Low-Speed Rotary Microtome. Used for the cutting of 1-2mm thick sections from the 6mm diameter epoxy resin mould. The cutting wheel used was a 5ins. diameter diamond wafering blade.

8.5. Determination of cross-sectional area circularity

In section **8.2.3** plant fibre comparative diameter dimensions were evaluated as diagnostic features and their diametrical ratios recorded using ImageJ software. The ImageJ software provides access to a range of support functions to facilitate shape analysis and comparison. The feature selected to improve the diagnostic determination of cross-sectional images was "Circularity" (Ct) the ratio of shape area to its perimeter.

$$\textbf{Circularity} = 4\pi \times \textbf{Area/Perimeter}^2$$

This equation relates the shape factor Ct, to the ratio comparison of the circularity of a true circle "1" to a line of minimum height circa "zero". The fibre cell shapes display a Ct range from polygonal (circa 0.7) to ovate (circa 0.5) and provide a valuable diagnostic differential.

8.5.1 ImageJ analysis of fibre circularity ratio

CSA fibre images are shown in **Figure 8.12**. these "technical fibres" images, circa 25-40 µm, illustrate the number of microfibres that make up the fibre bundle. Individual microfibers within the section were labelled, and their non-dimensional circularity (Ct) determined with ImageJ software. Ideally, this should be accomplished by the "analysis of particle measurement" also incorporated into the software.

Unfortunately, as is evident from **Figure 8.12,** the microfibre bundles are too entwined and overlapped to enable ImageJ "threshold" analysis of a binary black and white image.

Consequently, the attendant “watershed” manipulation to separate the microfibre images equidistant around their edges was inoperable (Broeke et al. .2015: 59). Ct measurements were achieved by manual placement around the individual microfibre and determination of Ct with ImageJ functions “Analyze”, and “Measure”.

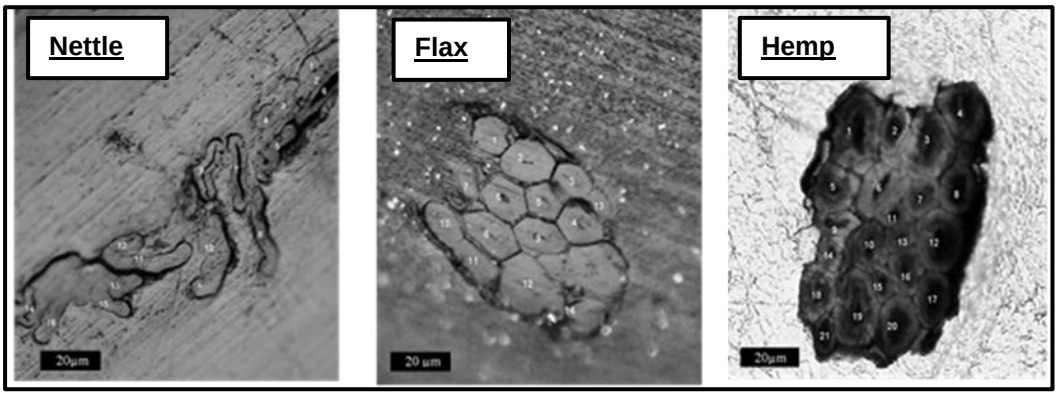

Figure 8.13 Microfibre cross-sectional Ct imaged with Nikon Optiphot under transmitted cross-polarised lighting (CPL). Typical CSA images analysed with ImageJ software to evaluate circularity, a non-dimensional ratio of CSA. **Left**. Nettle, (n=15), mean Ct 0.53, St. Dev. 0.109, SE. 0.028. **Centre.** Flax, (n=14), mean Ct 0.76, St. Dev. 0.05, SE. 0.13. **Right.** Hemp, (n=21), mean Ct 0.80, St. Dev. 0.06, SE. 0.013.
Note There was a variation in the number of microfibres contained within each “theoretical fibre” this variation reduces the number of microfibre samples available for measurement within the total assemblage.

The above sample preparation, sectioning and microscopic imaging were completed for samples from the following sources as detailed in **Chapter 4 Table 4.1** and partly repeated here for convenience **Table 8.4.**

Fibre	**Latin name and variety (where known)**	**Source**
Nettle	*Urtica dioica*	Wild (open woodland)
Hemp	*Cannabis sativa* v. n/a	Commercial crop
Flax	*Linum usitatissimum* v. Winterlyn	Commercial crop

Table 8.4 Plant fibre sources for nettle, hemp and flax. (from **Chapter 4** Table 4)

Microscope slides were prepared for the 2mm thick cross-sectional samples of “technical fibres”, circa 25-40µm, from each of the above species. The CSA’s were imaged with Nikon Optiphot under transmitted cross-polarised lighting (CPL). Ten samples from each species were mounted, and each fibre within the bundle labelled and analysed with ImageJ software to determine their Ct.

For each of the fibre species, it was apparent that their size and the quality of microfibrillar CSA displayed varied with the larger nettle fibre CSA presenting an average of 6 Ct measurements per sample, for the finer flax fibres there was an average of 13 and, for hemp 4. The data from the hemp samples was reduced due to the poor quality of CSA image presented. A sample of the microfibre image labelling and tabulation of the ImageJ analysis is shown in **Figure 8.1**

Label	Circularity
1	0.817
2	0.755
3	0.725
4	0.707
5	0.480
6	0.834
7	0.815
8	0.863
9	0.848
10	0.688
11	0.642
12	0.880
13	0.561
14	0.762
15	0.797
16	0.740
Mean Ct	0.744
St Dev.	0.110
St Error	0.027

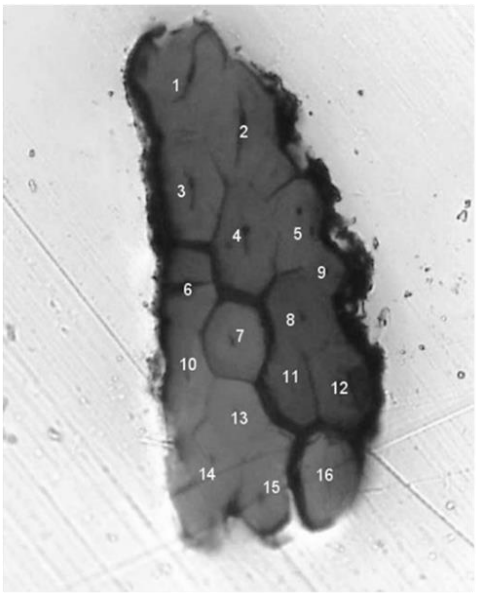

Figure 8.14 Flax W6 area cross-sectional Ct. Data assembled from ImageJ analysis of microfibrillar CSA.

The full data for each of the samples is shown in **Table 8.5 (a)** and **Table 8.5 (b)** with average, standard deviation and standard error detailed below each table. The database results are plotted in **Figure 8.15.**

Nettle: area cross-sectional circularity (Ct)							**Hemp: area cross-sectional circularity (Ct)**			
No	**Nettle Ct**	**No**	**Nettle Ct**	**No**	**Nettle Ct**		**No**	**Hemp Ct**	**No**	**Hemp Ct**
1	0.462	**21**	0.778	**41**	0.576		**1**	0.876	**23**	0.794
2	0.700	**22**	0.705	**42**	0.609		**2**	0.620	**24**	0.847
3	0.571	**23**	0.504	**43**	0.664		**3**	0.792	**25**	0.828
4	0.746	**24**	0.474	**44**	0.542		**4**	0.523	**26**	0.817
5	0.590	**25**	0.424	**45**	0.567		**5**	0.739	**27**	0.803
6	0.642	**26**	0.484	**46**	0.590		**6**	0.797	**28**	0.774
7	0.731	**27**	0.722	**47**	0.291		**7**	0.903	**29**	0.864
8	0.539	**28**	0.530	**48**	0.398		**8**	0.565	**30**	0.857
9	0.370	**29**	0.479	**49**	0.295		**9**	0.749	**31**	0.842
10	0.462	**30**	0.490	**50**	0.403		**10**	0.685	**32**	0.819
11	0.626	**31**	0.421	**51**	0.450		**11**	0.858	**33**	0.838
12	0.757	**32**	0.340	**52**	0.450		**12**	0.826	**34**	0.928
13	0.521	**33**	0.665	**53**	0.589		**13**	0.637	**35**	0.858
14	0.375	**34**	0.437	**54**	0.711		**14**	0.723	**36**	0.779
15	0.404	**35**	0.484	**55**	0.753		**15**	0.570	**37**	0.716
16	0.463	**36**	0.509	**56**	0.441		**16**	0.687	**38**	0.884
17	0.409	**37**	0.567	**57**	0.552		**17**	0.893	**39**	0.824
18	0.430	**38**	0.471	**58**	0.662		**18**	0.763	**40**	0.827
19	0.603	**39**	0.440	**59**	0.641		**19**	0.775	**41**	0.853
20	0.524	**40**	0.400	**60**	0.378		**20**	0.791	**42**	0.904
			Ave		**0.530**		**21**	0.821	**43**	0.590
			St. Dev.		**0.123**		**22**	0.857	**44**	0.542
			S.E.		**0.016**			**Ave.**		**0.778**
								St. Dev.		**0.105**
								S.E.		**0.016**

Table 8.5. (a) Ct determination for nettle and hemp fibres.
Nettle Ct. n= 60, Average = 0.530, St. Dev.= 0.123, SE= 0.016
Hemp Ct. = 44, Average = 0.778, St. Dev.= 0.105, SE= 0.016

Flax: area cross-sectional circularity (Ct)									
No.	**Flax Ct**	**No.**	**Flax Ct**	**No.**	**Flax Ct**	**No.**	**Flax Ct**	**No.**	**Flax Ct**
1	0.885	**27**	0.795	**53**	0.689	**79**	0.861	**105**	0.747
2	0.865	**28**	0.798	**54**	0.86	**80**	0.86	**106**	0.793
3	0.893	**29**	0.861	**55**	0.89	**81**	0.841	**107**	0.747
4	0.832	**30**	0.758	**56**	0.828	**82**	0.695	**108**	0.793
5	0.782	**31**	0.885	**57**	0.821	**83**	0.744	**109**	0.747
6	0.835	**32**	0.574	**58**	0.667	**84**	0.85	**110**	0.793
7	0.705	**33**	0.671	**59**	0.869	**85**	0.822	**111**	0.747
8	0.797	**34**	0.752	**60**	0.817	**86**	0.793	**112**	0.793
9	0.805	**35**	0.769	**61**	0.755	**87**	0.81	**113**	0.747
10	0.652	**36**	0.768	**62**	0.725	**88**	0.785	**114**	0.793
11	0.805	**37**	0.779	**63**	0.707	**89**	0.749	**115**	0.747
12	0.693	**38**	0.672	**64**	0.48	**90**	0.839	**116**	0.793
13	0.832	**39**	0.564	**65**	0.834	**91**	0.837	**117**	0.747
14	0.819	**40**	0.652	**66**	0.815	**92**	0.74	**118**	0.793
15	0.885	**41**	0.813	**67**	0.863	**93**	0.713	**119**	0.747
16	0.865	**42**	0.775	**68**	0.848	**94**	0.831	**120**	0.793
17	0.893	**43**	0.669	**69**	0.688	**95**	0.796	**121**	0.747
18	0.832	**44**	0.752	**70**	0.642	**96**	0.827	**122**	0.793
19	0.782	**45**	0.727	**71**	0.88	**97**	0.678	**123**	0.747
20	0.835	**46**	0.858	**72**	0.561	**98**	0.775	**124**	0.793
21	0.705	**47**	0.744	**73**	0.762	**99**	0.831	**125**	0.82
22	0.748	**48**	0.745	**74**	0.797	**100**	0.796	**126**	0.754
23	0.863	**59**	0.719	**75**	0.74	**101**	0.827	**Ave.**	**0.778**
24	0.872	**50**	0.699	**76**	0.847	**102**	0.678	**St. Dev.**	**0.079**
25	0.614	**51**	0.706	**77**	0.841	**103**	0.775	**S. E.**	**0.007**
26	0.814	**52**	0.774	**78**	0.86	**104**	0.673		

Table 8.5. **(b)** Ct determination for flax fibres. Flax Ct.
n= 126, Average = 0.778, St. Dev.= 0.079, SE= 0.007

The results above in **Table 8.5 (a) and 8.5 (b)** are presented in **Figure 8.14** to illustrate the statistical comparison of the mean and standard deviation of fibre cross-sectional circularity.

Note The data base in support of the above is included in Appendix C (1,2,3).

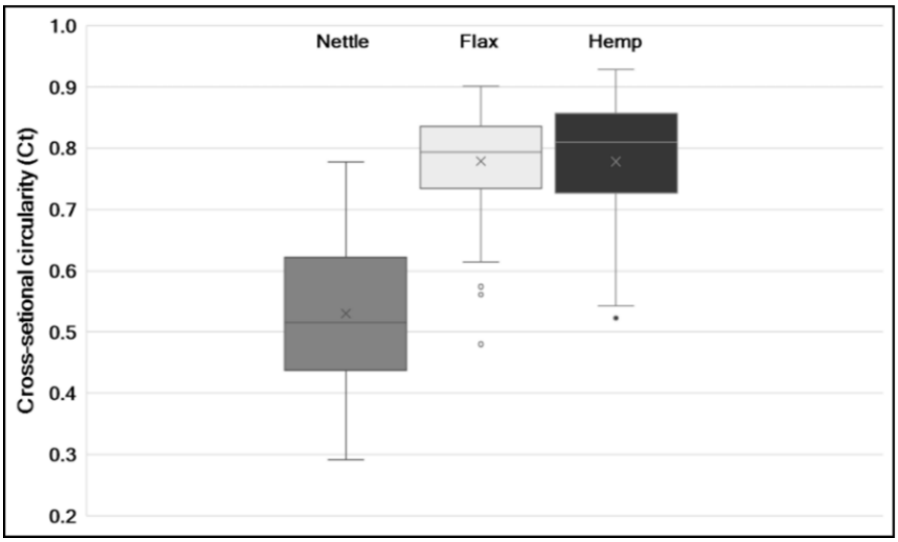

Figure 8.15 Plot of comparison of the mean and standard deviation of fibre cross-sectional circularity (Ct) for nettle, flax and hemp

Analysis of variance in fibre cross-sectional circularity (Ct) for 230 samples, Nettle (n 60), Hemp (n 44) and Flax (n 126), found there to be highly significant variation between the grouped samples ($F=144.148$, $df=229$, $p= <0.0001$). The plot shows a significant difference between Nettle and Flax ($T=16.56$, $df=184$, $p<0.0001$) and a significant difference between Nettle and Hemp ($T=10.78$, $df=102$, $p<0.0001$). There was no significant difference between Flax and Hemp.

8.6 Summary

The results achieved in the analysis of variance for Ct values supports the proposal of Ct as a diagnostic feature. In combination with MFA measurements these Ct features, as detailed in the previous chapter, provide the foundations for plant fibre diagnosis.

In a review. of the cross-sectional shapes attributed to plant fibre, the following six shape descriptions based on experienced subjective judgement for flax, hemp and stinging nettles from both unprocessed plant stems and processed (retted) fibres were listed Lukšová and Holst (2020).

Polygonal	Polygonal, slightly rounded
Oval	Irregular oval
Uneven, rounded edges	Flattened

(Lukšová and Holst 2020).

Similarly, in a programme, Wear Analysis and Visualizing Expert Systems (WAVE), to determine tool wear analysis, the difficulty, regarding the insufficiency in similarities of observation descriptions, in reconciling a comparison in the interpretations was reported (Van den Dries 1998: 45) The author record that,

> “(T)here was no absolute consensus within the discipline as to nomenclature: each expert developed his or her personal method of analysis and reasoning (Van den Dries 1998: 45)”.

The WAVE programme’s intended research outcome was to establish a descriptive consensus to enable tool wear data to be diagnosed within an Artificial Intelligence protocol. The analysis of plant fibre area cross-sections with an established computer software programme, ImageJ (Rasband 2016), offers an arithmetical determination that could serve as a base for consideration of computerised “Artificial Intelligence” (AI) as a diagnostic facility to support the subjective judgement of fibre CSA morphology.

Chapter Nine
Combination diagnosis, microfibrillar angle (MFA) and circularity (Ct)

9.0 Introduction

In the previous two chapters, the morphological features of microfibrillar angle (MFA) and cross-sectional circularity (Ct) have been assessed for a range of modern reference material. It is intended that these two diagnostic features be utilised in a two-stage binomial mode for fibre analysis.

9.1 Principal component analysis (PCA)

Initially, it was proposed that PCA would offer a statistical protocol to determine the MFA/Ct relationship. Unfortunately, PCA requires a large, circa 200, sample database and although Ct at 235 samples meets this requirement, MFA, with only 70 samples, is too low. Additionally, PCA requires a range of variables with a minimum of three and the database for MFA and Ct does not meet that criteria.

9.2 MFA/Ct Ratio analysis

Simple ratios of MFA/Ct are illustrated in **Table 9.1** to show the considerable overlap, 22 to 3, that covers the total values attained between the extremes of Max. MFA/Min. Ct and Min. MFA/Max. Ct ratios for the three modern reference fibres flax, nettle and hemp.

Fibre	Flax	Nettle	Hemp
Max. MFA	7.4	10.5	6.9
Min. Ct	0.48	0.48	0.542
Min. MFA	3.3	3.2	3.0
Max. Ct	0.778	0.78	0.928
Ratio Max. MFA/Min Ct.	15.4	21.9	12.73
Ratio Min. MFA/Max. Ct	4.24	4.10	3.23

Table 9.1. Ratio of maximum/minimum and minimum/maximum of MFA and Ct ratio values to illustrate the overlap.

A simple ratio of MFA v Ct would not provide an acceptable measure as the variation in the ratio factor for each fibre show a range between the maximum 21.9 to the minimum 3.23.

9.3 Vector Analysis

An alternative proposal was to construct a vector plot based on MFA and Ct mean values to reflect their relationship. The vectors are defined by their angular direction (α^{o}) and their magnitude (R)

Where $R = \sqrt{(\text{Mean MFA}^2) + (\text{Mean (Ctx10)}^2)}$

and

Cosine α^{o} = MFA/ R

The above ratios are listed in **Table 9.2** and angular direction and magnitude listed in **Table 9.3.**

	Hemp	Flax	Nettle
Mean MFA	4.59	-5.78	-6.5
Mean Ct x 10	8.12	7.76	5.30

Table 9.2 Tabulation of Mean values MFA and (Ct x 10)

R=	**$\sqrt{(MFA^2+(Ctx10)^2)}$**		
Cos.α⁰=	MFA/R		
	Hemp	Flax	Nettle
R=	9.3	9.7	8.4
Cosine =	0.49	-0.60	-0.77
α⁰ Radians	1.05	2.21	2.46
α⁰	61⁰	127 ⁰	141⁰

Table 9.3 Determination of vector angular direction and magnitude: calculated for MFA and Ct mean values

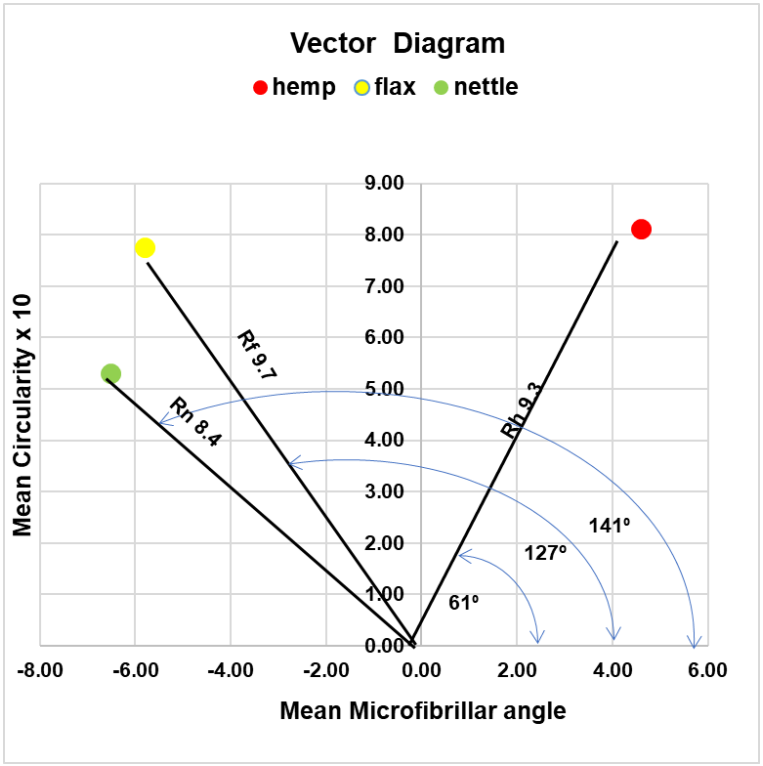

Figure 9.1. Vector diagram: based on the fibre mean values of MFA and (Ctx10)

The resultant vector diagram **Figure 9.1** plots the resulting vector direction and magnitude for each fibre's MFA and Ct mean values to illustrate their relationship.

9.4 Graphical relationship

The final option is to present the fibres' MFA and Ct mean values to illustrate their relationship in a graphical plot format **Figure 9.2** The plot also includes an annular representation of the 99% confidence level surrounding the mean value plots **Table 9.4** and **Figure 9.2.**

The range for 3xSt. Errors with maximum and minimum values						
	Hemp		**Flax**		**Nettle**	
MFA SE x3	0.72		1.05		1.29	
Ct SE x3	0.03		0.02		0.05	
	hemp max	**hemp min**	**flax max**	**flax min**	**nettle max**	**nettle min**
Mean MFA+/- 3SE	5.311	3.871	-4.733	-6.833	-5.231	-7.817
Mean Ct +/- 3SE	0.846	0.754	0.797	0.754	0.578	0.482

Table 9.4 Range of MFA and Ct maximum and minimum values: based on a 99% confidence level at 3 SE.

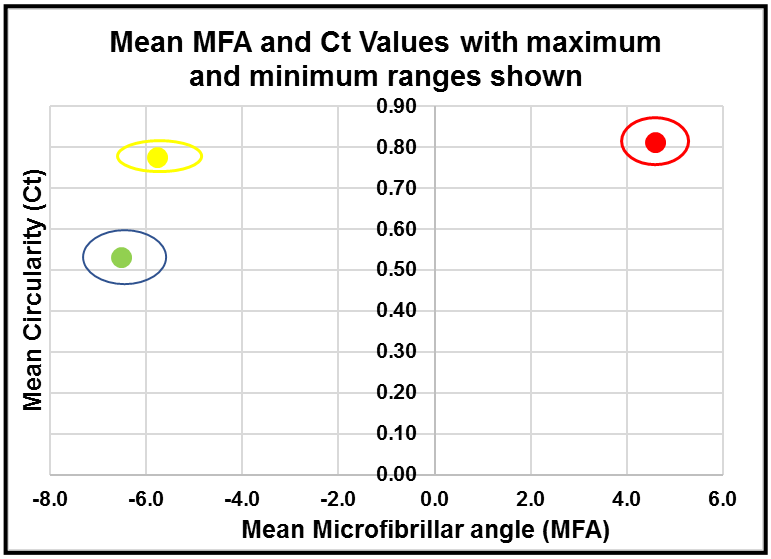

Figure 9.2. A plot of mean MFA v Mean Ct values**:** as determined for the three modern natural fibres flax (yellow), nettle (green) and hemp.(red) The enclosing circles define the 99% (3 St Errors) confidence range for each fibre type.

9.5 Summary

The vector depiction in **Figure 9.1** illustrates the potential for displaying the MFA/Ct relationship in a mathematical vector format. However, the display offers limited advantage over a basic graphical representation. It should however be recognised that the incorporation of an additional diagnostic feature within a 3D vector format would considerably advance the diagnostic capability This potential is examined further in **Chapter 13.**

Figure 9 illustrates the advantage in applying MFA/Ct in a coextensive coherence for the diagnosis of plant fibre species. However, prior to accepting MFA/Ct as a diagnostic process, it is necessary to evaluate the reliability of the procedure when applied to archaeological artefacts. Hence it was necessary to incorporate both an appraisal of a temperature accelerated degradation trial to confirm the stability of these morphological features, and a blind-test regime applied to randomised samples to confirm the reliability of MFA/Ct as diagnostic features.

The research outcomes for both conformation trials are reported in the following chapters for blind testing **Chapter 10** and for degradation trials **Chapter 11** Following this secondary appraisal, the research programme applied the diagnostic determinants to address archaeological textile artefacts to case study analysis. **Chapter 12** details the MFA/CT relationship determined within each category as a comparative measure of the efficacy of the dual diagnostic morphological features acting in combination in the evaluation of plant fibre species.**Note The data base in support of the above is included in Appendix D.**

Chapter Ten
Blind test - fibre MFA/CT appraisal

10.0 Introduction

Following the completion of the experimental research, the diagnostic features so established require the researcher to confirm the research findings within a defined and rigorously controlled test environment. The parameters established should be undertaken within prescribed environmental conditions and be conducted either by professionals, with knowledge in the research field, or through a blind-test routine whereby the researcher applies the experimental techniques to a random selection of samples to confirm the viability of the diagnostic parameters. There is a range of blind-tests undertaken in support of archaeological analysis, microwear analysis (Bamforth 1988; Bamforth et al. 1990; Gonzalez et al. 2003; Evans and Donahue 2005; Evans 2014a; Hayes et al. 2017), residue analysis (Evans and Donahue 2005; Lombard and Wadley 2007; Hayes et al. 2017), faunal remains (Gobalet 2001; Nims and Butler 2007; Morin et al. 2017) and radiocarbon dating (Nelson et al. 1988; Hart and Lovis 2007; Douka et al. 2010). However, reservations have been expressed regarding the efficacy of blind testing, for example, the discussion of microwear diagnosis (Newcome et al. 1986; Hurcombe 1988; Van-Den Dries1998) and, for problems arising from carbon-inclusion in radiocarbon dating, (Nelson et al. 1988; Grimm et al. 2009; Douka et al. 2010).

10.1 Experimental archaeology

Experimental archaeology is a scientific research science that formulates a research hypothesis for evaluation supported by experimentation in past methods and construct replication. However, there are concerns as to the validity of such replications in that the laboratory processes that are undertaken with modern reference material, plus the cultural input of the experiment, may not represent past conditions and circumstances accurately (Hurcombe 2007; Outram 2008). In a report on the diagnosis of Neolithic textile artefacts, the findings were criticised by other authors as unreliable in that Neolithic fingers were “too fat” to weave such textiles a response that serves to highlight the dissenters bias in the formulation of a valid hypothesis (Soffer and Adovasio 2014).

10.2 Experimental archaeological research programme

Some of the difficulties to be avoided in formatting an experimental archaeological research programme are noted (Outram 2008: 4-5). These include the lack of well-thought-out hypothesis, insufficient details on methods and materials and compromise using modern reference material. Additionally, Outram (2008) notes the lack of academic context and the setting of inappropriate parameters to address the archaeological questions The inclusion of ethnographic reports informing the research protocol is noted by Hurcombe (2000), who comments on the bias in the way that airborne pollen is incorporated into site deposits, and notes the problem of recognising and identifying naturally occurring wild plants as exploited species.

The author also remarks on the perception and prejudice of male ethnographic reporters who may not give appropriate recognition to female craft activities (Hurcombe 2000: 155-173).

10.2.1 Radiocarbon C14 Dating

To ensure radiocarbon dating quality and reliability on an international basis, comparative inter-laboratory testing is an essential requirement. From a range of sites and periods, sample materials such as wood, bone and soils, that have previously been dated by independent means, are prepared and labelled before distribution to the laboratories for blind testing. The programme exists to support confidence in the radiocarbon dating process. However, there are concerns regarding dating accuracy that can be modified by contamination from associated younger/older materials deposited from bioturbation or fungal and bacterial activity. An examination of eleven samples from Alaskan Arctic Holocene deposits of plant fibre and tree stumps created confusion with a recorded discrepancy of some 4000 years. The conclusion being that caution should be exercised when submitting bulk samples where the deposition may contain “dead carbon” (Nelson et al. 1988).

10.2.2 Fishbone identification

The considerable variation in the interpretation of fish bones, teeth and scales from the archaeological sites in San Luis Obispo County California USA undertaken by doctoral degree level specialists raised questions regarding the accuracy and inconsistency of recorded data (Gobalet 2001).

Gobalet proposes a review of the chosen specialist's diagnostic credibility be included and that data from non-peer reviewed "grey literature" should be avoided.

In contrast, a blind-test review on the analysis of 112,000 fish remains from a Native American site in Washington State USA, as documented by five different analysts, noted close agreement with only minor differences in the previous recording of species with a recommendation that a programme of quality assurance of experimental control and assessment could be beneficial (Nims and Butler 2017).

10.2.3 Faunal bone analysis

Blind testing of ungulate bone assemblages from two large samples were conducted to evaluate the abundance of elements individualy (Number of Identified Specimens (NISP) or taxa based (Minimum Number of Elements (MNE). Doubts have been expressed regarding the accuracy of both methods, and the blind-test was designed to compare the NISP and MNE diagnosis of bone fragmentation. The results are proposed as capable of providing replicable and accurate abundance ratios (Morin et al. 2017: 886-93).

10.2.4 Lithic use-wear (MicrowearAnalysis)

Bamforth (1988) reviewed the poor performance of blind-tests reported by other authors (Dumont 1982; Knutson and Hope 1984; Levi-Sala 1986) to identify problems with image processing, the design and scoring of the blind-test and the duration of use are noted.

In particular, for the latter case, the author notes

> "(T)he increasing level of correct identifications as related to the duration of use and notes that such tests as conducted within microwear analysis are unknown for other archaeological studies." (Bamforth 1988: 17).

More recent works, and the availability for modern reference lithic material to be utilised in use-wear analysis, has led several blind-test research programmes to evaluate the diagnostic potential for interpretation of the microwear associated with different edge tool/material interface and associated residue analysis (Gonzalez et al. 2003; Evans and Donahue 2005; Evans 2014a; Hayes et al. 2017). However, few research programmes for evaluating similar use-wear and residue diagnostic techniques, have been applied to grinding tools (Hayes et al. 2017).

Replication experiments with use-wear analysis of ground stone objects were carried out on a range of raw materials and included blind testing although the authors noted that there were still too few analytical frameworks for use-wear analysis (Van den Dries 1998; Dubreuil and Savage 2014). Research at Leiden University considered the potential for computer-assisted evaluation of use-wear analysis based on an artificial intelligence technique Wear Analysing and Visualising Expert System (WAVE). The system was based on data collated from descriptions of the observations reported by different use-wear analysts. However, there was an insufficient similarity of process description to afford comparisons. The results were subject to a blind test by students and experienced analysts.

The author noted that there was insufficient consensus within the discipline and that the descriptions of the observations given by different use-wear analysts did not support a meaningful comparison of interpretations (Van den Dries 1998).

In an extensive review of lithic microwear analysis, the importance of validating diagnosis through a blind testing protocol is proposed as an essential and necessary method (Evans 2014a). The author expresses concerns regarding the limited data set for functional analysis and notes the unacceptable level of accuracy and proposes,

> "(A) large dataset of consistently designed blind-tests in method evaluation and suggests that fields such as lithic microwear analysis would greatly benefit from such testing" (Evans 2014b: 5).

A summary of blind-test results from 40 tests records that 33 of the tests provided data suitable for determination with 42.7% accuracy in diagnosis. Again, the question of subjectivity, in describing the use-wear outcomes, is noted to propose the development of a database to be established to accommodate the variation in analytical skills and experience (Evans 2014a)

10.3 Blind testing - Aims and objectives

In formulating the experimental structure for the blind test protocol and in agreement with Outram (2008, 4-5), the hypothesis is proposed.

Can the textile plant fibre morphological features, microfibrillar angle MFA and fibre cross-sectional circularity Ct, serve as reliable diagnostic features?

In support of the above, the following aim and objectives are noted below.

Aim

To utilise a blind-test protocol to evaluate the viability and reliability of, CSA circularity (Ct) and microfibrillar angle (MFA) as plant fibre diagnostic features.

Objectives

- To use the statistical outcomes reported in **Chapters Seven** and **Chapter Eight** to establish a representative fibre sample size.
- To randomise the samples within a blind test protocol.
- From the eight modern reference fibre species, included within the Research Programme, to select fibre types that have been produced under basic processing techniques with minimum electro/mechanical or chemical enhancement.
- In agreement with the initial research protocol to utilise those established minimally invasive techniques in the blind test appraisal
- To evaluate and tabulate the results within a database suitable for statistical analysis.
- The data outcomes to be compared with the previously determined research findings and a summary of the blind test accuracy prepared.

10.4 Blind test protocol

The analysis of degraded archaeological specimens to determine fibre type are often challenging, partly due to uncertainties around the reliability of identification techniques. Here, two established diagnostic approaches are standardised, quantified, and blind tested in terms of their combined ability to separate reference material from nettle (*Urtica dioica* L.), flax (*Linum usitatissimum* L.) and hemp (*Cannabis sativa* L.). As noted in previous chapters the diagnostic feature to be evaluated within the blind test protocol are longitudinal microfibrillar angle (MFA) and cross-sectional circularity (Ct) used in a two-step procedure to analyse a set of randomly selected modern fibres (n=48, 16 from each species).

10.4.1 Introduction

The analysis of degraded archaeological specimens to determine fibre types is often challenging, partly due to uncertainties around the identification techniques' reliability. Here, the two diagnostic features reported in previous chapters are standardised, quantified, and blind tested in terms of their combined ability to separate reference material from nettle (*Urtica dioica* L.), flax (*Linum usitatissimum* L.) and hemp (*Cannabis sativa* L.). Current methodology for archaeological and historic fibre identification relies on autoptic microscopic analytical techniques (Suomela et al.2018). There have recently been many palaeoethnobotanical applications of fibre identification (Bergfjord et al. 2012; Skoglund et al. 2013; Lukešová et al. 2019). However, limitations to the methods are occasionally noted and rarely quantified.

One novel approach to this is blind testing, an established method for understanding the capability and appropriateness of identification techniques (Sheldrake 1999; Evans 2014) with a broad range of examples within archaeological science (Bamforth 1988; Nelson et al. 1988; Bamforth *et al.* 1990; Gobalet 2001; Gonzalez-Urquijo and Ibanez-Estevez 2003; Hart and Lovis 2007; Hayes *et al.* 2017; Morin *et al.* 2017; Douka *et al.* 2010). Since this approach is yet to be applied to bast fibre identification, understanding sources and degrees of error will make records more robust and valuable (Nims and Butler 2007). It can also drive improvements in techniques that will aid in the re-evaluation of some archaeological specimens and support discussion about the broad range of plant products in past societies.

As previously noted, the aim of the presented study is to evaluate the viability and reliability of a combined approach using cross-sectional circularity (Ct) and microfibrillar angle (MFA) measurements as a method for distinguishing between fibres of nettle, hemp and flax. These are considered to have been the three most commonly used bast fibres in prehistoric Northern Europe. Ct is a new method presented as a quantifiable alternative to shape interpretation, commonly used as presented by Suomela et al. (2018). MFA imaging is as presented by Bergfjord and Host (2010), with the addition of directly measuring the angle, and is a simpler alternative to the highly regarded modified Herzog test (Haugan and Holst 2013).

10.4.2 Method - sample size and source of fibres

The diagnostic features, MFA and Ct, outlined in **Chapter Seven** and **Chapter Eight** are proposed for the blind-test evaluation of fibre types with longitudinal microfibrillar angle (MFA) and cross-sectional circularity (Ct) used in a two-step procedure to analyse a set of randomly selected modern fibres. The sample size is determined by considering of Error Range and Students *t* Distribution for 95% confidence to calculate a sample size of 16 for each type giving a total sample size of 48 **Table 10.1.**

Fibre	Number(n)	√n	MFA	St. Dev (σ)	SE	Student " t @95% df =15	SD*t	Error range t x SD/√n
Nettle	16	4.00	6.524	2.157	0.135	2.131	4.597	-5.351 to -7.69
Flax	16	4.00	5.573	1.678	0.105	2.131	3.576	-4.906 to -6.694
Hemp	16	4.00	4.591	1.128	0.071	2.131	2.404	4.661 to 3.999

Table 10.1. Determination of blind test sample size (Drennan 2004: 132).

10.4.3 Method - the selection of fibre samples

Fibre	Source	Location	Process
Nettle	Testbed Crop	Bradford UK	Retted Manual decortication Basic combing
Hemp	Commercial Crop	Baswick UK	Retted Mechanical decortication Basic combing
Flax	Testbed Crop	Bradford UK	Retted Manual decortication Basic combing

Table 10.2. Blind test: fibre material sources.

Sixteen samples each of nettle, flax and hemp fibre were randomly selected and individually bagged in private as blind samples for analysis. Each sample typically included up to four technical fibres that were selected from fibre collections of each species. Bulk suppliers were not used as errors in selection have been known, Dunbar and Murphy (2009), hence the fibre samples used were harvested locally **Table 10.2**

10.4.4 MFA sample preparation and procedure

Following Petrco and Kubic (2004), samples of fibre, circa 2mm length, were cut with a scalpel. These were separated by hand, mounted on a slide in distilled water under a glass coverslip, then sealed with clear lacquer.

Samples were viewed in transmitted light under a Nikon Optiphot compound microscope, with cross-polarized lighting and a full-wave plate when necessary to enhance contrast. The MFA for each fibre was determined from the angle of variance measured twice, first, by direct angular variations indicated on the rotating stage scale and secondly, using Olympus AnalySIS software to measure the enclosed angle. The mean of these two angular measurements was used as the determinant value for classification purposes and the results are shown in **Figure 10.1** and **Table 10.3**

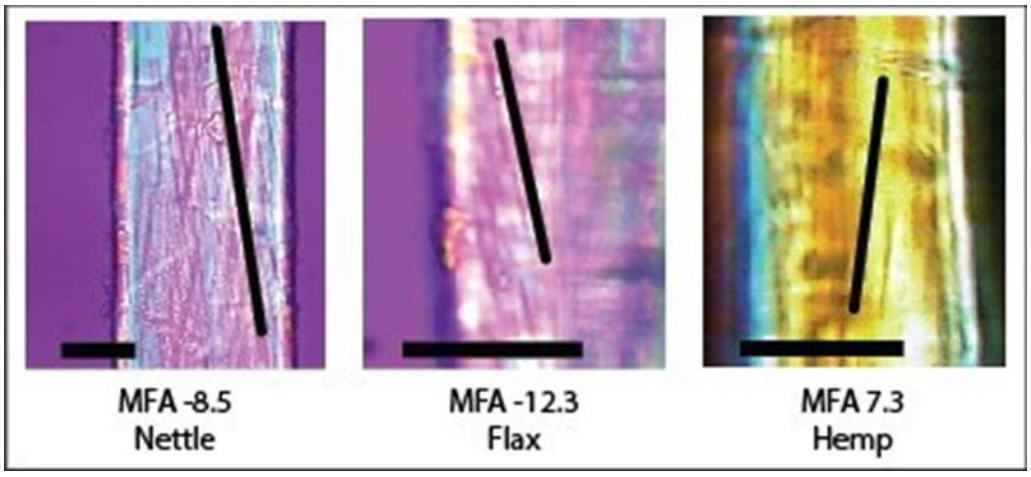

Figure 10.1. Examples of the three different fibres in the study: the measurement of MFA by direct observation, and digital angle measurement. Scale bar represents 25 µm.

When viewing the fibre, it is essential to focus on the anterior surface. With translucent fibres, the posterior view is also visible, and microfibre angles are therefore displayed in the opposite angle **Figure 10.2.**

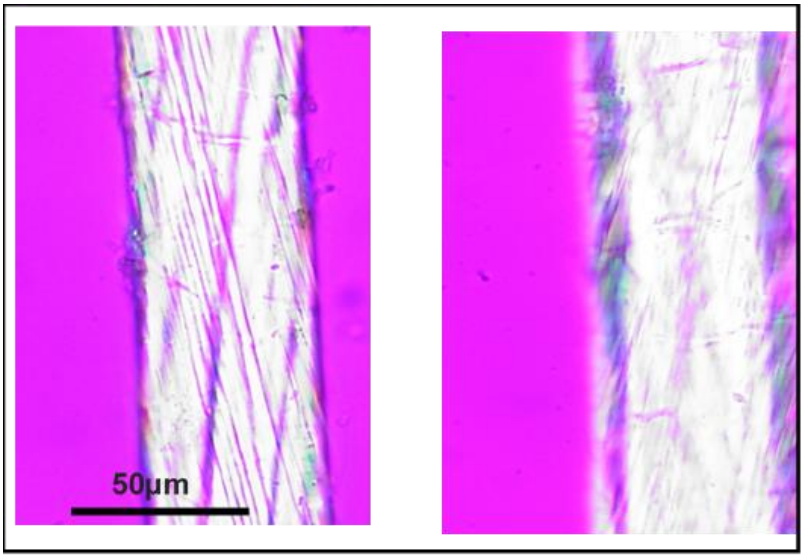

Figure 10.2. MFA displayed by BT 18 a nettle fibre. Left, the anterior view Right, the posterior view.

It is well established that the fibre's angular orientation within the stems of nettle and flax have a twist that is opposite to that of hemp. As a result, the measurement, and notation of a positive or negative angle, is usually considered a robust feature for distinguishing hemp from nettle/flax **Figure 10.3.**

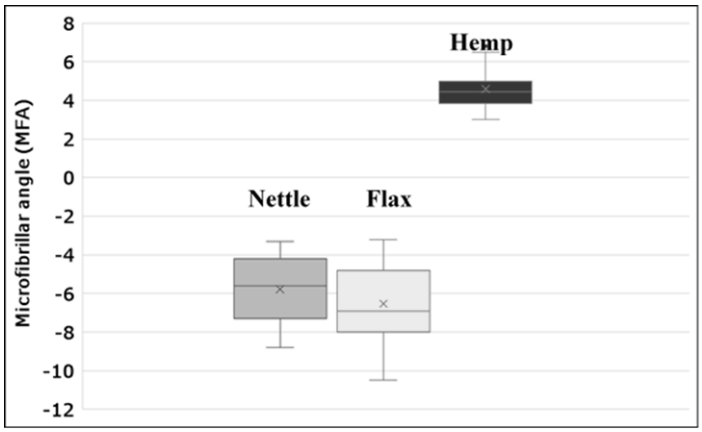

Figure 10.3. Box and whisker comparison of MFA for the three fibre species. (Previously noted reported **Figure 7.15**).

10.4.5 Cross-sectional circularity (Ct) sample preparation and procedure

A scalpel was used to cut 25mm lengths of each technical fibre, circa 15-25*µm* diameter. These were centralised vertically within a 6mm diameter mounting tube which was sealed at the lower end. The fibre was mounted and EpoFix (Struers (UK) Ltd. 2016) low viscosity epoxy resin was used to fill the tube and left to set. Following overnight curing, the moulded sections were end prepared and polished prior to microtome cutting of 1mm thick CSA samples suitable for microscope imaging. The CSA samples were mounted on glass slides with Eukitt mounting medium. A Nikon Optiphot compound microscope with BD Plan 40x 0.65NA objective lens was used to image each technical fibre bundles cross-sections in reflected light **Figure 10.4** and plotted in

Figure 10 5.

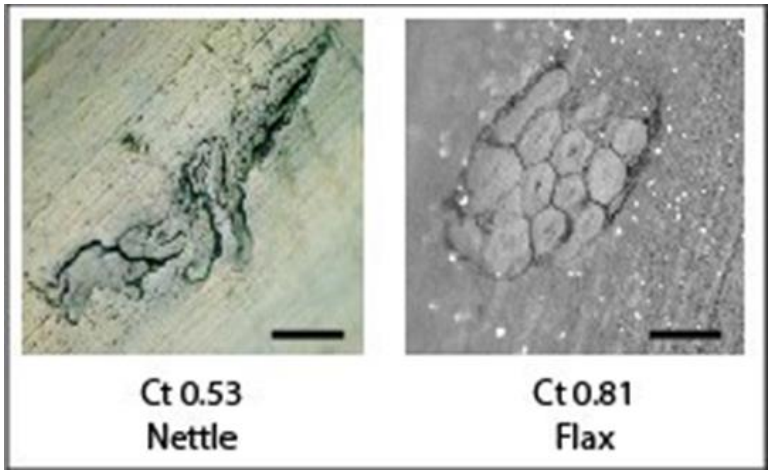

Figure 10.4. Examples of Nettle and Flax fibres differences in cross-sectional appearance and Ct measurement. **Scale bar is 25µm.**

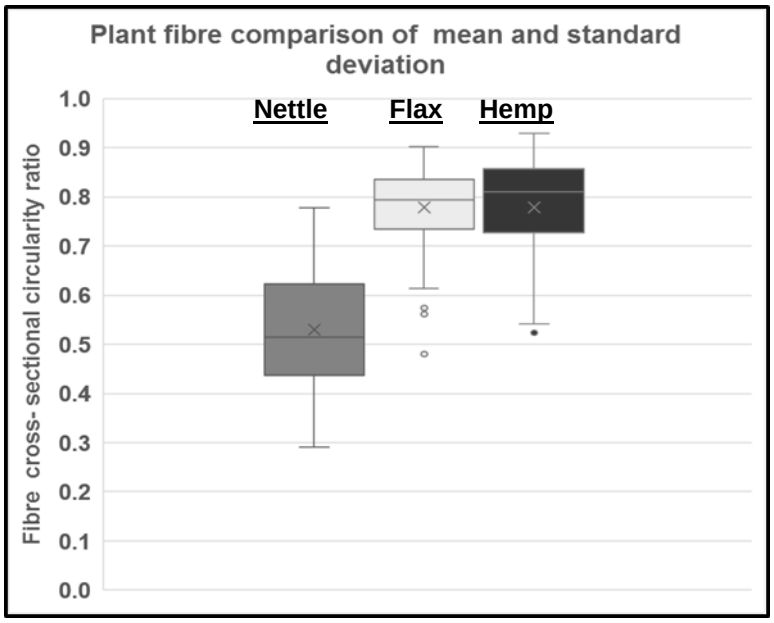

Figure 10.5. Database established for CSA Circularity **(See Figure 8.14)** The multi-fibre CSA images were evaluated using ImageJ software (Rasband 2016).

The groups of individual fibre cross-sectional outlines were manually traced within the image on the screen; the programme analysis displays and edits the image formats to calculate area, circularity, and shape ratios.

Six representative individual fibre images were selected from each grouped image. The samples were subsequently analysed in ImageJ software to record the circularity (Ct) ratios. A database of the measured fibre circularity for the 48 blind test samples is included in **Table 10.3** and summarised in **Table 10.4.**

	Nettle	Flax	Hemp	Rejects
Total samples	16	16	16	
Analysed for MFA	47			1
Grouping Based on MFA	29		18	
Analysed for Ct	27		n/a	2
Grouping based on MFA and Ct	11	16	18	
Number correctly identified	7	10	13	
Total accuracy	43.8%	62.5%	81.3%	62.5%
Accuracy without rejects	50.0%	66.7%	81.3%	66.7%

Table 10.3. Summary of blind test results and accuracy of diagnosis.

10.4.6 Statistical evaluation of MFA and Ct

Fibres are assigned to either flax or nettle on based on Ct value. If the Ct value is less than 0.696, it is determined to be nettle while, if it is larger than this value, it was determined to be flax. A Ct of 0.696 is selected as an appropriate cut-off value to separate Nettle from Flax. 88% of nettle samples fall below this value, while 80% of flax samples fall below. 95% of nettle samples have a Ct lower than 0.75 and, 95% of flax have a Ct above 0.65. Research presented here formalises shape analysis using a method of measuring circularity (defined as the ratio between the area and circumference of the fibre). To use Ct as the determinant criterion, the cross-sectional circularity of fibres from samples collected during the research programme was re-evaluated and the Ct was measured so the data could be used to propose a cut-off value.

Figure 8.14 and Tables 8.5a and 8.5b show the results of measuring the Ct of 230 samples of modern reference material. The ANOVA statistical test found a significant difference between the grouped samples (F=144.15, df=229, p**=>3.9E-41). For n=230, nettle (n=60), flax (n=126), hemp (n=44). The statistical difference results from the circularity of nettle being lower than that of flax and hemp. This data corroborates that of Suomela *et al.* (2018) in that the lower Ct reflects a more oval form relative to flax and hemp.

10.4.7 Results

All blind test results are included **Table 10.3** to summarise the Ct and MFA and the diagnostic outcomes for the 48 samples.

The overall accuracy of the two-step procedure is measured at 62.5%. Excluding results from specimens, that would not usually be studied due to faulty sample preparation producing inferior images, accuracy is reported at 66.7%. Accuracy for the individual species is 81.3% for hemp, 50.0% for nettle, and 66.7% for flax.

Following sample preparation, one sample (retrospectively identified as flax) was considered unsuitable for MFA analysis due to an inadequate image. MFA was measured on the remaining 47 slides and this feature was used to separate hemp (H) from flax/nettle (FN). Eighteen samples were identified as hemp due to a positive MFA twist angle. Only 13 of these were actually hemp, indicating that in these tests MFA, as a standalone approach, has accuracy in differentiating hemp from nettle and flax at 72%.

The 29 fibres identified as having a negative MFA, and thus likely to be flax or nettle, were subjected to the second stage of analysis.

Cross-sectional fibre circularity (Ct) was measured for each sample **Table 10.4 (a-d)** and used here to differentiate flax from nettle. Two of the samples (both retrospectively identified as nettle) could not be studied by this method. Samples were identified as nettle if their Ct was less than 0.696 and hemp if Ct was above this value. On this basis, 11 samples were diagnosed as nettle and 16 as flax. Seven of the 11 nettle samples were correctly classified to the nettle group and 10 of the 16 flax samples were correctly identified to the flax group.

The overall success rate for identification was 66.7% but this varied between the species. The results show differences in the efficacy of the methods. MFA distinguished between hemp and flax/nettle in the first stage, with 81.3% of the hemp samples being successfully identified. Twenty-seven samples proceeded to Stage 2 and were classified using Ct analysis after which, 66.7%% of all flax and 50.0% of all nettle samples were identified successfully. The results suggest that some evidence for the use of wild nettles may have been under-represented in archaeological reports. The 66.7% overall accuracy achieved in the blind test provides the first quantitative data illustrating the capability of two frequently used methods for differentiating between three common bast fibres. The result is 62.5% if only the samples that could be studied are included in the calculations. In the application those fibres may be replaced by a further fibre from the archaeological material

Table 4 (a-d) tabulates the MFA and Ct data determine and are summarised in **Table 4.5.**

Sample No.	Stage angle measurement start angle	Stage angle measurement finish angle	Stage Angle MFA	MFA as measured Olympus Analysis software	Average MFA	Identification based on MFA	Ct	Identification based on Ct	Identification made by blind analyst	Actual Fibre in the sample	Flax	Nettle	Hemp
1	145	139	-5.2	-8.2	-7	flax/nettle	0.7	nettle	nettle	flax	0		
2	117	106	-11	-7	-9	flax/nettle	0.8	flax	flax	flax	1		
3	12.6	5.4	-7.2	-6.8	-7	flax/nettle	0.7	flax	flax	flax	1		
4	80.8	71.9	-8.9	-4.5	-7	flax/nettle	0.6	nettle	nettle	nettle		1	
5	247	255	8	6.4	7.2	hemp	n/a	-	hemp	flax	0		
6	137	131	-5.8	-1.8	-4	flax/nettle	0.6	nettle	nettle	nettle		1	
7	336	345	8.9	8.1	8.5	hemp	n/a	-	hemp	hemp			1
8	332	325	-6.7	-3.4	-5	flax/nettle	0.8	flax	flax	flax	1		
9	57.7	50	-7.7	-7.7	-8	flax/nettle	0.5	nettle	nettle	nettle		1	
10	191	182	-9.3	-4.5	-7	flax/nettle	0.8	flax	flax	nettle		0	
11	29.1	38.6	9.5	9.2	9.4	hemp	n/a	-	hemp	nettle		0	
12	134	150	16.2	16.4	16	hemp	n/a	-	hemp	flax	0		

Table 10.4 (a). Comparison of BT diagnosis based on MFA and Ct compared to actual fibre identity (False=0, True =1).

Sample No.	Stage angle measurement start angle	Stage angle measurement finish angle	Stage Angle MFA	MFA as measured Olympus Analysis software	Average MFA	Identification based on MFA	Ct	Identification based on Ct	Identification made by blind analyst	Actual Fibre in the sample	Flax	Nettle	Hemp
13	275.2	269.5	-5.7	-5.4	5.6	flax/nettle	n/a	-	rejected	nettle		0	
14	32.6	39.9	7.3	8.6	8	hemp	n/a	-	hemp	hemp			1
15	253	248	-5.6	-7.5	-7	flax/nettle	0.7	nettle	nettle	nettle		1	
16	189	194	4.3	5.8	5	hemp	n/a	-	hemp	hemp			1
17	25.3	27.5	2.2	4	3.1	hemp	n/a	-	hemp	hemp			1
18	298	284	-13	-9.7	-12	flax/nettle	0.5	nettle	nettle	nettle		1	
19	241	232	-9.6	-9.4	-10	flax/nettle	0.7	nettle	nettle	nettle		1	
20	349	345	-4	-4.5	-4	flax/nettle	0.7	flax	flax	flax	1		
21	342	348	5.7	8.1	6.9	hemp	n/a	-	hemp	hemp			1
22	264	255	-8.7	-6.4	-8	flax/nettle	0.7	flax	flax	nettle		0	
23	203	211	8.4	5.6	7	hemp	n/a	-	hemp	hemp			1
24	203	208	4.7	9.2	6.9	hemp	n/a	-	hemp	hemp			1

Table 10.4 (b). Comparison of BT diagnosis based on MFA and Ct compared to actual fibre identity (False=0, True =1).

Sample No.	Stage angle measurement start angle	Stage angle measurement finish angle	Stage Angle MFA	MFA as measured Olympus Analysis software	Average MFA	Identification based on MFA	Ct	Identification based on Ct	Identification made by blind analyst	Actual Fibre in the sample	Flax	Nettle	Hemp
25	307	299	-8.3	-6.7	-8	flax/nettle	0.7	flax	flax	nettle		0	
26	312	305	-7.3	-7.3	-7	flax/nettle	0.8	flax	flax	flax	1		
27	n/a	n/a	n/a	-7.9	-8	flax/nettle	0.5	nettle	nettle	nettle		1	
28	26.2	29.7	3.5	4.6	4.1	hemp	n/a	-	hemp	hemp			1
29	324	329	5.3	3.8	4.5	hemp	n/a	-	hemp	flax	0		
30	246	240	-6.2	-4.2	-5	flax/nettle	0.6	nettle	nettle	hemp			0
31	4.6	14	9.4	4.1	6.8	hemp	n/a	-	hemp	nettle		0	
32	197	201	4.4	3.1	3.8	hemp	n/a	-	hemp	hemp			1
33	240	229	-11	-11	-11	flax/nettle	n/a	-	rejected	nettle		0	
34	271	267	-4.5	-3.8	-4	flax/nettle	0.6	nettle	nettle	hemp			0
35	244	235	-8.9	-3.7	-6	flax/nettle	0.7	flax	flax	flax	1		
36	345	341	-4.5	-9.5	-7	flax/nettle	0.7	flax	flax	hemp			0

Table 10.4 (c). Comparison of BT diagnosis based on MFA and Ct compared to actual fibre identity (False=0, True =1).

Sample No.	Stage angle measurement start angle	Stage angle measurement finish angle	Stage Angle MFA	MFA as measured in Olympus Analysis software	Average MFA	Identification based on MFA	Ct	Identification based on Ct	Identification made by blind analyst	Actual Fibre in the sample	Flax	Nettle	Hemp
37	160	153	-7.3	-4.2	-6	flax/nettle	0.8	flax	flax	nettle		0	
38	238	230	-7.9	-6.6	-7	flax/nettle	0.7	flax	flax	flax	1		
39	n/a	n/a	n/a	n/a	n/a	rejected	n/a	-	rejected	flax	0		
40	161	169	7.7	10.6	9.2	hemp	n/a	-	hemp	hemp			1
41	12.2	5.1	-7.1	-7.8	-7	flax/nettle	0.7	nettle	nettle	flax	0		
42	262	273	10.8	5.5	8.2	hemp	n/a	-	hemp	hemp			1
43	137	140	3.2	3.6	3.4	hemp	n/a	-	hemp	hemp			1
44	27.5	20.6	-6.9	-6.5	-7	flax/nettle	0.8	flax	flax	flax	1		
45	66.3	57.9	-8.4	-8.3	-8	flax/nettle	0.8	flax	flax	flax	1		
46	133	127	-6.1	-7.3	-7	flax/nettle	0.7	flax	flax	nettle		0	
47	318	312	-6.2	-6.9	-7	flax/nettle	0.8	flax	flax	flax	1		
48	278	281	3.1	7	5	hemp	n/a	-	hemp	hemp			1

Table 10.4 (d). Comparison of BT diagnosis based on MFA and Ct compared to actual fibre identity (False=0, True =1).

Summary for Table 10.4.(a-d)	Flax	Nettle	Hemp	Total
Number evaluated	16	16	16	48
Number successfully identified	10	7	13	30
Percentage successfully identified	62.5%	43.8%	81.3%	62.5%

Table 10.5. Summary of **Table 10.4.(a-d).** comparison of BT diagnosis.

10.5 Summary

In an applied scenario, the three excluded samples would be described as indeterminate. Deciding not to decide, (Dror and Langeburg 2019) is an important step in this process, where the selection criteria could be described as requiring further research. Considering the results from the plant species included in the test, it is clear that nettle fibres are the most likely to be misidentified (58% of all nettle sample submitted were incorrectly identified) and nettle fibres were the most likely to be rejected as bad samples.

In general, the results presented show that the method has performed relatively well within the test scenario. Random guessing would result in an accuracy of around 33%. The strongest element of the method is Stage 1 MFA analysis. 81% of hemp samples were correctly identified at this stage. A review of the data finds five samples (two nettle and three flax) were misidentified as having a positive MFA value. Revisiting the samples has confirmed that it is not that these samples have a positive MFA, but rather the viewing is complicated, and they were misreadings.

Image quality is one of the typical challenges faced by subjective procedures, and variation is likely to be seen in the MFA measurement, the analyst's experience, and the sample quality.

Beyond a test scenario, there is also the possibility for cognitive bias to influence the determination. It is widely understood that external influence can impact on the analytical capability of a specialist, see Nakhaeizadeh et al. (2014) for an example. Therefore, it is recommended that analysts attempt to shield themselves from external influence before conducting analysis, as recommended by Sevick (2015). Given the high possibility of this type of error, finding a replacement for the MFA procedure outlined here should be a high priority for research.

At stage 2, the results are more quantitative since Ct is determined from the image. To evaluate Ct, the hemp samples that erroneously proceeded to the second step are excluded, since their datapoints add little value in evaluating the Ct analysis quality for separating nettle and flax. In the second stage of analysis, 24 nettle and hemp samples were studied, 17 of which were correctly identified. This result places the accuracy of Ct analysis at 70.8%. Error in diagnosis here is influenced by overlaps in fibre form between the two species.

The presented methodology has caveats that have implications for the use of this method in broader applications. The cut-off value of Ct 0.696 to distinguish flax from nettle is based on a relatively limited dataset. Cross-sectional circularity data and the overlap between flax and nettle may vary much more than has been established to date.

There is a need for a larger reference collection to be evaluated for MFA and Ct in order to refine the criteria used in diagnosing unknown samples. Caveats relate to archaeological preservation and sample processing methods. In selecting samples to be subjected to the blind test, it was decided to concentrate on minimally processed fibres.

Further processing, by combing may have removed the more damaged bast fibres, this would have allowed for easier sample selection and microscopic imaging. However, given that only three samples (6%) could not be studied due to the poor condition of the image, this may not be a substantive issue. More significant is the effect of degradation on the quality of the fibres and therefore the ability to utilise the presented methods.

The outcome in blind-testing determinations is illustrate in **Figure 10.6** where the MFA and Ct results for the flax, nettle and hemp samples are compared with those factors derived in the test reported in **Chapters 7 8 and 9** and plotted in **Figure 9.3.**

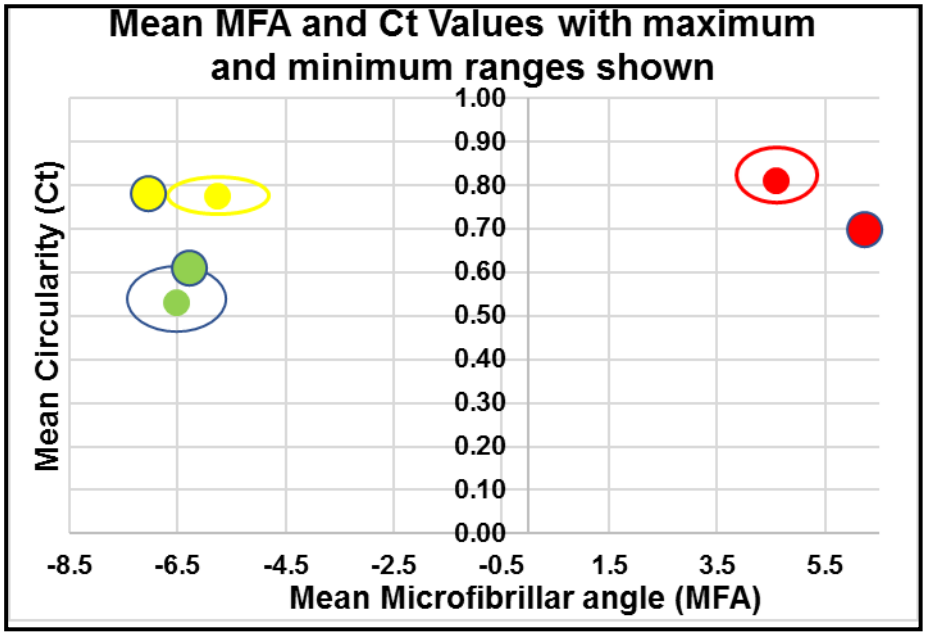

Figure 10.6. Comparison of fibre MFA/Ct**:** the plot (Taken from **Chapter 9**) shows the derived results plotted in **Figure 9.3** within their 95% confidence range defined by the surrounding circles. The determinations of MFA/Ct from the blind test results are included, flax (yellow), nettle (green) and hemp (red) with their data marks outlined.

Note The data base in support of the above is included in Appendix E.

Chapter Eleven
Fibre degradation - accelerated ageing evaluation

11.0 Introduction

The survival of natural plant fibres in archaeological sites is dependent on the burial environment, soil relative humidity, soil pedology and environment, such that organic textile materials deteriorate and only survive in exceptional circumstances. Most plant fibre archaeological finds are associated with waterlogged, frozen or arid conditions with a few from fibres held in direct contact with metal objects. Deterioration is defined as,

> "(T)hose processes which individually or in combination, result in changes to the properties of an artefact material or structure, thereby reducing their ability to perform any of their intended functions, or which serve to destroy, obscure, or confuse original intrinsic information" (Krueger 2011: 2036).

11.1. Background

In formulating the degradation study, it is necessary to consider those conditions in which the plant fibres are buried, and how these conditions can be replicated either within the laboratory or on a comparable site. Within the context of the primary research objectives previously discussed, the principal areas of experimental determination were to evaluate the degradation of the diagnostic features of the fibre cell morphology and material strength of samples of modern fibre reference material.

The physical dimensions of fibres and their moisture content, the environmental conditions, including temperature, water content, soils and the reactive nature of the fibre, are major factors affecting biodeterioration (Szostak-Kotowa 2004).

Additionally, Szostak-Kotowa reports on the breakdown of cellulose structure as being dependant on the fibre orientation “Z” or “S” and the microfibrillar angle

> “Moreover, the degree of orientation, the angle at which fibrils are positioned in relation to the long axis of the fibre, affects the biodeterioration process as well. Cellulose fibres of a high degree of orientation are less susceptible to microbial attack” *(*Szostak-Kotowa 2004: 166).

Kronkright (1990), advised that the study of the deterioration of plant material through chemical, physical, mechanical or biological activity is problematic and notes,

> “Plant materials in artefacts afford us none of the luxuries of isolation, homogeneity, or control. They are incredibly variable, even within a stem or leaf. Natural materials are formed under the influence of daily changes in the environment and reflect those changes in the organization of their structures” (Kronkright 1990: 139).

11.2 The degradation process

In the appraisal of plant fibre degradation, there are two principal aspects to consider, the microbiological and fungal processes driving the degradation and the resulting changes in morphological and material properties. Consideration of the fungal activity has been determined in terms of fungal biodegradability of cellulose content as measured by the loss of organic material and determined by the change in the weight of samples following ashing at 600ºC. (Lopez al 2006).

Archaeological textiles found in burial sites undergo the additional degradation factors associated with the decomposition of the human or animal remains or accompanying metal artefacts (Janaway 1987; Harris 2015; Higgitt 2011; Jones et al. 2011; Harris 2016). In extended time trials conducted on test burials of clothed pig carcasses from three sites in Ontario Canada, it was demonstrated that natural textile, held in contact with a buried decomposing body, would be preserved for longer periods of time when compared to the same textile buried directly in the soil. Additionally, the authors recorded minimal variation between the silty clay loam, fine sand and fine sandy loam soils (Lowe et al. 2013).

There are other factors which affect the rate of decomposition in a funerary context including the depth of burial, climatic conditions, physical conditions of the soil (texture, pH, and moisture), and the method of burial (clothing, wrappings, and metal inclusion). Clothing is often studied as a factor that can slow the rate of soft tissue decomposition. In contrast, the effect of soft tissue decomposition on the rate of textile degradation is usually reported anecdotally rather than being studied under controlled conditions. Many studies in this area have focused on the degradation of textiles buried directly in soil (Janaway 1987: 381; Kronkright 1990: 139; Peacock 1996: 35-47).

An investigation of the effect of soil texture, on the degradation and preservation of textile materials associated with buried bodies of a clothed pig (*Sus scrofa domesticus*) buried on three sites, in pasture, moorland, and deciduous woodland, were undertaken by the University of Bradford. In these trials, soil conditions were noted as having a marked effect upon soft tissue modifying the burial environment and impacting upon associated death-scene materials (Wilson et al. 2007).

Degradation of clothing contained within the burial environment is described by Janaway (2001: Table 20.5) who recorded the change in shape and weight of linen samples and the loss of tensile strength. In consideration of the water-logged effect on archaeological textiles, as determined by morphological changes, chemical analysis and tensile testing, it is reported that cellulose fabrics such as linen and cotton were less resistant to biodegradation than protein-based fabrics such as wool and silk (Peacock 1996).

In a five-year programme of research, trialled at Biskupin (Poland) to determine chemical and structural changes and mechanism of cellulose degradation in the natural environments, the authors compared the degradation of cellulose pulp, submerged in lake water, (pH 6.94-877), and peat (pH 7-8), the peat soil was found to be more conducive than lake water to the preservation of carbohydrates. The natural ageing in these two different burial conditions was evaluated to confirm the mechanism of cellulose degradation (Tamburini et al. 2017).

Research undertaken at the Chemnitz University of Technology (Germany) submitted flax and hemp fibres to a thermogravimetric analysis to note a decrease in the fibre's thermal stability and an increase in decomposition and degradation for temperatures above 160º C. (Wielage et al. 1999). These findings indicate that temperature would be a major limiting factor in the experimental design for accelerating of age degradation. The biodegradation of archaeological textiles in water degrading soil, loam (pH 6.5, moisture content 31%), and peat (pH 3.65, moisture content 75%) was investigated through the immersion of modern undyed natural fibre textile fabrics over a 34weeks (Peacock 1996)

Both Janaway (2002), and Peacock (1996), report the rapid degradation of linen and cotton in loam soil with total decomposition by the eighth week while silk and wool remained intact. Again, in peat soil linen and cotton were almost entirely decomposed by week 34, but silk and wool were still intact.

However, in agreement with Peacock (1996) and in consideration of the water-degraded archaeological textiles, this research programme is not constructed to consider microorganism or enzyme activities as such biodegradation is beyond the scope of this study.

Consequently, the principal degradation variables to be evaluated in this study are,

- **Physical properties** -The changes to the material properties of the fibre tensile strength and elasticity.
- **Changes in fibre CSA morphology** – Changes in fibre shape as evidenced by shrinkage or elongation of the fibre CSA and variations in microfibrillar angle.
- **Mechanical deformation -** Observation of fibre destruction, breakage and evidence of microbiological infestation or fungal growth.

11.3 General degradation procedure

As the reference plant fibre material is intended to replicate archaeological materials, the research initially considered the degradation of single fibre samples. While this evaluation concentrated on fibre degradation, the degradation presented indicates that additional tests on archaeological woven fabric should be considered. This facet is beyond the scope of this current study but could benefit from future consideration.

Soil burial is the preferred matrix, a procedure described in British Standard (BS) 6085:(1992:3) as “most severe” with the incubation temperature and moisture content specified as 28 ± 1ºC. and 25 ± 5% respectively and a pH level of 5.5 to 7. Recommendations regarding container size, burial depth, exposure time, post-extraction cleaning and storage are also included. In general terms, it was necessary to consider those conditions in which the plant fibre would be buried, and how we could replicate these either within the laboratory or on a comparable site. While the experimental design reflects the criteria described above, it is recognised that textile and fibre archaeological assemblages only survive in exceptionally rare environments.

A review of the uncertain diagnostic archaeological assemblages listed, **Chapter Three; Table 3.4,** gives guidance to those depositional environments that provide a degree of preservation to plant fibre remains. With the exception of the associated metallic finds, a large proportion of burial environments can be replicated in the following three proposed depositional soils for each period.

1) Peat-high relative humidity (RH 45%, pH3-4.5.

2) Loam-organically rich (RH 25%, pH 7-8.

3) Dry sand-arid (RH 5%, pH6-7) with the inclusion of an additional submerged water test for fibres in both peat and loam soils.

Fibres preserved in association with metallic artefacts, the largest assemblage, were included in an experimental programme to evaluate the formation of pseudomorphs formations that retain some of the fibre’s diagnostic features of through crystallised substitution of the original fibre morphology.

Janaway (1987), in an experimental “graveyard” deposition, evaluated the degradation of four textile samples; wool with copper; wool with iron; linen with copper; and linen with iron, to investigate the preservation of organic materials associated with metal objects. Regular exhumations were undertaken up to 226 days to evaluate the rate of deposition corrosion and degradation of the textiles. It was reported that iron corrosion deposition was more advanced than copper, and that linen was more susceptible to decay than wool in acidic conditions.

Evaluating three different textile fabrics from an Anglo-Saxon burial at Orsett UK, no actual fibres were preserved as they had been replaced by contact with metal oxides. However, there was enough pseudomorphic evidence to determine the spinning twist, “S” or “Z” and the weave pattern (Crowfoot 1985)

11.4 Method

A selection of the three modern reference fibres, nettle, flax, and hemp was sourced from various locations to reflect a variety of environmental conditions. Random fibre samples were extracted from these bulk supplies as identified in **Table 11.1** to provide ten single fibre selections for each of the four proposed degradation environments, with an additional ten single fibres selected and stored at normal laboratory conditions, (15-25ºC. RH 45% 75%), to act as “control specimens” for comparative tensile and fibre morphological evaluation.

A self-contained temperature and humidity data logger, “Tinytag Plus 2” (Gemini Data Loggers 2019), was installed to record laboratory temperature and humidity over the duration of the degradation period **Figure 11.1** summarises the data logger results.

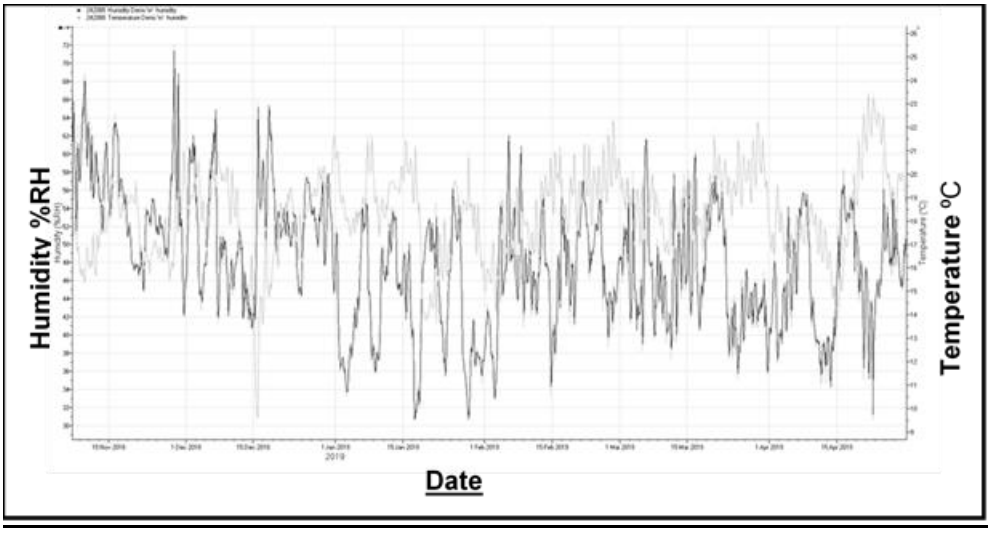

Figure 11.1. Laboratory temperature and relative humidity over the duration of the degradation test.

Ref.	Fibre	Description
NWO	Nettle (*Urtica dioica* L.)	Wild harvest (open woodland)
NWC	Nettle (*Urtica dioica* L.)	Wild harvest (closed woodland)
NU	Nettle (*Urtica dioica* L.)	Testbed planting
FW	Flax (*Linum usitatissimum* L.) v. Winterlyn	Commercial crop
FE	Flax (*Linum usitatissimum* L.) v. Eden	Commercial crop
FM	Flax (*Linum usitatissimum* L.) v. Marylyn	Testbed planting
HS	Hemp (*Cannabis sativa* L.) v. Santhica	Commercial crop
HC	Hemp (*Cannabis sativa* L.) v. n/a	Commercial crop

Table 11.1. List of varieties of fibre selection and cultivation environment.

11.4.1 Soil types

Soils are defined within British Standard (BS) 1377-1(2016) as an assemblage of discrete particles in the form of a deposit and are further sub-divided into cohesive, fine grain water-absorbing soils, and cohesionless granular soils such as gravel or sand. Each of these classes is grouped further into fine, medium or coarse-grained as determined by the percentage retention of soil particles remaining within decreasing sieve sizes. The Standard also includes general information relating to the tests, including common calibration and specification requirements, and general conditions for testing laboratories.

The deposition soils, **Table 11.2** were selected in accordance with BS 6085:(1992 Section 2.7: 2.1 Notes1 and 2) that propose the use of various types of soil including garden and natural fertile topsoil, compost and greenhouse potting soils

Soil type	pH	Moisture Content	Temp. ºC.
Peat	3-4.5	45%	40
Loam soil	7-8	25%	40
Dry sand	6-7	5%	40

Table 11.2. Selected soils. Moisture content and pH levels are shown. The burial temperature is determined as detailed below (**Section 11.4.5**).

11.4.2 Soil conditioning

Medium-grained soils were selected for the test. These soils are defined in British Standards (BS 1051-1 1981; BS 1377-1 2016).

- 1. Soils containing more than 10% retained on a 2 mm test sieve but not more than 10% retained on a 20 mm test sieve" (BS 1377-1. 2016:13).

- 2. Soil tests with medium-grained soils require a minimum sample mass of 500g. The soil dry weight was determined by heating in an electric oven, drying at 105º- 110º C. ± 0.05% down to constant weight, as measured at 15-minute intervals (BS 1051-1 1981).
- 3. Soil samples were subsequently adjusted to meet the designed test conditions, dry sand (pH7 moisture content 15%), loam (pH 7-8 moisture content 75%), and peat (pH 3.5 -4.0, moisture content 45%).

11.4.3 Sample mounting

The sample mounting is based on BS 1377-1 (2016) recommendations iwith modification for depositional environments and designed to avoid contamination from the mounting medium adhesive or supporting material **Figure 11.2.**

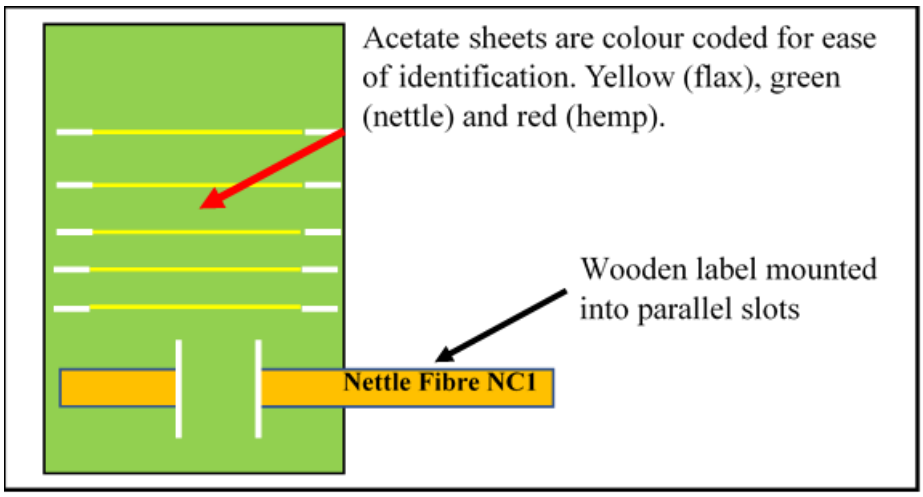

Figure 11.2. Carrier mounting and labelling of fibre samples**.** Numbered fibre samples mounted into slots cut into the acetate sheet carrier (no adhesive used).

Samples of fibres of various lengths were drawn at random from the bulk supplies of the plant fibre listed in **Table 11.2.**

Ten samples of each fibre were fixed to the plastic mounting for ease of recovery and placed on top of the first soil fill (15mm). A further layer of soil was added to provide an additional 30 mm of cover. Assemblages for each of the eight fibre types listed in **Table 11.2**, were subject to soil immersion tests in the three soil types, two submerged water tests in two soils types and one control assemblage held at laboratory atmospheric conditions.

Each container held eight mounted fibre samples labelled by burial period 12, 24 and 40 weeks requiring nine storage containers plus two submerged deposition, eleven containers of eight samples each. The containers were held at 40ºC. in a temperature-controlled heating cabinet for up to 40 weeks.

Additionally, ten samples of each fibre were stored at laboratory temperature and humidity levels. Following sample immersion, the polypropylene storage soil containers were fitted with lids to avoid moisture loss, labelled, and placed in a temperature-controlled electrically heated oven for the duration of the test of 12-40 weeks. The untreated samples were stored at standard laboratory conditions (BS 1051 1981), as shown in **Figure 11.1.**

11.4.4 Soil containers

BS 6085-(1992:7.1.1) recommend containers of glass or plastic of sufficient size to hold soil and specimens at the specified depth (45 mm to 65 mm) with a loose-fitting lid. However, as various levels of moisture content were to be maintained, sealed tight-fitting lids were added. A layer of soil was placed in the container to a minimum depth of 15 mm. and 30-50 mm of soil added above the samples. The electric oven was set to 40ºC., and a descriptive label attached to the oven time and temperature profiles recorded.

11.4.5 Burial temperature - accelerated ageing

Accelerated ageing experiments subject materials to aggravated conditions of heat, humidity, oxygen, sunlight, and vibration, to speed up the normal ageing processes and assist in the evaluation of long-term effects over shorter periods.

Temperature acceleration was included to ensure that the investigations would replicate an extended period as represented in the maintenance of embedded soil temperature. These acceleration rates were considered in the simulation of natural ageing of canvas paintings by evaluating the acceleration rate as determined under Arrhenius Law (2017) in a modified and tabulated format (Seves et al. 2000). In evaluating the degradation of these paint canvas, Seves (2000) offers a variation of the equation to determine the equivalent years of temperature ageing acceleration factor at temperatures higher than 25°C., **Table 11.3.**

Time length (TL) of thermal treatment (h)	Corresponding years of thermal ageing
93	42
144	65
357	160
528	237
700	315

Table 11.3. Ageing protocol**.** Times necessary for simulating 42-315year thermal ageing of paint canvas at 105 deg. C. (94kj/mol Activation energy) (Seves et al. 2000: 316 Table 1).

Wielage et al. (1999) determined the onset of thermal degradation of fibres at 160º C., humidity and ground conditions of acidity and alkalinity of natural soils were also noted as contributory factors. Consideration of the onset of degradation at 160ºC. and comparison with the temperatures shown in **Table 11.3,** plus concerns regarding water evaporation at higher temperatures, limits

the immersion temperature. The acceleration factor for a range of temperatures and their associated Acceleration Rate was determined by the Arrhenius Equation and are shown in **Figure 11.3.** and **Table 11.4.** In reflecting the above, the following degradation conditions were proposed. Furnace temperature to be employed was 40ºC. ± 2°C. with the moisture content recorded on a dried mass basis (BS 6085-1992:3 Note 2).

The Arrhenius formula for calculation of accelerated reaction factor $k=Ae^{(-Ea/RT)}$

Where T = Temperature (Kº)
E_A= Activation energy (joules/mol.) (50kj/mol.
(Rantuch and Balog 2014)
R = Gas constant 8.31j/kmol
e = Natural log base
A = Frequency factor (constant at low temperature)
k= Rate factor

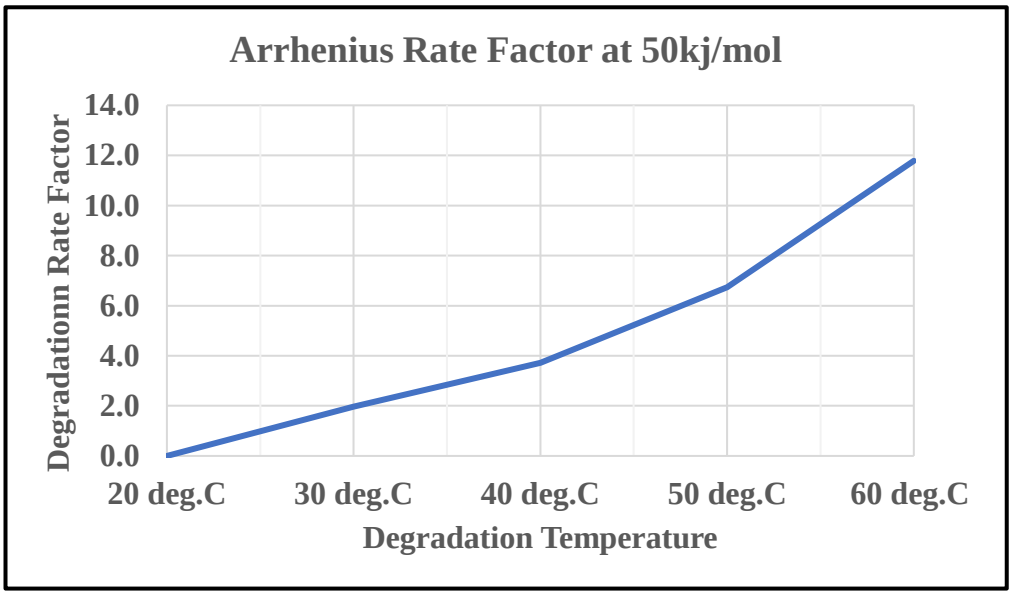

Figure 11.3. Degradation acceleration**.** Equivalent deposition rate factor for accelerated temperatures based on calculated temperature rate factors. (Acceleration factor 50kj/mol).

Weeks	30º C. (303 deg. K)	40º C. (313 deg. K)	50º C. (323 deg. K)	60º C. (333 deg. K)
Factor	**1.97**	**3.71**	**6.73**	**11.78**
12	24	45	81	141
24	47	89	162	283
36	71	134	242	424
40	79	149	269	471

Table 11.4. Arrhenius equivalent degradation periods in weeks for various acceleration temperatures**.** (Acceleration factor 50kj/mol).

11.4.6 Post-deposition treatment

At the end of each ageing process at 12, 24, 36 and 40 weeks, the samples were removed from the containers using two steel spatulas, to avoid disturbing the other samples, brushed and rinsed in water. Care was required to avoid damage to the potentially fragile specimens. The samples were dried at room temperature before submission for post-depositional analysis (BS 6085 1992:4).

11.4.7 Evaluation of fibre degradation

Evidence of fibre degradation was recorded for the three diagnostic features as detailed in section **11.2** above.

1) Physical properties

The changes in fibre physical properties, including tensile strength, strain and elasticity were determined by subjection to Mach 1 Biomomentum mechanical testing as detailed below.

2) Changes in fibre morphology, MFA evaluation and Circularity (Ct) measurements

Fibre CSA shape including changes in central lumen dimensions and Ct were recorded by ImageJ analysis of CSA sections and a database established (Rasband 2016).

3) Mechanical deformation or destruction of the fibre

The degraded fibres were observed visually and by microscopic examination for evidence of microbiological infestation or fungal growth. Breakages and increases in fibre deformation and ruptures were recorded.

11.4.8 Fibre - degradation of physical properties

As previously reported in **Chapter Six** the evaluation of Young's Modulus (*E)* resulted in a range of moduli values attributed to the modern reference materials of nettle, flax and hemp with variations presented by individual fibres within each type (See St. Dev. as attributed **Table 6)**. This variation in (E) may be attributable to the accumulative physical processing in fibre preparation such as to diminish its diagnostic features. However, as an indication of the loss of tensile strength attributable to the degradation process, the measurement of (E) serves to provide a general comparative measure within the confines of this experimental replication. **Chapter 6, Section 6.6.1** provides a summary of the method applied to fibre tensile testing with the Biomomentum Mach 1 mechanical testing equipment **Figure 11.4.** The (E) value for the surviving degraded fibres were evaluated similarly.

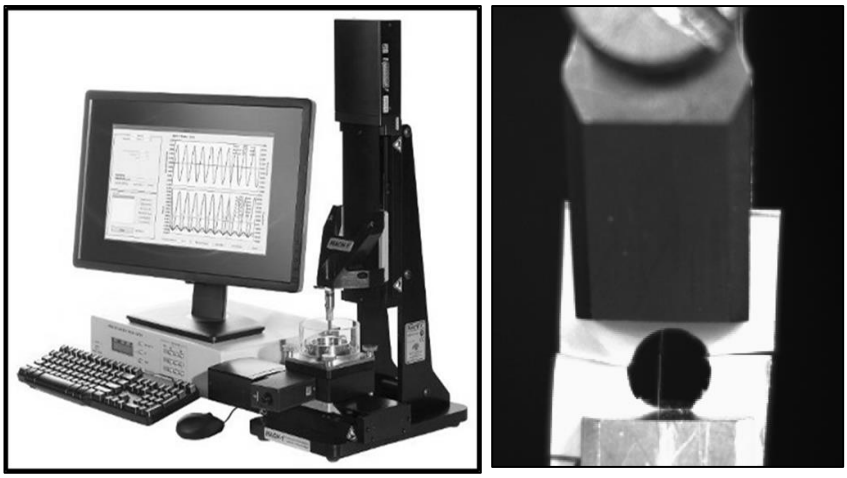

Figure 11.4. Biomomentum Mach-1TM Mechanical testing equipment. With camera mounting showing clamping arrangement. Card mounting details are shown right.

11.5 Fibre degradation - CSA geometric morphology (Shape analysis)

Plant fibre shape, material properties, and microscopic imagery have been used extensively to determine the genus of unknown plant material. Fibre dimension, fibre terminal shape, and fibre density are considered as diagnostic features (Catling and Grayson 1982; Ryder 1999; Bodros and Baley 2008; Horne et al. 2008). However, these dimensional features do not demonstrate a reliable diagnostic differential as dimensions vary within individual fibres and along the fibre length. Non-dimensional ratios such as lumen area/CSA and Circularity (Ct) offer comparative non-dimensional ratios for statistical comparison.

Identifying nettle, flax, and hemp plants in their natural growing environment, leaf and stem shapes, and flower colour and shape are distinct and recognisable diagnostic features. The research programme hypothesised that, while recognising that fibre dimension, even within each genus, varies considerably, fibre cross-sectional areas (CSA) may be compared statistically through evaluation of “Circularity” the ratio of area to perimeter.

(**Circularity = 4π x area/periphery^2**).

To appraise the deterioration due to degradation, fibre samples, circa 5-10μm diameter, were centralised vertically in a 6 mm diameter mountant moulding with an epoxy resin “Expo-Fix” (Sigma-Aldrich 2016).

The epoxy resin mounted samples were end-surface polished and sectioned into 1mm slices for viewing and imaging under polarised microscopy at 400x magnification. The Ct of the microfibrillar CSA was determined with ImageJ software (Rasband 2016).

11.5.1 Fibre - mechanical deformation

Plant fibre materials are subjected to a range of environmental conditions harvesting and production processes that modify the fibre’s characteristics as required by the end-use criteria. The growth conditions, processing and end-use, coupled with a lifetime utilisation serves to generate a complexity of deterioration mechanisms affecting fibre degradation determination (Janaway 1987: 381; Kronkright 1990: 139; Peacock 1996: 36).

The mechanical damage arising from the burial environment as shown by the tears, and fractures evident under visual or microscopic examination were determined. **Figure 11.5** shows the deformation marks visible under crossed polarised microscope (CPM) imaging of flax and nettle fibres. These nodal deformation zones are the “weak point” of failure under stress. It is also considered that fibre processing and utilisation, along with burial condition of biological attack from fungi, bacteria and insects will enhance the level of deformation (Baley 2002: 940; Thygesen et al. 2006).

Following post-depositional treatment, fibre samples recovered from the degradation tests were inspected for mechanical and nodal deformation by comparison with **Figure 11.5** and the control samples held at laboratory conditions.

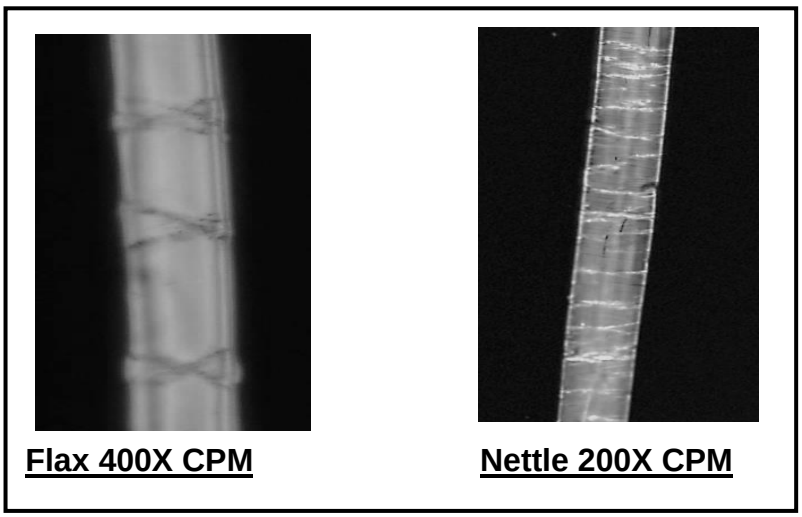

Figure 11.5. Images under cross-polarised light showing nodal deformation. Left. Flax 30µm dia. (400x) cross banding. Right. Nettle 90µm dia. (200x), showing straight striations (Waudby 2014, 60).

11.5.2 Soil sample - particle size and relative humidity

The recommendation from BS 1377-1 (2016) for the soil particle content, organic presence and moisture content prior to burial of degradation material was noted. The soil was subjected to a series of reduced particle diameter sieving 16mm. dia. to 2mm. dia. to determine the percentage retention rate for each particle diameter recorded. For organic presence, soil samples were subjected to an ignition test whereby the samples were placed in a furnace at 440ºC. +/- 25ºC. for 12 hours and the weight loss due to organic combustion recorded. Initial water content was determined by heating the soil sample to 105/110ºC. and reweighing after cooling **Table 11. 5.**

	Total weight	16mm retention	5mm retention	2mm retention	Above2mm retention	Above5mm, below 16mm retention	Organic content	Water content
Peat	33g	nil	6g	12g	36%	19%	5g	5%
Loam	141g	3g	18g	48g	49%	15%	1g	4%
Dry Sand	95g	nil	6g	12g	19%	6%	5g	nil

Table 11.5. Deposition soil properties and water content at the start of the experiment.

11.5.3 Correction of water content

To meet BS 6085 (1992) recommendation regarding moisture content, the water content required adjustment. The weight of water added was calculated as below.

Peat at 45%: Required moisture level and weight of water to add

Peat initial water content	5%
Required water content	45%
Total weight of soil and water	228g
Weight of water held	12g
Required water content	45%
Total weight after addition	T= 228 +0.45T (Hence 0.55T = 228g)
Total weight soil + water	T = 228/0.55 = 414g
Water content	0.45 x 414=186g

As the soil initially contained 5% water, weight to be added =186-12 =174g

A similar calculation for loam to achieve 25% from an initial level of 4% (28g) required the addition of 196g to achieve 25% moisture content. There was no requirement to add water to the dry sand.

11.5.4 Soil acidity measurement

The pH level for each of the eleven deposition soils was checked and adjusted to meet the BS recommendations. Soil pH levels were measured using a Jenway 3510 pH meter **Figure 11.6** calibrated using standard pH solutions at 4pH, 7pH and 9pH.

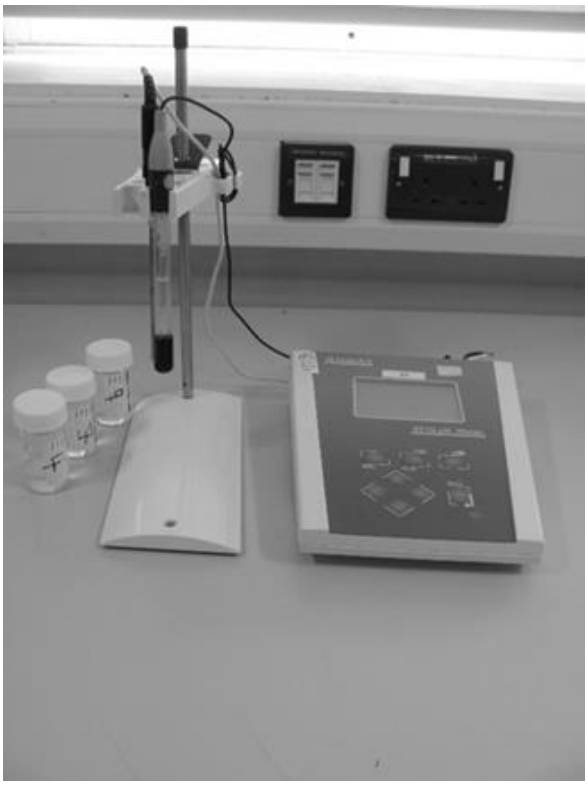

Figure 11.6. Jenway 3510 pH meter. Soil pH level measurement.

The soil types, pH levels, and sample number are listed below **Table 11.6.**

Soil	Period	Test sample	Acidity	No.
Peat	12 weeks	(1g immersed in DH_2O)	pH3.7	1
Peat	24 weeks	(1g immersed in DH_2O)	pH3.1	4
Peat	40 weeks	(1g immersed in DH_2O)	pH 2.7	7
Loam	12 weeks	(1g Deposit in water sample)	pH 5.6	2
Loam	24 weeks	(1g Deposit in water sample)	pH 5.8	5
Loam	40weeks	(1g Deposit in water sample)	pH 5.8	8
Dry sand	12 weeks	(1g immersed in DH_2O)	pH7.3	3
Dry sand	24 weeks	(1g immersed in DH_2O)	pH7.8	6
Dry sand	40 weeks	(1g immersed in DH_2O)	pH7.5	9

Table 11.6. Tabulation for numbered samples, deposition soils, period and pH levels**.** (Note, for operational reasons the end period was adjusted from 36weeks to 40weeks).

The samples were placed in a thermostatically controlled electric oven at 40ºC. and, to exclude any unauthorised adjustments, reserved solely for this experiment.

11.6 Results

At completion of each degradation period, the fibre samples were recovered from the deposition soil and inspected for mechanical and nodal deformation by comparison with **Figure 11.6** and with the controlled samples held under laboratory conditions.

There were four diagnostic features to be assessed to compare the effects of degradation upon the morphology and material properties.

- Surviving fibres were examined for consideration of the deterioration of the fibre as to its suitability for testing.
- Microfibrillar angle (MFA) was measured, and the quality of image presentation and ease of measurement noted.
- Evaluation of fibre area cross-section was undertaken with ImageJ software analysis of the fibre to determine the microfiber non-dimensional circularity.
- The degraded fibre was extracted from the sample containers and subjected to a comparative tensile test for comparison with non-degraded controlled samples.

The Biomomentum stress/strain data was inputted into a database for evaluation and statistical analysis of Youngs modulus "*E*" for the degraded samples **Figure 11.4.**

11.6.1 12week degradation results

The results presented at the end of the initial 12week period (Arrhenius 45week equivalent) are shown in **Table 11.7**

Sample	Flax (v.Winterlyn)	Flax (v.Marilyn)	Flax (v.Eden)	Nettle (Seeded (Uni. Testbed))	Nettle (Wild-Closed Space)	Nettle (Wild-Open ground)	Hemp Commercial (v. unknown)	Hemp Commercial (v.Santhica)	Survival Rate
Peat	N	N	N	N	N	N	N	N	**nil**
Dry sand	Y	Y	N	Y	Y	Y	Y	Y	**88%**
Loam	N	N	N	N	N	N	N	N	**nil**

Table11.7. Survival of samples after 12 weeks of degradation. (Arrhenius equivalent period of 45 weeks).

Fibres from the peat soil degradation were unavailable, there were no surviving samples. Examination of the mounting frame, depositional soil and retained pH level 3.8, failed to explain this anomaly and the rapid degradation, **Table 11.7.** While, for loam soil, there may be a high level of fungal and microbial deterioration with little or no survival, degradation of nettle samples within a peat deposition over such a short period was contradictory to those results reported by other authors (Peacock 1996; Janaway 1987; Janaway 2001; Wilson 2007).

In consequence of the poor results from the 12week peat deposition, it was proposed to initiate a separate 12week degradation test under the same conditions with fibres submerged in peat and dry sand.

Temperature variations from the set point of 40deg.C were recorded and supplemented with regular observations of thermometer readings of oven top and bottom temperatures A review of this secondary degradation exercise is included in **Section 11.9.**

The only failure from the 12week dry sand environment was flax (v. Eden), a commercial oilseed flax plant. However, in view of this poor performance at week 12 and, reflecting the archaeological depositions detailed in **Table 11.1** above, the selected depositions environments were extended to include two addition degradation soils, peat and loam, submerged underwater for 36weeks, and these have been added to the summary, **Table 11.9.**

11.6.2 24week degradation results

After 24weeks deposition (Arrhenius 89week equivalent) the survival rate for peat increased over the poor results obtained at 12 weeks with 63% of the

24week peat samples and 100% of the 24week dry sand available for determination of variation in morphology **Table 11. 8.**

Sample	Flax (v.Winterlyn)	Flax (v.Marylin)	Flax (v.Eden)	Nettle (Uni. Test bed)	Nettle (Wild-Closed Space)	Nettle (Wild-0pen ground)	Hemp Commercial v. unknown)	Hemp Commercial (v.Santhica)	Survival Rate
Peat	Y	Y	Y	Y	N	N	N	Y	**63%**
Dry sand	Y	Y	Y	Y	Y	Y	Y	Y	**100%**
Loam	N	N	N	N	N	N	N	N	**nil**

Table 11.8. Survival of samples after 24week degradation. (Arrhenius equivalent period 89weeks).

11.6.3 36week degradation of submerged fibres results

For the two 36week submerged depositions, it was decided to prepare soils that most closely reflect the archaeological depositions detailed in **Table 11.1.** Dry sand was excluded, and only peat and loam employed as the deposition soil. Notwithstanding the poor survival of the fibres in loam soil at 12weeks and 24weeks, the consideration was that total submergence underwater might serve to reduce the biological and fungal activity. The results did not support this hypothesis as none of the fibre samples within the loam soil survived. For peat samples, 75% survived although there were differences in that some fibres (**FM, NU** and **HS)** provided MFA samples others, (**FE** and **FW)** provided Ct. determinations from six survivors overall (75%) **Table 11.9.**

Sample	Flax (v.Winterlyn)	Flax (v.Marilyn)	Flax (v.Eden)	Nettle (seeds sown in test bed)	Nettle (wild-closed space)	Nettle (wild-open ground)	Hemp Commercial (v. unknown)	Hemp Commercial (Santhica)	Survival Rate
Peat	Y	Y	Y	Y	N	N	Y	Y	**75%**
Loam	N	N	N	N	N	N	N	N	**nil**

Table 11.9. Survival of samples after 36weeks submerged degradation**.** (Arrhenius equivalent period 134weeks).

11.6.4 40week degradation results

At 40weeks, (Arrhenius equivalent period 149 weeks), the degradation within the peat deposition was now total. Hence the only deposition still preserving the fibres was the dry sand (88%) with one fibre Winterlyn, commercial oilseed flax, degraded **Table 11:10.**

Sample	Flax (v.Winterlyn)	Flax (v.Marilyn)	Flax (v.Eden)	Nettle (Sown in test bed)	Nettle (wild-closed space)	Nettle (wild-open ground)	Hemp Commercial (v. unknown)	Hemp Commercial (Santhica)	Survival Rate
Peat	N	N	N	N	N	N	N	N	**nil**
Dry sand	N	Y	Y	Y	Y	Y	Y	Y	**88%**
Loam	N	N	N	N	N	N	N	N	**nil**

Table 11.10. Survival of samples after 40 weeks of degradation. (Arrhenius equivalent period of 149 weeks).

Degradation Soil	Deposition period	Mounting sample No.	pH Level at start	Deposition period weeks	Equivalent weeks (Arrhenius)	pH level at finish	Comments
Peat	12W	1	3.7	12	45	3.6	No fibres remaining
Loam	12W	2	5.6	12	45	5.6	No fibres remaining
Dry sand	12W	3	7.3	12	45	6.1	88% remaining
Peat	24W	4	3.1	24	89	3.1	50% remaining
Loam	24W	5	5.8	24	89	6.9	No fibres remaining
Dry sand	24W	6	7.8	24	89	5.1	100% remaining
Peat	40W	7	2.7	40	149	2.9	No fibres remaining
Loam	40W	8	5.8	40	149	5.7	No fibres remaining
Dry sand	40W	9	7.5	40	149	4.7	88% remaining
Peat	36W Submerged				134		75% remaining
Loam	36W Submerged				134		No fibres remaining
Control		10	Normal temperature and pressure (NTP) 100% remain				

Table 11.11. Summary of surviving fibres for each period. Deposition soils, period and pH levels. (Note. For operation reasons the end period was adjusted from 36 weeks to 40weeks and the additional submerged 36week period added).

The above tabulation details the change in pH level during the deposition period, the percentage survival rate and the calculated equivalent **Table 11.11.**

11.7 Considerations of survival of morphological features MFA and Ct.

The intention in formulating the degradation study of modern natural plant fibre, was to determine the extent to which the diagnostic features, microfibrillar angle (MFA) and fibre circularity (Ct), were affected by their burial environment over time.

The fibre survival rates **Figure 11.7** are compared to the Arrhenius equivalent periods **Table 11.5.**

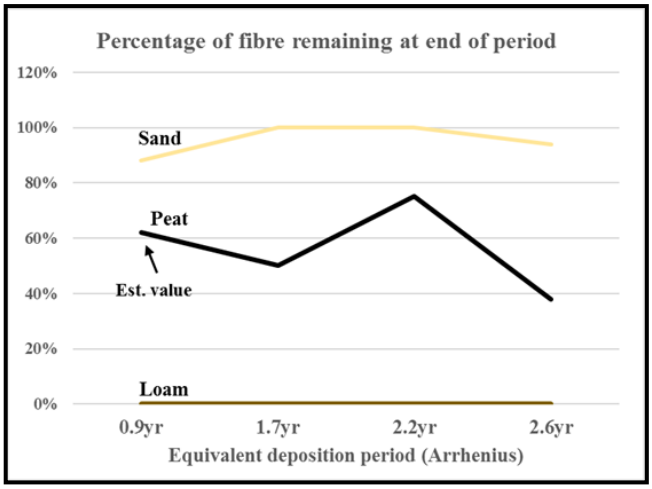

Figure 11.7. Percentage of fibre survivals over time. The peak for peat at 2.2yr results from the underwater submergence of the samples.

Of the three most resilient fibres, two, FM (Flax v. Marilyn) and NU (Nettle Uni.) had been harvested from the University testbed, soaked in the retting station and hand decorticated with minimum combing. The other resilient fibre was HS (Hemp v. Santhica) hand gathered from field cultivation with electro-mechanical decortication and no combing (East Yorkshire Hemp 2018).

11.7.1 Determination of degradation effects on the microfibrillar angle (MFA) of fibres

Surviving fibres were removed from the carrier frames and 2mm fibre l*o*ngitudinal sections mounted in distilled water under a glass cover for evaluation of MFA under crossed polarised light (CPL). Where additional clarity was required a 56nm “Red Shift” lens was introduced and the fibre lengths were examined for evidence of the MFA angular twist of the microfibre (Herzog 1965). evaluation of MFA under crossed polarised light (CPL).

Where additional clarity was required a 56nm “Red Shift” lens was introduced and the fibre lengths were examined for evidence of the MFA angular twist of the microfibre (Herzog 1965). Typical examples of the images presented are shown in **Figure 11.8.**

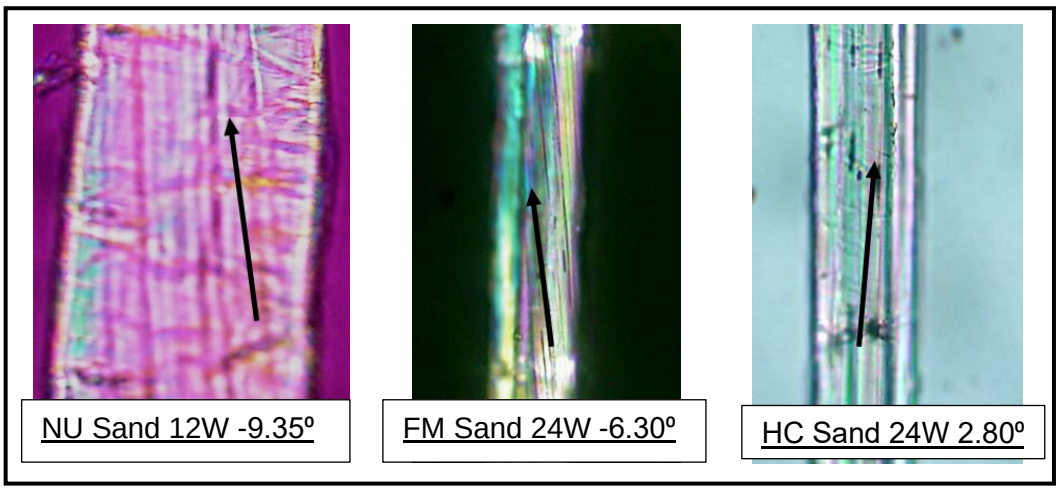

Figure 11.8. MFA**.** All surviving fibres were analysed, and MFA measured for the enclosed angle of microfibre using AnalySIS software. The “S” twist of both nettle and flax fibres at -9.35º and -6.30º are visible, the “Z”twist of the hemp fibre at 2.80º is also partially evident.

From the total of 88 fibre samples, eight types were buried in eleven environments. 48 samples did not survive and, from the remaining 40, seven samples failed to present measurable microfibre images.

Nine samples, from the 33 images assembled, failed to present measurable microfibrillar angles leaving 24 MFA images to compare. The Control Sample (Sample 10) had been mounted into holding frames and stored at normal temperature and pressure (NTP) and the microfibrillar angle measured. Measurements were recorded based on the change in rotational movement required to re-orientate the microfibre into the vertical plane, the rotary stage had an integral Vernier Scale to give accuracy to the measurement. A database of the surviving fibre MFA and Control MFA was assembled **Table 11.12.**

	FE	FM	FW	NU	NWC	NWO	HS	HC
Control MFA	-9.1	-8.0	-6.3	-5.1	-3.3	-3.6	3.4	6.3
12week sand		-6.2		-7.8	-9.4	-3.9		3.4
24week peat			-8.0	-6.3			8.9	
24week sand		-6.3		-6.2	-4.4	-6.0	4.0	2.8
36week peat submerged		-3.4		-8.7			2.2	
40week sand	-6.1	-7.5		-5.4	-8.4	-3.6	4.8	7.5

Table 11.12. Microfibrillar angles MFA. The data is assembled for the Control fibres and fibres from various depositions and periods. (Grey cells show where no measures were possible, black cell depict no survival).

There were no surviving fibres from the loam deposition. **Figure 11.9** and **Figure 11.10** plot the results.

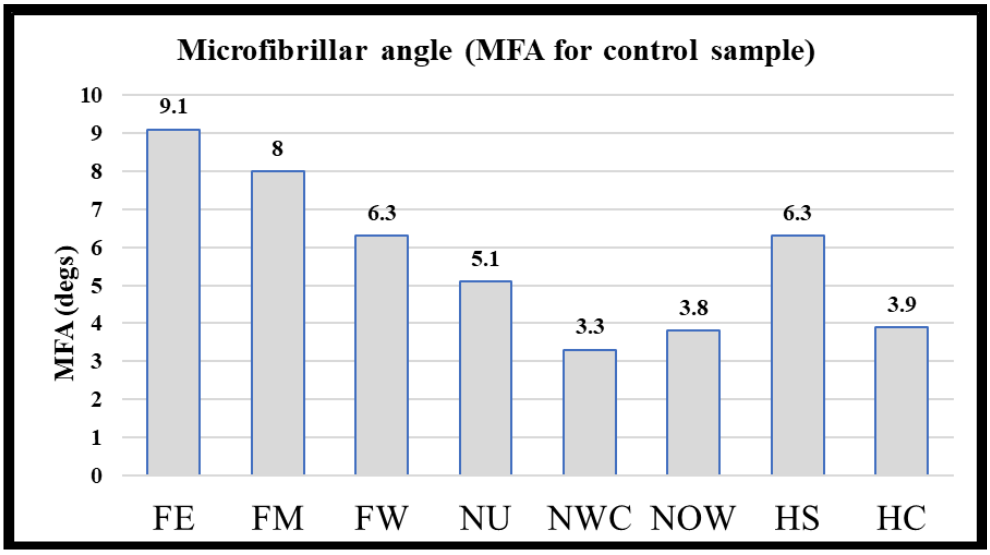

Figure 11.9. MFA of Control fibres. Individual fibre MFA measurements are shown above each fibre type. (For simplicity of display, the +/- angular orientation has been excluded from this representation

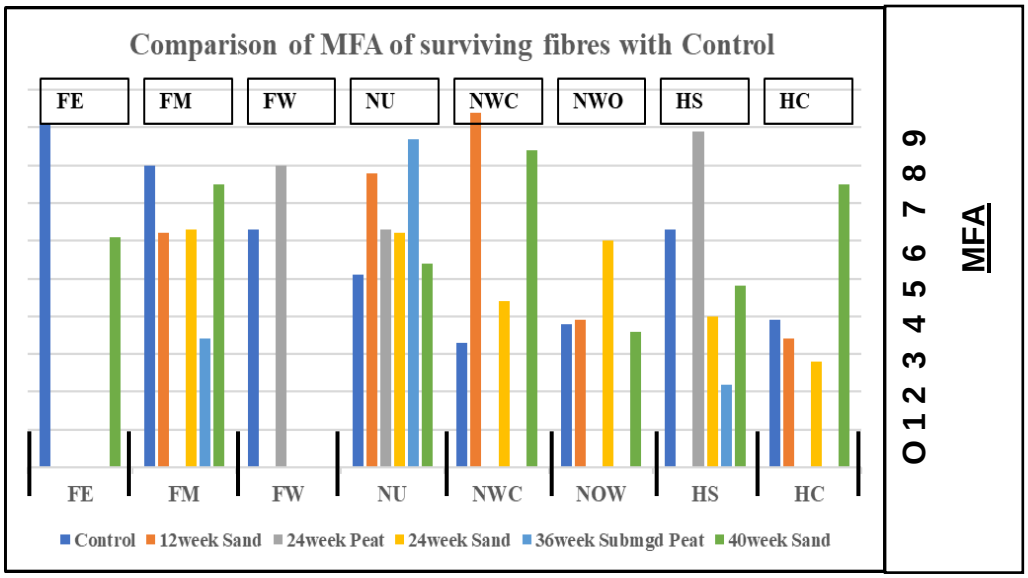

Figure 11.10. Comparison of MFA for surviving fibres against the Control fibre. The MFA for surviving fibres from each deposition soil and period are illustrated above the equivalent fibre species. The data labels depict the full range of samples deposited from 1) Control (blue) to (6) 40week in dry sand (green). The gaps show no result for degraded fibres. (For simplicity of display the +/- orientation has been excluded from this representation).

Images of MFA for surviving individual fibre species were investigated under cross polarised light (CPL) and the microfibrillar angle measured with angular changes determined from the rotary-stage re-orientation and confirmed with AnalySIS software. These are shown below **Figure 11.11a,** and **Figure 11.11b**. Close examination shows the range of image quality presented by these degraded fibres. Of the three most resilient surviving fibres two, FM (Flax v. Marilyn) and NU (Nettle Uni.) were both collected from the University testbed, soaked in the retting station and hand decorticated with minimal combing. The other resilient fibre was HS (Hemp v.Santhica), hand-gathered from field cultivation with electro-mechanical decortication and no combing

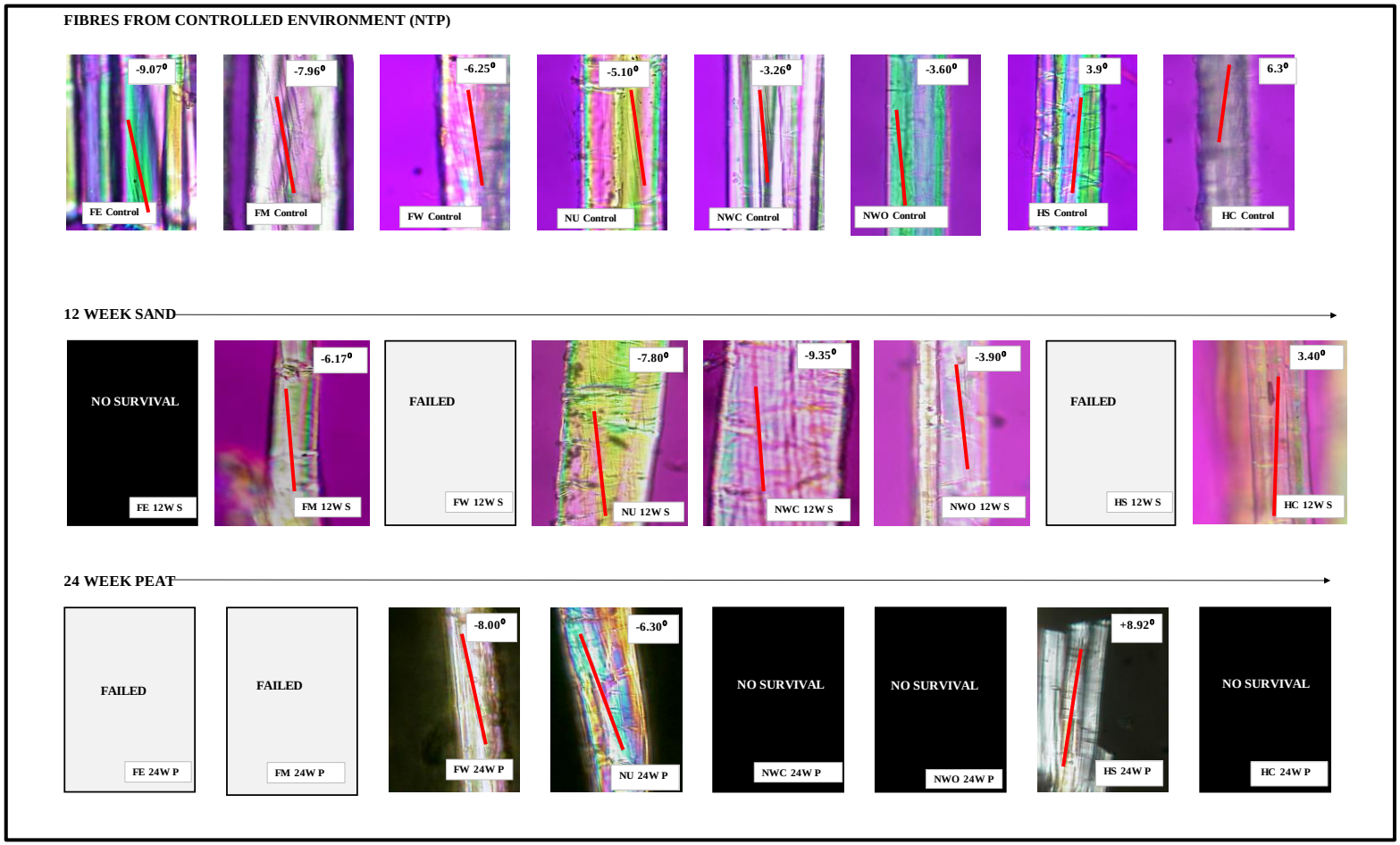

Figure 11.11a. MFA images for deposited fibres in each environment and different periods. Microfibrillar angled determined by rotational measurement and AnalySIS Software. (Black squares show non-survivors; blank squares show fibres failing MFA).

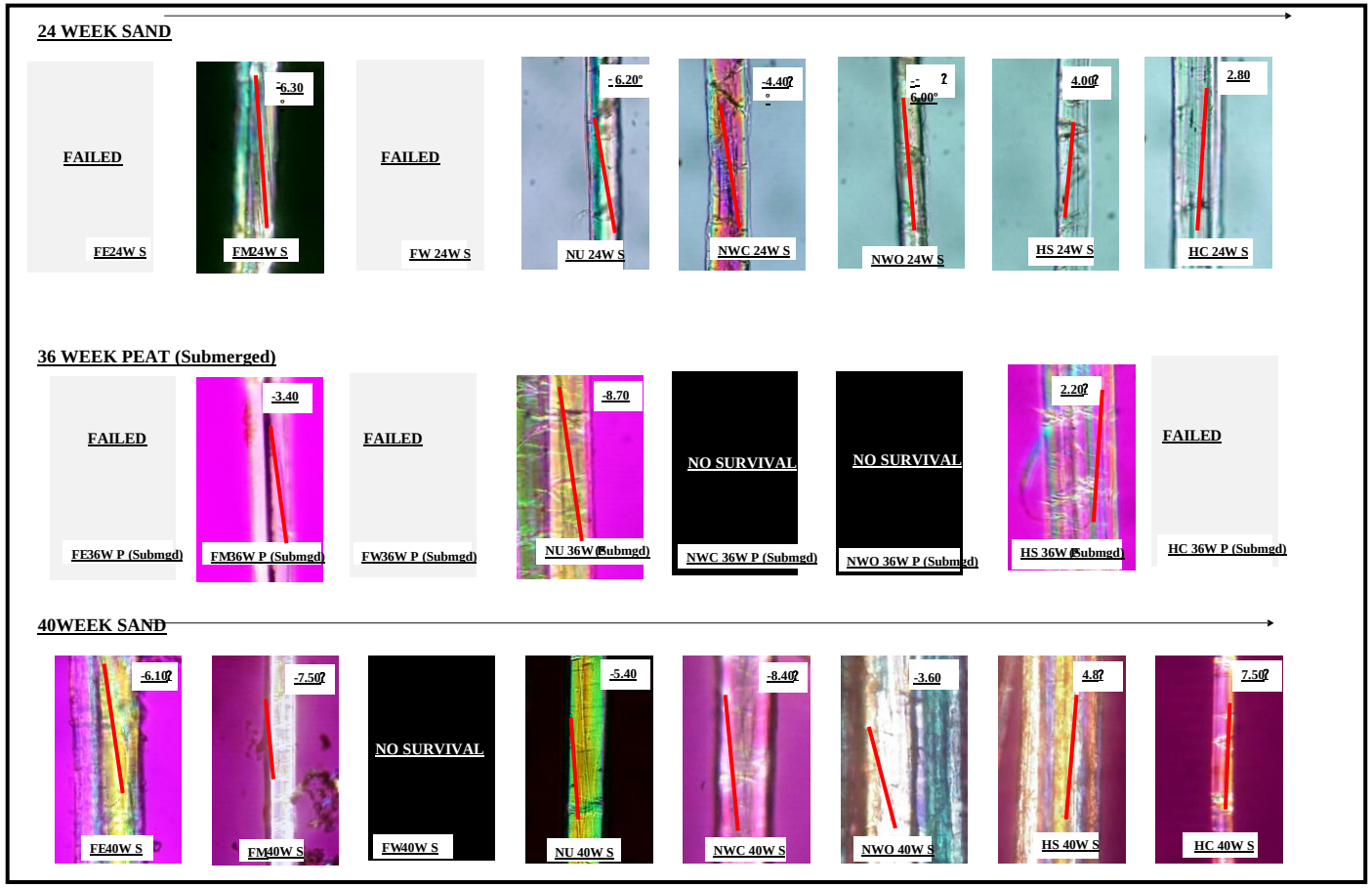

Figure 11.11b. MFA images for deposited fibres in each environment and for different periods. Microfibrillar angles determined by rotational measurement and AnalySIS Software. (The question marks denote uncertain diagnosis. Black squares show non-survivors; blank squares show fibres failing MFA presentation).

11.7.2 Measurement of MFA and Ct of surviving samples

Comparison of the MFA measurements for the surviving fibres from the three species are displayed in a box and whisker format **Figure 11.12.** These are grouped under fibre types, nettle, flax and hemp. A similar plot **Figure 11.13** taken from the original work described in **Chapter 7,** provides a comparison with non-degraded samples. The MFA measured for the degraded fibres confirm that, where a fibre survives deposition, the MFA can still serve as a diagnostic feature. While there are minor variations in MFA measurement, with hemp showing a more extensive range and nettle a reduced range, and notwithstanding the difficulty in obtaining quality images suitable for AnalySIS evaluation from degraded fibres, MFA as a diagnostic feature is still viable.

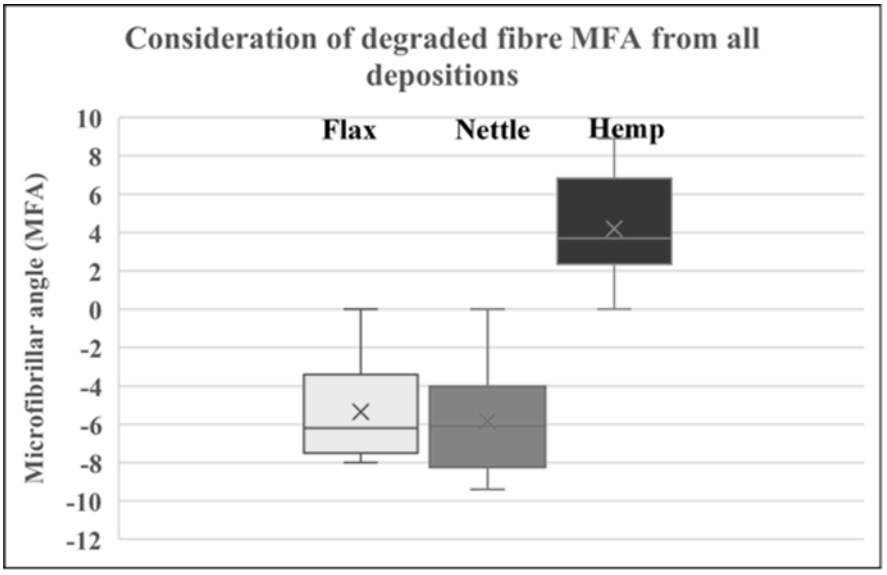

Figure 11.12. Comparison of the mean and standard deviation of fibre for MFA measurements for all surviving fibres (Control fibres excluded).

ANOVA Analysis of variance in fibre cross-sectional analysis of 24 samples nettle (n 11), flax (n 6), and hemp (7) shown in **Figure 11.13** found there to be highly significant variation between the grouped samples (F=71.84, df=23, p= <0.0001). The graph shows a significant difference between nettle and hemp (*T*=-10.53, df=16, p<0.0001) and a significant difference between flax and hemp (*T*=-8.44, df=10, p<0.0001). There was no significant difference between flax and nettle. Note. The control samples were not included in this analysis.

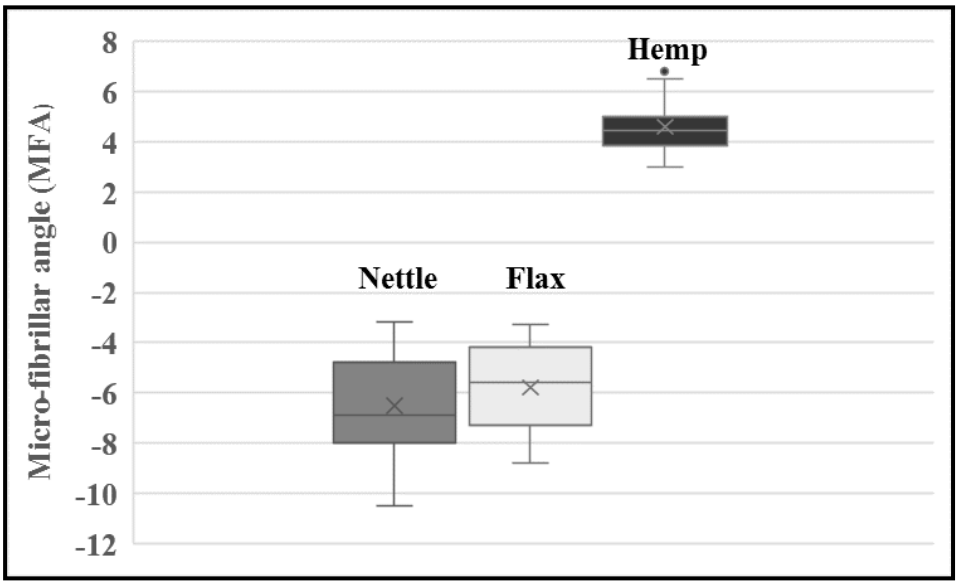

Figure 11.13. MFA of original non-degraded modern reference material (see **Chapter 9).**

11.7.3 Determination of degradation effects on the Circularity (Ct) of fibres

In addition to identifying MFA as a diagnostic feature, the circularity of the fibre cross-sectional area was also considered, and the effect of degradation evaluated. The same degradation periods, deposition soils and environments were used, and fibres of each sample were taken from the same acetate sheet carriers.

Lengths of 25mm of surviving fibres were extracted from the carriers and mounted in 6mm dia. EpoFix resin moulds, as previously described **Chapter 8**.

Following curing, the sections were end polished and 1mm sections microtomed for imaging under compound microscopy with CPL. The type of fibre selected for investigation described as “theoretical fibre” of some 25µm diameter presented several microfibre CSAs to be measured within the same image. These were identified and numbered.

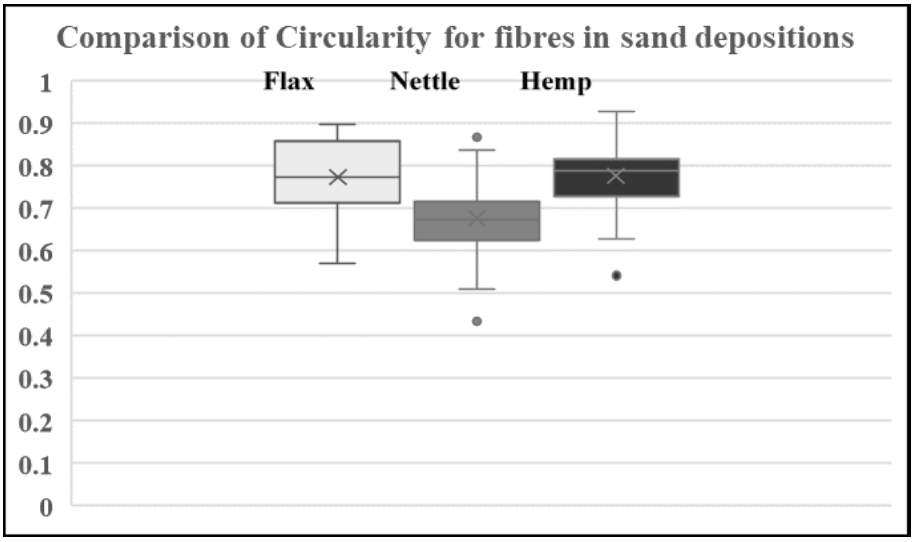

To achieve the same sample size, the test was limited to evaluating six fibre CSA measurements from each type to provide a comparable statistical comparison between the fibre types. The microscope images of CSA were compared with ImageJ software to measure Ct, and the data assembled in a spreadsheet for statistical analysis.

The circularity of 108 CSA fibres from dry sand deposits and 66 CSA fibres from peat deposits were collated with ImageJ analysis and show in **Figures 11.14** and **Figure 11.15.** A Single Factor ANOVA statistical analysis of the data coupled with a "*t*" distribution analysis.

Analysis of variance in fibre circularity of 108 samples deposited in dry sand. Nettle (n 36), Flax (n 36), and Hemp (36) shown in **Figure 11.14** found there to be highly significant variation between the grouped samples (F=16.0918, df=107, p= <0.0001). The graph shows a significant difference between Nettle and Flax *(t*=4.69, df=70, p<0.0001) and a significant difference between Nettle and Hemp (*t*=5.02, df=70, p<0.0001). There was no significant difference between Flax and Hemp.

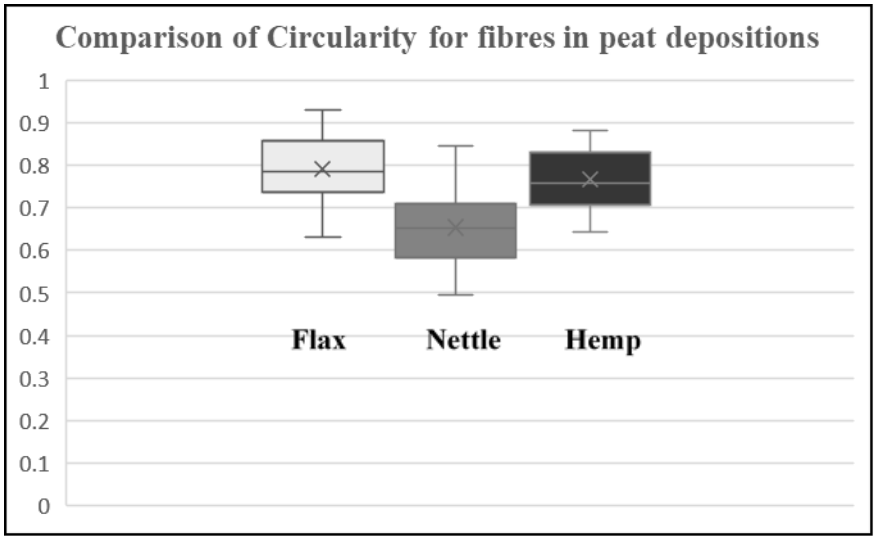

Figure 11.15. Plant fibre comparison of the mean and standard deviation of fibre circularity for 66 fibres deposited in peat.

Analysis of variance in fibre cross-sectional analysis of 66 samples deposited in peat. Nettle (n 24), Flax (n 24), and Hemp (18) shown in **Figure 11.15** found there to be highly significant variation between the grouped samples (F=19.54109, df=63, p= <0.0001).

The graph shows a significant difference between Nettle and Flax (*t*=5.76, df=46, p<0.0001 p<0.0001) and a significant difference between Nettle and Hemp (*t*=4.45, df=70, p<0.0001). There was no significant difference between Flax and Hemp.

Examples of flax FE (v. Eden) fibre images taken from fibre deposited in peat for 24 weeks, identified and analysed under ImageJ, are tabulated in **Table 11.13**. and shown in **Figure 11.16.**

Fibre (variety)	**Ct Average**	**Ct St. Dev.**
Flax (Eden)	0.806	0.057
Flax (Winterlyn)	0.858	0.054
Nettle (Uni. testbed)	0.628	0.062
Nettle (Wild closed)	0.699	0.132
Nettle (Wild open)	0.633	0.070
Hemp (Santhica)	0.777	0.077

Table 11.13. Fibres from 24week deposition**:** Ct determinations listed.

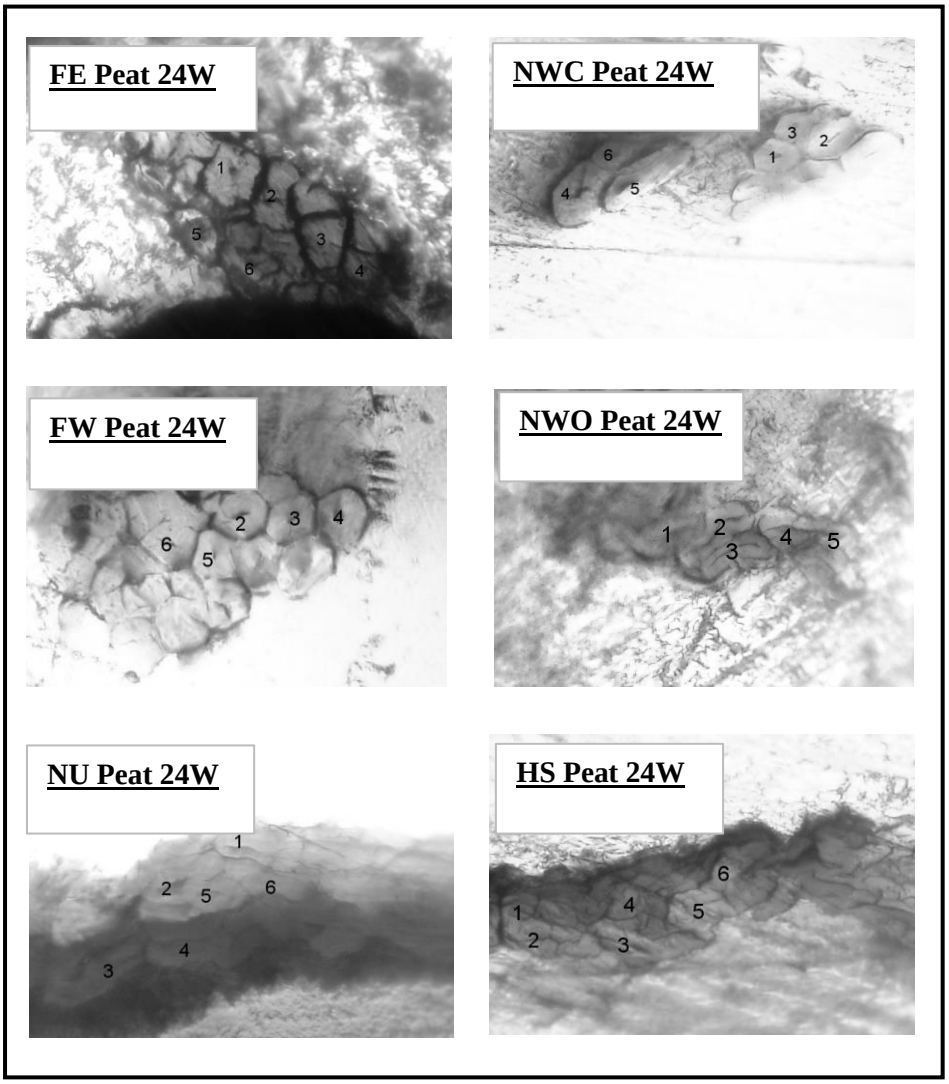

Figure 11.16. Fibres surviving 24week deposition: a selection of six CSA from each image was selected for measurement of Ct with ImageJ software.

11.8 Biomomentum tensile test of degraded samples

The level of degradation of the material properties of the degraded fibres, surviving sample fibre samples for each genus and deposition period was assessed by determination of their Modulus of Elasticity (*E*). Four fibres from each of the above were mounted on 6mm card holding frames prior to mounting onto the Biomomentum Mach-1TM for fibre stress and strain measurement and calculation. The data provided and downloaded from the test were added into an XL spreadsheet for analysis. A typical curve derived from the database is presented below **Figure 11.17a**. 12week dry sand deposition of wild nettle from a closed woodland area **NWC1** and **Figure11.17b**. 24week peat deposition from the University testbed **NU3** This tabulation was completed for all surviving fibres from each deposition soil and period. The results are tabulated below **Table 11.14.**

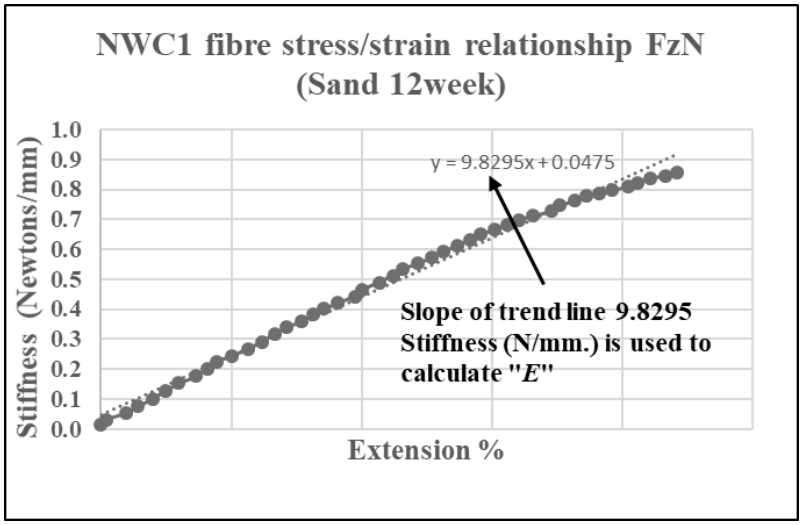

Figure 11.17a. Illustration of stress/strain database from Biomomentum test for NWC1.

Fibre, nettle from a closed woodland area, was held in Assemblage No.3 The trendline is added to determine the straight-line relationship “Stiffness” (Fz/N), used to calculate Young’s Modulus (*E*). (For determination of “*E*” data points preceding and following the straight-line elastic region have been removed).

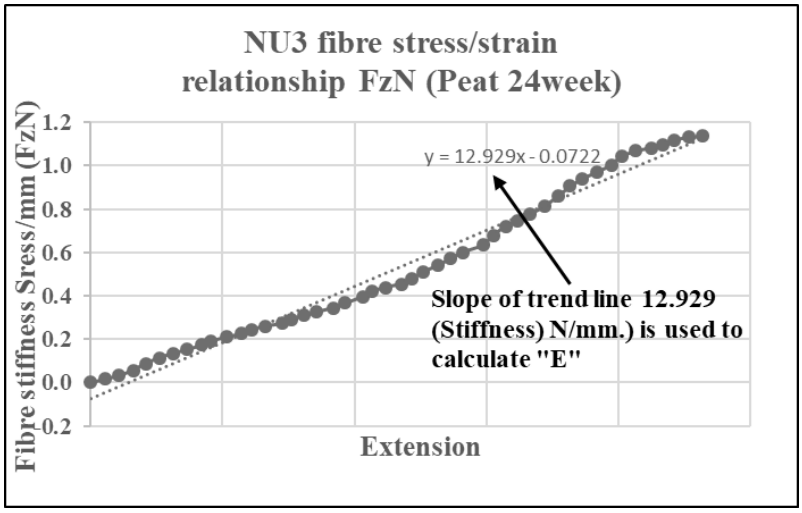

Figure 11.17b. Illustration of stress/strain database from Biomomentum test for NU3. Fibre, nettle from the University testbed, was held in Assemblage No 3. The trendline is added to determine the straight-line relationship, “Stiffness (Fz/N)”, used to calculate Young’s Modulus (*E*). (For determination of “*E*” data points preceding and following the straight-line elastic region have been removed).

The above graphs show the relationship between the stiffness of the fibre (FzN) (Newtons/mm) presented over the 6mm sampling length, a function which determines the stress imposed, over the extension (“z” denotes the vertical axis). The straight trendline relationship illustrates the elastic region for the fibre. To evaluate the degradation effects on the tensile strength of the surviving fibres from each soil and period, a selection of 20 fibres was taken from the carrier frames for submission to the Biomomentum mechanical testing machine for stress/elongation tabulation.

The twenty fibres were mounted across a 6mm gap onto a prepared card mounting (see **Figure 11.4)**. Young's Modulus is determined from the Biomomentum results and evaluated from the computer-generated slope of the FzN/Extension trendline line relationship.

The results for fibres from the 12week dry sand deposition are listed **Table 11.14.** Tabulation for all the surviving fibres is shown in **Table 11.15.**

Summary Sheet. Biomomentum database: Degradation 12wk dry sand							
Fibre	**Dia.**	**Max. Load**	**Stiff**	**Dia.**	**Area**	**Stress**	***E* Mod.**
	µm	**N**	**N/mm**	**mm**	**sq. mm**	**MPa**	**MPa**
Control	170	1.84	4.26	0.170	0.02270	81.18	4690
FW1	32	0.48	3.80	0.032	0.00080	596.75	28346
FW2	51	0.96	14.60	0.051	0.00204	469.88	42876
FW4	34	0.43	3.82	0.034	0.00091	473.55	25241
FM1	32	0.04	1.75	0.032	0.00080	49.73	13054
FM3	58	0.08	3.95	0.058	0.00264	30.28	8969
FE4	44	0.15	0.49	0.044	0.00152	98.64	1933
	Flax Ave.	**0.36**					**17872**
NU1	36	0.66	7.52	0.036	0.00102	648.32	44322
NU3	61	0.71	7.46	0.061	0.00292	242.91	15314
NU4	41	0.84	6.07	0.041	0.00132	636.16	27582
NWC1	49	0.86	9.83	0.049	0.00189	456.00	31273
NWC3	28	0.82	4.13	0.028	0.00062	1331.53	40238
NWO1	122	1.01	9.67	0.122	0.01169	86.39	4963
NWO2	76	0.44	5.31	0.076	0.00454	96.98	7022
	Nettle Ave	**0.76**					**24387**
HC1	46	0.43	3.19	0.046	0.00166	258.71	11515
HC2	61	1.48	6.17	0.061	0.00292	506.36	12666
HC3	45	1.00	6.70	0.045	0.00159	628.68	25273
HC4	90	1.36	7.70	0.090	0.00636	213.75	7261
HS1	160	1.39	2.98	0.160	0.02011	69.12	889
HS2	154	1.48	5.75	0.154	0.01863	79.45	1852
HS4	31	0.60	4.10	0.031	0.00075	794.84	32589
	Hemp Ave	**1.11**					**13149**
TOTAL SAMPLE		**32**					
TOTAL SURVIVAL		**20**					
% SURVIVE		**62.5%**					

Table 11.14. Young's Modulus for degraded samples from the 12week deposition in dry sand**.**

In **Table 11.15** four samples from each of the eight fibre types were tested, (the missing value, blank cells illustrate fibres that failed the test), and *E* values calculated as shown. Measurable stress could only be recorded for 62.5% of the samples.

Table 11.1Deposition period Soil type and "*E*" (GPa.)	**12 Wk. Dry Sand GPa.**	**24 Wk. Peat GPa.**	**24 Wk. Dry Sand GPa.**	**40 Wk. Dry Sand GPa.**	**40 Wk. Peat GPa.**	**36 WK. Peat (Submerged) GPa.**
Sample						
FW1 Flax (v.Winterlyn)	28.3					
FW2 Flax (v.Winterlyn)	42.9		0.1			
FW3 Flax (v.Winterlyn)			5.0			
FW4 Flax (v.Winterlyn)	25.2		13.2			12.6
FM 1 Flax (v.Marilyn)	13.0		6.1			
FM 2 Flax (v.Marilyn)						
FM 3 Flax (v.Marilyn)	9.0					
FM 4 Flax (v.Marilyn)			35.1			
FE1 Flax (v.Eden)		0.8	5.5	50.4		
FE2 Flax (v.Eden)						
FE3 Flax (v.Eden)						
FE4 Flax (v.Eden)	1.9					
NU1 Nettle (Uni. Test bed	44.3	2.4	5.5	5.7		
NU2 Nettle (Uni. Testbed)				1.7		
NU3 Nettle (Uni. Test bed)	15.3	0.8	2.6			25.6
NU4 Nettle (Uni. Testbed)	27.6		5.0	6.2		
NWC 1 Nettle (Wild-Closed)	31.3			7.3		
NWC 2 Nettle (Wild-Closed)			11.4			
NWC 3 Nettle (Wild-Closed)	40.2		14.2			12.9
NWC 4 Nettle (Wild-Closed)						5.6
NWO 1 Nettle (Wild-Open)	5.0			0.03		
NWO 2 Nettle (Wild-Open)	7.0					
NWO 3 Nettle (Wild-Open)						17.1

Table 11.15 (Part 1). Determination Young's Modulus "E" (GPa). Tests were conducted on four samples of each surviving fibre sample mounted (see Section 11.4.8 and Figure 11.4 above). (The shaded areas indicate fibres that were too fragile to survive the test loading).

Table 11.15 (cont.) Deposition period Soil type and "*E*" (GPa.)	**12 Wk. Dry Sand GPa.**	**24 Wk. Peat GPa.**	**24 Wk. Dry Sand GPa.**	**40 Wk. Dry Sand GPa.**	**40 Wk. Peat GPa.**	**36 WK. Peat (Submerged) GPa.**
NWO 4 Nettle (Wild-Open ground)				14.4		
HC 1 Hemp Commercial (v. unknown)	11.5					
HC 2 Hemp Commercial (v. unknown)	12.7					27.3
HC 3 Hemp Commercial (v. unknown)	25.3		7.9			6.5
HC 4 Hemp Commercial (v. unknown)	7.3		43.8			
HS 1 Hemp Commercial (v.Santhica)	0.9					7.9
HS 2 Hemp Commercial (v.Santhica)	1.9		26.5			15.9
HS 3 Hemp Commercial (v.Santhica)			45.2			7.6
HS 4 Hemp Commercial (v.Santhica)	32.6					7.5
Percentage surviving "*E*" Test	**62.5%**	**9.4 %**	**46.8 %**	**21.9 %**	**nil**	**34.3 %**

Table 11.15 (Part 2). Determination Young's Modulus "*E*" (GPa). Tests were conducted on four samples of each surviving fibre sample mounted (see **Section 11.4.8** and **Figure 11.4** above). (The shaded areas indicate fibres that were too fragile to survive the test loading).

These results are summarised in **Figure 11.18** and **Figure 11.19** and shown in box and whisker diagrams for "*E*" as calculated for sand and peat depositions.

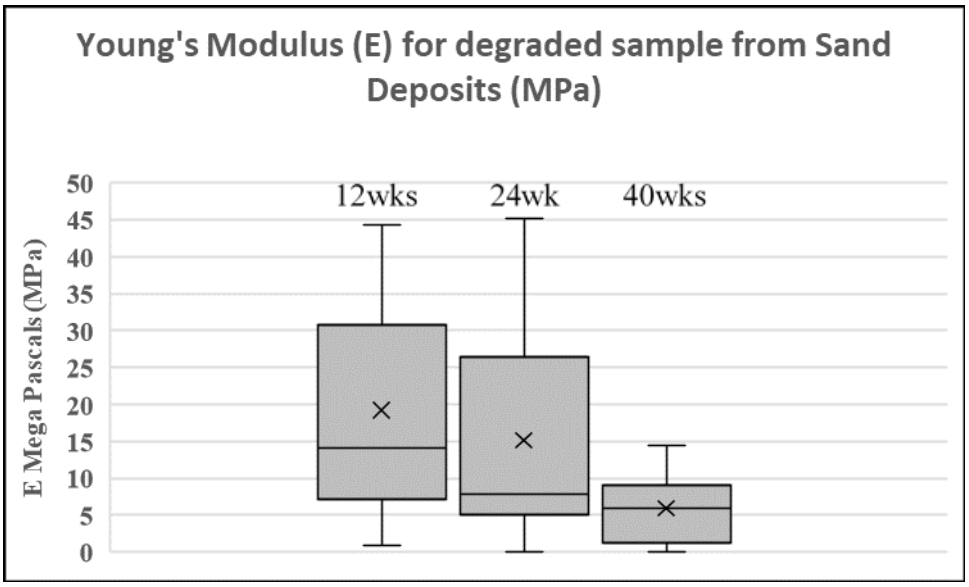

Figure 11.18. Representation of "*E*" values for dry sand deposition. Values calculated for a range of fibres deposited in dry sand for 12, 24 and 40 weeks taken from **Table 11.15**. (The decrease in modulus reflects the degraded tensile strength).

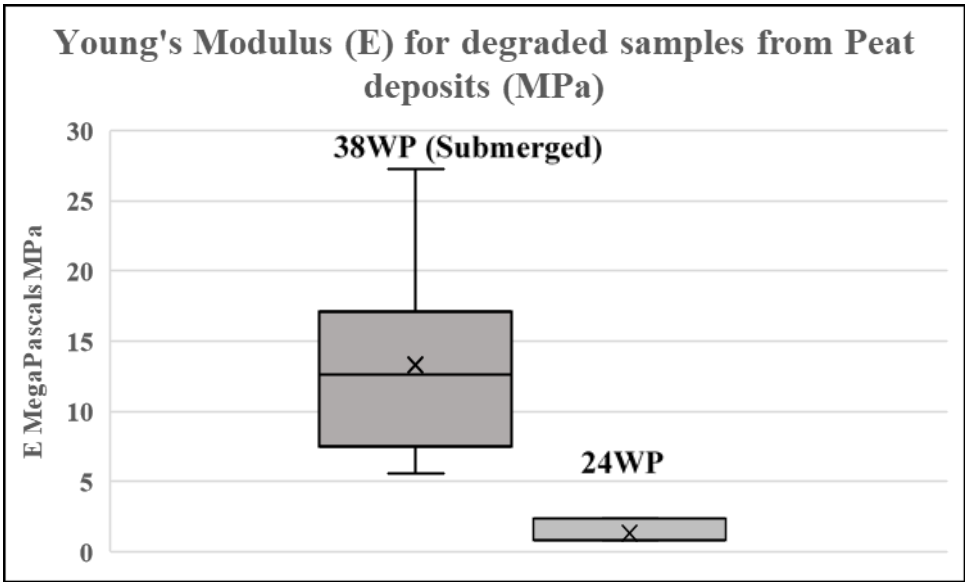

Figure 11.19. Representation of "*E*" values for peat deposition. Values calculated for a range of fibres deposited in peat for 24weeks and 36weeks submerged. (The decrease in modulus reflects the degraded tensile strength).

Figure 11.19 shows that the severe decrease in modulus for the 24week deposition, shown right, results from the degradation of tensile strength. In comparison, the increase in resistance to degradation, shown left, at 36 weeks results from sample total water immersion.

While tensile testing has been covered in more detail in earlier chapters, the results from the degradation trials can also be compared with Bodros and Baley (2008) report on nettle and flax fibres.

Plant Fibre	**Young's Modulus *E* (GPa) (Bodros and Baley 2008)**
Nettle	87 (±28)
Flax v. *Ariane*	58 (±15)
Flax v. *Agatha*	71 (±25)
Hemp	19.1 (±4.3)

Table 11.16. Comparative plant fibre Young's Modulus *E*. (Bodros and Baley 2008: Table 1. with additions).

	12 Wk.	**24 Wk.**	**24 Wk.**	**40 Wk.**	**40 Wk.**	**36 WK.**
Fibre	**Dry Sand GPa.**	**Peat GPa.**	**Dry Sand GPa.**	**Dry Sand GPa.**	**Peat GPa.**	**Submerged GPa.**
Flax	20.1	0.8	10.8	50.4		12.6
Nettle	24.4	1.6	7.7	5.9		15.3
Hemp	13.2		30.9			12.1

Table 11.17. Cumulative figures for mean values of *E* for each fibre species, within each deposition period, are provided for comparison with Table 11.16 above.

Except for *E* of flax at 40 weeks (50.4 GPa) and hemp at 24 weeks (30.9 GPa), there is a minimum correlation with the figures obtained by Bodros and Bailey (2008), particularly for nettle.

Practical experience, from the tensile degradation trial, where there was difficulty in mounting some specimens into the load-bearing assemblage, would suggest that the differential could be attributed to degradation.

11.9. Supplementary testing - a re-evaluation of 12week peat deposit

Consideration of the 12week (Arrhenius 45week) and 24week (Arrhenius 89week) survival rates for the acidic peat soil gave cause for concern in that, while all the fibres in the 12week peat deposit failed, 63% of the fibres survived within the 24week deposit. In view of this discrepancy, it was decided to run an additional 12week peat soil test with samples drawn from the original assemblage held in three containers positioned top, middle and bottom of the oven. Three dry sand containers with similar samples were also placed in the oven chamber as control samples. To assist in the degradation comparison, the six containers were positioned at equal intervals within the oven and temperature sensors were added at oven top and bottom to allow monitoring and recording **Figure 11.20**. The test was completed at 12 weeks and the fibre samples and pH levels analysed for degradation and survival rates **Table 11.18.**

Location	Fibre Type	Survived	Remains
Bottom	Hemp (Santhica)	**3**	Fibres
	Flax (Eden)	**1**	Fragment
	Flax (Marylin)	**1**	Fragment
Middle	Hemp (Santhica)	**1**	Fragment
	Flax (Eden)	**1**	Fragment
	Flax (Marylin)	**1**	Fragment
	Nettle (Wild-closed)	**1**	Fragment
	Nettle (Wild-open)	**1**	Fragment
Top	Hemp (Santhica)	**1**	Fragment
	Hemp (Commercial)	**1**	Fragment
	Flax (Marylin)	**2**	Fibre and Fragment
	Nettle (Wild-open)	**1**	Fragment

Table 11.18. Fibres surviving 12 weeks (Arrhenius 45weeks) in peat soil. The fragments surviving this supplementary12week peat were too fragile to evaluate MFA or Ct. All control samples from the dry-sand deposit survived.

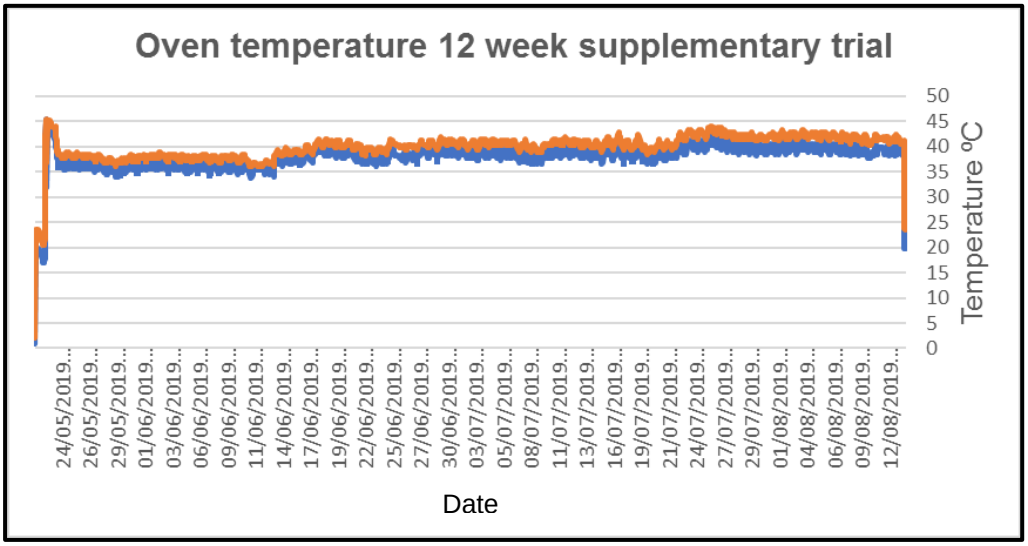

Figure 11.20. Plot of recorded oven temperature: variation for 12week period of supplementary degradation trial for set-point at 40º.

At the completion of the supplementary test of the 24 samples held within the peat soil, 15 survived in a heavily degraded condition. These were small fragments unsuitable for morphological evaluation or tensile testing.

The findings confirm that the original discrepancy in the survival from peat deposition over the initial 12 and 24week periods was not an anomaly but as *Janaway (2000) noted that a*,

"(W)ide range of intrinsic and extrinsic factors resulting in differential loss or preservation*"* (Janaway 2002:398).

11 10 Summary- fibre degradation evaluation

The principal research objective, in conducting the degradation trials was to determine the extent to which the derived diagnostic morphological features MFA and Ct, as summarised in **Chapter Nine**, were retained. The comparison of principal diagnostic features, MFA and Ct retained under degradation are compared in Figure 11.21.

11.10.1. Tensile properties of degraded fibres

There is a significant variation in the results achieved with the mean values recorded from degraded fibres compared with the Bodros and Baley (2008) tensile testing for "Young's Modulus" **Table 11.16:** However, the poor survival of fibres from the deposition are broadly in agreement with those reported by others and confirm that plant fibre degrade in all but the most advantageous soil deposition (Bodros and Baley 2008; Summerscales et al. 2010; Baley and Bourmaud 2014).

11.10.2 Degradation- associated metallic assemblages

The extent to which the pseudomorphic representation replicates the MFA and Ct diagnostic feature are uncertain. As reported **Chapter Three**, for the assemblages listed, the description and identification of the replicated spun fibre's twist S or Z, thread count, and weave structure are indicative of the potential for a more extensive review of such assemblages. In support, of the potential for the diagnosis of fibre residue Forte et al. (2019) conducted experimental work on the fibre retention deposited on replicated spindle whorls **Chapter 4, Section 4.9.3.** Their findings offer a comparison that could serve as a foundation for initiating a future experimental diagnostic appraisal programme.

11.10.3 Degradation: MFA/Ct comparison

The plot **Figure 11.21** illustrates the post-depositional determinations of MFA and Ct values compared with the experimentally derived values reported in **Chapter Nine.**

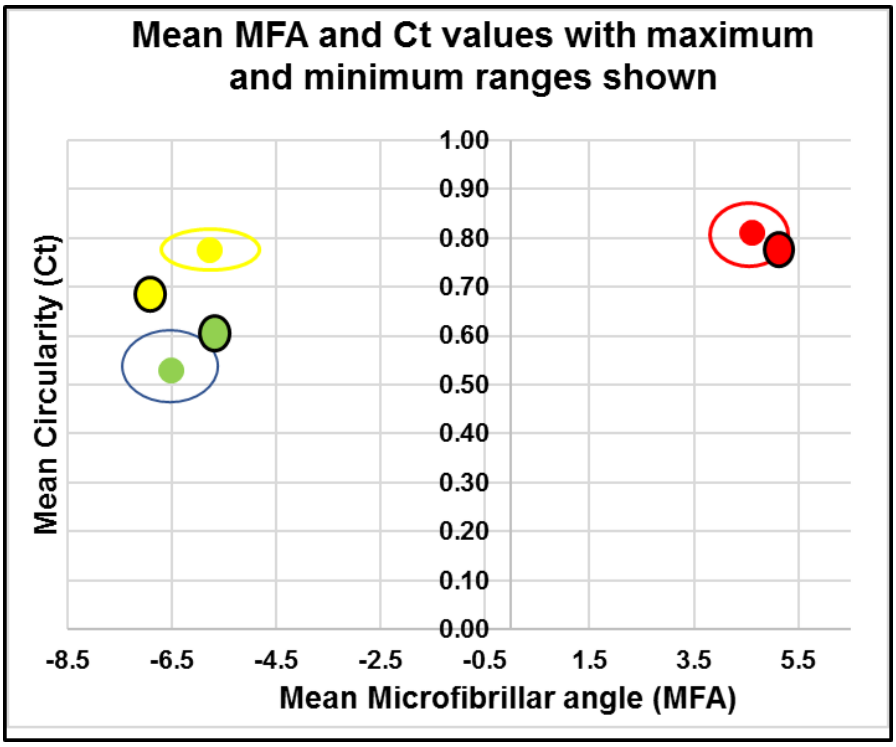

Figure 11.21. The plot shows a comparison of MFA/Ct diagnostic features **Chapter 9** with the added results from the degraded fibres, flax (yellow), nettle (green) and hemp (red). The degraded samples are outlined in black.

Note The database in support of the above is included in Appendix F.

Chapter Twelve
Archaeological assemblages - Case Studies

12.0 Introduction - archaeological assemblages

A range of diagnostic techniques applicable to plant fibre identification has been reported and evaluated in previous chapters to propose that the morphological features of microfibrillar angle (MFA) and fibre area cross-sectional circularity (Ct) offer potential as diagnostic features that meet the research aims and objectives. Subsequent chapters have considered the durability of these features with their diagnostic suitability reviewed within a Blind Test protocol conducted upon minimally processed modern reference material, Chapter 10, and their degraded age-related reliance when subjected to accelerated degradation trials Chapter 11. In this chapter, the application of MFA and Ct, diagnostic features to archaeological assemblages, are reviewed for the following case studies.

1. Confirmation of the diagnosis of 16th to late 19th century samples held at Temple Newsam Museum and labelled as unknown bast fibre.

2. Evaluation of loose fibres from the Cliffe Castle Coptic Collection.

3. Application of the diagnostic techniques to textile collected from the 600 AD mass grave at Kasr-el-Yahud (Qasr-el-Yahud) Jordan.

12.1. Case Study 1 - Confirmation of diagnosis attributed to samples held at Temple Newsam (Leeds Museums and Galleries)

12.1.1 Introduction

In order to substantiate the validity of the determined diagnostic features based on modern reference material, it was decided that there was a need to obtain access to museum and archaeological collections to evaluate the long-term effects on textile fibres resulting from their initial production processes and their depositional and conservation environments.

There are rightful concerns expressed by Museum Curators regarding the accessibility of textile artefacts for research purposes, particularly where these artefacts may be subjected to destructive or invasive concerns. Leeds City Museums (LCM) offers encouragement to researchers who may wish to examine their collections but do so within a strict policy and procedure regarding the destructive sampling of collections. Access is administrated through a formal application process with permission granted at the Acquisition and Disposal Committee monthly meeting. After considering the proposed fibre preparation method, the evaluation techniques and the small sample sizes, the preparation and mounting processes to be applied were judged to be acceptable.

12.1.2 Review of textile diagnostic features

As previously noted for plant fibre diagnostic features, the research described to date has concentrated on evaluating modern reference material. The techniques described include cross-sections morphology, tensile strength evaluation, and micro-fibrillar fibre orientation.

It is recognised that textile materials excavated from archaeological sites, materials held in museum collections, or textiles still present and preserved in their original environment in stately homes or national collections, offer the opportunity to consider the effects on the diagnostic features resulting from the deposition environment. It is evident from the low level of textiles present within the archaeological record, that preservation is limited by soil types, pH levels, relative humidity and temperature that corrupt or destroy the textile fibres. Only in exceptional circumstances such as water-logged, arid conditions or in association with metal cathodic protection would the fibres survive (Janaway 1987: 381; Kronkright 1990: 139; Peacock 1996: 35-47; Peacock 2003: 32-34).

12.1.3 The Roger Warner Textile Collection Temple Newsam (Leeds) UK

Roger Warner accumulated collections over fifty-years period from the mid-1930s and presented them to Leeds City Museums from 1985 onwards. Now housed as part of the Temple Newsam collection of decorative arts the textiles are available for public inspection and scholarly interpretation. Helen Bower, the Assistant Curator, conducted an extensive review of the collection and published a catalogue of her findings covering 187 artefacts of dress and furnishing textiles from the sixteenth to late-nineteenth-century European origins (Bower 2000).

The range of textile examples detailed within the catalogue reflects Warner's interest in the decorative arts, and association with wallpaper manufacturers Jefferey and Company.

The company's designs were influenced by original examples obtained from France, the Low Countries and Italy. However, in partnership with established designers of the day, a range of designs for block-printed wallpaper some of which achieved an award at the 1873 London Annual International Exhibition was published (Yorkshire Post 2009).

It was against this background that Warner developed an interest in textile design, including complete furnishings and dressing and textile fragments as items of historical interest for both their pattern weaving construction and the innovation in their design. The collection benefitted from Warner's purchase of antiques for an antique dealership opened in 1936 in Burford Oxfordshire UK. Post First World War the collection was extended by the acquisition of textile material from the sales of the contents from country houses. These English country estates were subject to extensive death duties and changes in social structures. Unlike furniture, textile items were not considered for their monetary value as antiques and their historical value was of little interest to collectors. Consequently, they were often auctioned as inexpensive agglomeration of furnishing fragments.

12.1.4 The Warren collection catalogue

The textile assemblage review was aided by Bower's (2000) catalogue that allowed an examination of the full range of artefacts to identify suitable textiles for further evaluation and diagnosis. The catalogue listed 180 artefacts from the group of furnishing or heavyweight fabric remains including curtains, chair covers and valences.

In agreement with the research objectives, attention was directed to two items described as constructs of wool or cotton weft upon an unidentified bast fibre warp. Artefact Leeds Warren ALWAG. RW0337 and artefact ALWAG. RW0338 were selected.

12.1.5 Artefacts selected for fibre identification.

As noted above. there were artefacts within the collection for which only the broad description of bast fibre had been applied **Figure 12.1.1** and **Figure 12.1.2.**

Figure 12.1.1. RW 337. A 19th. Century seat cover (Ginsberg Catalogue No. 154). Late 19th-century cotton and bast furnishing of Brocatelle weave. 46.3 x 57.1 cm. Cotton warp ends 12/cm Z twist (average dia. 0.64mm). Bast fibre weft picks 28/cm 2ply Z twist (average dia.0.8mm).

The furnishing is listed as a chair seat cover with tack-holes around the edges. For the catalogue, the item was photographed from the back and described as,

> "Woven with a faintly streaky ground in imitation of a faded late 17th or 18th-century silk" (Bower 2000: 37).

Figure 12.1.2. RW 338. A late 19th- century furnishing (Ginsberg Catalogue No. 176). Late 19h century of Damask weave 57 x 90 cm acquired from S.W. Wolsey Ltd. London.

RW 338 is listed as wool and bast furnishing. Twill Weave late 19th century Damask weave 57 x 90 cm. Bast fibre warp ends 10/cm “Z” twist (average dia. 0.64mm) and weft picks 18/cm 2ply, “Z” twist (average dia.0.8mm).

These two items were of interest to the research programme as they both carried the indeterminate identification as “bast fibres”, a diagnosis which can be addressed.

12.1.6 Weave construction and description

In appraising the fibres utilised in these furnishing fabrics, it is necessary to understand the construction method and to determine the preferred choice of fibre most often used in the weaving of such material. The textiles are detailed in the catalogue as shown above with RW337 described as a Brocatelle weave and RW 338 a Damask weave.

Brocatelle Weave Originally a description of fabrics produced on Florentine looms, a technique similar to Damask, this twill weaving produces a bold symmetrical pattern of an embossed structure raised by alternating the ratio of the warp and weft carry over. The distinctive change in pattern colour is recognised in this design and, unlike Damask the cloth is not reversible. This weaving technique was applied with great success following the introduction of Jacquard loom weaving perfected by Joseph Marie Jacquard in 1800-1804

While the Jacquard system produces embossed figures in a compact woven warp, Brocatelle is a heavier thicker double weave of silk and linen that shows the pattern in high relief particularly suitable for hard-wearing chair covers (Bower 2000: 106; Pritchard 2006: 146; Droß and Schieck 2014: 220; Vintage Fashion 2019).

Damask Weave A single warp and weft self-patterned reversible fabric in which the pattern is formed by contrasts in warp and weft weaving techniques (Bower 2000: 106; Pritchard 2006: 146).

12.1.7 Determination of microfibrillar angle and circularity for samples

An agreement was reached with Leeds City Museums for the collection 25mm samples from the two textile assemblages nominated. The samples were removed under supervision and were taken from loosely adhering fibres attached to the textile fragments RW 337 and RW 338. For MFA and Ct evaluation the fibres were prepared as previously reported in **Chapters Seven and Eight.**

From the catalogue description, the fibres are described as,

RW 337 A bast fibre from chair seat covering, a light brown Z twist fibre.

RW 338 A bast fibre from RW 338 furnishing.

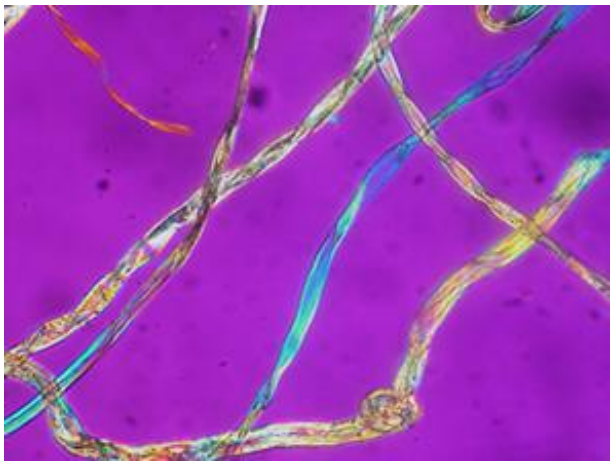

Figure 12.1.3. MFA and Ct RW 337 Cotton warp fibre imaging. Images of the cotton fibre under CPL multi-colour changes along fibre length are identified as cotton (Bouchard and Tengberg 2011: Fig.3; Petraco and Kubic 2004: 104).

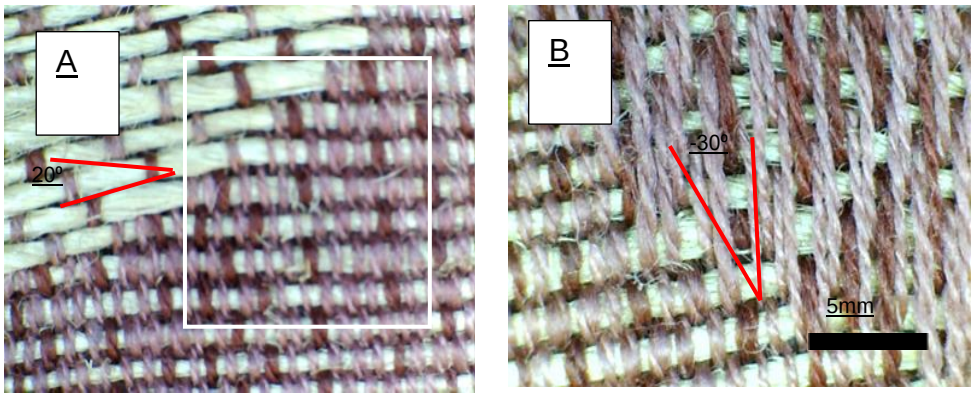

Figure 12.1.4. RW 337 Images of chair seat cover cotton and bast construct. A) Front view of chair cover showing white cotton fibre weft 8/cm, 2ply Z twist (20º) average fibre diameter 0.8mm. **B)** Reversed side of chair seat cover showing purple bast fibre warp 18/cm, 2ply S twist (-30º) average fibre diameter 0.6mm. (The 1cm square aids the thread count).

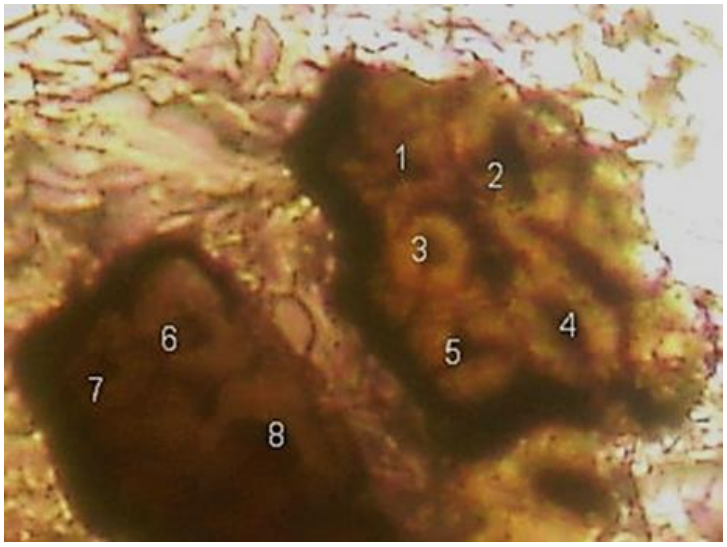

Figure 12.1.5. RW337. Area cross-section for bast fibre sample. Individual fibre CSA's identified for ImageJ analysis of circularity.

Temple Newsam	
RW337 Fibre No.	**Circularity**
ImageJ (Ct)	
1	0.918
2	0.895
3	0.937
4	0.909
5	0.944
6	0.864
7	0.922
8	0.919
Mean	**0.914**

Table 12.1.1. RW337. Individual fibre circularity. Circularity (Ct) for identified fibres with a mean of 0.914.

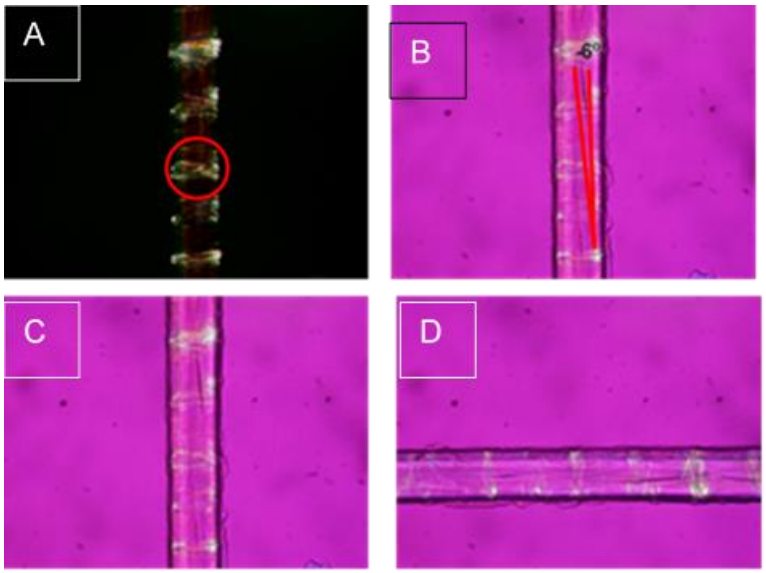

Figure 12.1.6. RW 337 Bast weft fibre imaging. A) Fibre rotated under CPL to attain extinction. B) Image under CPL with 56nm Red Plate inserted MFA illustrated at -6º. C) Image viewed under 56nm Red Plate at 90º, image colour a vague red. D) Image rotated to 180º, some green/blue colour change noted.

Figure 12.1.6 Shows bast fibre rotated under CPL with 56nm Red Plate in line. **A)** Fibre image is in extinction under CPL with some nodal deformations displayed (red circle). **B)** A section of a fibre of constant colour with an MFA (-6º) identified and located. **C)** Image rotated 90º shows red colouration that changes at **D)** 180º, to mainly blue colouring

This red/blue colour change under the 56nm Red Plate plus the MFA at -6º with X deformation marks and a Ct value of 0.914 indicates that this is a flax fibre.

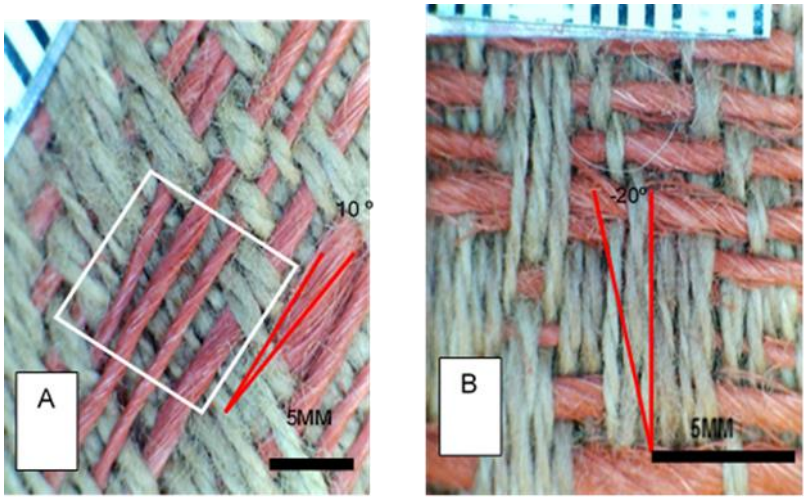

Figure 12.1.7. RW 338 Images of wool and bast furnishing. **A**) Front view showing bast fibre warp 6/cm Z twist (10º), average fibre diameter 0.5mm. **B)** Reversed side with wool weft fibre10/cm 2ply S twist(-20º) twist average fibre diameter 0.8mm. (The 1cm square aids the thread count).

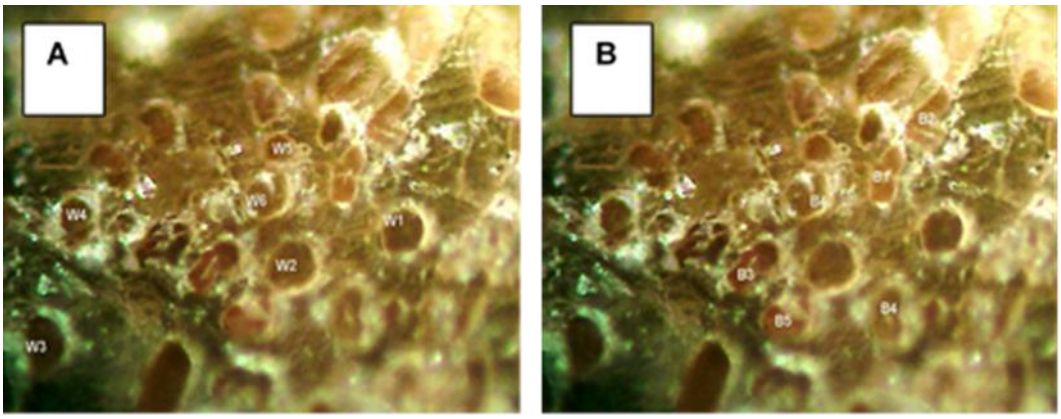

Figure 12.1.8. RW388 Wool (A) and bast fibre (B) identity: fibre Ct determined with ImageJ Table 12.1.2.

RW388 Wool Ct		RW388 Bast Ct	
Sample	**Ct**	**Sample**	**Ct**
Wool 1	0.944	**Bast 1**	0.840
Wool 2	0.857	**Bast 2**	0.897
Wool 3	0.956	**Bast 3**	0.793
Wool 4	0.933	**Bast 4**	0.924
Wool 5	0.896	**Bast 5**	0.822
Wool 6	0.928	**Bast 6**	0.890
Mean Wool	**0.919**	**Mean Bast**	**0.89**
St.Dev.Wool	**0.04**	**St. Dev Bast**	**0.05**

Table12.1.2. Tabulation of Ct values: wool and bast fibres identified in Figure 12.1.8**.**

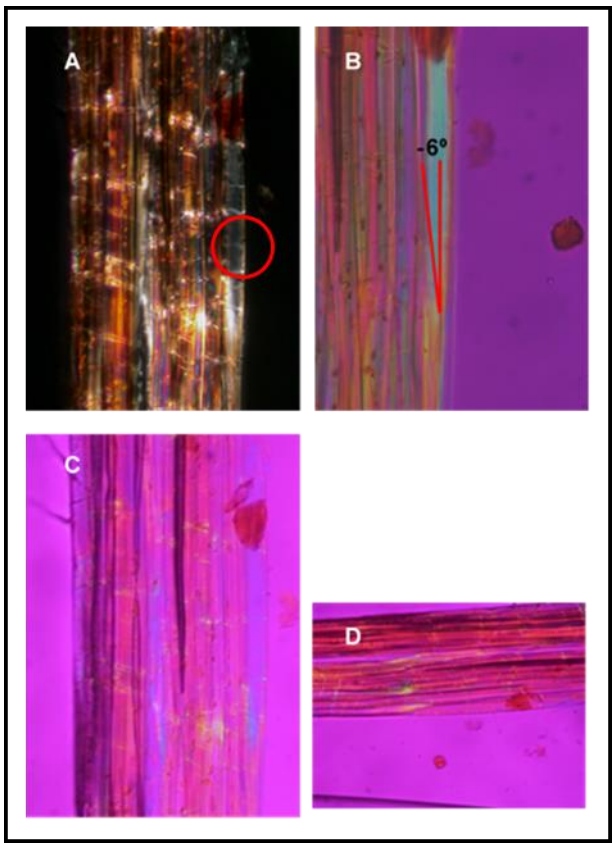

Figure 12.1.9. RW 338 Wool and bast weft fibre imaging. **A)** Fibre rotated under CPL to attain extinction. **B)** Image under CPL with 56nm Red Plate inserted MFA illustrated at -6º. **C)** Image with 56nm Red Plate at 90º, poor quality image vague red. **D)** Image rotated to 180º, a poor-quality image with some green/blue colour change noted.

Figure 12.1.9 Shows bast fibre rotated under CPL with 56nm Red Plate in line. **A)** Fibre image is in extinction under CPL with some nodal deformations displayed, but these are low quality dislocation marks (red circle). **B)** A section of a fibre of constant colour with an MFA(-6º) of low visibility identified and located. Minimal colour change under Herzog Test (Petraco and Kubic 2004: 89-93; Lukšová 2017) and poor-quality nodal dislocation marks, red circle on **(A),** indicates a flax fibre. **C)** fibre rotated to 90º for CPL imaging under 56nm Red Plate to show mainly blue colouring**.** **D)** CPL imaging and 56nm at 180º with the colour changed to red. This colour change from red to blue is usually indicative of a positive Z MFA fibre such as jute or hemp (Haugan and Holst 2013).

The above diagnosis, based on the Herzog Test, would be incompatible with fine furnishings.

If the MFA at -6º plus a Ct value of 0.89 with the X nodal marking is acceptable, then a tentative diagnosis for the bast fibre RW338 would be flax.

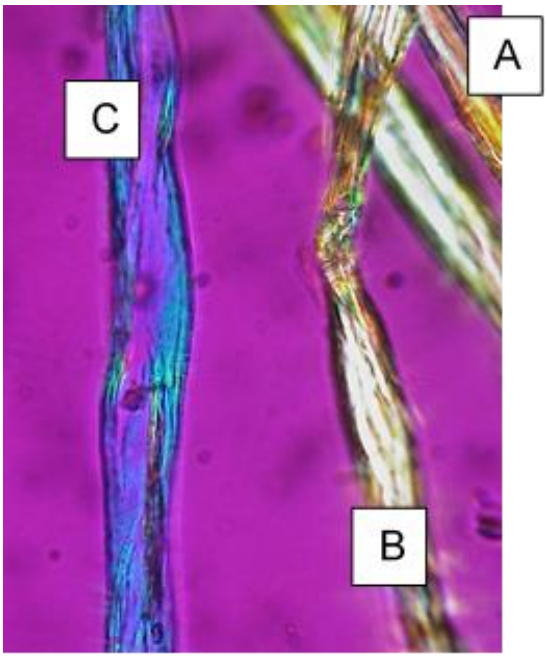

Figure 12.1.10. This a section from RW 338 of fibre imaging under CPL that shows three different fibres in the same location. A) bast fibre B) cotton fibr.e and C) a fibre that responds to Red Plate shift. (See comments in **12.1.8** below).

12.1.8 Comments on Temple Newsam Warren Collection

There was some success in diagnosing the samples provided from the collection, particularly with MFA and Ct determination for Sample RW 337. However, there was less success with the bast fibre from RW 338 where both MFA and Ct measurements were compromised and the Herzog Test proving unreliable due the reduction in image quality.

In general, when the method for the accumulation of these textiles is considered, in comparison with personal clothing and without knowledge of their post-acquisition cleaning and conservation, there are concerns regarding the possible cross-contamination of these utilitarian textiles with other fibres. The multi-fibre image **Figure 12.1.10** illustrate the concerns.

12.2. Case Study 2 - Cliffe Castle Egyptian Coptic Collection

To confirm that the morphological diagnostic features, as described in previous chapters, could be employed successfully on ancient, potentially degraded textile samples, access to the Egyptian Coptic Collection at Cliffe Castle was arranged (Cliffe Castle 2019). Previous authors had expressed concerns regarding the limited provenance for items that are mainly described as originating from a Petrie excavation possible from the Upper Egyptian sites Akhmim, Fayum and el Lahun. (Pritchard 2004: 1-3; Riggs 2012: 156-157).

12.2.1 Principal sites excavated by Petrie

Fayum was a major granary area in the Greco-Roman period probable destroyed due to mismanagement of the irrigations system and subsequently abandoned allowing a rapid covering of sand that preserved the archaeological sites. The late 19th and early 20th-century reclamations revealed several sites with the first survey conducted by Petrie in 1890 who recorded circa twenty sites and concluded the excavations at Hawara south-east of Fayum in the 1888/9 season. Examination of funeral offerings, including coinage, was used to determine the continued usage of the burial sites extended from the Ptolemaic period to the sixth century (Smalley 2015). Further excavations were undertaken within the el-Lahun corridor were Petrie discovered finely woven textiles from this 5th-century site in the ruins of the Valley Temple (Riggs 2012: 156-157).

The Whitworth Collection, described in **Section 12.3,** was provided by donations from private collections with additional donations of 260 textiles from Petrie in 1897. This latter selection of textiles is reputed to have come from the el-Lahun cemetery excavations at Fayum. Other donations in the early 20th century were gifted to textile collections in Halifax (Bankfield Museum) and Bolton (Bolton Library and Museum) by supporters of Petrie's Egyptian excavations. Similarly, the Cliffe Castle Collection is also based on donations from private collections assembled in the late 19th and early 20th centuries. The commercialisation of Coptic remains raises issues regarding the world-wide distribution of textiles particularly where this resulted in larger samples being cut into sections to meet the increase in demand (Linscheid 2001: 75-80; Pritchard 2004: 1; Riggs 2012: 56-57; Bankfield Museum 2018).

Stevenson (2014) reviewed both the British collection and distribution of Egyptian finds to museums, 1880—1915, the Pitt Rivers Collection of 134,000 at the University of Oxford to identify 112 collections of Egyptian artefacts being held in the UK. The author also notes that Petrie's work in the late 1880s became contingent upon support from donations and that one of Petrie's principal supporters was Jesse Haworth (1835-1912) who donated his share of artefacts to the Manchester Museum (Pritchard 2004: 4; Shamir and Baginski 2013: 77-88; Stevenson 2014: 10).

> "(T)he excavated artefact continues to be a source of western values, capitalist gains and imperial authority. ---------In such transactions for the continuing dispersal of objects, their associated contexts become easily detached (Stevenson 2014: 12).

12.2.2 Tunic fibre construction Qumran (Jordan)

Textile remains from the original 1950 excavation of Qumran were reported as being dispersed to various locations, poorly recorded and stored in inappropriate facilities which hindered the publication of relevant data. This problem has only now been corrected some 50years later (Sukenik and Shamir 2011: 206-225; Wild and Wild 2014: 721-783). The utilisation of plant fibres, their growth, harvesting and subsequent processing and assemblage provides a framework supporting the understanding of the social, economic and political structure of society. Garment shape and structure, including or excluding design ornamentation, can also inform societal, hierarchal and religious structures (Shamir and Baginski 2013: 77-88). The presence or absence of particular fibres through ages are noted as reflected the religious embargo imposed under Judean Law when the inclusion of wool within the textile was banned under *Sha'anezl Law* as the fibre taken from a living creature of God's creation was demeaned. (Bible Contemporary English version (2000), Deuteronomy 22: 1; Leviticus19: 19).

12.2.3 Tunic Design

Benaki Museum (Athens Greece) holds a collection of Egyptian textiles from the 3rd to the 10th century AD, a period of religious, political and cultural turmoil in the Eastern Mediterranean (Tsourinaki 1960). Among the collection, from the arid regions of Egypt, there were a many preserved textile pieces available for evaluation including tunics, shawls and furnishings. In particular tunics, the shirt type dress worn by men, women and children, and adopted by several cultures from the Roman Empire to Early Medieval times.

A range of fibre types, construction methods, decorations, and weaving styles presented typologies that serve to identify both period and culture.

From this collection, Tsourinaki (1960) examined the construction method from the early Egyptian Roman Period 30BCE to the Christian, Coptic Period 395AD to 642AD. Early linen or wool tunic constructions were short or long with wide sleeves and woven as a single cross-shaped piece on vertical twin beamed looms. While the looms did not survive there is evidence-based surviving pin beaters, loom weights and combs to determine the process. The weaving method to accommodate the large width required two weavers working side by side to complete, an arrangement that required joint conformity of pattern and style.

This one width style only required a single rolled side seam to complete with rolled hem and horizontal neck opening. Decorations, vertical shoulder bands (*clavi)*, woven bands (t*abulae*) or medallion circles (*orbiculi)* sewn at chest and knee height, were either woven into the garment or added as separate tapestry and embroidered features. These highly decorative styles included Christian and Pagan images as indicative of their period, a typology that assists period determinations along with symbolic images of rank and status. (Pritchard 2006: 33-34; Shamir 2005: 162-168; Shamir 2015: 48-60).

An individual illustration of tunic manufacture and design is presented by an artefact from the Benaki Museum Collection. Tunic (No. 7169) is a single width red woollen tunic of vertical symmetry from a cross-shaped loom Tsourinaki (1960: 209-212). The 2.52m full-length tunic was embellished with undyed woven bands (3.8cm), and four multi-coloured tapestry medallions at knee and chest depict leaves and flowers along with heraldic back-to-back yellow birds.

In common with other collections of Coptic textile artefacts, the provenance for the garment is unknown. However, evidence of body fluid staining indicates a burial find.

Access to similar textile artefacts from the same period was obtained from the Bankfield Museum Halifax UK to evaluate their Coptic collection assembled from Flinders-Petrie's excavation of the late 19th century and donations from other private collectors.

12.2.4 Bankfield Museum - tunic tapestry and embordered features

In support of the understanding of tunic design and fabrication access to the Coptic collection at Bankfield Museum was granted to examine the tunic assemblage. The broad appeal for donations of collections is evident from the museum list of donors that shows the entry immediately below Flinders Petrie as,

> "Donated from Mrs Ling-Roth nee Haigh. Born of English parents in Roubaix France". Courtesy of Bankfield Museum (2019).

The preservation of these Late 19th-century textile fragments is impressive, the fabric weaving structure, decoration style (weaving/embroidery/tapestry) can all be determined. In particular, it is the 1400year durability of the fibre colouring that is the most striking. As noted above the inclusions of symbols of Christianity and symbolic *maenad* aids interpretation of cultural and structures typologies and provenance **Figure 12.2.1, Figure 12.2.2.**

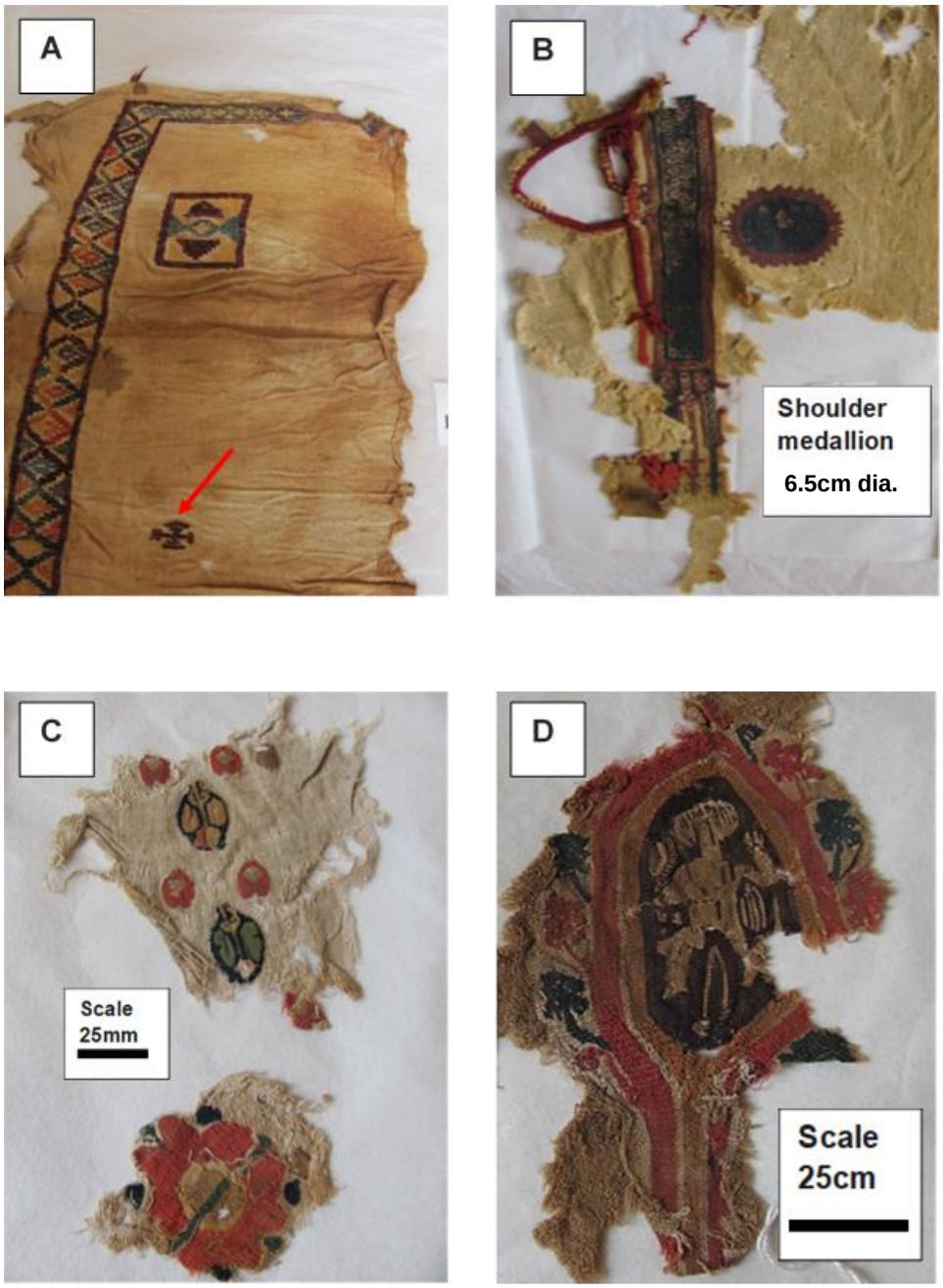

Figure 12.2.1. Illustrations of tunic tapestry and embroidery decorations A. Hemline embroidered geometric border and cross (indicated on image); the cross has been interpreted as a Christian symbol. Fragment size 50x30cm. B. Part of a clavus with a small 6.5cm diameter medallion. C. A range of flower shapes woven into a light-coloured tunic. D. Maenads (dancing figures) with flower surround woven into the clavus. Images courtesy of Bankfield Library and Museum Halifax UK.

Figure 12.2.2. Tunic 40cm diameter central medallion: geometric embroidery design. Courtesy of Bankfield Museum Halifax.

12.2.5 Sample preparation and determination of MFA and Ct

In discussion with the Cliffe Castle Museum Archivist and having consideration for the continuing conservation of the Collection, the existing conservation and durability of the Coptic artefacts were assessed. With agreement, small samples 25mm were selected from these fibres for diagnosis. For the aged, degraded fibres of limited strength, it was necessary to redesign the sample moulding and fibre extraction procedures to be employed.

12.2.6. Method for preparation of fibre mounting and analysis

The initial mounting method employed a vertical weighted presentation around a wire support. The 230µm wire support served as a location indicator for the fibre sample of circa 15-30µm diameter, as illustrated in **Figure 8.8.**

It was necessary to redesign the mounting to limit the stress applied to the degraded fibre; a horizontal orientation would be preferred. However, this would also require the inclusion of an opening for the deposition of the epoxy resin encapsulation **Figure 12.2.3.**

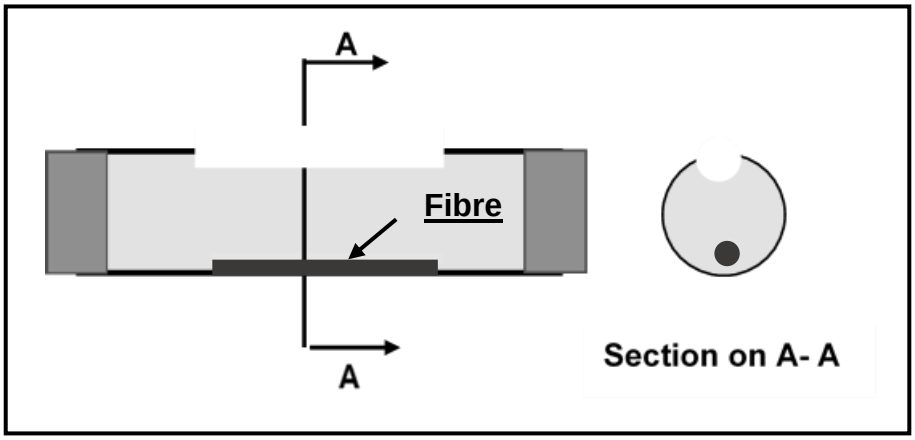

Figure 12.2.3. The revised design of mounting for degraded 5mm length archaeological fibre circa 25µm diameter. The design included an opening in the upper surface of the 9mm diameter plastic forma with wooden sealing blocks secured at each end.

The mounting was filled with EpoFix epoxy resin and cold cured in a fume cupboard for 24 hours and subjected to end grinding and polishing. 1mm sections were diamond cut and polished for microscope examination under a Nikon Optiphot compound microscope under cross-polarised light (CPL) at 40x magnification viewed with a Nikon BD Plan 40/0.65 objective lens. The fibre CSA images produced were subjected to ImageJ analysis to determine their Ct.

For MFA imaging of potentially degraded fibre samples, these were initially placed in a lightweight plastic container and submerged under distilled water and floated within a sonic water bath for 10minutes cleaning.

The fibres were removed and dried before separation in distilled water under magnification to obtain individual fibres of circa 10µm diameter suitable for MFA and Herzog Red-Plate testing and microscope imaging.

12.2.7. Fibre diagnosis Cliffe Castle assemblages

Sample CC9 from the Cliffe Castle collection was subjected to both MFA and Ct diagnosis and the results are shown in the tabulation included in **Figure 12.2.4.** The MFA angle of -8º is shown, image left reflecting the microfibrillar angle displayed bottom centre. Ct values obtained from the six fibre area cross-sections are tabulated and the mean value of 0.871 with a standard error of 0.082 is listed.

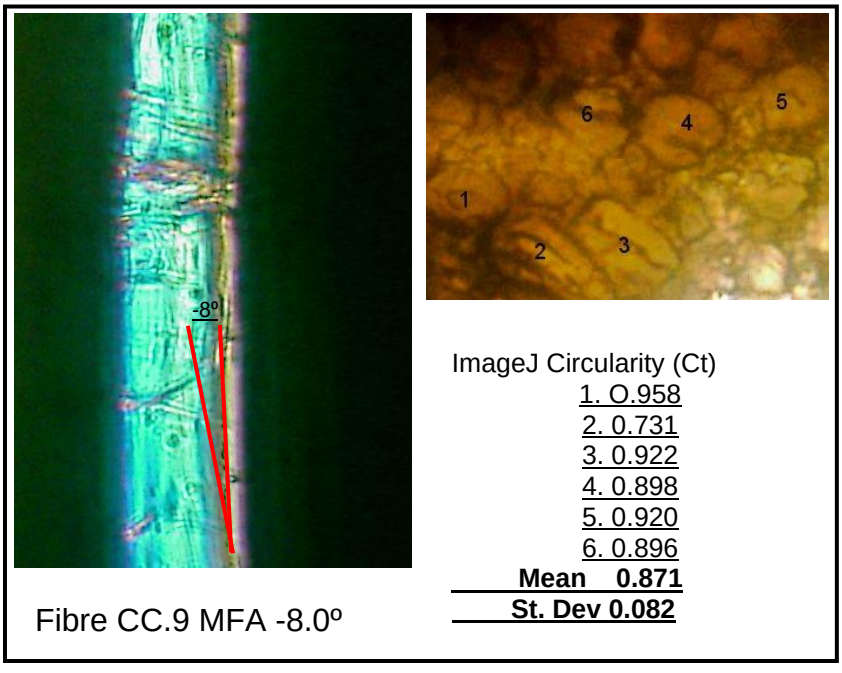

Figure 12.2.4. Details of MFA and Ct measurements. Sample No CC9 from Cliffe Castle Coptic fibre (DMU 95/071.1-13). Courtesy of Cliffe Castle Museum Keighley UK.

In a supplementary test, for Red Plate shift (Herzog Test), fibre from sample CC9 was rotated under CPL to achieve extinction before inserting the red plate at 45º. The colour change from red at 90º to blue at 180º is indicative of a negative microfibrillar angle (MFA) associated with flax and nettle fibres **Figure 12.2.5.**

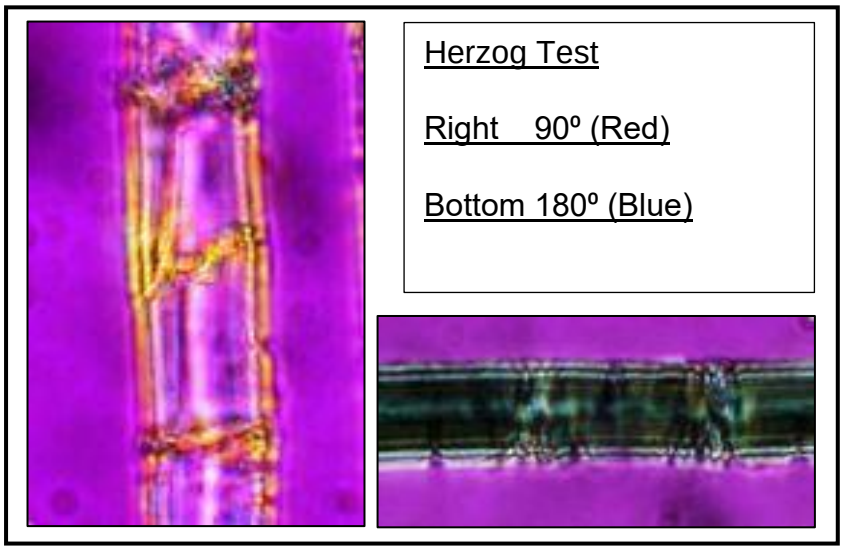

Figure 12.2.5. Details of Herzog Red Plate Test for MFA**.** Sample No 9 from Cliffe Castle Coptic fibre (DMU 95/071.1-13). Courtesy of Cliffe Castle Museum Keighley UK.

The MFA angle of -8.0º and mean Ct of 0.871, coupled with the Herzog Test results confirmed the sample fibre to be flax. The crossed image at the nodal points adds to the diagnosis.

A similar analysis procedure was completed for Sample CC1 from the same assemblage (DUM 95/071.1-13).is shown in Figure 12.2.6. Unfortunately, the image of the microfibrillar angle MFA is indetermined due to the poor-quality imaging. However, as with CC9, Ct values were obtained from six fibre area cross-sections to determine a mean value for Ct at 0.903 with a standard deviation of 0.042. The Herzog Red Plate Test were also indeterminate, the fibre could only be identified as a “bast fibre”.

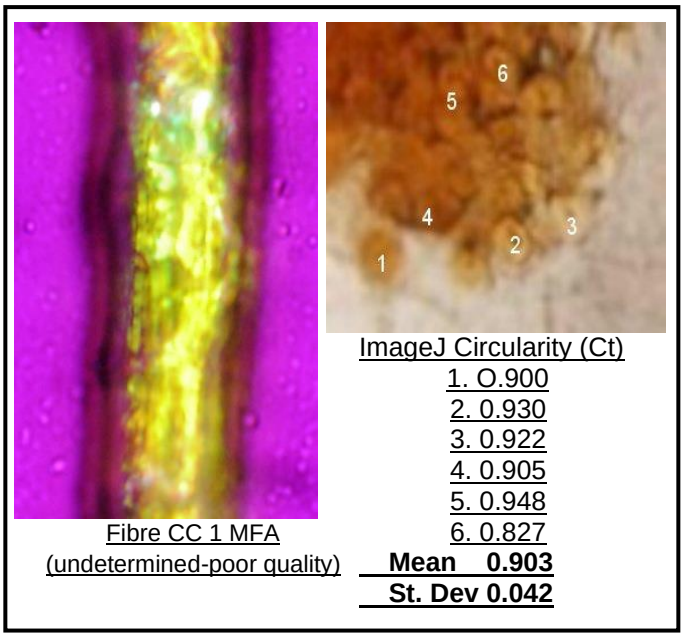

Figure 12.2.6. MFA and Ct determination for sample CC1**.** Left**.** Inadequate quality image for MFA analysis. Right. CSA with fibres numbered, Ct visible but outline obscure.

Figure 12.2.7. Herzog Test. Sample CC1 imaged but not a clear indication of Red Plate shift.

12.2.8 Cliff Castle: discussion and resume

As noted, in determining the research objectives, there are understandable restrictions that limit access and sample size available from archaeological samples. Ideally access to the additional assemblages in this collection would serve to extend the diagnostic statistics but such assemblages are rightly now well conserved with few associated loose fibres available. The reported improvement in minimally intrusive diagnostic techniques, based on minimum sample size, to determine MFA and Ct as diagnostic features may provide reassurances in diagnosing archive assemblages.

12.3 Case 3- Mass burial rescue excavation - Kasr-el-Yahud (Qasr-al-Yahud) Jordan

Kasr-el-Yahud (Qasr-al-Yahud) a baptism site on the River Jordan, according to tradition Jesus was baptised here by John the Baptist. Monasteries and |churches were first established here in the Byzantine Period, often called the Eastern Roman Empire or Byzantium (AD 330 to 1453). The change, following the Muslim conquest of Roman Egypt in (AD 639-646) and an earlier invasion by the Persian Sassanid Empire (AD 616-629), made conditions difficult and the monasteries became places of refuge and protection (Zias 1988: 197-200; Janaway 2002: 386; Shamir 2005: 162-168). Jerusalem was captured in the early 7th century, under a Jewish and Persia alliance, and it is recorded that thousands of Christians were massacred. However, there are doubts regarding the actual figures of up to 65,000 men women and children being slaughtered (Crawford 2013: 57-61). With one notable exception, Mamilla pool, the archaeological record does not support the reported figures for victim numbers and proposes that the figures were exaggerated to gain Christian support. The site at Kasr-el-Yahud has been identified as a massacre site with an associated mass burial in AD 614 (Zias 1988: 197-200).

When baptisms came under Turkish control, the site was abandoned and remained so until the introduction of British Rule following the Crusades of the 12th and 13th centuries. With the site now more secure, baptisms and pilgrimages were renewed with churches of many denominations being built stretched along 3.3km of the west bank. **Figure 12. 3.1** The 1956 earthquake caused severe damage to the site and the subsequent Six-Day War saw Israel take control of the West Bank.

Currently, the baptism site is inaccessible due to landmines, and tourism and pilgrimages are now directed to Yardenit located south of the Sea of Galilee.

12.3.1. Geographic location Kasr-el-Yahud (31.84ºN- 35.54ºE)

The site is on the west bank of the River Jordan 10km east of Jericho, and 6km north of the Dead Sea, and lies on the Jordan Plain east of Jericho. Jericho sits on a raised plateau at -852 feet (-352m) below sea level; the valley is a further 165 feet (53m) feet below the plateau. Temperature varies from a high of 35ºC in January to 22ºC in July. Precipitation is very low at an average of 81mm per month with September being the driest. The arid desert climate of the Judean Desert assists in the preservation of burial textiles and garments (Shamir 2015: 48-60).

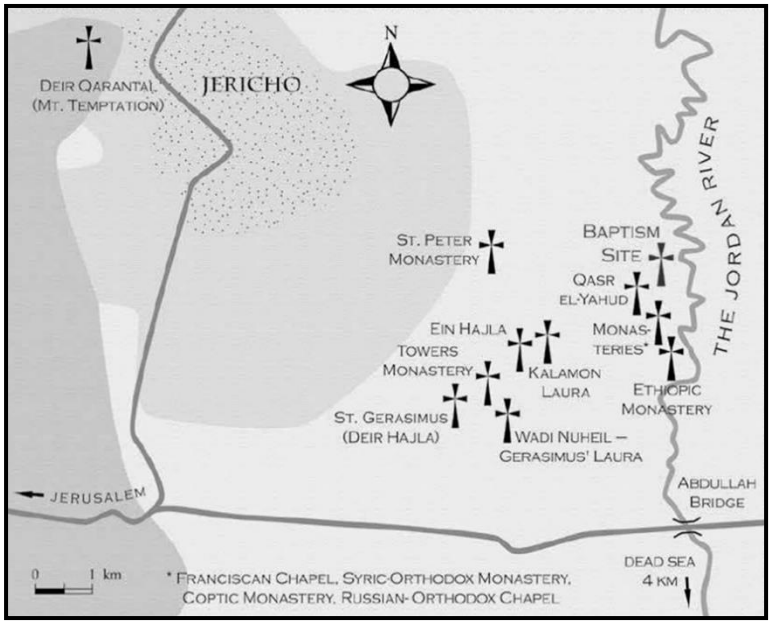

Figure 12.3.1. The vicinity of Qasr el-Yahud. **(**Dina Shalem 2019, Ostracon, Israel Nature and Parks Authority).

At this Jordan/Israeli border, created on the West Bank of the River Jordan following the 1968 Six Days War, work was undertaken in 1983 to reinforce the border which exposed the remains of a mass grave. The grave contained skeletal remains of 300 men, women and children, 90% of which had been destroyed by the construction work (Shamir and Baginski 2018: 77-88). However, 34 skeletons were retrieved in a rescue excavation in 2002 (Shamir 2013: 49) This mass grave, with bodies skeletonised and laid on top of each other in an East to West Christian alignment, was attributed to the AD614 Byzantine-Persian invasion and slaughter of the hospital patients. From anthropological evidence, the bodies were identified as probably Egyptian or, by reference to skull shape, Nubian. The skeletal analysis showed evidence of tuberculosis, leprosy and facial disfiguration of the hospital patients (Zias 1988: 197-200; Janaway 2002: 386; Shamir 2005: 162-168). Some of the body parts were clothed with substantial textile remains around the limbs with other, more degraded textiles evident around and below the body cavity Similar body wrappings are noted at Qarara Moyenne -Egypt (Huber 2015: 120-125).

The Christian burials indicate a subsequent intervention following the massacre, although the presence of faecal pellets in the grave attests to attack by jackals before access for burial was possible. The delay is attributed to period awaiting the retreat of the Byzantine /Persian forces. There were two hundred and thirty-seven textile fibres identified in a rescue excavation undertaken in an unsafe environment with severe time constraints (Shamir 2005: 162-168; Shamir 2015: 48-60; Janaway 2002: 386).

The largest sections recovered from the long-sleeved ankle-length tunics came from the sleeve, shoulder and neck regions with the largest pieces in the range 550 to 1190mm by 1550mm. Fibres were mainly undyed linen or cotton with only three wool remains identified The low survival rate was attributed to microbial degradation with a proviso that the actual fibre mix of linen, cotton and wool would most likely reflect the fibre mixture for garments of a similar age (Janaway 2002: 386; Fuller 2008: 1-26). However, in the report from the excavation at Qumran, it was noted that, for this site located south of Kasr-el-Yahud, the tunics were all bleached linen with minimal decoration. The authors attribute the basic tunic design as indicative of a group who wished to preserve this style as a religious differential (Sukenik and Shamir 2011: 206-225). In particular, the authors record the Torah Law's influence of prohibiting the wearing of cloth containing both wool and linen *(shaʿaṭnez)*. As the Ksar el Yahud site is a Christian burial, this restriction would not be applicable although the textile manufacturing/design criteria could influence garments manufactured under textile production associated with patients who have travelled from other regions.

12.3.2. Egyptian Tunic design, construction and decoration

Tunic manufacturing methods have changed from the one-piece textile "woven to shape", with no cutting required and finished with a single seam, to two basic types sleeveless and sleeved. The sleeveless tunics were produced from horizontal tunic lengths mounted along the weft run and woven by two weavers working side by side.

Alternatively, sleeveless tunics could be completed with two components assembled across a shoulder seam, or one single length folded in half with a side seam.

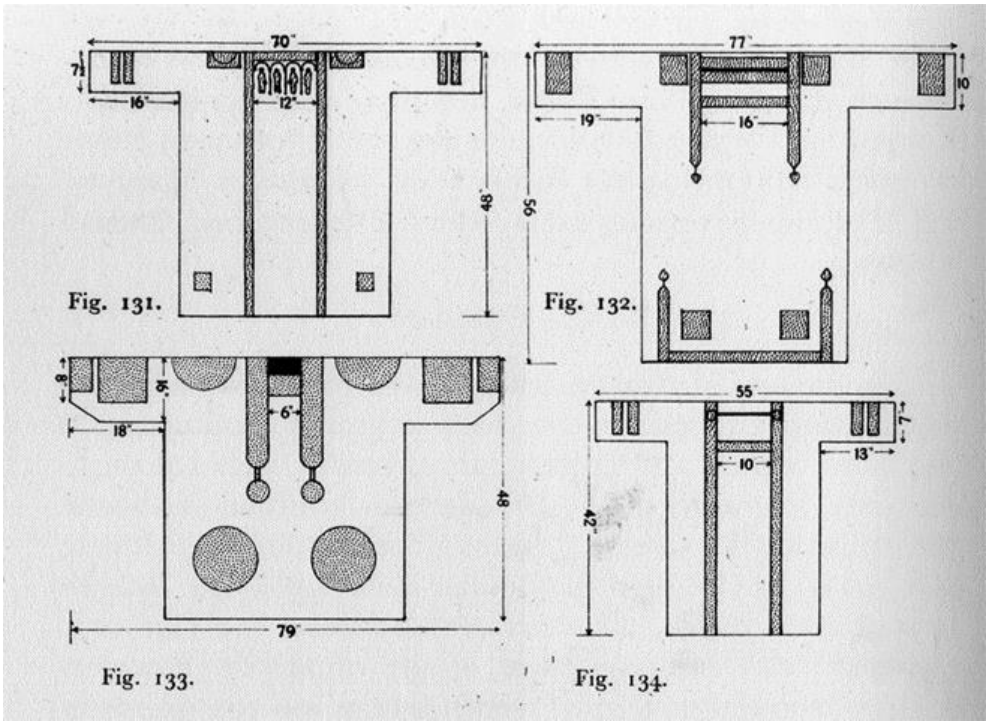

Figure 12.3.2. Diagrams of ornamented tunics (M. Houston, Ancient Greek, Roman and Byzantine Costume and Decoration. London 1931: Fig.131-134). Dimensions in inches

Tunics were also manufactured with three components, a tunic top and two attached skirt lengths, with a central horizontal rolled seam and two side rolled seams (Pritchard 2006: 66-68; Shamir and Baginski 2013: 77-88).

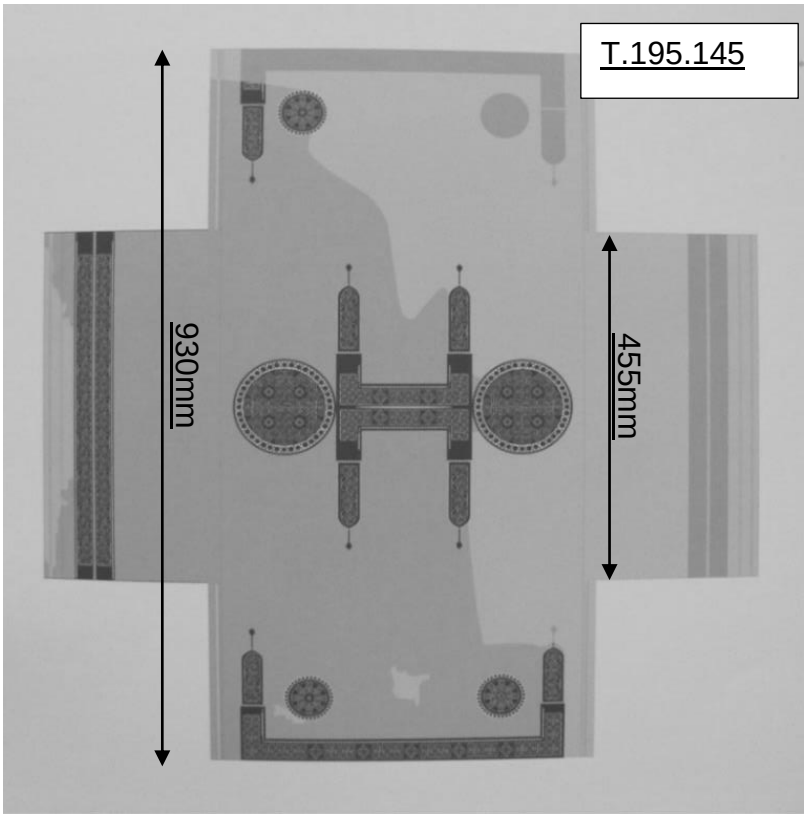

Figure12.3.3. Diagram of wide-sleeved linen tunic T.1995.145. (Pritchard 2004: 53) Photographs courtesy of Whitworth Museum Manchester

The tunics also carried shoulder and kneecap square or oval ornamental medallion decorations. Sleeve and hem bands were occasionally included **Figure 12.3.4, 12.3.5, 12.3.6** and **12.3.7.** Features depicted within the decoration include pattern repeats, plant and animal representations and human figures, dancing maidens, *maenad,* mythological figures, *satyrs* and winged gods, *erotes.*

Figure 12.3.4. ‘Leukyon´e’; A. Gayet, Fantˆomes d’Antino´e (Paris 1904) (Thomas 2007: 139).

Figure 12.3.5. Details of Coptic child's tunic design. Whitworth Museum ID T 1993.27**.** Childs linen tunic (585 mm height) with simple neck and sleeve bands the tunic has side gores inserted to fit larger sizes. (Pritchard 2004: 110) Photograph courtesy of Whitworth Museum Manchester.

Figure 12.3.6. Detail of sleeve band design Whitworth Museum ID T 8397**.** Sleeve bands from a linen tunic. The tongues of the hare and lion and the duck's beaks and feet are highlighted with red wool. (Pritchard 2004: 62). Whitworth Museum ID T 1993.27. Photograph courtesy of Whitworth Museum Manchester.

Figure 12.3.7. Detail of wide-sleeved tunic design Whitworth Museum ID T 1995.145. Wide-sleeved linen tunic (1.19m height) showing short clavi with terminals, shoulder medallions (260mm diameter) with smaller medallion repeats at the knee, and hem and sleeve bands. The sleeves are 565mm wide. (Pritchard 2004, 110) Photograph courtesy of Whitworth Museum Manchester.

12.3.3 Nature of fibre sample recovered from Kasr-el-Yahud

From the original 1989 excavation of 237 items, a proportion was held in storage at the University of Bradford for future investigation. This assemblage consists of 40+ congealed and degraded samples of mixed textiles that were held in separate packages and labelled according to the site location within the mass grave. Of necessity, because of the limited time available for this rescue excavation, there was insufficient time to wash and prepare all but the largest samples for evaluation on-site (Janaway 2002: 379-402).

The assemblage available for this research programme was accessed from a University of Bradford collection composed of small textile sections with a range of fibre type, fibre diameter, weaving mode and colour.

The fragile nature of the collection can be envisaged from the detail below of one highly commingled assemblage recovered from the site unlabelled **Figure 12.3.8.** As noted above the time constraint placed upon this recovery excavation site and the overlay of the skeletal remains limited site provenance for the individual remains and on-site post-excavation cleaning and washing. Two hundred and thirty-seven textile samples, mostly linen and cotton with minimum survival of wool fibres were recovered. There was no apparent differential survival between the linen and cotton material. For the assemblage available from the University of Bradford collection the fragments were mostly of limited size although larger fragments were recovered on-site, 550 x 1550cm, 1550 x 1190 cm from sleeve, shoulder and neck regions. However, textiles from below the body were generally in worst conditions (Janaway 2002: 386).

Figure 12.3.8. Kasr-el-Yahud textile assemblage: typical comingled assortment of textile fibre recovered.

12.3.4 General assessment of the collection

Initial examination of the collection assemblages indicates a range of fibre colouring, weave structure and fibre dimensions **Figure 12.3.9**

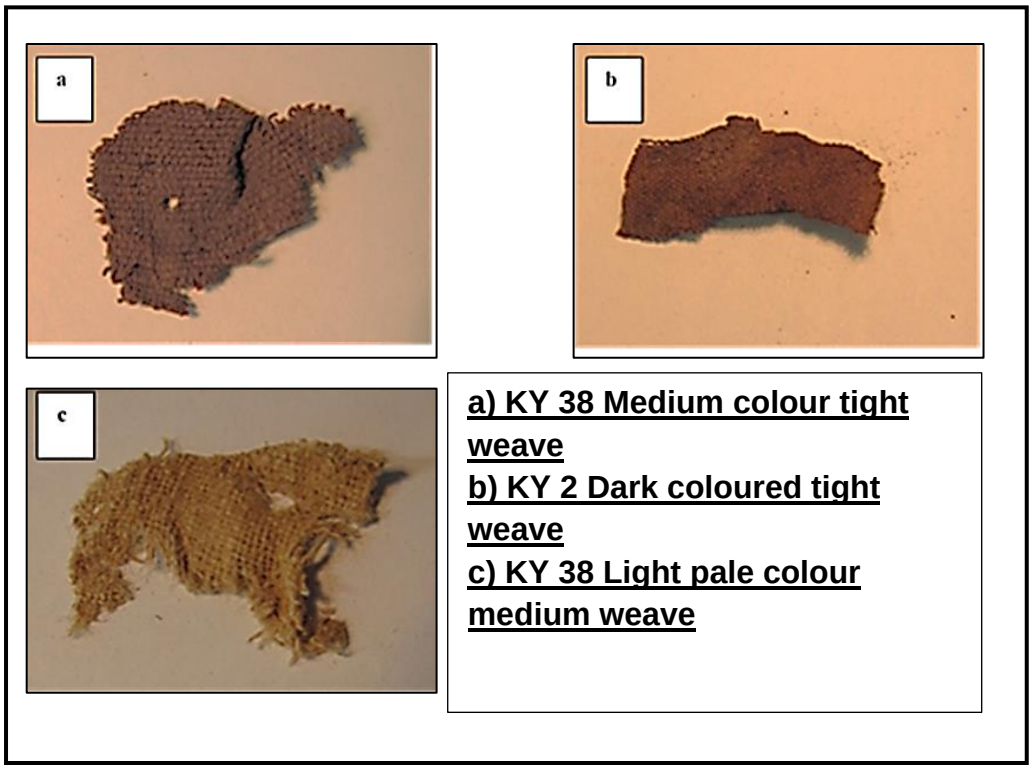

Figure 12.3.9. Illustrations of textile colour range that may be related to fibre type.

Several samples, similar to the above, were present within the research assemblage including two larger dried and congealed textile pieces. The first, a congealed dehydrated sample, was rehydrated with a spray of distilled water before reshaping, flattening and drying **Figure 12.3.10.**

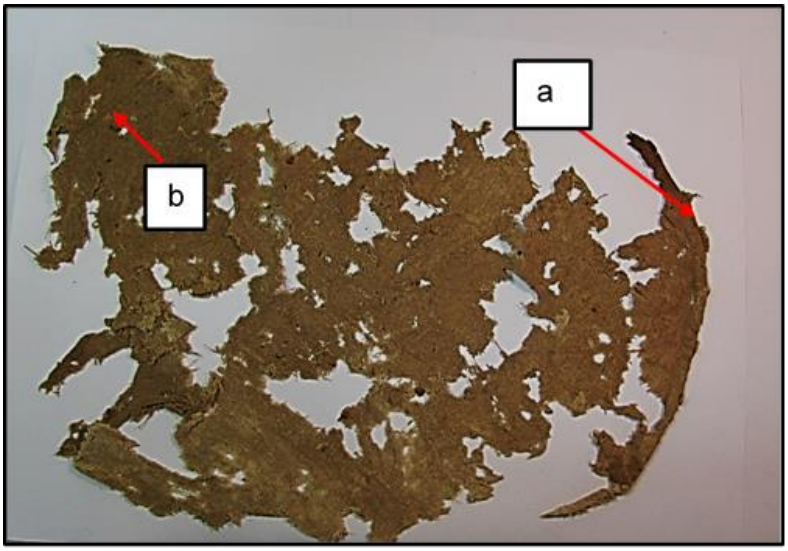

Figure 12.3.10. Sample KY7 Rear of tunic: rolled neck seam evident on the right(a) and rolled side seam top-left (b). Size 38 x 23cm.

A similar section of rolled seam from (KY2) is shown in **Figure 12.3.11** there is evidence of the rolled seam at the bottom left, there is no evidence for shoulder decoration, *calvi* or medallions. The rolled side seam assembly is seen **A** bottom left.

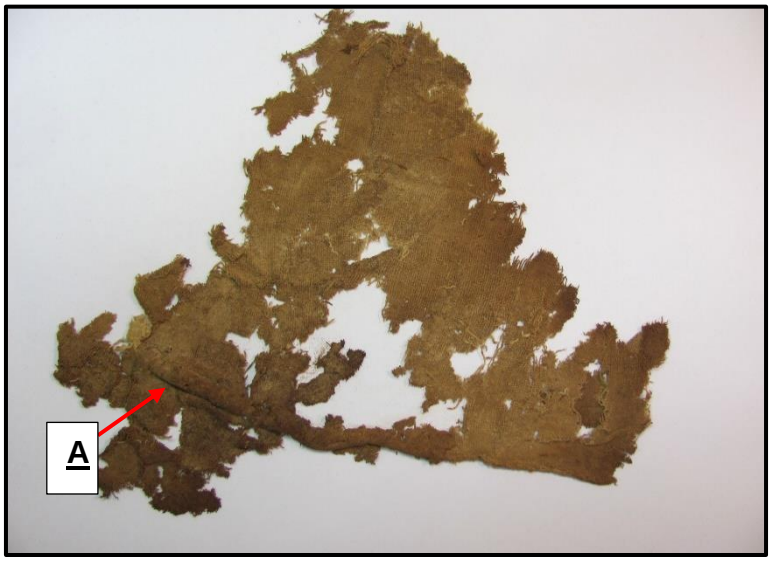

Figure 12.3.11. KY2 Large textile fragment: evidence of rolled side seam at bottom left at “A”. Size 24x21 cm.

While there was no evidence for tunic decoration, one sample of simple dark banding, was woven into a tunic piece **Figure 12.3.12.**

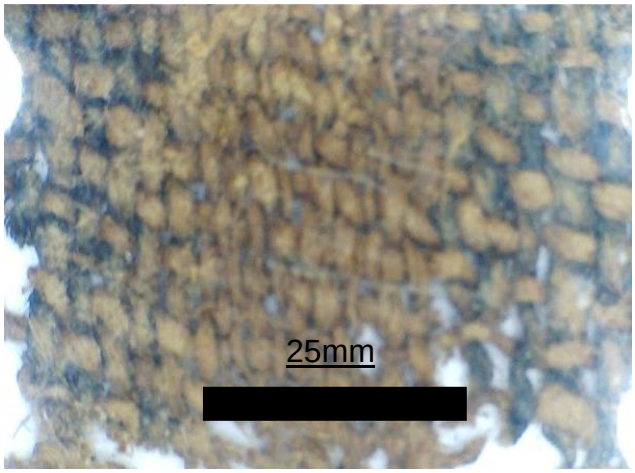

Figure 12.3.12. Detail of dark banding woven into tunic fabric: banding shown on both left and right edges.

12.3.5 Method- preparation of sections and imaging

The principal aim of this examination of these Kasr-el-Yahud (KY) was to evaluate the durability of the MFA and Ct diagnostic features proposed in this work. Unfortunately, the long-term degradation of the fibres within the burial environment made them friable and unsuitable for suspension within the previously reported vertical mounting structure. A compromise was required, and this was achieved by moulding the fibre samples in larger 9mm plastic tubes held in the horizontal plane with plugs at each end and a gap created along the top of the plastic mould for access (See Section 12.2.8). Thus, semi-circular moulds of the fibres were produced for grinding, polishing, and sectioning into 1mm slices for microscopic examination and imaging

12.3.6 Determination of microfibrillar angle (MFA) and circularity (Ct) for KY 12 fibre

The method, for determination of the Ct of modern and minimally processed fibres, has been described in detail in previous chapters. However, for archaeological textiles, which may have been subjected to degradation environments, there was an overriding need to limit sample size sectioning and processing. Additionally, the fibre production techniques and the ability to produce fine fibres of less than 10µm challenged the imaging techniques employed within the programme. Consequently, there was a challenge to establish if those techniques could measure MFA and Ct to achieve meaningful results.

An initial trial of a single fibre from KY12 was conducted to confirm the practicality of mounting, polishing, and sectioning prior to submitting the samples to imaging and evaluation. The modified design for horizontal mounting was utilised on 25mm of fibre from KY12 and the following section produced **Figure 12 3.13**. The image was obtained with transmitted light with Nikon Optiphot compound microscope under cross-polarised light (CPL) at 40x magnification viewed with a Nikon BD Plan 40/0.65 objective lens. The images were subsequently analysed with ImageJ software to determine particle dimensions (Rasband 1987; Broeke *et al.* 2015). There is a need for caution in separating the fibre CSA from similar circular sand particles included within the image. It was decided that the presence of lumina would serve as a guide **Figure 12.3.13.**

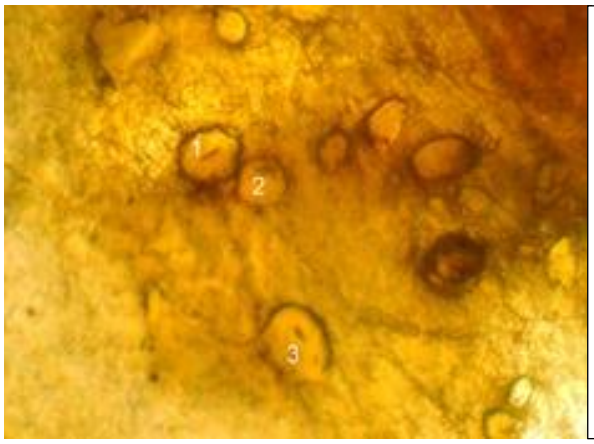

Fibre CSA No.	Circularity Ct ImageJ
1	0.945
2	0.951
3	0.944
Mean	0.947

Figure 12.3.13. **KY 12** Circularity of fibre samples. ImageJ analysis of fibres in cross-sectional area of K12.

In previous chapters the determination of MFA has been achieved by either or both direct measurement of observed angle displayed by microscope imagery and Herzog Red Plate Test, both outcomes are shown below **Figure 12.3.14** and **Figure 12.3.15**

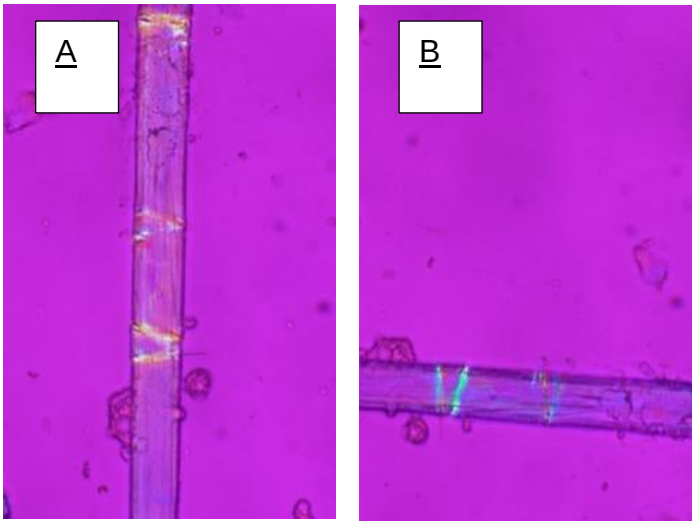

Figure 12.3.14. KY12 fibre 12µm diameter rotated from extinction at 90º. With Red Plate (56nm) introduced, the colour change is evident from red at 90º to blue at 180, a flax fibre.

The subsequent birefringence colour change, a) Red shading evident at 90º to, b) Blue tinge evident at 180º, indicate the negative microfibrillar angle. Hence this is flax. The Herzog Test does not measure the degree of negative angle and the determination must qualify this difference between the sample and other bast fibres presenting negative MFA orientations.

In previous chapters, it is noted that observation of fibres under CPL can provide images of microfibres. These displays are difficult to determine but, they can be located with due care and diligence, and the MFA angle assessed with AnalySIS software Image **Figure 12.3.15.**

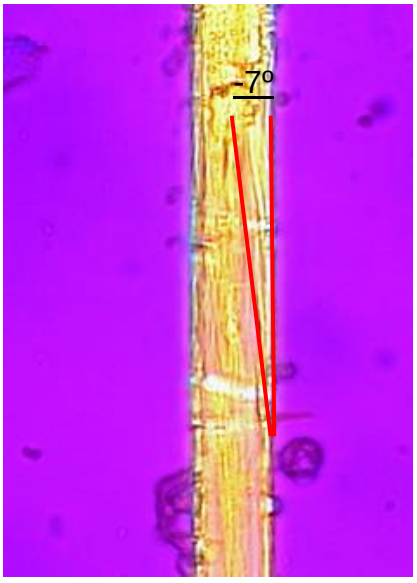

Figure 12.3.15. KY 12 Determination of MFA Transmitted light under CPL with 56nm Red Plate inserted**.** The angle of microfibrillar at -7ºcan be seen to the right of the sloping line.

The success achieved in the measurement of MFA and Ct in this trial was extended to include similar tests to be applied to a random sample of 25% of the KY fibre assemblages available within the collection.

12.3.7 Extension of MFA and Ct evaluation to random samples drawn from the Kasr-el-Yahud collection

There are 40 labelled and site locations detailed in the catalogue of fragments held in the University of Bradford collection of excavated assemblages recovered from the mass-burial. The intention is to compare the results obtained from the analysis of KY 12 to determine the efficacy of the MFA/Ct diagnostic technique applied.

The random listing selected 9 locations, **KY11, KY26, KY36, KY3, KY8, KY22, KY31, KY37 and KY41**, these plus **KY12** above would provide 25% of the assemblages available. The following images, **Figures 12.3 16 to 25,** show the range of assemblages selected. The first images presented are for the cotton fibres **KY11, KY26 and KY36.**

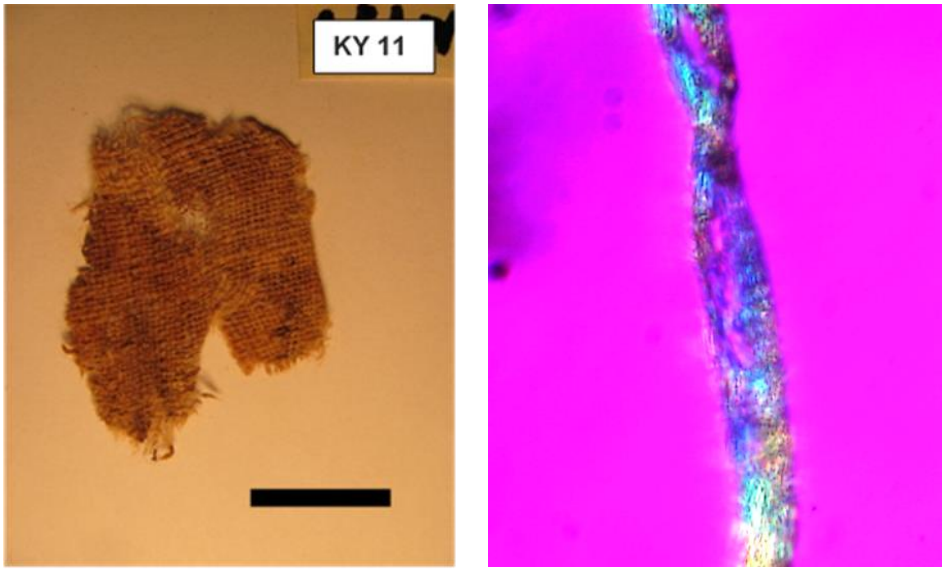

Figure 12.3.16. KY 11 Left. Fragment of textile basic tabby weave 9/9 threads per. cm. Right. 13µm thread under 56nm Red Plate, no extinctions are shown and there was no attendant colour change. A degraded cotton fibre, no CSA imagining was possible. Scale 25mm.

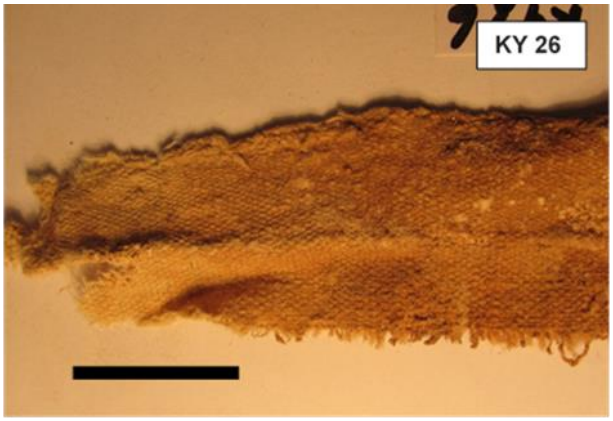

CSA Unsuitable for

ImageJ analysis

Figure 12.3.17. KY 26. Fragment of textile basic tabby weave 16/16 threads per cm. Seam present along the centre. Right. 8µm thread under 56nm Red Plate, no extinction shown and no attendant colour change. A degraded cotton fibre, no CSA imagining was possible. Scale 25mm**.**

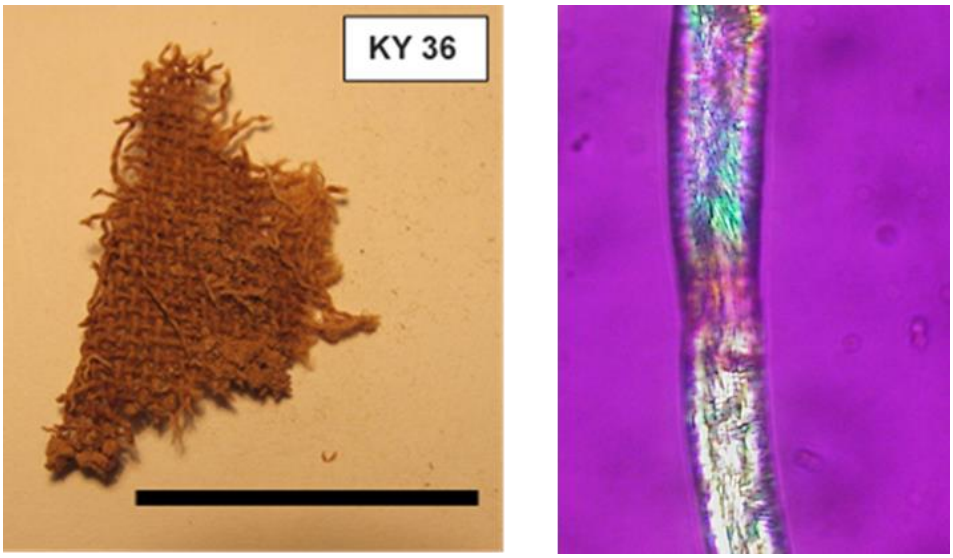

Figure 12.3.18. KY 36. Left. Fragment of textile basic tabby weave 9/9 threads per.cm. Right. 22µm thread under 56nm Red Plate, no extinction shown and no attendant colour change. A degraded cotton fibre, no CSA imagining was possible. Scale 25mm**.**

The cotton fibre appears to have degraded more rapidly than the flax fibres to the extent that their cross-sectional images are unsuitable for ImageJ Analysis. From the ten fibres included in this random sample, three (30%) were diagnosed as cotton.

The following fibres were diagnosed as flax with fibre diameters ranging from 20µm down to 10µm. At this lower fibre diameter presentation of microfibrillar within the image is unlikely.

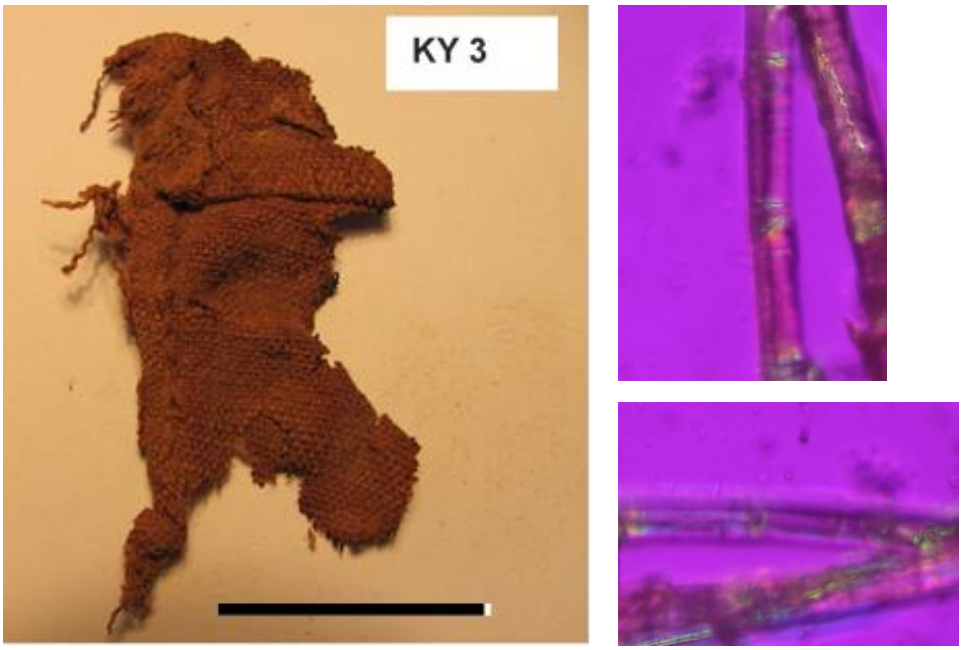

Figure 12.3.19. KY 3 Left. Fragment of textile basic tabby weave 16/16 threads per cm. Repaired section visible centre bottom and horizontal seam visible near the top. Top Right. 15µm thread under 56nm Red Plate. Top Right Red at 90º. Bottom Right. Blue showed at 180º. A flax fibre. Unfortunately, the CSA image was of poor quality and unsuitable for ImageJ analysis. There was no visible MFA included within the imaging Scale 25mm.

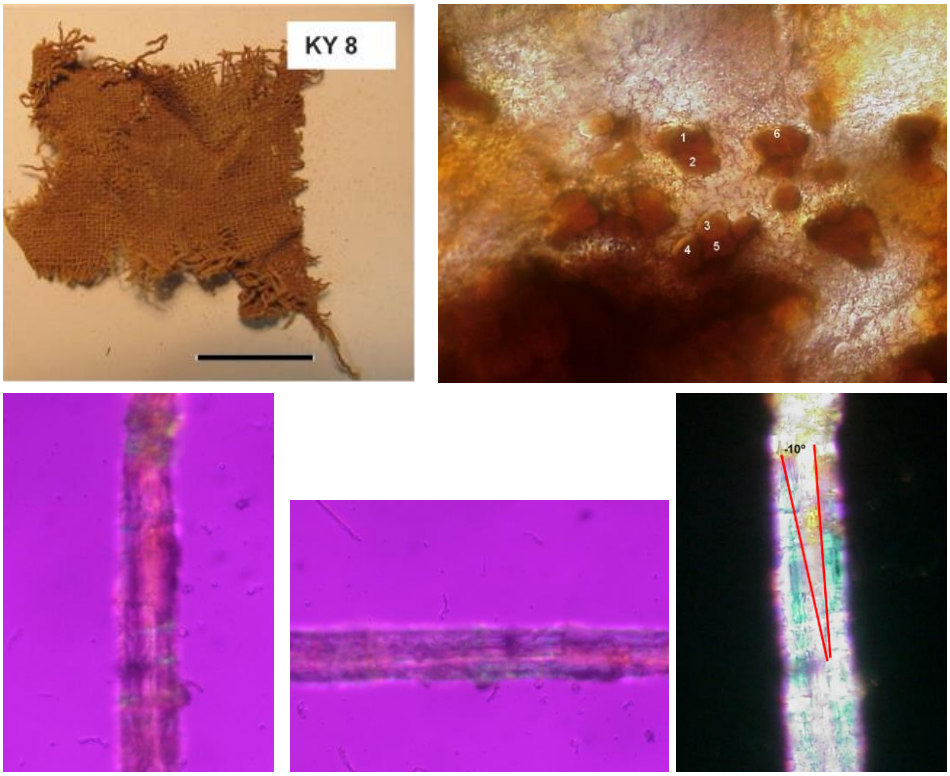

Figure 12.3.20. KY 8. Top Left Fragment of textile basic tabby weave 16/16 threads per cm**.** Bottom Left. 10µm thread under 56nm Red Plate, red at 90º. Bottom centre, blue shown at 180º, a flax fibre. Bottom Right, **MFA (-10º)** measurable here with microfibrillar visible top right of the image. Top Right cross-sectional image suitable for measurement of Ct with ImageJ **Table 12.3.1.** Scale 25mm.

KY 8 CSA Image No.	Circularity (Ct)
1	0.743
2	0.772
3	0.921
4	0.912
5	0.923
6	0.848
Mean	0.853

Table 12.3.1. KY 8 ImageJ analysis of circularity (Ct). Fibres identified 1-6 on area cross-sectional image in Figure 11.4.

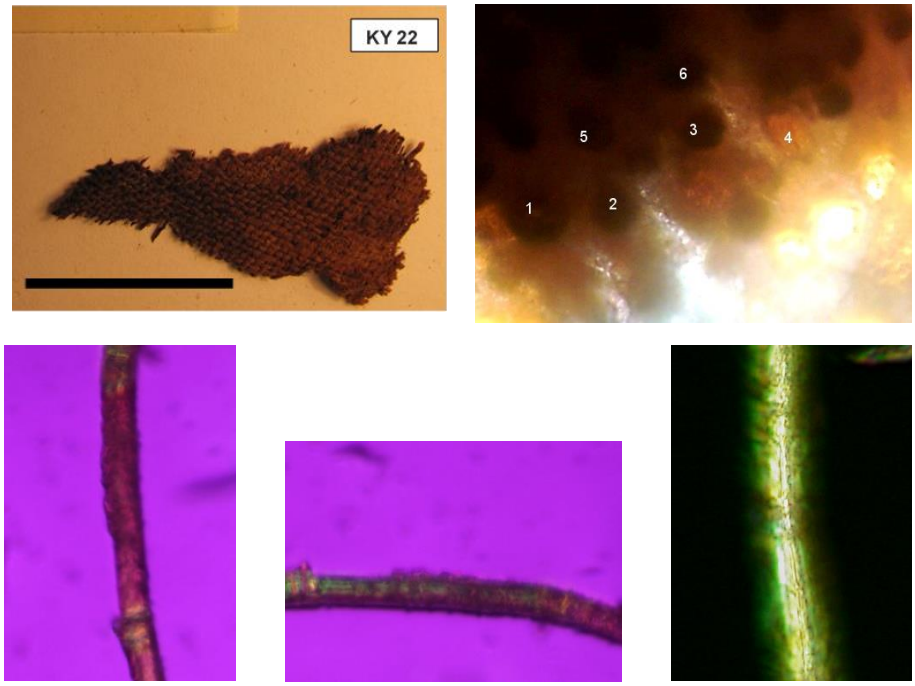

Figure 12.3.21. KY 22 Top Left. Fragment of textile basic tabby weave 12/12 threads per.cm. Bottom Left. 13µm thread under 56nm Red Plate, red at 90º. Bottom Centre, blue shown at 180º, a flax fibre. Bottom Right. MFA no microfibrillar visible. Top Right cross-sectional image suitable for measurement of Ct with ImageJ **Table 12.3.2. Scale 25mm.**

KY 22 CSA Image No.	Circularity CT
1	0.939
2	0.932
3	0.909
4	0.866
5	0.919
6	0.894
Mean	0.910

Table 12.3.2. KY 22. ImageJ analysis of circularity (Ct). Fibres identified 1-6 on area cross-sectional image in Figure 12.3.21.

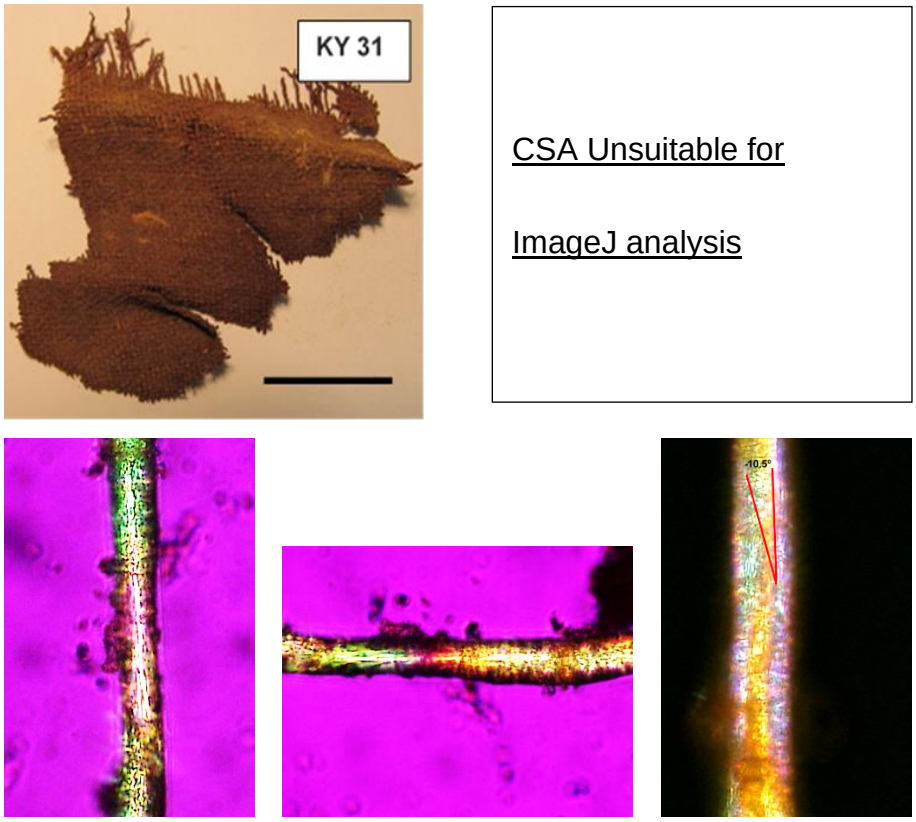

Figure 12.3.22. KY 31. Top Left. Fragment of textile basic tabby weave 12/12 threads per cm**.** Bottom left. 13µm thread under 56nm Red Plate, red at 90º. Bottom Centre, green shown at 180º, possibly a flax fibre. Bottom Right, MFA microfibrillar visible at 10.5º. Top Right cross-sectional image unsuitable for measurement of Ct with ImageJ Scale 25mm.

The images for KY 31 are of poor quality, microfibrillar angle (MFA) as measured at -10.5 is based on a single presence at centre right. The CSA images are also inconclusive. Hence the diagnosis of KY31 is suspect.

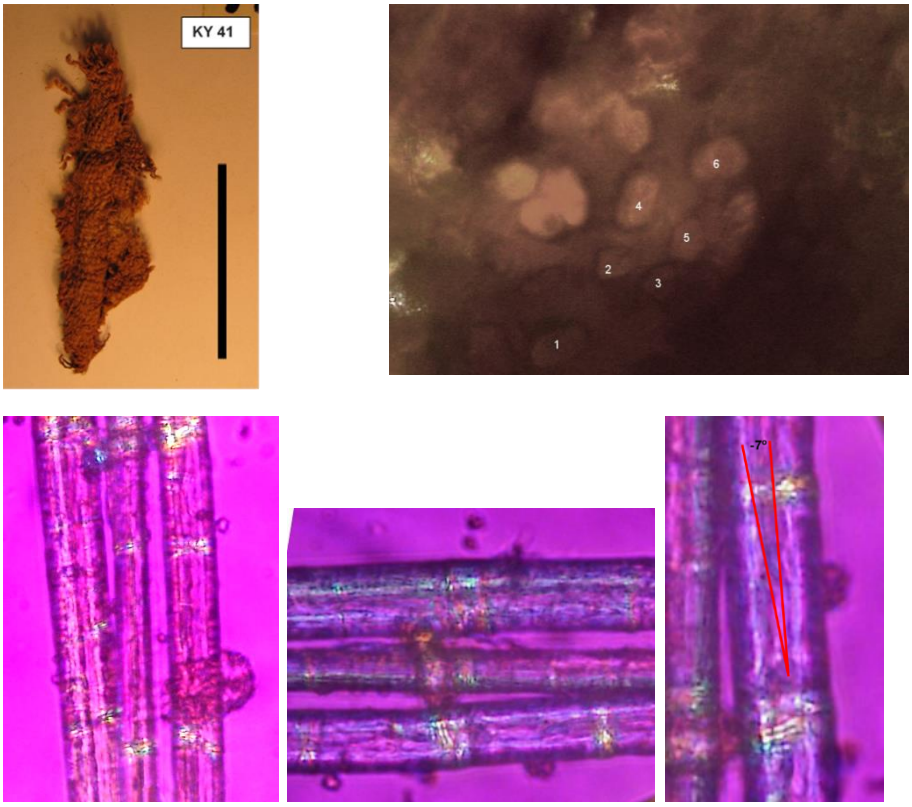

Figure 12.3.23. KY 41. Top Left. Fragment of textile basic tabby weave 14/12 threads per cm, with rolled seam evident on the right. Bottom Left. 18µm (average diameter of three threads), under 56nm Red Plate, red at 90º. Bottom Centre, blue shown at 180º, a flax fibre. Bottom Right, MFA microfibrillar visible at 10.5º. Top Right cross-sectional image for measurement of Ct with ImageJ **Table 12.3.3.** Scale 25mm.

KY 41 CSA Image No.	Circularity CT
1	0.798
2	0.899
3	0.900
4	0.872
5	0.910
6	0.912
Mean	0.882

Table 12.3.3 KY 41. ImageJ analysis of circularity (Ct). Fibres identified 1-6 on area cross-sectional image in **Figure 12.3.23.**

12.3.8. Review of diagnosis of MFA and Ct for Kasr-el-Yahud collection

There are difficulties in diagnosing the KY collection in that there are considerable levels of degradation for these 1400-year-old textile fibres. However, the Ultrasonic Water Bath cleaning provides some samples suitable for MFA analysis. The fibre needle separation method under distilled water separates the fibres down to the “ultimate” circa 10μm level, a level that limits the presence of microfibrillar surrounding the “theoretical fibre “. Hence, fibre type determination relies upon the Herzog Test and does may not detail the actual microfibrillar angle.

12.4 Summary and plot of archaeological assemblage diagnostic determinants

The following confirmation of the case study diagnostic features identified are reviewed below.

12.4.1 Review of Case Study 1: Temple Newsam

The Temple Newsam collection has been catalogued and reviewed by Bower (2000) and unidentified fibre labelled as bast fibres. As these assemblages from the Roger Warner collection were mainly from the 18th and 19th-century and described as bast fibres, therefore not wool and hence most likely to be flax. However, when the method for the accumulation of these textiles is considered, and without knowledge of their post-acquisition cleaning and conservation, there are concerns regarding the possible cross-contamination with other fibres due to variation in storage and lifetime usage of furnishing materials. The multi-fibre image **Figure 12.1.10** illustrated the concerns.

The diagnosis had some success with the determination of area-cross sectional circularity, with RW337 at Ct 0.914 mean value and RW388 at Ct 0.89 mean value. Unfortunately, the fibres were too intermingled, and the MFA values were indetermined.

12.4.2 Review of Case Study 2: Cliff Castle

For the two fibre samples provided CC1 and CC9, the area cross-sectional circularity was successfully measured with CC1 at Ct 0.903 mean value and CC9 at Ct 0.871 mean value. Diagnosis of MFA was only partially successful with a value for CC9 MFA -0.8º.

The CC1 fibre presented an unsuitable MFA image and the alternative Herzog Test suggested a negative MFA angle indicative of flax or nettle; however, the colour shift was inconsistent. The results tabulated above, to determine MFA and Ct as diagnostic features, were achieved from the diagnosis of two 12mm sections. While the prepared sample mountings, MFA determinations from glass-slide mountings under glass coverslips, and Ct measurements from 6mm tubular epoxy resin mountings remain available for future diagnostic measurements. For the sample size the indeterminate MFA imaging was disappointing.

12.4.3 Review of Case Study 3 Kasr-el-Yahud

The need to expedite the excavation of this mass- burial site for the recovery of skeletal and textile assemblages understandably resulted in a compromise in post-excavation sample cleaning and storage. However, there are compensations in that the commingled assemblages retained their association with their original depositional environment, an arrangement conducive to further archaeological investigation.

Consideration of the Ct and MFA determinations achieved, from the aged and degraded plant fibres, indicate the potential for the application to larger sample size. The sample selection, preparation, imaging, and Ct analysis techniques require improvement for fibres recovered from such sites. As previously noted, images of individual fibres under the Herzog Red Plate required a subjective judgement of the attendant colour changes that was not entirely satisfactory.

12.4.4. General MFA/Ct determinants from Case Studies compared with experimental results.

The MFA and Ct diagnosis results for the nine archaeological textile fibres reviewed above are tabulated below **Table 12.5.1** and plotted in **Figure 12.5.1.** for comparison

Sample	Source	MFA	Ct
Temple Newsam	**TN 337**	-6.0	0.914
Temple Newsam	**TN 338**	-6.0	0.890
Cliffe Castle	**CCI**	-8.0	0.903
Cliffe Castle	**CC9**	(-8.0)	0.871
Kasr-el-Yahud	**KY 8**	-10.0	0.848
Kasr-el-Yahud	**KY 12**	-7.0	0.947
Kasr-el-Yahud	**KY 22**	(-8.5)	0.894
Kasr-el-Yahud	**KY 31**	-10.5	(0.900)
Kasr-el-Yahud	**KY 41**	-7.0	0.882

Table 12.5.1. Tabulation of archaeological MFA and Ct. diagnosis: results for indeterminant figures have been averaged and are shown in shaded cells above

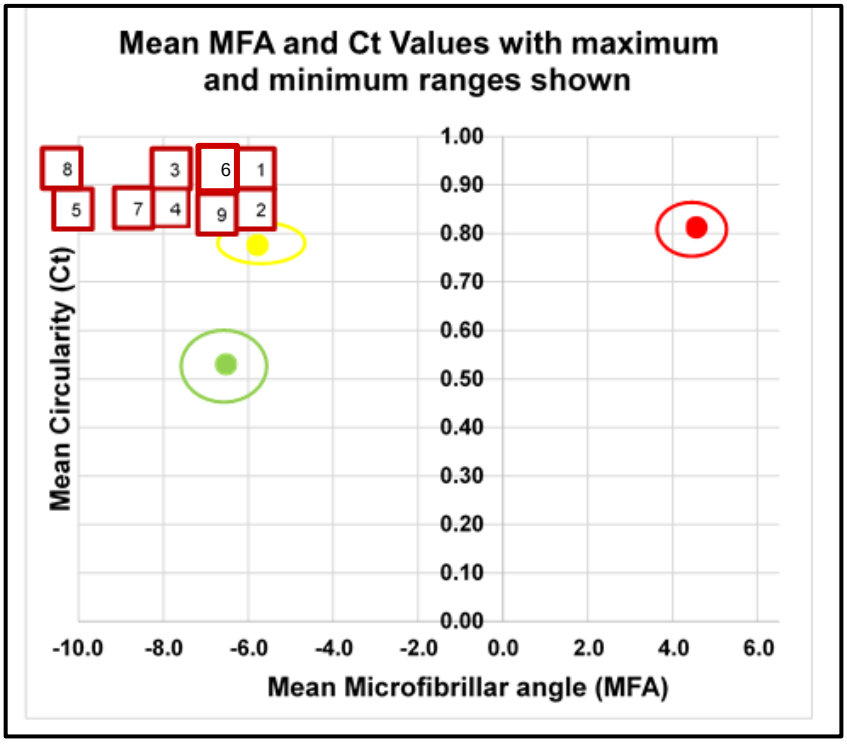

Figure 12.5.1 A plot of MFA/Ct relationships as determined from diagnosis of fibres from archaeological assemblages: the results are labelled as identified in Table 12.5.1 and plotted on the comparative plot assembled in **Chapter 9**. Flax (yellow), nettle (green) and hemp (red).

The plot shows that the fibres identified by MFA and CT diagnosis from the small range of textile assemblages are predominantly flax. The assemblages cover a wide range of depositional periods from the Coptic period AD400- 620 to the late 18th century. The techniques employed serve to identify the majority of the fibres presented but would benefit from application over a wider range of archaeological textile assemblage.

Chapter Thirteen
Discussions and conclusions

13.0 Introduction

In reviewing the research programme for the diagnosis of the three plant fibres, the similarity in the fibre morphology for the three species flax nettle and hemp highlights the interpretative dilemma encountered. The limited survival rate of fibres directs the diagnosis to the inferential interpretation of associated artefact assemblages. Spindle whorls and loom weights attest to the textile/fibre assemblage and flax and hemp seeds, associated with retting pits, denote aspects of the chaîne opératoire processing. In the latter case nettle seeds, recovered from rigorous flotation processes, add to the diagnostic predicament whereby reports of the presence of nettle, in close association with the fibre retting process may be disregarded. However, as noted for Reading Business Park, **Sector 4.7,** the presence of nettle was reported as indicative of their possible participation in the process.

While summaries are included at the end of each chapter, to detail the findings and their potential contribution to the overall objective, the following sections review the broader issues.

a) The research programme results are reviewed and evaluated with respect to the initial overall aims and objectives.

b) The potential applying MFA and Ct diagnostic techniques to fibre residues and pseudomorph structures is appraised.

c) The opportunities presented to enhance the accuracy and graphical representation of the MFA and Ct determination are detailed.

13.1 Review of research programme results

Initially, it was appropriate to examine the botanical structure of the selected plant fibres flax, hemp and nettle and to review the diagnosis of past archaeological assemblages. **Chapter 2** appraised plant fibre structure and the cultural history of the introduction of non-native flax and hemp plant fibre as they evidence the changes in technological/chronological horizons. The similarities in the plant fibre area-cross-sectional of cells held within the plant stem are apparent and confirm the difficulty in determining a reliable diagnosis based on subjective judgement. If an interpretive dilemma is apparent at this initial stage, where the stems' structure constrains the fibre, this diagnosis is even more difficult after extraction, processing and depositional degradations are considered.

In the review of archaeological assemblages, **Chapter 3**, the limitations in subscribing identifications to circa 300+ textile fibre are recorded. It is apparent, as detailed in **Chapter 3**, that a principal factor influencing the fibre underdiagnosis is their close association with metallic artefacts and the attendant pseudomorphic modifications.

The summaries included in these early chapters highlight the problem in identifying plant fibre. Also, it should be recognised that these comments, referencing the research programmes selection of flax, hemp and nettle as the plant fibres to be appraised, may also be relevant to the diagnosis of other bast fibres, notably from trees (Rast Eicher 2005, 117-132; Medard 2004).

These early chapters formed the basis for deriving the principal research hypothesis and associated aims and objects included in **Chapter 3.**

In addition to considering the diagnosis of fibres following their initial harvesting and preparation processes, as detailed in the chaîne opératoire, textile tools such as spindle whorls and loom weights may also serve as inferential diagnostics features to complement fibre identification and utilisation. This topic was addressed in **Chapter 4** to detail the spindle whorl Moment of Inertia (MI) assessment as indicative of spun fibre quality and operational efficiency. Loom weights are also quantified regarding the mounting stress for warp fibre's that limits load bearing, and the associated fineness of thread count that can be achieved. The summary of **Chapter 4** considered the analysis of residues retained on spindle whorls and the archaeobotanical analysis of textile remains associated with textile production tools.

In the initial stages of the plant fibre diagnostic evaluation, chemical analysis and material properties were prioritised. Although the samples were minimally processed modern reference materials, the results, summarised in **Chapters 5 and 6,** were inconsistent. The ADF/NDF chemical analysis was compared with a review of testbed samplings reported by other authors, **Chapter 5, Section 5.2,** who recorded inconsistent variations in chemical constituents along the fibre length. FTRS spectrographic investigations from the Federal University Juiz de Flora Brazil, revealed variations for specific wavelengths. However, as reported in **Chapter 5**, replication of these results was less effective. Furthermore, the comparison of tensile stress revealed significant divergences in the calculation of Young's moduli compared with similar trials

Given these inconsistencies and the unreliability of the results achieved, it was deemed that the costs for more extensive laboratory tests of ADF/NDF and FTRS could not be justified.

13.1.2 Response to results achieved in the initial research phase

The results from this initial phase of the research programme were disappointing in that they failed to address the aims and objectives outlined in **Chapter 3.** Consequently, it was decided to refocus the diagnostic research programme.

Chapter 7, Figure 7.4 reviews the 19th century illustration of the total plant assemblages that displays the potential for morphological as diagnostic indicative representations. Additionally, **Figure 7.1, 7.2** and **73** include images of seeds recovered from Neolithic sites in Germany and Syria to illustrate the variation in flax seed dimensions. It was this joint representation of shape uniformity that redirected investigations to focus the research parameters on the determination of the plant fibre morphological features as presented by minimally processed fibre. **Chapter 7**, and **Chapter 8**

The MFA/Ct research results derived from the range of fibre samples tested are listed and their statistical variations evaluated to compare their validity and determination as appropriate to the research aims and objectives. The summary and graphical representation included in **Chapter 9** confirm their efficacy and suitability as diagnostic parameters

Finally, to address the reliability and durability of the findings, the derived MFA and Ct diagnostic features were reappraised within a blind-test protocol and temperature accelerated degradation deposition. Again, these results were summarised at the end of each chapter.

13.1.3 Plant fibre morphology - MFA/Ct analysis

The research programme's diagnosis of morphological features confirms the potential for microfibrillar angle measurement (MFA) and circularity (Ct), a non-dimensional determination of cross-sectional shape evaluation, as diagnostic features **Chapter7** and **Chapter 8**. Results indicate that the Herzog Red Plate Test can inform the analysis of the MFA direction but has limitations in quantifying the angular measurement, a prime diagnostic differential between flax and nettle **Sector 7.6.2.** Measurement of MFA, as presented by images of "theoretical fibres" under microscopic CPL, was provided. for ImageJ recording and measuring. The appraisal has limitations, particularly for extremely fine fibres circa <10μm, an "ultimate fibre". At 10μm the CPL microscopy evaluation would present a limited set of microfibre for appraisal with few MFA observations visible. Hence, in those circumstances, the Herzog test is proposed as a secondary, less effective, alternative.

It was decided that in the determination of cross-sectional shape, the non-dimensional ratio, "circularity" (Ct), would provide a comparison of fibre shape irrespective of variations in actual size. In the past fibre diagnosis was based broadly on the subjective judgement of the fibre shape as either oblong (nettle) circular (flax) or polygonal (hemp) (see comments **Section 13.1.7**).

The application of computer-based ImageJ software, plus the attendant statistical analysis was a major contributary factor in the accuracy of Ct determinations.

13.1.4 Blind-test protocol

From the sixteen samples from each of the fibre species subjected to the blind test, the MFA and Ct determinations achieved 62.5% success in plant fibre identifications. This result is reasonable but could be improved. The positive outcomes were reduced by the poor quality of fibre samples provide for examination. The intent was to ensure that the modern reference material samples, replicated minimally processed prehistoric fibre material. In that respect, these samples proved to be more diagnostically challenging.

It would be more effective to evaluate the blind-test efficacy if the initial blind test determinations were conducted on modern processed material of improved quality This series of tests could then be extended with samples obtained from decreasing fibre processed quality levels. This approach would offer the ability to compare and contrast the relationship of MFA/Ct diagnosis to fibre processing quality.

13.1.5 Accelerated degradation effects

In submitting the fibre samples to a range of soil and temperature depositions the principal objective was to appraise the retention of MFA/Ct morphologies as reliable diagnostic features. In that respect, as detailed and summarised in **Chapter 11,** the surviving samples retained their diagnostic morphological feature. However, and as expected, the material tensile stress properties were considerably reduced. While, as noted in **Chapter 11, Section 11.2,** the research programme was not constructed to evaluate the microbiological and fungal processes driving the intensity of the degradation process, the total loss of fibre samples from the peat soil at 12 weeks required re-evaluation to ensure that no inadvertent variations in protocol had been introduced. The results from the supplementary 12week test-run demonstrated a similar outcome. A result that confirms Janaway's (2002) comments,

> "(W)ide range of intrinsic and extrinsic factors resulting in differential loss or preservation" (Janaway 2002, 398).

13.1.6 Absence of evidence

This research work acknowledges the underrepresentation of plant fibre assemblages within the archaeological record. In consideration of the wide range of depredating depositions, it is understandable that the oft repeated "mantra",

Absence of evidence is not evidence of absence.

is proposed as a statement of fact.

However, it should be recognised that such “absence interpretations” hold within them an interpretive dilemma. The dilemma arises from the assumption that plant fibre artefacts would survive their presence, whereas evidence suggests the opposite. There are significant differences between organic and inorganic archaeological survivals.

The assumed absence of inorganic material, such as lithic, ceramic or precious metal assemblages reflects the expectation that an inorganic deposition would survive. This assumption can be qualified by the determination of the statistical probability of their presence.

Drennan (2004, 255-259) addresses and tabulates the determination of the sample size required to qualify the “absence” at high confidence levels of low probabilities.

Organic materials deposited in similar circumstances and subjected to a statistical appraisal of absence evaluations may not be confirming their absence but confirming their loss in degradation.

13.1.7 Subjective Judgement

The subjective judgement of plant fibre morphology was examined in **Chapter 8** to address the attributes of plant fibre cross-sectional shapes. As with other archaeological diagnoses, the principal features of seriation and typology are essential contributions to identifying a range of shape descriptions and variations. These variations are considered in the adaptations of manufactured artefacts that represent chronological and cultural diversifications.

Textile production also shares product typological attributes particularly in weaving structures and clothing style assemblages. However, both unprocessed and processed fibres share similarities in their MFA and Ct morphological variations. Similarities, as itemised in **Chapter 8, Section 8.6,** that demonstrate the challenge facing application of descriptive terms based on subjective judgements, notably when compared to those reported for tool wear analysis.

Also as previously reported, **Chapter 10, Section 10.5,** there is the potential for cognitive bias and external influences to misdirect artefact diagnostic representations Because of these concerns, it is proposed that a project for research into alternative shape analysis protocol to enhance the determination of MFA be established.

While the research programme shows that minor variations in Ct measurement are statistically quantifiable under ImageJ software, there is the potential to improve the software application to consider additional plant fibre morphological attributes. This factor is addressed in **Section 13.3.2**.

13.2 Potential for MFA and CT diagnosis in future research programmes

In the reviews of archaeological assemblages and inferential textile tool diagnosis**, Chapters 3 and 4,** noted that fibres were present in pseudomorphic format or as residue in association with the textile tools. In view of the limited presence of plant fibres, unaffected by degradation modifying processes, would these pseudomorphic fibres offer an alternative, albeit modified, source for diagnostic appraisal?

13.2.1 Plant fibre pseudomorphic presence

As previously noted, and reviewed in detail in **Chapter 11,** archaeological plant fibre assemblages are highly perishable and survive only in cold environments, extreme dryness, or oxygen-depleted anoxic conditions. Additionally, as confirmed in the fibre assemblage tabulation, **Chapter 3, Table 3.2,** 65% of the 322 surviving fibres exhibited various degrees of modified pseudomorphic forms. These pseudomorphs, held in close association with metallic objects, presented limitations to their botanical identifications.

The above comments referenced the survival, in pseudomorph form, of fibre utilised in the textile or thread count construction.

As the recorded data, **Table 3.2,** shows in many cases there was sufficient retained textile fabrication details held in pseudomorphic representation to determine the fibre spin angle and associated thread count.

However, from the observed pseudomorphs listed, there were insufficient fibre morphological features to allow the fibre species to be determined. Hence positive fibre identification was only possible for a few samples (4%).

Recommendations 1. MFA/Ct Diagnosis of fibre pseudomorphic material

The research programme has identified that microfibre angle (MFA) and area cross-sectional circularity (Ct) can be employed coextensively to identify plant fibre diagnostic features. It is feasible to address the research work to evaluate the extent to which MFA and Ct fibre morphological details, presented from retained fibres held in metallic artefacts, may also be represented in their pseudomorph images.

13.2.2 Textile tool plant fibre residue

In the examination of spindle whorl reside deposited upon replication studies as described in **Chapter 4, Section 4.9.3** the authors described the initial results for residue analysis as limited. However, the possibility of extending this work was noted to recognise the potential for future fibre MFA/Ct analysis of residue retained on textile tools.

Also, the archaeobotanical excavation of Quartier Mu V. relates the recovery of a small 6cm x 9cm sample of woollen archaeological textile from the sediment flotation of residue retained in the drainage system. The textile thread details are recorded as 0.3mm diameter with a thread count of 20 threads/cm in alternative S and Z spin **Chapter 4, Section 4.12.**

Recommendation 2. MFA/Ct analysis of textile tool residues

The above site report illustrates the importance of detailed archaeobotanical appraisal of site environments, particularly where there may be fibre held by, or closely related to, textile tool assemblages excavated from advantageous depositions environments.

13.2.3 The flaxseed oil/fibre, primary/secondary product dilemma

Chapter 2, Section 2.10.2 references the evaluation of the distribution of domestic flaxseeds and capsules, **Figure 2.11**, and archaeological finds of wild flax, **Figure 2.12.** Considerations of Late Neolithic flaxseed refers to the seed diameter as illustrative of the primary flax product being oil are discussed in **Chapter 4**, **Figure 7.1.**

This interpretation is questioned as, based on the evidence for flax fibre production, **Chapter 4, Section 4.4,** flax plants are pulled from the ground before maturity; consequently, the seed capsules would also be under-mature and smaller. However, some mature flax fibre capsule would have to be retained to provide seeds for future flax crops.

As noted, the oil/fibre dichotomy has been addressed in detail in a Special Report published in Vegetation History and Archaeobotany (2011) whereby the authors' general conclusions were that there was insufficient evidence to support oil as the primary flax product. The second consideration to take into account is that flax plants rely on adequate water supplies to ensure capsule maturity as a shortfall in irrigation would result in the immature seed capsules not achieving full oilseed capacity. Hence, the early harvesting for the secondary fibre product becomes more suitable as textile fibre.

Recommendation 3. Determination of flaxseed dimension pre and post-harvest

The concept of flaxseed dimensional evaluation, to assess the differential in seeds gathered from flax fibre retting and seeds reserved for crop sowing, would support a future testbed research project.

3.2.4 Tree bast fibre

The research work reported above was centred on the three principal plant fibre flax hemp and nettle but recognises the contribution of bast fibre fabrications in basketry, cord and netting that predate them (Gleba and Harris 2019, 2329-2346; Médard 2005, 99-105; Rast-Eicher 2005,118; Harris 2010, 1070; Rast-Eicher 2016, 81-86). **Chapter 2, Section 2.4**.

As noted by Rast-Eicher (2005) Medard (2019), these fabrication skills, employed in the Mesolithic and Early Neolithic, were proposed as a technological foundation for the development of more complex weaving techniques **Chapter 4, Section 4.5.** Ötiz (The Iceman) (3.4kya-3.1kya) discovered in the Ötzal Alps in 1992 wore a range of fur fabrics over a woven grass skirt this bast fibre assemblage is significant in that it coexistent with the early Central European adaptation of flax and hemp. In **Chapter 3, Table 3.4** the first entries were described as bast fibre material from the Palaeolithic period, Lascaux Cave-France, Ohalo-Israel, Dzudzuana-Caucasus and Bouldnor Cliff-England, however, these diagnoses are recorded as unreliable.

Recommendation 4. Tree bast diagnosis with MFA/Ct determinants

Rast-Eicher (2005), reporting on bast fibre preceding wool, and comments from Médard's (2019) on tree bast fibres, support the need for prioritising additional research **Chapter 4, Section 4.5.** The diagnostic features, MFA/Ct, derived in the programme would support this proposal for the evaluation of tree bast fibres and notes the potential for their application in evaluating their morphological feature.

13.3 Enhancement of MFA/Ct determinations and coextensive representations

MFA/Ct diagnostic features were reviewed and summarised in **Chapter 9** to appraise and their co-extensive relationship and graphical representation under various protocols discussed. The following areas for enhancing the research implementation are proposed.

a) Plant fire reference material processing. In a reflection of the research programme findings, the dichotomy of a principal research protocol of “minimally invasive archaeological assemble appraisal” and the attendant “minimally processed modern reference materials” deliver contrasting outcomes. While the concerns regarding the detrimental effect upon the archaeological assemblages are paramount, the adaptation of the principle to fibre preparation processing raises issues.

Consideration of Pre-Historic textile assemblages illustrates the quality and craft skills of the past. In preparing modern plant fibre material, the end-product delivered for appraisal would be more influential if the findings reflected these craft skills. It is recognised that including more refined processing, particularly fibre combing, would provide improved fibre dimensional consistency to the reference material. A consistency that may enhance or reduce the efficacy of the diagnostic features identified. The Blind Test protocol illustrated these concerns.

Recommendation 5. Review of reference plant fibre material preparation

Any future Research Programme should address these concerns regarding modern reference material pre-test processing

b) Vector analysis. MFA and Ct joint relationships were plotted in the 2D vector analysis included in **Chapter 9.** However, vector format representation could be improved if an additional diagnostic parameter could be identified, an identity to format a third axis and permit 3D representation **Section 13.3.1.**

c) Computer shape analysis. An improvement in the Ct representation as derived from computer-based shape analysis, under artificial intelligence appraisal would be beneficial. (see **Section 13.3.2**)

13.3.1 Vector analysis, diagnosis of nodal dislocations spatial location

In **Chapter 7, Section 7.4,** the nodal dislocation marks, for the three fibre types under review, were described as distinctive cross-shaped representations visible under CPL viewing of longitudinal fibre images and defined as a diagnostic criterion. While there are queries regarding the viability of this variation in nodal deformation for fibres presenting an acceptable diagnostic feature. The differential exhibited by the cross-shaped nodal deformations displayed by nettle and flax display an anomaly.

It was observed that, in the numerous images obtained within the programme, the cross-shaped deformation marks were always presented with the origins fixed on the left and right extremes of the fibre image irrespective of the fibre orientation.

Recommendation 6. Determination of a non-dimensional representation of nodal dislocation

The anomaly presented by nodal deformations would benefit from further investigation. The proposal is to consider nodal dislocations as an additional third determinant to compliment MFA and Ct with the potential to incorporate three axis in formulating a 3D vector analysis.

13.3.2 Fibre Ct determine by computer-based artificial intelligence (AI)

In a reflection of the above concerns, the application of computer-based artificial intelligence (AI) was reviewed to propose a potential for future plant fibre cross-sectional morphological research. A pilot trial, of AI computer appraisal, using samples of fibre cross-sectional area (CSA) prepared as detailed in **Chapter 8**, was completed with encouraging results.

AI evaluations induce a variation to the CSA image in terms of size, colour, focal distance, image quality and orientation to evaluate AI's ability to optimise a shape dimension classification for each fibre species. While the initial results are encouraging, there is a requirement to provide an extensive database of fibre CSA images to qualify the potential for AI analysis.

Recommendation 7. To establish a research protocol for AI appraisal of plant fibre cross-sectional Ct.

The hypothesis is proposed that AI could provide an accurate and robust diagnosis of fibre CSA. This proposal is under consideration to form the basis of an application for future research funding.

13.4 Case study reviews

In undertaking comparative studies based on replications of modern reference material, the outcomes are determined by the degree of pre-treatment of the plant fibre from harvesting and retting to the pre-weaving preparation.

While the protocol defines the replication in relation to the overall objectives as minimally invasive, applying a similar directive to the reference material limits the authenticity of the finished properties as they reflect the quality of the end product. Reference to the archaeological assemblage, Sector 3.5.1.1-35.1.9, illustrates the quality of fibre preparation achieved.

The preparation of modern reference material for this research programme was limited to primary combing and fibre selection following completion of retting. As such the fibre submitted for testing may include fibres of inferior quality. These fibres would have been removed if a more intensive combing process had been undertaken; this is particularly relevant to the blind-test protocol efficacy where minimally processed fibres were included.

There is always the dichotomy in proposing the efficacy of research resolutions based on diagnostic techniques applied to experimental reproductive evaluations of modern reference material as sufficiently non-destructive to alleviate the Museum Archivist’s rightful concerns. In reflection of the above concerns the author records appreciation of the support and access to archaeological assemblages provided by Museum Archivists.

13.4 1 Case study 1: Temple Newsam furnishing fabrics

Here the mixed results achieved on the evaluation of furnishing fabrics are noted. There are marked differences in the production and utilisation of such textile assemblages compared with personal clothing attire. Furnishing assemblages address functional requirements that require substantial weight-supporting fabric construction, the softness of comfortable seating, and potential amalgamation of fibres to give a pleasing decorative effect.

These constraints, plus consideration of the pre-auction inadequacies in conservation and the commingling of antique fabric collections, need to be addressed. Additionally, it is recognised that, in contrast to personal clothing, the extensive lifestyle usage of utilitarian products may present difficulties in achieving adequate diagnostic determinations.

13.4 2 Case study 2: Cliffe Castle

Samples, from the Egyptian Coptic Collection at Cliffe Castle Museum, were collected for evaluation. The 5^{th}-06^{th} century textile fragments were part of original tunic fragments excavated from the dry sand environment were fragile, although well preserved. Compared to the furnishing textiles noted above these aged single fibre samples offered a less commingled assemblage There were concerns regarding the contamination from sand crystals that required attending, and it was necessary to submit the fibre samples to sonic water cleaning. Subsequently, the MFA (-8.0º) and Ct (0.0871) diagnosis of fibre CC9 was completed satisfactorily, with MFA confirmed by Herzog Test as negative “S” format.

Unfortunately for the second fibre CC1 only Ct at 0.903 could be confirmed. MFA measurement and determination by Herzog was unsuccessful, although there where high auto-fluorescence levels present.

The difficulty associated with autofluorescence interference with image quality obtained from other analytical techniques was noted previously in Sections 2.6.1 and 5.5.1. For future fibre imaging, it may be beneficial to consider modified or filtered CPL light sources.

13.4.3 Case Study 3 Kasr el Yahud

As noted in Section 12. 3. 3. a proportion of the 237 mixed fibre assemblages recovered from this 7th century mass burial arid climate site was available for evaluation. The time constraints imposed upon site excavations of this massacre site limited on-site cleaning or conservation of the fibre assemblage.

Consequently, fibres, held in commingled bundles, required a degree of pre-treatment with distilled water spray washing sonic bath treatment and needle separation to release individual fibres for diagnostic evaluation.

There were limited woollen fibre adornments finds reported held within the tunic design. However, the textile structures suggest some individuality in personnel attire, a differential possibility demonstrated by the presence of “S” spun cotton fibre of Nubia style. Additionally, the enforced delay in the interment, attested by the presence of animal faecal matter, is reported as resulting in a variety of burial practices whereby some shrouds were improvised by overwrapping existing personal tunic material as shrouds.

It was fortunate that the selection of KY 12 as an initial trial served to confirm both MFA (-7º) and Ct (0.947) measurements and was instrumental in supporting a randomised evaluation of 25% of the archaeological assemblage.

The research programme protocol emphasises the need to limit pre-evaluation preparation to a minimally invasive process. However, the site report notes the time restraints that limited the opportunity for on-site washing and preparation, although some of textile assemblage features imaged and reported demonstrate the benefits derived from post-excavation treatments.

Recommendation 8 Comparison with other post excavation fibre treatments

In addition to the outcomes and protocol reported above, it would be advantageous if details of the post-excavation treatments were available for replication such that future sample preparation would not compromise the compatibility of on-site/off-site excavations.

13.5 Conclusions

The research report confirms that the limited availability of fibre assemblages highlights the requirements for robust, reliable and minimally destructive diagnostic programmes. It is recognised that depositional limitation may also influence fibre recovery whereby the presence of multiple inorganic artefacts may direct post-excavation attention away from textile fibre recovery and evaluations to concentrate on the more substantial inorganic artefacts.

There were areas of disappointment in the research outcomes, particularly for chemical analysis and considerations of fibre material properties.

However, there were compensations, the development and appraisal of MFA and Ct morphological diagnostic techniques working as coextensive parameters are encouraging. This combination can be used as a stand-alone diagnostic procedure or in support of other conventional evaluations. The work raises awareness of the potential for blind testing as a reliable technique for the qualification of diagnosis based on subjective judgement.

Also, the survival of MFA and Ct diagnostic features in advantageous degradation studies could offer support to encourage site recovery rates for seeds and fibres from soil depositions.

As noted above, the research work also supports considerations of MFA and Ct diagnostic features for tree-bast fibres used in the Mesolithic, accompanied by computer-based artificial intelligence interpretations that would offer a challenging future research project. The minimally destructive techniques described in this research work and the application of improved imaging analysis could prove beneficial to the diagnosis of prehistoric plant fibre usage and are recommended.

REFERENCES

Adams, N. K. (2007) Political affinities and economic fluctuations; the evidence from textiles. In Gillis, C. and Nosch, M-L. B. (eds.) *Ancient textiles; production, craft and society.* Oxford: Oxbow; 201-207.

Adovasio, J. M., Soffer, O., Illingworth, J. S., and Hyland, D.C. (2014) Perishable fiber artifacts and Paleoindians: new implications. *North American archaeologist*, 35 (4), 331-352.

Alfaro, C. (2019) Spain. In Gleba, M. and Mannering U. (eds.) *Textiles and Textile Production in Europe from pre-history to AD 400.* Chapter 16, 334-348.Oxford: Oxbow.

Allaby, R. G. Peterson, G. W., Merriwether, D. A., and F. Yong (2005) Evidence of the domestication history of flax (Linum usitatissimum L.) from genetic diversity of the sad2 locus. *Theoretical applied genetics* (2005) 112, 58–65.

American Society Testing Materials (ASTM) International (1989) *Designation: D 3379 – 75 (Reapproved 1989). Standard test method for tensile strength and young's modulus for high-modulus single-filament materials* (available online) www.astm.org Accessed 28/02/2014.

American Society Testing Materials (ASTM). 2014. *International designation: C1557 -14.* Standard test method for tensile strength and Young's modulus of fibers. Accessed 13/02/2018 https://www.astm.org.

Andresen, S. T, and Karg, S (2011) Retting pits for textile fibre plants at Danish prehistoric sites dated between 800 B.C. and A.D. 1050. *Vegetation history and archaeobotany.* 20, 517-526.

Andersson-Strand, **E., B. (2010)** Textile tools and production during the Viking Age. In Andersson-Strand, E., Gleba, M., Mannering, U., Munkholt, C. and Ringgaard, M. (eds) (2010) *North European symposium for archaeological textiles X.* Oxford: Oxbow, 1-3.

Andersson-Strand, E., Gleba, M., Mannering, U., Munkholt, C. and Ringgaard, M. (eds) (2010) *North European symposium for archaeological textiles X.* Oxford: Oxbow.

Andersson Strand, E. Nosch, M.-L. and Cutler, J. (2013) Textile tools and textile production- studies of selected Bronze Age sites: introduction. In Andersson Strand, E. and Nosch, M.-L. (eds.) Tools, textiles and contexts; investigating textile production in the Aegean and Eastern Mediterranean Bronze Age. *Ancient textiles series* 21 Chap.6.1, 191-196.

Andualem, D., Negessee, T. and Tolera, A. (2015) Biomass yield, chemical composition, and *in vitro* (L.) organic matter digestibility of stinging nettle (*Urtica simensis* L.) from four locations at three stages of maturity. *Livestock research for rural development* 27 (8), 1-9.

Aslan, M., Chinga-Carrasco, G., Sørensen B. F. and Madsen, B (2011) Strength variability of single flax fibres. *Journal of material science* 46, 6344-6354).

Austenson, H. M., Wenhardt, A. and White, W. J. (1970) Effects of summer fallowing and rotation on yield of wheat, barley and flax. *Canadian journal of plant sciences* 50, 659-666.

Bacci, L., Baronti, S., Predieri, S. and Di Virgilio, N. (2009) Fiber yield and quality of fiber nettle (Urtica dioica L.) cultivated in Italy. *Industrial crops and products* 29 (2–3), 480-484.

Bacci, L., Di Lonardo, S., Albanese, L., Mastromei, G. and Perito, B. (2011) Effect of different extraction methods on fiber quality of nettle (Urtica dioica L.). *Textile research journal* 81 (8), 827-837.

Baley, C. 2002. Analysis of the flax fibres tensile behaviour and analysis of the tensile stiffness increase. *Composites: Part A* 33, 939–948.

Baley, C. and Bourmaud, A. (2014) Average tensile properties of French elementary flax fibres. *Material letters.*2 (30), 1-3.

Ball, T., Chandler-Ezell, K., Dickau, R., Duncan, N., Hart, T. C., Iriarte, J., Lentfer, C., Logan, A., Lu, H., Madella, M., Pearsall, D. M., Piperno, D. R., Rosen, A. M., Vrydaghs, L., Weisskopf, A. and Zhang, J. (2016) Phytoliths as a tool for investigations of agricultural origins and dispersals around the world. *Journal of archaeological science* 68, 32-45.

Bamforth, D. B. (1988) Investigating microwear polishes with blind tests - the institute results in context. *Journal of archaeological science.* 15, 11–23.

Bamforth, D., Burns, G. R. and Woodman, C. (1990) Ambiguous use traces and blind test-results - new data. *Journal of archaeological science.* 17, 413–430.

Bank- Burgess, J. (2019) Case study: the textiles from the Princely Burial at Eberdingen-Hochdorf, Germany. In Gleba, M and Mannering, U.(eds.) Textiles and textile production in Europe from Prehistory to AD400. *Ancient textiles Series 11*, 139-152.

Bar-Adon, P. (1980) T*he cave of treasures. The finds from the cave in Nahal Mishmar Jerusalem.* Israel Exploration Society.

Barber, E., J., W. (1991) *Prehistoric textiles; the development of cloth in the Neolithic and Bronze Age.* Princeton: Princeton University Press.

Barbulée, A. and Gomina, M. (2017) Variability of the mechanical properties among flax fiber bundles and strands. *Procedia Engineering* 200, 487–493.

Bar-Yosef, O., Belfer-Cohen, A., Mesheviliani, T., Kakeli, N., Bar-Oz, G., Boaretto, E., Goldberg, P., Kvavadze, E. and Mtskevich, Z. (2011) Dzudzuana: an Upper Palaeolithic site in the Caucasus foothills (Georgia). *Antiquity* 11, 331-349.

Bazzenella, M. (2003) Italy Neolithic and Bronze Age. In Gleba, M. and Mannering U. (eds.) *Textiles and Textile Production in Europe from pre-history to AD 400*.Oxford: *Ancient textiles series* 11 Chap. 8, Oxbow, 203-214.

Beck, C. B. (2010) *An introduction to plant structure and development, plant anatomy for the twenty-first century.* (2nd ed.) New York: Cambridge University Press.

Belanová-Štolcova, T. (2019) Slovak and Czech Republics. In Gleba, M. and Mannering, U. (eds.) *Textiles and textile production in Europe from prehistory to AD 400. Ancient textiles series 11* Chap. 15, 306-331.

Bello, S.M., Parfitt, S. A., De-Groote, I. and Kennaway, G. (2013) Investigating experimental knapping damage on an antler hammer: a pilot-study using high-resolution imaging and analytical techniques. *Journal of archaeological science (40), 4528-4537.*

Bender-Jørgensen, L. (2005) Hallstatt and La Téne textiles from the archives of Central Europe. In Bichler, P., Grömer, K., Hoffmann-de Keijzer, R., Kern, A. and Reschreiter, H. (eds.) Hallstatt textiles, technical analysis, scientific investigation and experiment on Iron Age textiles. *BAR International series. 1351*, 133-150.Oxford: Archaeopress.

Bender-Jørgensen, L. (2007) The world according to textiles In Gillis, C. and Nosch, M-L. B. (eds.) *Ancient textiles; production, craft and society.* Oxford: Oxbow, 7-12.

Bender Jørgensen, L. and Grömer K (2013) The archaeology of textiles-recent advances and new methods. *Pregledni rad Predan* 30 (11), 91-111.

Bender Jørgensen, L. and Rast Eicher, A. (2018) Raw materials: creativity and materials. Fibres for Bronze Age textiles. https://www.cambridge.org/core. https://doi.org/10.1017/9781108344357.004. Accessed 5/8/2020.

Bergfjord, C. and Holst, B. (2010) A procedure for identifying textile bast fibres using microscopy: flax, nettle/ramie, hemp and jute. *Ultramicroscopy* 110, 1192-1197.

Bergfjord, C., Karg, S., Rast-Eicher, A., Nosch, M. L., Mannering, U., Allaby, R. G., Murphy, B. M. and Holst, B. (2010) Comment on “30,000year-old wild flax fibers”. *Science* 328, 1634.

Bergfjord, C., Mannering, U., Frie, K. M., Gleba, M., Scharff, A. B., Heinemeier, J., Nosch, M.L. and Holst, B. (2012) Nettle as a distinct Bronze Age plant. *Science report* 2 (664), 1-4.

Bible (2000) *Contemporary English version (2000),* Deuteronomy 22:1; Leviticus19, 19).

Black L (1973) The Nivkh (Gilyak) of Sakhalin and the Lower Amur. *Artic anthropology* 10 (1), 112 Madison: University of Wisconsin Press.

Bleed, P. (2001) Trees or chains, links or branches: Conceptual alternatives for consideration of stone tool production and other sequential activities. *Journal of archaeological method and theory,* 8 (1), 101-127.

Bodros, E. and Baley, C. (2008) Study of the tensile properties of Stinging Nettle fibre (U*rtica dioica). Materials letters* 62 (14), 2143-2145*.*

Bolohan, N.and Lazanu, C.-C. plant textiles in a grave mound of the Early Bronze Age in eastern Romania. In Siennicka, M., Rahmstorf, L. and Ulanowska, A. (eds) *First textiles, the beginnings of textile manufacture in Europe and the Mediterranean. Oxford: Oxbow, 143-150.*

Bos, H. L. and Donald, A.M. (1999) In situ ESEM study of the deformation of elementary flax fibres. *Journal of materials science* 34, 3029-3034.

Bosch, A., Chinchilla, J., and Tarrús, J. (2006) Els objects de fusta del poblat : Neolític de La Draga, excavations 1995-2005*. Monografies del casc 6 Museu d'arqueologia de Catalunya centre d'arqueologia subaquàtica de Catalunya*. 2006, 1-186.

Bosi, G., Rinaldi, R. and Mazzanti, M. B. (2011) Flax and weld; archaeobotanical records from *Mutina* (Emilia Romagna, Northern Italy, dated to the Imperial Age, first half 1st century A.D. *Vegetation history and archaeobotany* 20, 543-548.

Bouchard, C., Tenberg, M aánd Dia-Prá, P. (2011) Cotton cultivation and textile production in the Arabian Peninsula during antiquity; the evidence from Madain Salih (Saudi Arabia) and Qal'at al-Bahrain (Bahrain) *Vegetation History Archaeobotany.*

Bourmaud, A., Morvan, C., Bouali, A., Placet, V., Perré, P. and Baley, C. (2013) Relationships between micro-fibrillar angle, mechanical properties and biochemical composition of flax fibers. *Industrial crops and products* 44, 343–351.

Bower, H. (2000) *Textiles at Temple Newsam:* The Roger Warner collection. Leeds: Leeds Museum and Galleries.

Bowdery, D. (2001) Phytolith and starch data from an obsidian tool excavated at Bitokara, New Britain Province, Papua New Guinea: A 3400year old hafting technique. In Meunier JD and Colin F (eds) *Phytoliths: applications in earth sciences and human history.* Lisse: Balkema, 225-238.

Bouayoun, T, Stambouli, H., Ez Zoubi, Y., El Bouri, A., Farah, A. and Tabyaoui, M (2018) Hemp seed oil: chemical characterisation of three non-drug varieties cultivated in Morocco. *Journal of applied biology and biotechnology* 6 (5), 37-41.

Bozarth, S. R. (1992) Classification of opal phytoliths formed in selected dicotyledons native to the Great Plains. In Rapp, G. Jr. and Mulholland, S. C. (eds.) *Phytolith systematics: Emerging issues.* New York: Plenum Press, 193-215.

Bredemann, G. (1950) Nutrient absorption and nutrient requirement of fibre nettles. biological abstracts 24 (5) number 13238 [Cited in Horne, M. R.L., Harwood, R. J, McCormick, B. P., and Harwood, J. L. (2008) stinging nettle (Urtica dioica) fibres for use in textiles: team research, De Montfort University, Leicester, UK. *Conference proceedings 86th textile world conference Nov. 2008.* Hong Kong: Institute of Textiles and Clothing, 63-70.

Bremond, L., Alexandre, A., Hély, C. and Guiot, J. (2005) A phytolith index as a proxy of tree cover density in tropical areas: calibration with Leaf Area Index along a forest–savanna transect in southeastern Cameroon. *Global and planetary change* 45 (4), 277-293.

Breniquet, C. (2013) Functions and uses of textiles in the ancient Near East. Summary and perspective. In Nosch, M. L., Koefoed, H. and Andersson-Strand, E. (eds) *Textile production and consumption in the ancient Near East.* Oxford: Oxbow Books, 1-25.

British Standards 1051 (1982) *Terms relating to the conditioning, testing and mass determination of textiles.* London: British Standard Institute.

British Standard 1377-1 (2016) *Methods of test for soils for civil engineering purposes-Part 8: Shear strength tests (effective stress).* London: British Standard Institute.

British Standard 6085 (1992) *Methods for the determination of the resistance to microbiological deterioration.* London: British Standard Institute.

British Standard ISO 9276-6 (2008) *Representation of results of particle size analysis; part 6- Descriptive and qualitative representations of particle size*. London: British Standard Institute.

British Standard EN ISO 13906 (2008) *Animal feeding stuffs. Determination of acid detergent fibre (ADF) and acid detergent lignin (ADL) contents*. London: British Standard Institute.

British Standard EN ISO 16472. (2006) Animal feeding stuffs. *Determination of amylase-treated neutral detergent fibre content (aNDF).* London: British Standard Institute.

Broeke, J., Pérez, J. M. M. and Pascau, J. (2015) *Image processing with ImageJ (2nd Ed*); Extract and analysis data from complex images with ImageJ. Birmingham: Packet.

Cambridge Archaeological Unit (2016) Must Farm; dig diary 6. http://www.mustfarm.com/progress/site-diary-6-textiles/ Accessed 03/11/2016.

Cameron, E., Harris, S. and Mould, Q. (2016) The textile and animal-skin object. In Jones, A. M. (ed) *Preserved in the peat. An extraordinary Bronze Age burial on Whitehorse Hill, Dartmoor, and its wider context.* Oxford: Oxbow Books, 148-156.

Canti, M. G. (2003) Aspects of the chemical and microscopic characteristics of plant ashes found in archaeological soils. *CATENA* 54 (3), 339-361.

Cartwright, C. (2016) Report on the scanning electron microscope (SEM) examination of the basketry container and other organic artefacts from Whitehorse Hill cist. In Jones, A. M. (editor) *Preserved in the peat. An extraordinary Bronze Age burial on Whitehorse Hill, Dartmoor, and it's wider context.* Oxford: Oxbow Books, 267-273.

Catling, D. and Grayson, J. (2012) *Identification of vegetable fibres.* Springer Science and business Media.

Charlet, K., Jernot, J. P., Gomina, M., Bréard, J., Morvan, C. and Baley, C. (2009) Influence of an Agatha flax fibre location in a stem on its mechanical, chemical and morphological properties. *Composites science and technology* 69 (9), 1399-1403.

Chmielewski, T and Gardynski L. (2010) New frames of archaeometrical descriptions of spindle whorls, a case study of the late Eneolithic spindle whorls from the 1c site in Gródek, District of Hrubieszów, Poland. *Archaeometry* 52 (5), 869-881.

Clarke, R. C. and Merlin, M.D. (2013) "Cannabis." *Evolution and ethnobotany.* Berkeley: University of California Press.

Coles, J. M., Coutts, H. and Ryder, M. L. (1964) A late Bronze Age find from Pyotdykes, Angus, Scotland, with associated gold, cloth, leather and wood remains. *The prehistoric society* Vol. XXX (No 1), 186-198.

Coles, J. M., Hibbert, F.A. and Orme, B. J. (1973) Prehistoric roads and tracks in, Somerset: The sweet track. *Proceedings of the prehistoric society* 39, 256-293.

Conto, G., Carfi, F. and Pace, V. (2011) Chemical composition and nutritive value of ramie plant [Boehmeria nivea (L.)) and its by-products from the textile industry as feed for ruminants. *Journal of agricultural science and technology* A1, 641-646.

Crawford, P. (2013) *The war of the three gods, the seige of Jerusalem.* Basrnsley: Pen and Sword Military.

Crowfoot, E. (1985) Textiles. In Hedges, D., and Buckley, D., G. Anglo-Saxon burials and later features excavated at Orsett, Essex. *Medieval archaeology* 29 (1), 1-24.

Cruikshank, P. (2011) Flax in Croatia: traditional production methods, the use and care of linen in folk costumes and implications for museum conservation. *Textile history* 42 (2), 239–260.

Cummings, V. and Harris, O. (2011) Animals, people and places: the continuity of hunting and gathering practices across the Mesolithic–Neolithic transition in Britain. *European journal of archaeology* 14 (3), 361-393.

Cutler, D. F. and Stevenson, D. W. (2008) *Plant anatomy, an applied approach*. Malden (USA): Blackwell.

Cutler, J., Andersson Strand, E. and Nosh M.-L. (2013) Textile production in Quartier Mu.V. In Nosh M.-L. B., Cutler, J. and Andersson Strand, E. (eds.) Fouilles excécutées à Malia. Le Quartier Mu V. *Études Crétoises* 34 Chapter 5, 95-118 and Appendix Pl, 1-8.

Cybulska, M., Florczak, T. and Maik, J. (2010) Virtual reconstruction of archaeological textiles. In Andersson-Strand, E., Gleba, M., Mannering, U., Munkholt, C. and Ringgaard, M. (eds) (2010) *North European symposium for archaeological textiles X.* Oxford: Oxbow,36-40.

Dai, D. and Fan, M. (2010) Characteristic and performance of elementary hemp fibres. *Material sciences and applications* 1, 336-342.

Dark, P. (2004) Plant remains as indicators of seasonality of site-use in the Mesolithic Period. *Journal of environmental archaeology* 9, 39-45.

Day, P. M. and Kiriatzi, E. (1999) Group therapy in Crete; a comparison between analysis by Neutron Activation Analysis (NAA) and thin section petrography of Early Minoan Pottery. *Journal of archaeological science* 26, 1025-1036.

De Lucia Brolli, M. A. (1998) Una tomba orientalizzante da "falerii": contributo alla conoscenza della Necropoli dei Cappuccini. *Archeologia Classica* Vol. 50, 181-211.

Densmore, F. (1979) *Chippewa customs.* St Paul Minnesota: Minnesota historical society. (1979 reprint).

Dimmock, J. P. R. E., Bennett, S. J., Wright, D., Edward-Jones, G. and Harris, I. M. (2005) Agronomic evaluation and performance of flax varieties for industrial fibre production *Journal of agricultural science* 143, 299–309.

Dimova, B. (2016) Textile production in Iron Age Thrace, *European journal of archaeology* 19 (4), 652-680.

Di-Virgilio, N. (2013) Stinging Nettle: a neglected species with a high potential as multi-purpose crop. Summer School of FIBRA Catania-Italy July *2013 Fibre crops as sustainable source of bio-based material for industrial products in Europe and China*. (2013: npn.) (available on-line *www.fibrafp7.net)* (accessed 7/7/2014).

Di-Virgilio, N., Papazoglou, E. G., Jankauskiene, Z., Lonardo, S., Praczyk, M. and Wielgusz, K. (2015) The potential of stinging nettle (*Urtica dioica* **L**) as a crop with multiple uses. *Industrial crops and products* 68, 42-49.

Domínguez-Rodrigo, M. (2008) Conceptual premises in experimental design and their bearing on the use of analogy: an example from experiments on cut marks. *World archaeology* 40, 1:67-82.

Dounias, E. (2001). The management of wild yam tubers by the Baka Pygmies in Southern Cameroon. *African study monographs* 26, 135–156.

Douka, K., Higham, T. and Sinitsyn (2010) The influence of pre-treatment chemistry on the radiocarbon dating of Campanian Ignimbrite-aged charcoal from Kostenki 14 (Russia) *Quaternary research* 73, 583–587.

Drennan, R.D. (2004) *Statistics for archaeologist: a common approach.* New York: Springer.

Dreyer, J., Dreyling, G. and Fieldmann, F. (1996) Cultivation of stinging nettle (Urtica dioica) with high fibre content as a raw material for the production of fibre and cellulose: Qualitative and quantitative differentiation of ancient clones. *Journal of applied botany-Angewandte botanik* 70 (1-2), 28-39.

Drobß-Krüpe, K. and Peutz-Schieck. (2014) The tangled threads of ancient embroidery, a compilation of written sources archaeologically preserved textiles. In Harlow, M. and Nosch, M-L. *Greek and Roman textiles and dress*. Oxford: Oxbow, 1-33.

Dror, I. E. and Langeburg, G. (2019) "Cannot Decide": the fine line between appropriate inconclusive determinations versus unjustifiably deciding not to decide. *Journal of forensic science* 64, No. (1), 10-15.

Drucker, P. (1953 reprint) *The Northern and Central Nootkan Tribes.* Washington: Supt. of Docs. U.S. Govt.

Dubreuil, L. and Savage, D (2014) Ground stones: a synthesis of the use-wear approach. *Journal of archaeological science* 48, 139-153.

Dunbar, M. and Murphy, T. M. (2009) DNA analysis of natural fiber rope. *Journal of forensic sciences* 54 (1), 108-113.

Dunsmore, S. (2006*)* *The nettle in Nepal: A cottage industry*. Surbiton; Land Resources Development Centre.

Edom, G. (2010) F*rom sting to spin- a history of nettle fibre*. Bognor Regis; Urtica Books.

Edwards, H. G. M., Ellist, E., Farwell, D.W. and Janaway, R. C. (1996) Preliminary study of the application of Fourier Transform Raman spectroscopy to the analysis of degraded archaeological linen textiles*. Journal of raman spectroscopy* 21, 663-669.

Edwards, H. G. M., Farwell, D. W. and Webster, D. (1997) FT Raman microscopy of untreated natural plant fibres. *Spectrochimica.* Part A (53), 2383-2392.

Edwards, H. (2014) *Email FTRS fibres analysis at Federal University of Juiz de For a, Brazil, for samples of nettle, flax and hemp* [Personnel communication 18/11/2014).

Evans, A.A. (2014a) Standardization, calibration and innovation: a special issue on lithic microwear method. *Journal of archaeological science* 48, 1-4.

Evans, A.A. (2014b) On the importance of blind testing in archaeological science: the example from lithic functional studies. *Journal of archaeological science* 48, 5-14.

Evans, A.A., and Donahue, R.E. (2005) The elementary chemistry of microwear traces: an experiment. *Journal of archaeological science* 32, 1733-1740.

Evert, R. F. (2009). *Esau's plant anatomy: meristems, cells, and tissues of the plant body: their structure, function, and development*. (3rd ed). Berlin: De Gruyter.

Farwell, D. W. (2014) *University of Bradford Molecular Studies Group* (MSG) (pers. comm.). Trial investigation of plant fibre samples. 21/07/2014 (by email)).

Forte, V., Coletti, F., Ciccarelli, E. and Lemorini, C (2019) The contribution of experimental archaeology in addressing the analysis of residue on spindle whorls. *Journal of experimental archaeology* 4, 1-8.

Foss Analytical (2016) Email, Fibretec 8000 analysis of flax and nettle fibre. Personnel communication (21/01/2016).

Frahm, E. and Brody, L. R. (2019) Origins of obsidian at the Pompeii of the Syrian Desert, sourcing lithic artefacts from the Yale-French excavations in Dura- Europos. *Journal of archaeological science. Reports* 24, 608-622.

Frangipane, M., Andersson-Strand, E., Laurito, R., Möller-Wiering, S., Nosch, M. L. and Wisti-Lassen, A. (2009) Arslantepe, Malatya, (Turkey), Textiles, tools and imprints of fabrics from the 4th to the 2nd millennium BCE. *Paléorient* 35 (1), 5-29.

Franzén, M-L, Sundström, A., Lundwall, E. and Andersson-Strand, E. (2019) Sweden. In Gleba, M. and Mannering U. (eds.) *Textiles and Textile Production in Europe from pre-history to AD 400. Ancient textiles series* 11 Chap. 17, Oxford: Oxbow, 349-366.

Fuller, D. Q. (2008) The spread of textile production and textile crops in India beyond the Harappan zone: an aspect of the emergence of craft specialization and systematic trade. In Osada, T. and Uesugi (eds.) *Linguistics, archaeology and the human past,* 1-26.

Fuentes, C. A., Willekens, P., Petit, J., Thouminot, C., Mussig, J., Trindade, L.M. and Van Vuure. A. W. (2017) Effect of the middle lamella biochemical composition on the non-linear behaviour of technical fibres of hemp under tensile loading using strain mapping. *Composites: Part A* 101, 529–542.

Gaffney, V., Garwood, G. and Momber, G. (2015) How sedimentary DNA brought wheat to Mesolithic Bouldnor Cliff. *British archaeology* May/June, 24-27.

Gale, R. and Cutler, D. (2000) *Plants in archaeology*: *identification manual of vegetative plant materials used in European and Southern Mediterranean to circa 1500.* Otley: Westbury and Royal Botanical Gardens Kew.

Garside, P., and Wyeth, P. (2006) Identification of Cellulosic Fibres by FTIR Spectroscopy: Differentiation of flax and hemp by polarized ATR FTIR. *Studies in conservation* Vol. 51 (No. 3), 205-211.

Gierlinger, N., Keplinger, T. and Harrington, M. (2012) Imaging of plant cell walls by confocal Raman microscopy. *Nature protocols* 7 (9), 1694-1708.

Gillis, C. and Nosch, M-L. (2007) *Ancient textiles, production, craft, and society.* Oxford: Oxbow.

Gilligan, I. (2006) Clothing and farming origins: the Indo-Pacific evidence. In *Indo-Pacific Prehistory Association Conference (IPPA): Manilla* 2006.

Gleba, M. (2008) Textile production in Pre-Roman Italy *Ancient textiles series 4*. Oxford: Oxbow.

Gleba, M. and Harris, S. (2019) The first plant bast fibres technology, identifying splicing in archaeological textiles. Archaeological and anthropological sciences 11, 2329-2346.

Gleba, M. and Mannering, U. (2019) Introduction: textile preservation, analysis and technology: *Textiles and Textile Production in Europe: From Prehistory to AD 400,* 1-26.

Gleba, M and Turfa, J.M. (2007) Digging for archaeological textiles in museums: “New” finds in the University of Pennsylvania Museum of Archaeology and. *Proceedings of the 9th North European Symposium for Archaeological Textiles, NESAT IX,* 35-40

Glory, A. (1959) Débris de cord paléolithique à la Grotte de Lascaux. *Mémoiries de la société préhistorique Française* 5, 135-169.

Gobalet, K. W. (2001) A critique of faunal analysis: Inconsistency among experts in blind tests. *Journal of archaeological science.* 28, 377–386.

Gostenčnik, K. (2010) The Magdalensberg textile tool, a preliminary assessment In Andersson Strand, E., Gleba, M., Munkholt, C. and Ringgaard, M. (eds.) *North European symposium for archaeological textiles X*. Oxford: Oxbow, 73-90.

Gonzalez-Urquijo, J.E., and Ibanez-Estevez, J.J. (2003) The quantification of use-wear polish using image analysis. First results. *Journal of archaeological science* 30, 481-489.

Goodway, M. (1987) Fibre identification in practice. *Journal of the American institute for conservation.* 26 (1), 27-44.

Greaves, P. H., Saville, B. P. and Royal Microscopical Society (1995) *Microscopy of textile fibres.* Vol. 32. Oxford: BIOS Scientific.

Grimm, E.C., Maher Jr, L.J. and Nelson, D.M. (2009) The magnitude of error in conventional bulk-sediment radiocarbon dates from central North America. *Quaternary research* 72, 301–308.

Grömer, K. (2005) Efficiency and technique-experiments with original spindle whorls. In Bichler, P., Grömer, K., Hofmann-de Keijzer, R., Kern, A. and Reschreiter, H. (eds.) Hallstatt textiles; Technical analysis, scientific investigations and experiments on Iron Age textiles. *BAR International Series* 1351, 107-116.

Grömer, K. (2013) Discovering the people behind the textiles: Iron Age textile producers and their products in Austria. In Gleba, M. and Judit, P.(eds.) Making Textiles in Pre-Roman and Roman Times: People, Places, Identities. *Ancient Textiles Series* 13, 30-59.

Grömer, K. (2019) Austria: Bronze and Iron Age. In Gleba, M. and Mannering U. (eds.) Textiles and Textile Production in Europe from pre-history to AD 400 *Ancient textiles series* 11 Chap. 1. Oxford: Oxbow, 27-64.

Grömer, K. and Kern, D. (2010) Technical data and experiments on corded ware. *Journal of archaeological science* 37 (12), 3136-3145.

Guzowski, M., Becks, R., Andersson Strand, E., Cutler, J. and Nosh M.-L. (2015) Textile tools from Troia, western Anatolia. In Andersson Strand, E. and Nosch, M.-L. (eds.) Tools, textiles and contexts; investigating textile production in the Aegean and Eastern Mediterranean Bronze Age. *Ancient textiles Series* 21 Chap.6.13, 309-328.

Haag, K. and Müssig. J. (2016) Scatter in tensile properties of flax fibre bundles: influence of determination and calculation of the cross-sectional area. *Journal of material sciences* 51, 7907–7917.

Hald, M. (1980) Ancient Danish textiles from bogs and burials: a comparative study of costume and Iron Age textiles (Olsen, J. trans) A*rchaeological-historical series vol. XX1.* Copenhagen: National Museum (Stiftsbogtrykken), 124-128.

Haumptmann, A., Schmitt-Strecker, S., begemann, F. and Pa;lmieri, A. (2002) Chemical composition and lead isotopy of metal objects from the “Royal Tomb andc related finds at Arslanjtepe, Eastern Anatolia. *Paléorient* 28 (2), 43-70.

Hanninen, T., Thygesen, A., Mehmood, S., Madsen, B. and Hughes, M. (2015) Mechanical processing of bast fibres: the occurrence of damage and its effect on fibre structure. *Industrial crops and products* 39, 7–11.

Hardy, B. L., Moncel, M. H., Kerfant, C., Lebon, M., Bellot-Gurlet, L. and Mélard, N. (2020) Direct evidence of Neanderthal fibre technology and its behavioural implications. *Scientific reports nature research 10, 4889.*

Hardy, K. (2016) Plants as raw materials In Hardy, K. and Kubiak-Martens, L. (eds) Wild Harvest, plants in the hominin pre-agrarian human world. *Studying scientific archaeology* 2, 71-90.

Harris, D. R. (1989) Foraging and farming: an evolutionary continuum of people-plant interaction. In Harris, D. R and G. C. Hillman (eds) *Foraging and farming: the evolution of plant exploitation.* London: Unwin Hyman. Chap1, 11-26.

Harris, S. (2010) Smooth and cool or warm and soft; investigating the properties of cloth in prehistory. In Andersson Strand, E., Gleba, M., Munkholt, C. and Ringgaard, M. (eds.) *North European symposium for archaeological textiles X*. Oxford: Oxbow,104-112.

Harris, S. (2014) Flax fibre: innovation and change in the early Neolithic a technological and material perspective. *Textile Society of America Symposium Proceedings. Paper, 913. 9.*

Harris, S. (2015) Folded, layered textiles from a Bronze Age pit pyre excavated from Over Barrow 2, Cambridgeshire, England**.** In Grömer, K. and Pritchard, F. (editors). *Aspects of the design, production and use of textiles and clothing from the Bronze Age to the early modern era. Proceedings of NESAT Xll Conference* (2014) Hallstatt, Austria.

Harris, S. (2016) The charred textiles from the cremation. In Jones, A. M. (ed) *Preserved in the peat. An extraordinary Bronze Age burial on Whitehorse Hill, Dartmoor, and its wider context.* Oxford: Oxbow Books, 49-51.

Harris, S., Haigh, S., Handley, A. and Sampson, W. (2017) Material choices for fibre in the Neolithic: an approach through the measurement of mechanical properties. *Archaeometry* 59 3, 574–591.

Hart, J.P. and Lovis, W.A. (2007) A multi-regional analysis of AMS and radiometric dates from carbonized food residues. *Midcontinental Journal of archaeology* 32, (2):201-261.

Harwood, J. and Edom. (2012) Nettle fibre: its prospects, uses and problems in historical perspective. *Textile history*, 43 (1), 107–119.

Haseloff, J. (2003) Old botanical techniques for new microscopes *Bio techniques* 34, 1174-1182.

Haugan, E., Holst, B. (2013) Determining the fibrillar orientation of bast fibres with polarized light microscopy: the modified Herzog test (Red Plate Test) explained. *Journal of microscopy* Vol. 252 (Issue 2), 159-168.

Haugan, E. and Holst, B. (2014) Flax look-alikes: pitfalls of ancient plant fibre identification. *Archaeometry* 56 (6), 951-960.

Hayes, E. H., Cnuts, D., Lepers, C. and Rots, V. (2017) Learning from blind tests: Determining the function of experimental grinding stones through use-wear and residue analysis. *Journal of archaeological science:* Reports 11, 245–260.

Hearle, J.W.S. (1963) The fine structure of fibers and crystalline polymers: III. interpretation of the mechanical properties of fibers. *Journal of applied polymer science 7, 1207–1223.*

Herbig, C. and Maier, U. (2011) Flax for oil or fibre? Morphometric analysis of flax seeds and new aspects of flax cultivation in Late Neolithic wetland settlements in southwest Germany. *Vegetation history archaeobotany. 20, 527–533.*

Henriksen and Runge (2009) Archaeological evidence of flax production 500 BC–1000 AD–examples from Funen, Denmark. Communicating culture. The International Flax Network. Abstracts, 20-21.

Hernandez -Estrada, A., Gusoviusb, H-J., Müssigc,J. and Hughes, M. (2016) Assessing the susceptibility of hemp fibre to the formation of dislocations during. *Industrial crops and products* 85, 382–388.

Herzog, A. (1985) *Identification of textile materials*. The Textile Institute Manchester.

Higgitt, C., Harris, S., Cartwright, C., and Cruikshank, P. (2011) Assessing the potential of historic archaeological collections: a pilot study of the British Museum's Swiss lake dwelling textiles. *British Museum technical bulletin* 5, 81-94.

Hilger, M.I. (1951) *Chippewa child life and its cultural background*. Washington: U.S. Govt. Print 1951, 204.

Horne, M. R. L., Harwood, R.J., McCormick, B.P. and Harwood, J. L. (2008) Stinging Nettle (Urtica dioica) fibres for use in textiles: team research, De Montfort University, Leicester, UK. *Conference proceedings 86th textile world conference Nov. 2008. Hong Kong: Institute of textiles and clothing,* 63-70.

Houston, M. (2003) *Ancient Greek, Roman and Byzantine costume and decoration*. Dover: Dover Publications.

Huber, B. (2015) Qarara: une affaire de linceuls (Trans, A review of shrouds)**.** In *Proceedings of the 8th Conference of the Research Group "Textiles from the Nile Valley"* Antwerp 4-6 October 2013.Tielt: Lannoo, 120-25.

Hurcombe, L. (1988). Some criticisms and suggestions in response to Newcomer et al. (1986). *Journal of archaeological science* 15 (1), 1-10.

Hurcombe, L. M. (2000) Plants as raw material for crafts. In Fairbairn, A. S. (ed.) *Plants in Neolithic Britain and beyond: Neolithic Studies group seminar papers 5*. Oxford: Oxbow Books, 155-173).

Hurcombe, L. M. (2007) *Archaeological artefacts as material culture.* London: Routledge. Cornell University Press.

Hurcombe, L. M. (2008) Organics from inorganics: using experimental archaeology as a research tool for studying perishable material culture. *World archaeology* 40 (1), 83-115.

Hurcombe, L. M. (2010) Nettle and bast fibre textiles from stone tool wear traces? The implications of wear traces on archaeological late Mesolithic and Neolithic micro-denticulate tools. In Andersson–Strand, E., Gleba, M., Mannering, U., Munkholt, C. and Ringgaard, M. (eds.). *NESAT X.* Oxford: Oxbow, 129-139.

Hurcombe, L. (2014) *Perishable material culture in prehistory: investigating the missing majority.* London: Routledge/Taylor and Francis Group.

Jacomet, S. (2006) Plant economy of the northern Alpine lake dwellings 3500-2400 cal. BC. *Environmental archaeology* 11 (1), 65-85.

Janaway, R., C. (1987) The preservation of organic materials in association with metal artefacts deposited in inhumation graves. In Boddington, A., Garland, A., N., and Janaway, R., C. (eds.) *Death, decay and reconstruction: An approach to archaeology and forensic science.* Manchester: Manchester University Press.

Janaway, R.C. (2002). Degradation of clothing and other dress materials associated with buried bodies of both archaeological and forensic interest. In Hagland, W. D and Sorg, M. H. (editors) *Advances in forensic taphonomy method, theory, and archaeological perspectives.* Washington D. C: CRC Press, 379-399.

Jensen H. J. (1994) *Flint tools and plant working: Hidden traces of stone age technology*. Aarus: Aarus University.

Jinqiu, Z. and Jianchun, Z. (2010) Effect of refined processing on the physical and chemical properties of hemp bast fibers. *Textile research journal* 80 (8), 744-753.

Jochelson W (1908) *The Koryak: Memoir of the Jesup North Pacific Expedition*. New York: American Museum of Natural History.

Jones, A. M., Marley, J., Quinnell, H., and Hartgroves, S. (2011) On the Beach: New Discoveries at Harlyn Bay, Cornwall. *Proceedings of the Prehistoric Society* 77, 89–109.

Kania, K. (2015) Soft yarns, hard facts, evaluating the results of a large-scale hand-spinning experiment. *Archaeological anthropological science* 7, 113-130.

Karg, S. (2011) New research on the cultural history of the useful plant Linum usitatissimum L. (flax), a resource for food and textiles for 8,000 years. *Vegetation history and archaeobotany* 20, 507–508.

Kenward, H. K. and Hall, A. R. (1995) *Biological evidence from Anglo-Scandinavian deposits at 16-22 Coppergate.* York: CBA.

Kislev, M. E., Simchoni, O., Melamed, Y. and Maroz, L. (2011) Flax seed production; evidence from the early Iron Age site of Tel Beth-Shean, Israel and from written sources. *Veget hist and archaeobot* 20, 579-584.

Kronkright, D. P. (1990) Deterioration of artefacts made from plant materials. In Florian, M-L., Kronkright, D. P. and Norton, R. E. *The conservation of artefacts made from plant materials.* Princeton: Princeton University Press, 139-194.

Krueger, J. (2001) Taxonomy of degradation. In Buschow, J. K. H., Cahn, R. W., Fleming, M. C., Ilschener B., Kramer, E. J. and Mahajan, S. *Encyclopedia of materials science and engineering* Vol.3, 2036-2040. Oxford: Pergamon Press.

Kühn, M. and Heitz- Weniger, A. (2015) Vegetation history and plant economy in the Circum-Alpine region Bronze Age and Early Iron Age environments; stability or changes? In Menotti, F.(ed.) *The end of the lake dwellings in the Circum-Alpine Region*. Oxford: Oxbow, 125-178.

Kubiak-Martens, L. (2016) The plant food component of the diet at the late Mesolithic (Erteb0lle) settlement at Tybrind Vig, Denmark. *Vegetation history archaeobotany 8, 117-127.*

Küster, H. (1984) Neolithic plant remains from Eberdingen –Hochdorf Southern Germany. in Van-Zeist, W. and Casparie, W. A. (ed.) *Plants and ancient man: studies in palaeoethnobotany.* Proceedings of the sixth symposium of the international work group for palaeoethnobotany. Boston; Balkema, 307-312.

Larsson, M. and Lageras, P. (2015) New evidence on the introduction, cultivation and processing of hemp (*Cannabis sativa* L.) in southern Sweden. *Environmental archaeology* 20 (2), 111-119.

Lee, R. B. (1979) *The !Kung San. Men, women, and work in a foraging society.* Cambridge: Cambridge University Press.

Lefeuvre, A.,Bourmaud, A., Morvana, C. and Baley, C. (2014) Elementary flax fibre tensile properties: Correlation between stress–strain behaviour and fibre composition. *Industrial crops and products* 52, 762–769.

Levi Sala, I. (1986). Use wear and post-depositional surface modification: a note of caution. *Journal of archaeological science* 13, 203-218.

Leuzinger, U.and Rast-Eicher, A (2011) Flax processing in the Neolithic and Bronze Age pile-dwelling settlements of eastern Switzerland. *Vegetation history and archaeobotany* 20 (6), 535-542.

Levy, J. and Gilead, I. (2013) The Emergence of the Ghassulian Textile Industry in the Southern Levant Chalcolithic Period (c. 4500-3900 BCE). In Nosch, M. L., Koefoed, K. and Andersson-Stranded, E. (eds.) Textile production and consumption in the ancient near east: Archaeology, epigraphy, iconography*. Ancient textile series* Vol. 12. Oxford: Oxbow, 26-44.

Linscheid, P. (2001) Late antique to Early Islamic textiles from Egypt, *Textile history, 32:1, 75-80*.

Lipkin, S. (2012) Textile-making in Central Tyrrhenian Italy from the Final Bronze Age to the Republican Period. *BAR International Series 2369.*

Liu, M., Fernando, D., Daniels, G., Madsen, B. Meyer, S., Ale, M. T. and Thygesen, A. Effect of harvest time and field retting duration on the chemical composition, morphology, and mechanical properties of hemp fibers. *Industrial crops and products* 69, 29–39.

Lombard, M. and Wadley, L. (2007) The morphological identification of micro-residues on stone tools using light microscopy: progress and difficulties based on blind tests. *Journal of archaeological science* 34, 155-165.

Lopez, M. J., Vargas- Garcia, M del C., Suarez-Estrella, F. and Moreno, J. (2006) Bio-delignification and humification of horticultural plant residues by fungi. *International biodeterioration and biodegradation* 57, 24–30.

Lowe, A. C., Beresford, D. V., Carter, D. O., Gaspari, F., O'Brien, R. C., Stuart, B. H. and Forbes, S. L. (2013) The effect of soil texture on the degradation of textiles associated with buried bodies. *Forensic science international* 231, 331–339.

Lumb, D. R. A. (2013) Textiles, value, and the early economies of North Syria and Anatolia. In Nosch, M.L., Koefoed, K. and Andersson-Stranded, E. (eds) Textile production and consumption in the ancient near east: Archaeology, epigraphy, iconography*. A*n*cient textile series* Vol. 12*.* Oxford: Oxbow.

Lundström-Baudais, K. (1984) Paleoethnobotanical investigations of plant remains from a Neolithic lakeshore site in France; Clairvaux Station lll. in Van-Zeist, W. and Casparie, W., A. (eds.) *Plants and ancient man: studies in palaeoethnobotany.* Proceedings of the sixth symposium of the International Work Group for Palaeoethnobotany. Boston: Balkema, 293-306.

Luniak, B. (1953) *The identification of textile fibres: Qualitative and quantitative analysis of fibre blends.* London: Pitman.

Lukšová, H. (2014) *University Museum of Bergen.* Refractive index of mountant. (pers. comm.). (04/07/2014 by email)).

Lukšová, H (2017) Application of the Herzog Test to archaeological plant fibre textiles the possibilities and limits of polarised light microscopy. *Presentation at NESAT X111 Conference Liberec 2017*. (with kind permission from the Author).

Lundström-Baudais, K. (1984) Palaeoethnobotanical investigations of plant remains from a Neolithic lakeshore site in France; Clairvaux Station lll. In Van-Zeist, W. and Casparie, W. A. (eds) *Plants and ancient man: studies in palaeoethnobotany.* Proceedings of the sixth symposium of the International Work Group for Palaeoethnobotany. Boston; Balkema, 293-306.

Mabey, R. (1996) *Flora Britannica.* London: Sinclair-Stevenson.

Maier, U. and Schlichtherle, H. (2011) Flax cultivation and textile production in Neolithic wetland settlements on Lake Constance and in Upper Swabia (south-west Germany) *Vegetation history and archaeobotany* 20, 567–578.

Maik, J. (2019) Poland. In Gleba, M. and Mannering U. (eds.) Textiles and Textile Production in Europe from pre-history to AD 400. *Ancient textiles series* 11 Chap. 14, Oxford: Oxbow, 293-305.

Mannering, U., Gleba, M and Bloch-Hansen, M (2019) Denmark. In Gleba, M. and Mannering U. (eds.) Textiles and Textile Production in Europe from pre-history to AD 400. *Ancient textiles series* 11 Chap. 3, Oxford: Oxbow, 91-121.

Margariti, C., Eastop, D., Moraitou, G. and Wyeth, P. (2010) Potential and limitations of the application of FTIR microscopy to the characterisation of textiles excavated in Greece. In Andersson–Strand, E., Gleba, M., Mannering, U., Munkholt, C. and Ringgaard, M. (eds.). *North European Symposium for archaeological textiles NESAT X.* Oxford: Oxbow, 162-166.

Martin, E. and Murphy, P. (1988) West Row Fen, Suffolk: a Bronze Age fen-edge settlement site. *Antiquity* 62, 353-358.

Mazare, P. (2014) Investigating Neolithic and Copper Age textile production in Transylvania (Romania): applied methods and results. In Harlow, M., Michel, C. and Nosch, M.-L. (eds.) *Prehistoric, ancient near eastern and Aegean textiles and dress*. Oxford: Oxbow Chap.1, 1-42.

Médard, F. (2003) Textile remains and threading activities on the Neolithic site at d'Arbon Bleach3 (TG, Suisse). *Bulletin de la Prehistoric Society Francaise* 100 (2), 375-391.

Médard, F. (2005) Les textiles préhistoriques. *Collection archaeologica* 3, 99-104.

Médard, F. (2012) Switzerland: Neolithic period. In Gleba, M. and Mannering, U. (eds.) Textiles and textile production in Europe from prehistory to AD 400. *Ancient textiles series* 11 Chap. 18, *Ancient textiles series* 11 Chap. 18, 367-377.

Menotti, F. (2015) The lake-dwelling phenomenon: myth, reality and archaeology. In Menotti, F.(ed.) *The end of the lake dwellings in the Circum-Alpine Region.* Oxford: Oxbow, 1-14.

Militello, P. (2007) Textile industry and Minoan Palaces. In Gillis, C. and Nosch, M.-L. B. (eds.) *Ancient textiles; production craft and society.* Oxford: Oxbow Part 2 (4), 36-45.

Moffat, B. (1989) The third report on researches into the medieval hospital at Soutra, Lothian/Borders Region Scotland. In *Sharp practice* 3, 38.

Möller-Wiering, S. (2019) Germany. Bronze and Pre-Roman Iron Ages. In Gleba, M. and Mannering U. (eds.) Textiles and Textile Production in Europe from pre-history to AD 400. *Ancient textiles series* 11 Chap. 4, Oxford: Oxbow, 122-138.

Moore, J. and Jennings, D. (eds.) (1992) Reading Business Park, A Bronze Age landscape. Oxford: Oxford Archaeological Unit National Institute of Health (USA) (2010) *ImageJ, image processing and analysis in Java. http://imagej.nih.gov/ij/download.html* Accessed 29/03/2016.

Morin, E., Ready, E., Boileau, A., Beauval, C. and Coumont, M. P. (2017) Problems of identification and quantification in archaeozoological analysis, Part I: insights from a blind test. *Journal of archaeological method theory* 24, 886–937.

Nadel, D., Danin, A., Werker, E., Schick, T., Kislev, M. E. and Stewart, K. (1994) 19,000-year-old twisted fibres from Ohalo II. *Current anthropology* 35 (4), 451-458.

Nakhaeizadeh, S., Dror, I. E. and Morgana, R.M. (2014) Cognitive bias in forensic anthropology: Visual assessment of skeletal remains is susceptible to confirmation bias. *Science and justice* 54, 208–214.

Nelson, R.E., Carter, L.D. and Robinson, S.W. (1988) Anomalous radiocarbon ages from a Holocene detrital organic lens in Alaska and their implications for radiocarbon dating and Paleoenvironmental reconstructions in the Arctic. *Quaternary research* 29, 66-71.

Nims, R. and Butler, V. (2007) Assessing reproducibility in faunal analysis using blind tests: A case study from north-western North America. *Journal of archaeological science* 11, 750–761.

Outram, A., K. (2008) Introduction to experimental archaeology. *World archaeology* 40 (1), 1-6.

Pals, J. P. (1984) Plant Remains from Aartswoud a Neolithic settlement in the coastal area. In Van-Zeist, W. and Casparie, W.A. (eds.) *Plants and ancient man: studies in palaeoethnobotany*. Proceedings of the sixth symposium of the International Work Group for Palaeoethnobotany. Boston; Balkema, 313-330.

Pandey, B. P. (2012) *Plant Anatomy* (7th ed.). New Delhi (India): Chand.

Parry, D. W. and Kelso, M. (1975) The distribution of silicon deposits in the roots of *Molinia caerulea* (L.) Moench. und Sorghum bicolor. Moench. *Annals of botany* 39, 995-1001.

Parry, D. W. and Winslow, A. (1977) Electron-probe micro-analysis of silicon accumulation in the leaves and tendrils of *Pisum sativum* L. following root severance. Electron-probe micro-analysis of silicon accumulation in the leaves and tendrils of *Pisum sativum* L. following root severance. *Annals of botany* 41, 275-278.

Peacock, E., E. (1996) Characterization and simulation of water degraded archaeological textiles: a review. *International biodeterioration and biodegradation* 38 (1), 35-47.

Peacock, E. E. (2003) The biodeterioration of textile fibres in wet archaeological contexts with implications for conservation choices *Intrecci Vegetali e Fibre Tessili da Ambiente Umido: Analisi Conservazione e Restauro: Atti (Trento, 28–30 Maggio 2003), Incontri di Restauro*, 32-47.

Peacock, E. E. (2001) The contribution of experimental archaeology to the research of ancient textiles. Chapter 21 In Walton Rogers, P., Bender Jørgensen, L. and Rast-Eicher, A. (eds.) *The Roman textile industry and its influence: A birthday tribute to John Peter Wild.* Oxford; Oxbow, 181- 192.

Pearsall, D., M. (1989) *Paleoethnobotany: a handbook of procedures*. London: Academic Press.

Pearsall, M. D. and Dinan, E. H. (1992) Developing a phytolith classification system. In Rapp, J. G. and Mulholland, S. C. (eds) *Phytolith systematics: emerging issues.* New York: Plenum Press, 37-64.

Peetla, P., Schenzel, C. and Diepenbrock, W. (2016) Determination of mechanical strength properties of hemp fibers using near-infrared Fourier transform Raman micro- spectroscopy. *Applied spectroscopy* 6, 692-699.

Peeters, J. H. M. and Momber, G (2014) The southern North Sea and the human occupation of northwest Europe after the Last Glacial Maximum. *Netherlands Journal of Geosciences-Geologie en Mijnbouw* 93 (1/2), 55-70.

Petraco, N. and Kubic, T. (2004) *Colour atlas of microscopy for criminalists, chemist and conservators.* London: CRC Press.

Peyronel, L. (2007) Spinning and weaving at Tell Mardikh-Ebla (Syria): Some observations on spindle whorls and loom-weights from the Bronze and Iron Ages. In Gillis, C. and Nosch, M. L. B. (eds) *Ancient textiles production, craft and societies: Proceedings of the first international conference on ancient textiles, Lund (Sweden) and Copenhagen (Denmark) March 2003.* Oxford: Oxbow, 26-35.

Piccardo, P., Amendola, R. and Ervas, A. (2010) Metallographic investigations and experimental replication of an Etruscan bronze mirror. *Journal of historical metallurgy society* 44 (1), 10-14.

Pillin, I., Kervoelen, A., Bourmaud, A., Goimard, J., Montrelay. N. and Baleya, C. (2011) Could oleaginous flax fibers be used as reinforcement for polymers? *Industrial crops and products* 34, 1556–1563.

Piperno, D. R. (1988) *Phytolith analysis: an archaeological and geological perspective.* San Diego, Calif (USA): Academic Press.

Piperno, D. R. (2006) *Phytoliths: a comprehensive guide for archaeologists and paleoecologists.*

Pique, R., Romero, S., Palomo, A., Tarrus, J., Terradas, X. and Bogdanovic, I. (2016) The production and use of cordage at the early Neolithic site of La Draga (Banyoles, Spain) *Quaternary international* XXX, 1-9.

Placet, V., Day, A. and Beaugrand J. (2017) The influence of unintended field retting on the physicochemical and mechanical properties of industrial hemp bast fibres. *Journal of materials science* 52, 5759–5777.

Pounds, N. J. G. (1974) *An economic history of medieval Europe*. New York: Longman.

Powers, A. H. (1992) Great expectations: a short historical review of European phytolith systematics**.** In Rapp, G. J. and C., M. S. (eds) *Phytolith systematics: emerging issues.* New York: Plenum Press, 15-36.

Prieto, A., Yusta, I. and Arrizabalaga, A. (2019) Defining and characterising quartzite; sedimentary and metamorphic processes in the lithic assemblages of El Habario and El Arteu (Cantabrian Mountains, Northern Spain). *Archaeometry* 61 (1), 14-30.

Pritchard, F. (2006) *Clothing culture: dress in Egypt in the First Millennium AD. Clothing from Egypt in the collection of The Whitworth Art Gallery. Manchester:* The University of Manchester.

Raffrenato and Amburgh (2011) Technical note: improved methodology for analyses of acid detergent fiber and acid detergent lignin. *Journal of dairy science* 94 (7), 3613-3617.

Raffrenato, E., Van Soest, P. J. and Van Amburgh, M. E. (2011) Effect of lignin type on extent and rate of neutral detergent fibre digestion and potential energy yield. *South African Journal of animal science* 40 (5), 153-156.

Randsborg, K. (2011) *Bronze age textiles, men women and wealth*. Bristol; Bristol Classic Press.

Rantuch, P and Balog, K. (2014) Thermogravimetric analysis of cellulose insulation and determination of activation energy of its thermo-oxidation using non-isothermal, model-free methods *Polymers advanced technologies* 2014 25, 1169–1174.

Rasband W. S. (2016) ImageJ, U.S. National Institutes of Health, Bethesda, Maryland, USA, https www. imagej.nih.gov/ij/ Accessed 28/02/2017.

Rast-Eicher, A. (2016) *Fibres, microscopy of archaeological textiles and furs*. Budapest: Archaeolingua Alapítvány.

Renker, A. and Gunther, E. (1990) Makah. In Suttles, W. (ed.) *Handbook of North American Indians. Northeast. Vol. 7*. Washington, D.C.: Smithsonian Institution, 1990, 422-430.

Riggs, C. (2012) *The Oxford handbook of Roman Egypt*. Oxford: Oxford university press. Fayum, 156—157.

Rosen, A., M. (1992) Preliminary identification of silica skeletons from Near Eastern archaeological sites; an anatomical approach. In Rapp, G. J. and C., M. S. (eds) *Phytolith systematics: Emerging issues.* New York: Plenum Press, 129-147.

Ryder, M. L. (1999) Probable fibres from hemp (*Cannabis sativa* L.) in Bronze Age Scotland. *Environmental archaeology* 4 (1), 93-95.

Ryder, M. L. and Gabra-Sanders, T. (1987) A microscopic study of remains of textiles made from plant fibres. *Oxford journal of archaeology* 6 (1), 97-108.

Ryndina, N., Indenbaum, G. and Kolosova, V. (1999) Copper production from polymetallic sulphide ores in the Northeastern Balkan Eneolithic culture. *Journal of archaeological science* 26, 1059-1068.

Sabatini, S., Bergerbrant, S., Brandt, L O, Margaryan, A and Allentoft, M. E. (2019) Approaching sheep herds origin and the emergence of the wool economy in continental Europe during the Bronze Age. *Archaeological and anthropological sciences* 11, 4909-4925.

Sangster, A. G., and Hodson, M. J. (1992). Silica deposition in subterranean organs. *Phytolith systematics* 239-251). Springer: Boston MA, 239-251.

Sarpaki, A. (2007) Résultants archéobotanique: preliminaries dans divers secteures de Malia. In *Journées maliotes Malia, ville et territoire: organisation desespaces et exploitation des ressources, colloque organisé a l'Ecole française d'Athènes les 2-3 Novembre 2007*, 880-884.

Sauvage, C. (2013) Spinning from old threads; the whorls from Ugarit at the Musée d' Archaéologie Nationale (Saint-Germain-en-Laye) and the Louvre. In Nosch, M.-L., Koefoed, K. and Andersson Strand E. (eds.) *Textile production and consumption in the ancient Near East. Ancient textiles series* 12 Oxford: Oxbow Chap.11, 189-214.

Sauvage, C. (2014) Spindles and distaffs. Late Bronze Age and Early Iron Age Eastern Mediterranean use of solid and tapered ivory/bone shafts. In Harlow, M., Michel, C. and Nosch, M.-L. (eds.) *Prehistoric, ancient near eastern and Aegean textiles and dress*. Oxford: Oxbow: Chap.9, 184-226.

Schaffer, E. (1981) Fibre Identification in ethnological textile artefacts. *Studies in conservation* 26, 119-129*.*

Schellenberg, H. C. (1908) The remains of plants from the North Kurgan Anan. In Pumpelly, R. Explorations in Turkestan. Washington: Carnegie Institute. In Rovner, I. (1983) Plant opal phytolith analysis: Major advances in archaeobotanical research. *Advances in archaeological method and theory* 6, 225-266.

Schiere, I. (2005) Experiments with weaving and weaving tools; basic considerations after 20 years of work. In Bichler, P., Grömer, K., Hofmann-de Keijzer, R., Kern, A. and Reschreiter, H. (eds.) Hallstatt textiles; Technical analysis, scientific investigations and experiments on Iron Age textiles. *BAR International Series 1351*, 97-100.

Schiere, I. (2005) Experiments with warp-weighted loom of Gars-Thunau, Austria. In Bichler, P., Grömer, K., Hofmann-de Keijzer, R., Kern, A. and Reschreiter, H. (eds.) Hallstatt textiles; Technical analysis, scientific investigations and experiments on Iron Age textiles. *BAR International Series 1350,* 101-106.

Schrenck, L. (1854) The people of the Amur Region. *In Reisen und Forschungen im Amur-Lande in den Jahren 1854-1856 - Vol. 3* St. Petersburg: Kaiserliche Akademie der Wissenschaften.(npn).

Seves, A. M., Sora, S., Scicolone, G., Testa, G., Bonfatti, A. M., Rossi, E., and Seves, A. (2000) Effect of thermal accelerated ageing on the properties of model canvas paintings. *Journal of cultural heritage* 1, 315–322.

Sevick. K. (2015) Science and the law: forensic labs explore blind testing to prevent errors. Evidence examiners get practical about fighting cognitive bias. *Science* 31, 6247, 462 463.

Shalem, D. (2019) *The vicinity of Kasr el Yahud* Ostracon, Israel Nature and Parks Authority.

Sharma, H. S. S., Faughey, G. and Lyons, G. (1999) Comparison of physical, chemical, and thermal characteristics of water-, dew-, and enzyme-retted flax fibres. *Journal of applied polymer science* 74, 139-143.

Sharma, H. S. S. and Faughey, G. J. (1999) Comparison of subjective and objective methods to assess flax straw cultivars and fibre quality after dew-retting. *Annals of applied biology* 135 (2), 495-501.

Shamir, O. (2005) Tunics from Kasr al-Yahud. In Cleland, L., Harlow, M and Llewellyn-Jones, L. (editors) *The clothed body in the ancient world*. edited by Liza Cleland et al, 162-8. Oxford: Oxbow, 162-168.

Shamir, O. (2015) Egyptian and Nubian textiles from Qasr el-Yahud, 9th-century AD. In *Proceedings of the 8th Conference of the Research Group "Textiles from the Nile Valley" Antwerp 4-6 October 2013.*Tielt: Lannoo, 48-60.

Shamir, O. and Baginski, A. (2013) Textile Hoard from Jericho Cave 38 in the Qarantal Cliff. In *Hoards and Genizot as chapters in history*. Haifa, 77-88.

Shamir, O. and Baginski, A. (2018) Stories behind archaeological textiles fragments from the Early Islamic Period till the Medieval Period in the land of Israel. In *Proceedings of the ICOM Costumes London 2017. http://network.icom.museum/fileadmin/user_upload/minisites/costume/pdf/ICOM_Costume_London_2017_Proceedings_-_Shamir.pdf.*Accessed 17 November 2019.

Sherratt, A. (1983) The secondary exploitation of animals in the Old World. *World archaeology* 15 (1), 90-104.

Sheldrake, R. (1999) How widely is blind assessment used in scientific research? *Alternative therapies in health and medicine* 5, 88–9.

Sirelius, U. T. (1932) Die Handarbeiten der Ostjaken u, Wolgulen. *Journal de la société Finno-Ougrienne XXII 1904:19. (Meinande, K. K. trans.). Finlands folklig kulture 1932.* [Cited in Hald, M. 1980, 125 and 144 (Note 4)].

Skoglund, G., Nockert,. Holst, B. (2013) Viking and early middle ages Northern Scandinavian Textiles proven to be made with hemp. *Scientific reports* 3, Article No. 2686.

Smalley, R. (2015) Identifying provenance: Flinders Petrie's textile collection at the Victoria and Albert Museum. *Journal of the history of collections* vol. 27 (2), 135–146.

Soffer, O., Adovasio, J. M. and Hyland, D. C. (2000) The "Venus" figurines: textiles, basketry, gender, and status in the Upper Palaeolithic. *Current anthropology* 41 (4), 511-537.

Soleimani, M., Tabil, L., Panigrahi, S. and Opoku, A. (2008) The effect of fiber pretreatment and compatibilizer on mechanical and physical properties of flax fiber-polypropylene composites. *Journal of polymers and the environment* 16 (1), 74-82.

Soltvedt, E. C. and Henningsmoen, K. E. **(2016)** Agricultural and household activities in Vestfold, Southeast Norway, as illustrated by pollen data and the charred remains of crops and wild plants. *Environmental archaeology* 21, 1:11-3.

Spantidaki Y. and Moulherat (2019) Greece. In Gleba, M. and Mannering U. (eds.) Textiles and Textile Production in Europe from pre-history to AD 400. *Ancient textiles series* 11 Chap. 7, Oxford: Oxbow, 185-202.

Stevenson, A. (2014) Artefacts of excavation: The British collection and distribution of Egyptian finds to museums,1880 – 1915. Journal of the history of collections 26 (1), 89–102.

Štolcová, T. B. and Grömer, K. (2005) Loom-weights, spindles and textiles: Textile production in central Europe from the Bronze Age to the Iron Age. In Andersson–Strand, E., Gleba, M., Mannering, U., Munkholt, C. and Ringgaard, M. (eds) *North European Symposium for archaeological textiles NESAT X.* Oxford: Oxbow, 9- 20.

Stone, E. A. (2010) Wear on Magdalenian bone tools: a new methodology for studying evidence of fibre industries. In Andersson-Strand, E., Gleba, M., Mannering, U., Munkholt, C. and Ringgaard, M. (eds.) (2010) *North European Symposium for archaeological textiles* (*NESAT X).* Oxford: Oxbow, 225-232.

Sukenik, N. and Shamir, O. (2011) Qumran textiles and the garments of Qumran's inhabitants. In *Dead sea discoveries* 18, 206-225.

Summerscale, J., Dissanayake, N.P. J., Virk, A. S. and Hall, W. (2010) A review of bast fibres and their composites. Part 1- Fibres as reinforcements. *Composites:* Part A (41), 1329-1335).

Suomela, J., Vajanto, K. and Räisänen, R. (2018) Seeking nettle textiles – utilizing a combination of microscopic methods for fibre identification. *Studies in conservation*, 63 (7), 412-422.

Swanton, M. J. (1975) *Anglo-Saxon prose.* London: Dent and Sons.

Szostak-Kotowa, J. (2004) Biodeterioration of textiles. *International biodeterioration and biodegradation* 53,165 – 170.

Tamburini, D., Lucejko, J., J., Zborowska, M., Modugno, F., Cantisani, E., and Mamo, M. (2017) The short-term degradation of cellulosic pulp in lake water and peat soil: A multi-analytical study from the micro to the molecular level. *International biodeterioration and biodegradation* 116, 243-259.

Thomas, J. (1996) The cultural context of the first use of domesticates in continental and northwest Europe. In Harris, D. R. *The origins and spread of agriculture and pastoralism in Eurasia*. London: UCL, 310-322.

Thomas, K. (2007) Coptic and Byzantine textiles found in Egypt: Corpora, collections, and scholarly perspectives. *https://www.nyu.edu/gsas/dept/fineart/people/faculty/Thomas_PDFs/TKThomas%20Coptic%20and%20Byzantine%20Textiles.pdf.* (Accessed 17 November 2019).

Thomé, **T. W. (1885)** *Flora von Deutschland, Österreich und der Schweiz in Wort und Bild für Schule und Haus* (Flora of Germany, Austria and Switzerland in Word and Picture for School and Home) Gera-Germany

Thomason, J. L., Carruthers, J., Kelly, J. and Johnson, G. (2011) Fibre cross-section determination and variability in sisal and flax and its effects on fibre performance characterisation. *Composites science and technology* 71, 1008-1015.

Thuault, A. Bazin, J., Eve, S., Bréard, J. and Moussa, G. (2013) Numerical study of the influence of structural and mechanical parameters on the tensile mechanical behaviour of flax fibres. *Journal of industrial textiles*. 44, 1.

Thygesen, A., Daniel, G., Lilholt, H. and Thomsen, A. B. (2006) Hemp fibre microstructure and use in fungal defibration to obtain fibres for composite materials. *Journal of natural fibres* 2 (4), 19-37.

Tsourinaki, S. (1960) A narrow-sleeved woollen tunic from Byzantine Egypt. In Maravelia, A. (editor): *En Quete de la Lumiere: Melanges Sadek. BAR International Series*1960*, 1.*

Tutin T. G., Heywood, V. H., Burges, N. A., Moore, D. M. Valentine, D. H., Walters, S. M., and Webb, D. A. (1990) *Flora Europa: Vol. 2: rosaceae to umbelliferae* (2nd ed.). Cambridge: Cambridge University Press.

Tutin T. G., Heywood, V. H., Burges, N. A., Valentine, D. H., Walters, S. M. and Webb, D. A. (1993) *Flora Europa: Vol. 1: psilotaceae to platanaceae* (2nd ed.). Cambridge: Cambridge University Press.

Twiss, P. C. (2001) A curmudgeon's view of grass phytolithology. In Meunier, J. D. and Colin, F. (2001) *Phytoliths: applications in earth sciences and human history.* Abingdon; Balkema, 7-26.

Uranić, I. (2006) Contributions to the provenance of the Zagreb Mummy Acta *Antiqua Hungary* 46,195–200.

Valamoti, S. M. (2011) Flax in Neolithic and Bronze Age Greece; archaeobotanical evidence. *Vegetation history and archaeobotany* 20, 549-560.

Vakirtzi, S., Koukouli- Chryssanthaki C.and Papadopoulos, S. (2014) Spindle whorls from two prehistoric settlements on Thassos, North Aegean In Harlow, M., Michel, C. and Nosch, M.-L. (eds.) *Prehistoric, ancient near eastern and Aegean textiles and dress*. Oxford: Oxbow Chap.2, 43-56.

Vakirtzi, S. (2019) Pierced sherds and clay spindle whorls. In Nikolakopoulou I. (ed.) Akrotiri, Thera: Middle Bronze Age pottery and stratigraphy. Volume 1 stratigraphy, ceramic typology and technology, weaving equipment. *The archaeological society at Athens Library series* 318: Chap 4.1, 479-500.

Van Den Dries, M., H. (1998) *Archaeology and the application of artificial intelligence: case-studies on use-wear analysis of prehistoric flint tools*. PhD thesis. Leiden University Chapter 5, 41-45. https://openaccess.leidenuniv.nl/handle/1887/13148 Accessed 26/12/2019.

Van Gijn, A. and Little, A. (2016) Tools, use wear and experimentation: extracting plants from stone and bone. In Hardy, K. and Kubiak-Martens, L. (ed) Wild harvest: plants in the hominin and pre-agrarian human worlds. *Studying scientific archaeology* 2, 135-153.

Van Soest, P. J. (1967) Development of a comprehensive system of feed analysis and its application to foragers. *Journal of animal science* 26 (1), 119-128.

Van-Zeist, W. and Casparie, W.A. (1984) *Plants and ancient man: Studies in palaeoethnobotany.* Proceedings of the sixth symposium of the International Work Group for Palaeoethnobotany. Boston; Balkema.

Van-Ziest, W and Bakker-Heeres, A. H. (1975) Evidence for linseed cultivation before 6000 BC. *Journal of archaeological science* 2, 215-219.

Verdin, P., Berger, J. F., Lopez-Saez, J. A. (2001) Contribution of phytolith analysis to the understanding of historical agrosystems in the Rhone Mid-Valley, (Southern France). In Meunier, J. D. and Colin, F. (2001) *Phytoliths: applications in earth sciences and human history.* Abingdon; Balkema, 155-172.

Verhecken, A. (2010) The Moment of Inertia, a parameter for the functional classification of worldwide spindle-whorls. In Andersson Strand, E., Gleba, M., Munkholt, C. and Ringgaard, M. (eds.) *North European symposium for archaeological textiles X.* Oxford: Oxbow, 257-270.

Verhecken, A. (2013) Spinning with a hand spindle; an analysis of the mechanics and its implications on yarn quality. Archaeological textile series 55, 97-101.

Viklund, K. (2011) Flax in Sweden: The archaeobotanical, archaeological and historical evidence. *Vegetation history and archaeobotany* 20, 509–515.

Vogl, C.R. and Hartl, A. (2003) Production and processing of organically grown fibre *Journal of alternative agriculture* 18 (3), 119-128.

Walton Rogers, P. (1997) Textile production at 16-22 Coppergate. York Yorkshire Archaeological Trust.

Wasylikowa, K. (1984) Fossil evidence for ancient foods plants in Poland. In Van-Zeist, W. and Casparie, W. A. (eds.) *Plants and ancient man: studies in palaeoethnobotany.* Proceedings of the sixth symposium of the International Work Group for Palaeoethnobotany. Boston; Balkema, 257-266.

Waudby, D. B. (2014) *Reconstruction studies of British prehistoric stinging nettles* (*Urtica dioica* L.*); plant fibre utilisation* (Unpublished MA dissertation (available University of Bradford).

Wiener, J., Kovačič, V. and Deilová, P (2003) Differences between flax and hemp *AUTEX research journal* 3 (2), 58-67.

Weiss, E. and Zohary, D. (2011) The Neolithic southwest Asian founder crops their biology and archaeobotany. *Current anthropology* 52 (S4), 237-254.

Wielage, B., Lampke, T., Marx, G., Nestler, D., and Starke, D. (1999) Thermogravimetric and differential scanning calorimetric analysis of natural fibres and polypropylene. *Thermochimica acta* 337 (1-2), 169-177.

Wild, J. P. (1970) *Textile manufacture in the northern Roman Provinces*. (2008 digital print) Cambridge: Cambridge University Press.

Wild, J. P. (2007) Methodology introduction*:* In Gillis, C. and Nosch, M. L. B. (eds.) *Ancient textiles production, craft and society*. Proceedings of the first international conference on ancient textiles Lund Sweden/Copenhagen Denmark March 2003. introduction to textile background studies and application. Oxford: Oxbow, 1-6.

Wild, J. P. and Wild, F. (2014) Qasr Ibrim: New perspectives on the changing textile cultures of Lower Nubia. In O'Connell, R. (editor) *Egypt in the first millennium AD. perspectives from new fieldwork.* British Museum Publications on Egypt and Sudan 2, 721-83.

Williams, H. (2016) The micro-excavation and conservation of the artefacts. In Jones, A. M. (ed) *Preserved in the peat. An extraordinary Bronze Age burial on Whitehorse Hill, Dartmoor, and its wider context.* Oxford: Oxbow Books, 25-32.

Wilson, A. S., Janaway, R. C., Holland, A. D. Dodson, H. I., Baran, E., Pollard, A. M. and Tobin, D. J. (2007) Modelling the buried human body environment in upland climes using three contrasting field sites. *Forensic science international* 169, 6–18.

Wylie, A. (1989) The interpretive dilemma. In Pinsky, V. and Wylie, A. (eds.) *Critical traditions in contemporary archaeology*. Cambridge: Cambridge University Press, 18-27.

Yan, L., Chouw, N. and Jayaraman, K. (2014) Flax fibre and its composites – a review *Composites:* Part B 56, 296–317.

Zias, J. (1988) Leprosy and tuberculosis in the Byzantine monasteries of the Judean Desert. In *Human paleopathology: current synthesis and future options. International congress of anthropological and ethnological sciences.* Zagreb Yugoslavia 22-31 July 1988, 197-199.

Zohary, D. and Hopf, M. (2000) *Cultivated plants in West Asia, Europe and the Nile Valley.* Oxford: Oxford University Press.

INTERNET SITES ACCESSED

AnalySIS

Ankom Technology (2016) *Ankom 220: NDF/ADF analytical processor.* *https://www.ankom.com/product-catalog/ankom-200-fiber-analyzer* Accessed 05/07/2018.

Arrhenius Law (2017) Activation energy of reaction mechanisms *http://www.chem1.com/acad/webtext/dynamics/dynamics-3.html* Accessed 23/03/2017.

Bankfield Museum Halifax (2019) *https://museums.calderdale.ac.uk* Accessed 6/5/2018

BioMomentum. (2016) *Biomomentum Mach-1 Mechanical testing equipment.* *http://www.biomomentum.com* Accessed 10/12/2019.

Bradford District Guild of Handweavers, Spinners and Dyers (2014) *http://bradfordguild.btck.co.uk* Accessed 12/03/2014.

Camira Fabrics Mirfied (2014) Information *http://www.camirafabrics.com/fabrics* *Accessed 15/06/2018.*

Cliffe Castle (2019) Coptic collection https://www.bradfordmuseums.org/venues/visit/cliffe-castle-museum Accessed 26/12/2019.

Dartmoor National Park (2017) Whitehorse Hill project *http://www.dartmoor-npa.gov.uk/lookingafter/laf-culturalheritage/whitehorse-hill-burial* Accessed 2/04/2017.

East Yorkshire Hemp (2017) Flax and hemp suppliers. https://eastyorkshirehemp.co.uk Accessed 2/04/2019.

Foss Analytics . (2016) *Textile analysis: Fibertec TM Analyser.* https://www.fossanalytics.com/en/blog/feed-and-forage?industryId=ad36c5d4-2613-489a-a760-f227266b873f Accessed 13/10 2018.

Ghent University (2016) *Analytical techniques in aquaculture research: Proximate analysis Van Soest fibre analysis.* *http://www.aquaculture.ugent.be/Education/* Accessed 05/07/2016.

Instron European. (2017) *Instron 5564 Electro mechanical load frame* http://www.instron.co.uk/en-gb accessed 05/05/2017.

Sigma-Aldrich (2016) EpoFix.

https://www.sigmaaldrich.com Accessed 11/03/2016).

Van Den Dries, M., H. (1998) Archaeology and the application of artificial intelligence: case-studies on use-wear analysis of prehistoric flint tools. PhD thesis. Leiden University Chapter 5:41-45. https://openaccess.leidenuniv.nl/handle/1887/13148 Accessed 26/12/2019.

Vintage Fashion_(2019) Brocatelle https://vintagefashionguild.org/fabric-resource/brocatelle Accessed 7/122/2019.

Whitworth Museum Manchester (2019) Whitworth collection https://www.whitworth.manchester.ac.uk

Yale University, Human Relations Area File (eHRAF) (2013) *https://hraf.yale.edu* Accessed on line 15/03/13.

Yorkshire Post (2019) Roger Warner collection *https://www.yorkshirepost.co.uk/news/treasures-of-unique-collector-go-under-hammer-1-2330975* Accessed on line 15/12/201.

APPENDIX

The research work is supported by the following database held within Microsoft XL Files as listed below.

A) Original database for tensile tests of flax, hemp and nettle fibres.

B) Determination of fibre MFA based on deviation of tensile test trendline

C) Original database for evaluation of MFA and Ct

D) Vector and statistical analysis of combined MFA/Ct relationship.

E) Blind test database includes MFA and Ct determinants of fibre samples.

F) Database for evaluations of MFA, Ct and Young's moduli for surviving fibres

dbw 17/2/2021